PhD degree in Molecular Medicine

European School of Molecular Medicine (SEMM)

University of Milan and University of Naples "Federico II"

Faculty of Medicine, BIO/11

# A NEW CLASS OF NON-CODING RNA CONTROLS THE DNA DAMAGE RESPONSE AND DNA REPAIR

*Flavia Michelini*

IFOM – FIRC Institute of Molecular Oncology, Milan

Matricola n. R08902

| | |
|---|---|
| Supervisor | Dr. Fabrizio d'Adda di Fagagna<br>IFOM, Milan |
| Internal co-supervisor | Dr. Gioacchino Natoli<br>IFOM, Milan |
| External co-supervisor | Dr. Javier Martinez<br>IMBA, Vienna |

Anno accademico 2012-2013

*To Dad*

# Table of Contents

**LIST OF ABBREVIATIONS** 11

**TABLE OF FIGURES** 15

**ABSTRACT** 19

**INTRODUCTION** 23

1. DNA DAMAGE AND THE DNA DAMAGE RESPONSE 24
   - 1.1 Different types of DNA damage 24
   - 1.2 The DNA damage response 25
     - *1.2.1 DNA damage sensors* 27
     - *1.2.2 DNA damage signaling* 29
     - *1.2.3 Crosstalk between chromatin and DDR* 31
   - 1.3 The DNA damage checkpoints 33
   - 1.4 DNA damage induced senescence 35
   - 1.5 The DNA repair pathways 36
   - 1.6 Defects in DNA repair and checkpoint pathways 39
2. THE RNA WORLD 41
   - 2.1 Different RNAs from different RNA polymerases 41
   - 2.2 The RNA "dark matter" 43
   - 2.3 Non-coding RNA 44
   - 2.4 Non-coding RNA in human diseases 47
3. RNA INTERFERENCE 49
   - 3.1 The discovery of RNA interference 49
   - 3.2 miRNA, siRNA and the RNAi pathway 50
   - 3.3 DROSHA and DICER 54
   - 3.4 miRNA in cancer and diseases 56

4. DDR AND RNA 58

4.1 DDR and RNA transcription 58

4.2 DDR proteins and RNA 59

4.3 DDR and miRNA 60

4.4 DDR and lncRNA 63

4.5 Non-canonical small RNA in DDR and DNA repair 64

**MATERIALS AND METHODS 67**

CELL CULTURE 68

IONIZING RADIATION (IR) 68

PLASMID TRANSFECTION 69

RNA INTERFERENCE 70

LNA TRANSFECTION 71

LENTIVIRAL INFECTION 72

ADENOVIRAL INFECTION 73

G2/M CHECKPOINT ASSAY 73

INHIBITION OF RNA TRANSCRIPTION 74

RNASE A TREATMENT AND RNA COMPLEMENTATION EXPERIMENTS 75

ANTIBODIES 77

IMMUNOFLUORESCENCE 77

IMAGING 78

IMMUNOBLOTTING 79

REAL-TIME QUANTITATIVE REVERSE TRANSCRIPTION PCR (QRT-PCR) 80

SMALL RNA PREPARATION 82

RNA EXTRACTION FROM GEL 83

NORTHERN BLOTTING 83

RNA SEQUENCING 85

MICROINJECTION 86

SINGLE STEP PHOTOBLEACHING 87

STATISTICAL ANALYSES 87

**RESULTS 89**

1. IR-INDUCED DDR FOCI ARE SENSITIVE TO RNASE A TREATMENT, ARE RESCUED BY TOTAL RNA RE-ADDITION AND ARE RNA POLYMERASE II DEPENDENT 90

1.1 IR-induced DDR foci are sensitive to RNase A treatment 90

1.2 Total RNA addition restores DDR foci in RNase A-treated cells 93

1.3 IR-induced DDR foci are RNA polymerase II dependent 93

2. THE RNA SPECIES INVOLVED IN DDR ACTIVATION ARE IN THE SIZE RANGE OF DROSHA AND DICER PRODUCTS 101

3. DICER OR DROSHA INACTIVATION IMPAIRS IR-INDUCED DDR FOCI FORMATION AND ESTABLISHMENT OF CELL CYCLE CHECKPOINTS 103

3.1 IR-induced DDR foci are sensitive to DICER or DROSHA knockdown independently from the canonical RNAi pathway 103

3.2 DNA damage recognition by MRE11–RAD50–NBS1 complex is affected by the lack of DICER or DROSHA 105

3.3 IR-induced DDR foci are dependent on the ribonuclease activity of DICER 107

3.4 DICER RNA products are required for DDR foci reformation in RNase A-treated cells 110

3.5 DICER or DROSHA inactivation impairs G1/S and G2/M DNA damage checkpoints and allows senescent cells to re-enter into cell cycle 110

4. DDR FOCUS FORMATION AT A DEFINED GENOMIC SITE REQUIRES DAMAGE SITE-SPECIFIC DDRNAS THAT ACT IN A TRANSLATION-INDEPENDENT, MRN-DEPENDENT, MANNER 114

4.1 An inducible DDR focus can disappear and reform in a RNA-dependent manner at a unique and traceable locus 114

4.2 DDR-regulating RNAs are site-specific 116

4.3 DDR-regulating RNAs act in a translation independent manner 118

4.4 DDR-regulating RNAs act in an MRN-dependent manner 119

5. DDR-REGULATING RNAS ARE DNA DAMAGE SITE-SPECIFIC DICER AND DROSHA PRODUCTS 122

5.1 DICER and DROSHA are necessary for the generation of DDRNAs in NIH2/4 cells 122

5.2 DDRNAs are not detectable by Northern blot analysis 124

5.3 Deep sequencing of nuclear small RNA reveals a peak of DDRNAs around 22-23 nt that is DICER dependent 127

5.4 DDRNAs generated in vitro by a recombinant DICER are sufficient to restore DDR foci 132

6. SYNTHETIC BIOLOGICALLY ACTIVE DDRNAS AND DDRNA ANTAGONISTS MODULATE THE DDR ACTIVATION AT THE DAMAGED LOCUS 135

6.1 Synthetic DDRNAs are sufficient to restore 53BP1 focus after RNase A treatment in NIH2/4 cells 135

6.2 Locked Nucleic Acids block DDRNAs function in living cells 137

7. DDRNAS AND DNA DAMAGE REPAIR 140

7.1 DICER knockdown impairs DNA damage repair in NIH2/4 140

7.2 Locked Nucleic Acids block DDRNAs function in DNA damage repair 142

8. DDR FOCI CONTAIN RNA MOLECULES 144

8.1 Synthetic cy5-DDRNAs rescue 53BP1 focus in RNase A-treated NIH2/4 cells 144

8.2 cy5-DDRNAs localize at the damaged site and co-localize with the 53BP1 focus 145

8.3 cy5-DDRNAs but not an unrelated cy5-RNA localize at the locus 147

8.4 cy5-DDRNAs localize more at the damaged than the undamaged locus 149

8.5 Deconvolved cy5-DDRNAs localize at the locus 153

**DISCUSSION 155**

1. DNA MAKES RNA PROTECTS DNA 156

1.1 A novel class of non-coding RNA regulates the DNA damage response 156

1.2 RNA-dependent DDR foci assembly and maintenance: the imperturbable γH2AX and the strange case of 53BP1 157

1.3 RNA polymerase II transcription at the DSB: a possible reconciliation? 161

2. BIOGENESIS AND FEATURES OF DDRNAS 164

2.1 DICER and DROSHA direct involvement in DDR: differences between DDRNAs and miRNAs 164

2.2 Biogenesis of DDRNAs by DROSHA and DICER: a hypothetical model 166

2.3 Are other components of the RNAi machinery involved in DDRNA generation and function? 168

2.4 DDRNA features and abundance 169

3. ROLE OF DDRNAS IN DDR AND DNA DAMAGE REPAIR 171

3.1 DDRNAs in DDR signaling: a structural component of the focus? 171

3.2 DDRNAs in DDR signaling: a chromatin-mediated mechanism? 172

3.3 DDRNAs and MRN complex: an intimate relationship 172

3.4 DDRNAs in DNA damage repair 173

4. LOOKING FOR SEQUENCE-SPECIFIC DAMAGED LOCUS 176

5. PHYSIOLOGICAL RELEVANCE OF DDRNAS 179

5.1 DDRNAs as new guardians of the genome 179

5.2 LNA technology to counteract site-specific DNA damage 180

5.3 A new vision of DICER and DROSHA in pathology and cancer 180

**REFERENCES 183**

**ACKNOWLEDGMENTS 209**

# List of Abbreviations

| | |
|---|---|
| 53BP1 | p53 binding protein 1 |
| 9-1-1 | RAD9-RAD1-HUS1 |
| AGO | argonaute |
| AMO | anti-miRNA oligonucleotide |
| ASO | antisense oligonucleotide |
| A-T | ataxia-teleangectasia |
| ATCC | american type culture collection |
| ATM | ataxia telangiectasia mutated |
| ATR | ataxia telangiectasia and Rad3-related |
| ATRIP | ATR-interacting protein |
| BARD1 | BRCA1 associated RING protein 1 |
| BER | base excision repair |
| BLM | Bloom syndrome |
| BRCA1 | breast cancer 1 |
| BrdU | bromodeoxyuridine |
| BSA | bovine serum albumin |
| CDK | cyclin-dependent kinase |
| ceRNA | competing endogenous RNA |
| circRNA | circular RNA |
| CLIP | cross-linking immunoprecipitation |
| CTD | carboxy-terminal domain |
| CtIP | CtBP-interacting protein |
| DAPI | 4',6-diamidino-2-phenylindole |
| Dcr | Dicer |
| DDR | DNA damage response |
| DDRNA | DDR-regulating RNA |
| DGCR8 | DiGeorge syndrome critical region 8 |
| diRNA | DSB-induced RNA |
| DMSO | dimetilsolfossido |
| DNA-PKcs | DNA-PK catalytic subunit |
| DSB | double-strand break |
| dsDNA/dsRNA | double-stranded DNA or RNA |
| dsRBD | double-stranded RNA binding domain |
| EMT | epithelial-to-mesenchimal transition |
| endo-siRNA | endogenous small interfering RNA |
| EV | empty vector |
| EWSR1 | Ewing sarcoma breakpoint region 1 |
| FACS | fluorescence-activated cell sorting |
| FUS | fused in sarcoma |
| GFP | green fluorescent protein |
| GR | glucocorticoid receptor |

| | |
|---|---|
| GW182 | glycine-tryptophan protein of 182 kDa |
| Gy | gray |
| HDAC | histone deacetylase |
| HNF | human normal fibroblasts |
| HOTAIR | HOX antisense intergenic RNA |
| HOX | homeobox |
| HP1 | heterochromatin protein-1 |
| HR | homologous recombination |
| IR | Ionizing radiation |
| KAP1 | KRAB-associated protein 1 |
| KSRP | KH-type splicing regulatory protein |
| JMJD2A | Jumonji domain 2 A |
| LNA | locked nucleic acid |
| lincRNA | long intergenic non-coding RNA |
| lncRNA | long non-coding |
| MDC1 | mediator of DNA damage checkpoint 1 |
| miRNA | microRNA |
| miRISC | miRNA-induced silencing complex |
| MMR | mismatch repair |
| MMEJ | microhomology-mediated end joining |
| MRN | MRE11-RAD50-NBS1 |
| mRNA | messenger RNA |
| NBS | Nijmegen breakage syndrome |
| ncRNA | non-coding RNA |
| NER | nucleotide excision repair |
| NHEJ | non-homologous end joining |
| NuRD | Nucleosome Remodeling Deacetylase |
| OIS | oncogene-induced senescence |
| PANDA | p21 associated ncRNA DNA damage activated |
| PARP | poly(ADP-ribose) polymerase |
| PAZ | Piwi Argonaute Zwille |
| PFA | paraformaldehyde |
| PIK | phosphatidylinositol 3-kinase |
| piRNA | piwi interacting RNA |
| PIWI | P-element-induced wimpy testis |
| pre-miRNA | precursor microRNA |
| pri-miRNA | primary microRNA |
| rasiRNA | repeat associated small interfering RNA |
| rDNA | ribosomal DNA |
| RdRP | RNA dependent RNA polymerase |
| RIDDLE | Radiosensitivity, Immunodeficiency, Dysmorphic features and LEarning difficulties |
| RISC | RNA-induced silencing complex |
| RNA pol | RNA polymerase |
| RNAi | RNA interference |
| RNase | ribonuclease |

| | |
|---|---|
| ROS | reactive oxygen species |
| RPA | replication protein A |
| RPP0 | Ribosomal protein large P0 |
| RT | room temperature |
| rRNA | ribosomal RNA |
| SA-β-gal | senescence-associated-β-galactosidase |
| SAHF | senescence-associated heterochromatin foci |
| SASP | senescent-associated secretory phenotype |
| SDS | sodium dodecyl sulphate |
| sem | standard error of the mean |
| shRNA | short hairpin RNA |
| SINE | short interspersed elements |
| siRNA | small interfering RNA |
| snoRNA | small nucleolar RNA |
| snRNA | small nuclear RNA |
| SSB | single-strand break |
| ssDNA/ssRNA | single-stranded DNA or RNA |
| TA | triamcinolone acetonide |
| tel-sRNA | telomer specific small RNA |
| TERRA | telomeric repeat-containing RNA |
| TopBP1 | topoisomerase II binding protein 1 |
| TRBP | transactivation-responsive RNA binding protein |
| tRNA | transfer RNA |
| UDR | ubiquitination-dependent recruitment |
| UTR | untranslated region |
| UV | ultraviolet |
| WSTF | Williams-Beuren syndrome transcription factor |
| WT | wildtype |
| XUT | Xrn1-sensitive unstable transcripts |
| XIST | X-inactivation specific transcript |
| XPO5 | Exportin 5 |

# Table of Figures


FIGURE 1. THE DNA DAMAGE RESPONSE PATHWAY. 27

FIGURE 2. MULTIPLE FUNCTIONS OF THE MRN COMPLEX. 29

FIGURE 3. THE DNA DAMAGE REPAIR PATHWAYS. 38

FIGURE 4. BIOGENESIS AND FUNCTION OF MIRNA. 54

FIGURE 5. INTERPLAY BETWEEN DDR AND MIRNA. 62

FIGURE 6. SCHEME OF RNASE A TREATMENT. 91

FIGURE 7. IR-INDUCED DDR FOCI ARE SENSITIVE TO RNASE A TREATMENT. 92

FIGURE 8. RNA POLYMERASE II INHIBITION FOR 24 HOURS LEADS TO AN IMPAIRMENT IN DDR FOCI FORMATION BUT ALSO TO A DECREASE OF DDR PROTEIN AND MRNA LEVELS. 95

FIGURE 9. RNA POLYMERASE II INHIBITION FOR 8 HOURS IN PERMEABILIZED CELLS LEADS TO AN IMPAIRMENT IN DDR FOCI FORMATION WITHOUT DETECTABLY ALTERING MRNA LEVELS OF DDR PROTEINS. 96

FIGURE 10. RNA POLYMERASE I IS NOT INVOLVED IN DDR FOCI FORMATION. 97

FIGURE 11. RNA POLYMERASE III IS NOT INVOLVED IN DDR FOCI FORMATION. 98

FIGURE 12. RNA POLYMERASE II BUT NOT RNA POLYMERASE I INHIBITION PREVENTS DDR FOCI REFORMATION AFTER RNASE A TREATMENT. 99

FIGURE 13. INCUBATION WITH 20-35NT LONG RNAS IS SUFFICIENT TO RESTORE DDR FOCI FORMATION IN RNASE-TREATED CELLS. 102

FIGURE 14. DICER OR DROSHA INACTIVATION IMPAIRS DDR FOCI FORMATION IN IRRADIATED CELLS. 104

FIGURE 15. DICER OR DROSHA KNOCKDOWN IN OIS CELLS IMPAIRS RAD50 AND NBS1 FOCI FORMATION. 106

FIGURE 16. DICER KNOCKDOWN IMPAIRS RAD50 FOCI FORMATION IN HELA CELLS. 107

FIGURE 17. DDR FOCI ARE SENSITIVE TO DICER OR DROSHA KNOCKDOWN AND DDR FOCI FORMATION IS RESCUED BY WILDTYPE BUT NOT MUTANT DICER. 108

FIGURE 18. IMPAIRED DDR FOCI FORMATION IN DICEREXON5 CELLS IS RESCUED BY WILDTYPE BUT NOT MUTANT DICER. 109

FIGURE 19. DICER RNA PRODUCTS ARE REQUIRED FOR DDR FOCI REFORMATION. 111

FIGURE 20. LOSS OF G2/M CHECKPOINT ACTIVATION IN DICER-INACTIVATED CELLS IS RESCUED BY WILDTYPE DICER RE-EXPRESSION. 113

FIGURE 21. AN INDUCIBLE DSB SYSTEM AT A UNIQUE AND TRACEABLE LOCUS. 114

FIGURE 22. A SINGLE DDR FOCUS AT A DEFINED LOCUS CAN DISAPPEAR AND REAPPEAR IN AN RNA DEPENDENT MANNER. 115

FIGURE 23. MOLECULAR MECHANISMS OF ACTION OF DDRNAS: TWO ALTERNATIVE MODELS. 117

FIGURE 24. TWO ISOGENIC CELL LINES THAT DIFFER ONLY FOR AN INTEGRATED EXOGENOUS SEQUENCE. 117

FIGURE 25. DDR-REGULATING RNAS ARE SITE-SPECIFIC. 118

FIGURE 26. THE MECHANISM OF DDR FOCUS REFORMATION TRIGGERED BY DDRNAS IS NOT AFFECTED BY MODULATION OF TRANSLATION. 119

FIGURE 27. PATM AND MRE11 FOCI IN CUT NIH2/4 CELLS ARE SENSITIVE TO RNASE A TREATMENT. 120

FIGURE 28. SITE-SPECIFIC DDRNAS ACT IN A MRN-DEPENDENT MANNER. 121

FIGURE 29. SITE-SPECIFIC RNAS THAT ALLOW REFORMATION OF DDR FOCI IN RNASE A-TREATED CELLS ARE DICER AND DROSHA DEPENDENT. 123

FIGURE 30. PROBE GENERATION FOR NORTHERN BLOT AND TESTING FOR DNA CONTAMINATION OF RNA PREPARATIONS. 124

FIGURE 31. NORTHERN BLOT ANALYSIS OF TOTAL RNA FROM NIH24 CELLS DOES NOT SHOW ANY SPECIFIC SIGNAL OF RNA TRANSCRIPTS AT THE LOCUS UPON CUT. 125

FIGURE 32. SMALL RNA FRACTION IS ENRICHED FOR RNAS BELOW 200NT IN LENGTH AND IT IS DEVOID OF LONGER RNA. 126

FIGURE 33. NORTHERN BLOT ANALYSIS OF SMALL RNA FROM NIH2/4 CELLS DOES NOT IDENTIFY ANY SPECIFIC SIGNAL OF DDRNAS UPON CUT. 127

FIGURE 34. SMALL NUCLEAR RNA PREPARATION FOR NEXT GENERATION SEQUENCING. 128

FIGURE 35. SMALL NUCLEAR RNA FRACTION IS MORE ACTIVE IN RESTORING 53BP1 FOCUS FORMATION COMPARED TO TOTAL RNA IN RNASE-TREATED CELLS. 129

FIGURE 36. DISTRIBUTION OF DDRNA READS ALONG THE LOCUS SEQUENCE. 130

FIGURE 37. DICER AND DROSHA KNOCKDOWN AND I-SCE I CUT CONTROLS. 131

FIGURE 38. DDRNAS ARISING FROM THE LOCUS ARE DICER (AND DROSHA) DEPENDENT AND SHOW A 5' AND 3' BASE BIAS. 133

FIGURE 39. IN VITRO-GENERATED DICER RNA PRODUCTS ARE SUFFICIENT TO RESTORE DDR FOCUS FORMATION IN RNASE-A-TREATED CELLS IN A SEQUENCE-SPECIFIC MANNER. 134

FIGURE 40. SYNTHETIC DDRNAS MAP. 135

FIGURE 41. SYNTHETIC DDRNAS ARE SUFFICIENT TO RESTORE 53BP1 FOCUS FORMATION AFTER RNASE A TREATMENT. 136

FIGURE 42. LNA MAP. 138

FIGURE 43. LNA TRANSFECTION IMPAIRS DDR AT THE LOCUS IN CUT NIH2/4 CELLS. 139

FIGURE 44. AN INDUCIBLE I-SCE I TO STUDY DNA REPAIR IN NIH2/4 CELLS. 140

FIGURE 45. DICER KNOCKDOWN IMPAIRS DNA REPAIR. 141

FIGURE 46. LNA TRANSFECTION IMPAIRS DNA REPAIR AT THE LOCUS IN CUT NIH24 CELLS. 142

FIGURE 47. SYNTHETIC CY5-DDRNAS ARE ABLE TO RESTORE 53BP1 FOCUS FORMATION IN RNASE A-TREATED CELLS AS UNLABELLED ONES. 145

FIGURE 48. CY5-DDRNAS PATTERNS IN THE NUCLEUS OF NIH24 CELLS. 146

FIGURE 49. CY5-DDRNAS LOCALIZE AT THE LOCUS IN RNASE A-TREATED CELLS. 147

FIGURE 50. 3D RECONSTRUCTION OF CY5-DDRNAS AT THE DAMAGED LOCUS. 148

FIGURE 51. CY5-DDRNAS BUT NOT AN UNRELATED CY5-RNA CO-LOCALIZE WITH THE LOCUS. 149

FIGURE 52. CY5-DDRNAS CO-LOCALIZE WITH THE LOCUS MORE IN CUT THEN IN UNCUT RNASE A-TREATED CELLS. 150

FIGURE 53. SYNTHETIC CY5-DDRNAS CO-LOCALIZE WITH THE LOCUS IN MICROINJECTED NIH24 CELLS AT DIFFERENT CONCENTRATIONS. 151

FIGURE 54. LARGER AGGREGATES OF CY5-DDRNAS CO-LOCALIZE WITH THE LOCUS UPON INDUCTION OF DNA DAMAGE. 152

FIGURE 55. DECONVOLVED SYNTHETIC CY5-DDRNAS PAIRS CO-LOCALIZE WITH THE LOCUS. 153

FIGURE 56. DIFFERENCES AND SIMILARITIES BETWEEN DDRNAS, MIRNAS AND DIRNAS. 165

FIGURE 57. A POSSIBLE WORKING MODEL FOR DDRNAS AND DIRNAS IN DDR AND DNA DAMAGE REPAIR. 169

FIGURE 58. TWO HYPOTHETICAL MODELS OF SEQUENCE RECOGNITION BY DDRNAS. 177

**Note about the figures.**

Figures 7, 13, 14, 17, 18, 19, 20b-c, 22, 25, 27, 28a-b, 37a, 38, 39b-c-d and 41 describe the work that has been published, so they are considered as adapted from Francia et al., 2012.

# Abstract

DNA is the most precious molecule in our cells, thus it has to be protected from damage and alterations and, if damaged, it has to be repaired efficiently. The DNA damage response (DDR) is a signaling cascade that follows the generation of a lesion in the DNA double helix and promptly arrests cell proliferation in order to attempt DNA repair. It has been proposed that mammalian genomes are pervasively transcribed, also in non-coding regions. Non-coding RNAs (ncRNAs) have been involved in an increasing number of cellular events and some of them are processed by members of the RNA interference (RNAi) pathway. So far, RNAi and DDR pathways have not been demonstrated to directly interact. During my PhD, I contributed to uncover an unexpected layer of DDR regulation by a new class of DICER- and DROSHA-dependent small non-coding RNA, named DDRNA.

DDR foci stability is sensitive to RNA polymerase II inhibition and to RNase A treatment. Incubation of RNase A-treated cells with DICER- and DROSHA-dependent RNA products restores focal accumulation of DDR factors. DICER and DROSHA are indeed necessary to trigger DDR upon exogenous DNA damage in human cells, and DICER processing activity is necessary to activate DDR. Moreover, DICER and DROSHA knockdown impacts on checkpoint activation and allows senescent cells to re-enter S-phase. Differently, inactivation of GW182, a component of the RNAi machinery involved downstream of DICER and DROSHA in mRNA translational control, does not impact on DDR foci formation and detection. In a mammalian cell system in which a single DNA double-strand break can be generated at a defined exogenous integrated locus, DDR focus formation requires site-specific RNA molecules. RNA deep sequencing confirmed the presence of 22-23-nucleotide sequence-specific transcripts arising from the damaged locus, which are DICER-dependent. These DDR-regulating RNAs (DDRNAs) act at the first steps of the DDR cascade, in an MRN-dependent manner and have an impact also on DNA damage repair. Importantly, DDRNAs, both chemically synthesized or generated *in vitro* by DICER cleavage, are biologically active and antisense LNA oligonucleotides reduce

DDR activation in living cells. Finally, by the use of fluorescently labeled molecules, DDRNAs have been demonstrated to localize at the site-specific damaged locus.

Collectively these results suggest an unanticipated direct role of DICER and DROSHA in the production of small ncRNAs that control DDR activation at sites of DNA damage. Given the known tumor suppressive functions of DDR and the implication of its activation in a number of biological relevant processes, such as senescence, this discovery may have a significant impact on our understanding of ageing and cancer.

# Introduction

# 1. DNA damage and the DNA damage response

## *1.1 Different types of DNA damage*

In the cell, genomic DNA is the most precious molecule that, if damaged, cannot be replaced. Yet, endogenous and exogenous damages to the DNA are events that occur frequently in a living organism and the failure to deal properly with these aberrations can result in mutations, loss of genetic information and tumorigenesis (Jackson and Bartek, 2009).

A major source of genomic alterations is the generation of mismatches and small insertions or deletions during DNA replication (Branzei and Foiani, 2008). In addition, cellular metabolism produces reactive oxygen species (ROS): superoxide anions, hydroxyl radicals and hydrogen peroxide, generated by oxidative respiration, and products of lipid peroxidation may lead to a variety of oxidative modifications of DNA, but also RNA, proteins and lipids (De Bont and van Larebeke, 2004). Spontaneous reactions can cause hydrolysis of nucleotides resulting in abasic sites or deamination of cytosine, adenine, guanine and 5-methylcytosine that are converted to uracil, hypoxanthine, xanthine and thymine, respectively (De Bont and van Larebeke, 2004; Lindahl, 1993).

Exogenous sources of DNA damage include the ultraviolet (UV) component of sunlight, ionizing radiation (IR) such as X-rays and γ-rays from cosmic radiation, medical treatments or radiotherapy, aromatic compounds that intercalate into DNA and various other genotoxic agents (Iliakis et al., 2003; Povirk, 1996; Rastogi et al., 2010). For example, bleomycin is a glycopeptide antibiotic used in cancer therapy, which once chelated to a metal ion, reacts with oxygen to produce superoxide and hydroxide free radicals that directly cleave DNA (Hecht, 2000). Etoposide is an alkaloid derived from a plant toxin that inhibits DNA topoisomerase II, preventing re-ligation of the DNA strands broken during DNA unwinding (Soubeyrand et al., 2010). Crosslinking agents, like mytomicin C, cisplatin and psoralen, but also UV and IR, introduce covalent links between

bases of the same DNA strand (intrastrand crosslinks) or different DNA strands (interstrand crosslinks) (Deans and West, 2011). Physiological events such as meiotic recombination and telomere shortening as well as pathological events such as oncogene activation or viral infections are also dangerous for the DNA (Jackson and Bartek, 2009). Single-strand breaks (SSBs) are discontinuities of the sugar-phosphate backbone in one strand of the DNA double helix and can be caused by ROS, IR or erroneous activity of cellular enzymes such as DNA topoisomerase I (Caldecott, 2008). Double-strand breaks (DSBs) are breakages of the sugar-phosphate backbone in both strands and can be generated by IR, radiomimetic drugs or ROS. DSBs can also arise when a replicative DNA polymerase encounters a DNA single-strand break or other types of lesion causing the so-called "fork collapse" (Branzei and Foiani, 2010; Helleday et al., 2007). Transcription is also known to impair replication progression, and stalled replication forks can lead to genomic instability (Bermejo et al., 2012). Additionally, DSBs can be generated as intermediates of biological events such as class switch and V(D)J recombination in lymphoid cells (Jackson, 2002). DSBs can also occur during the hyper-proliferative phase triggered by oncogene activation, as a result of fork stalling following oncogene-induced replication stress (Di Micco et al., 2007). Among the various lesions, DSBs are particularly dangerous for the cell, since both strands of the DNA are broken: if left unrepaired, they can lead to translocations ultimately resulting into loss of genetic information and/or tumorigenesis (Chapman et al., 2012; Jackson and Bartek, 2009).

### *1.2 The DNA damage response*

Maintenance of genomic integrity and stability is of prime importance for survival of a cell and consequently of an organism. Thus any kind of damage introducing discontinuities in the nuclear DNA double helix elicits a prompt cellular reaction. The DNA damage response (DDR) is a coordinate set of events that follows the generation of a lesion in the DNA double helix. Thanks to this evolutionary-conserved mechanism, cells can promptly

arrest the cell cycle and attempt DNA repair, thus avoiding the dangerous replication of a damaged template (Polo and Jackson, 2011). Until a lesion has not been fully repaired, cell proliferation is normally not resumed.

Powerful activators of the DDR are ruptures of the sugar-phosphate DNA backbone, leading to the generation of DSBs or to the exposure of single-stranded DNA. These two types of lesions are sensed by specialized complexes that recruit and activate two large protein kinases, ataxia telangiectasia mutated (ATM) or ataxia telangiectasia and Rad3-related (ATR), respectively, at the site of the DNA lesion (Figure 1) (Nam and Cortez, 2011; Shiloh and Ziv, 2013). ATM and ATR are members of the phosphatidylinositol 3-kinase-like family of serine/threonine protein kinases (PIK kinases) and phosphorylate their substrates on a serine or threonine followed by glutamine, the S/TQ motif (Bensimon et al., 2010; Langerak and Russell, 2011). The recruitment of either of these apical kinases to the lesion leads the local phosphorylation *in cis* of the histone H2AX at serine 139 (named γH2AX), a key step in the nucleation of the DDR. Indeed γH2AX acts as a recognition mark for the retention of other DDR proteins at sites of DNA damage (Martin et al., 2009). This establishes a positive feedback loop and fuels the spreading of γH2AX along the chromatin up to 1-2 megabases away from the DNA damage site (Iacovoni et al., 2010), generating a molecular 'velcro' that attracts and retains a large number of DDR factors. This results in the formation of cytologically detectable nuclear foci, whose size increases over time, leading to the spreading of the signal from the site of the lesion and the accumulation of multiple copies of DDR factors (d'Adda di Fagagna, 2008; Polo and Jackson, 2011).

Probing damaged cells with antibodies that recognize DDR factors generates a distinctive nuclear pattern of discrete bright foci. As foci detection reveals the number and the position of DNA lesions within a cell, immunocytological staining is generally considered a highly sensitive and informative approach because it allows the detection of even a single

event of damage and therefore gives information on the activation of a cellular response at the single-cell level.

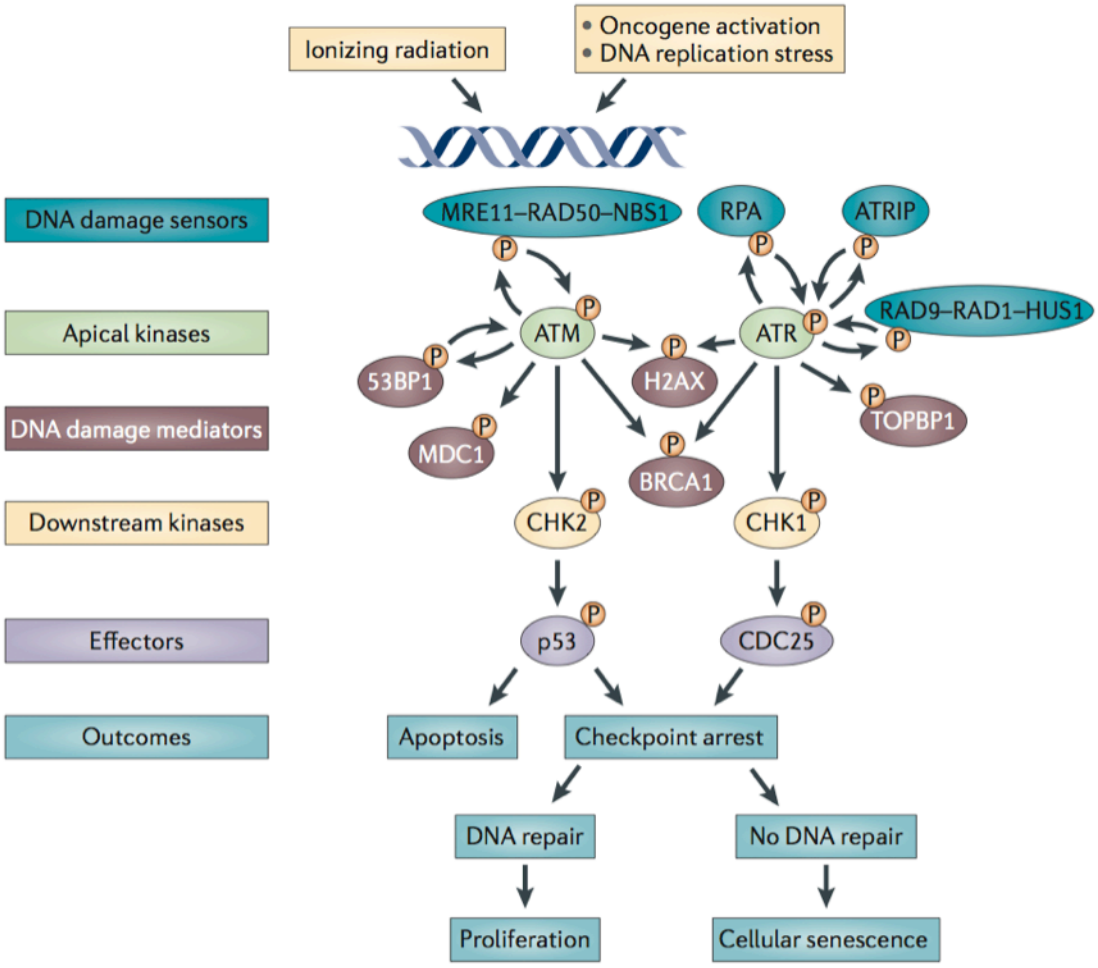


adapted from Sulli et al., 2012

**Figure 1. The DNA damage response pathway.**
DSBs are initially sensed by the MRE11-RAD50-NBS1 (MRN) complex, while ssDNA is recognized by RPA and the RAD9–RAD1–HUS1 (9-1-1) complex. The two different DNA damage sensors recruit the apical kinases ATM and ATR, respectively. ATR is in complex with ATRIP and its kinase activity is further stimulated by TOPBP1. ATM and ATR phosphorylate (P) the histone variant H2AX on Ser139 (known as γH2AX) to recruit other components of the DDR cascade such as MDC1, 53BP1, BRCA1. The diffusible downstream kinases CHK2 (mainly phosphorylated by ATM) and CHK1 (mainly phosphorylated by ATR) spread the signal to the effectors like p53 and CDC25. Depending on the cellular context, the three possible outcomes of DDR activation are cell death by apoptosis, transient cell cycle arrest to attempt DNA repair, or cellular senescence.

### *1.2.1 DNA damage sensors*

To ensure the efficient signaling and repair of DNA damage, DDR proteins must relocate to the right place at the right time, assembling at the site of breaks in a sequential

coordinated manner. Although the DNA damage response is an extensively studied pathway, the precise mechanism by which a cell detects DNA lesions is still under debate.

The recruitment of DDR factors to SSBs is very rapid and transient and involves poly(ADP-ribose) polymerase-1 (PARP-1) and PARP-2, whose binding to DNA breaks triggers poly-(ADP-ribosyl)ation of numerous proteins, a crucial modification that leads to the recognition and subsequent repair of the lesion (Gagne et al., 2006). PARP-1 and PARP-2 activity can be also stimulated by DSBs (Polo and Jackson, 2011).

The accumulation of DDR factors to DSBs has been described as a two-phase process in which the initial recruitment occurs by a direct recognition of the DNA lesion in a γH2AX-independent manner, followed by retention of DDR proteins at the damaged site in a γH2AX-dependent manner (Celeste et al., 2003; Yuan et al., 2010). It appears that in the first step of DNA damage recognition the MRE11-RAD50-NBS1 (MRN) complex plays important roles (Figure 2), together with histone modifications and changes in chromatin environment around the damaged site (Stracker and Petrini, 2011; Yuan and Chen, 2010). RAD50 interacts with MRE11 via its ATPase domains and creates the globular head of the complex that associates with the DSB. Then MRE11 dimerization ensures stable DNA binding, and RAD50 dimerization tethers the two DNA ends together (Kanaar and Wyman, 2008). In addition, MRE11 has 3'-to-5' exonuclease and 5' overhang endonuclease activities, important for the initial steps of DNA end resection and subsequent DNA repair via homologous recombination or HR (Kanaar and Wyman, 2008). NBS1, the third component of the complex, interacts with MRE11 and CtIP (CtBP-interacting protein) and associates with ATM via its C-terminal domain, promoting the recruitment of the kinase to DSBs, where ATM gets activated by the MRN complex via a yet undefined mechanism, possibly involving the formation of ssDNA oligos during DNA end resection (Jazayeri et al., 2008).

DSBs are also recognized by KU70/80 heterodimer, a ring-shaped complex that encloses DNA ends and recruits DNA-PK catalytic subunit (DNA-PKcs), which phosphorylates

itself and other targets initiating the non-homologous end joining (NHEJ) repair pathway (Mahaney et al., 2009). Like ATM and ATR kinases, also DNA-PKcs can phosphorylate H2AX in response to DNA damage (An et al., 2010).

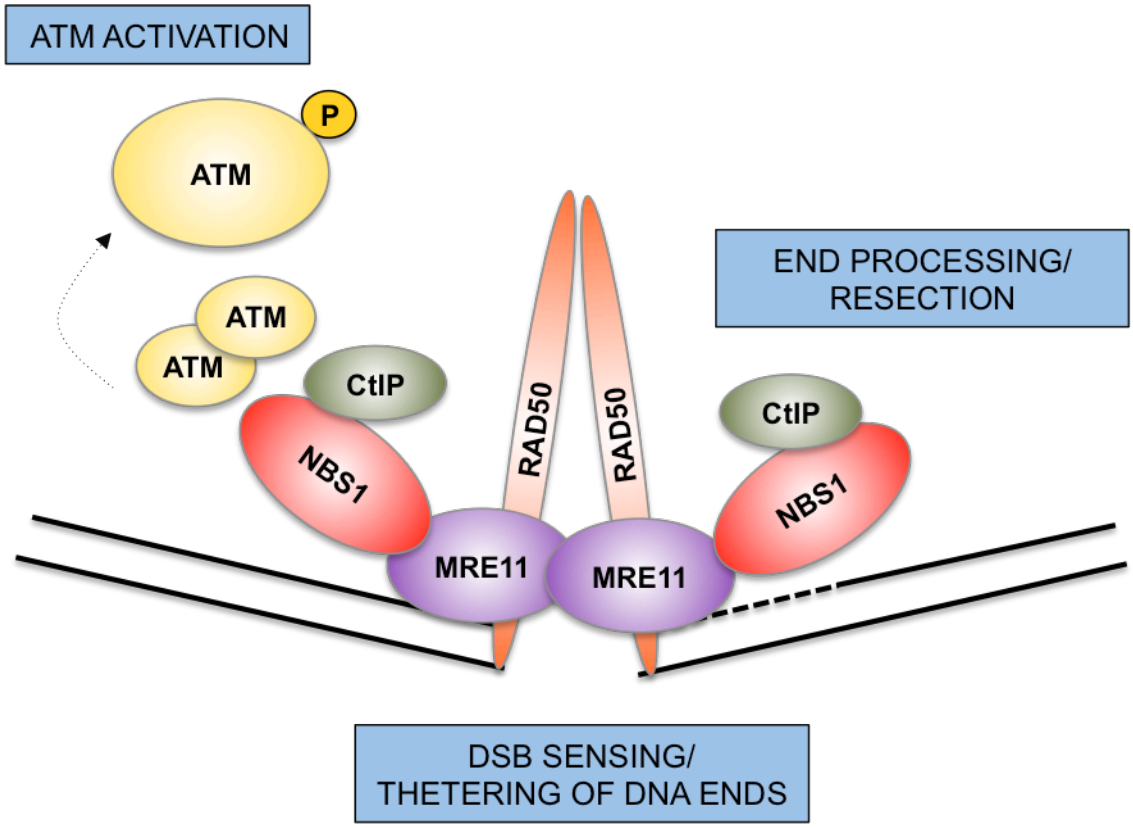


**Figure 2. Multiple functions of the MRN complex.**
RAD50 interacts with MRE11 shaping the globular head of the MRN complex that associates with the DSB. MRE11 dimerization ensures stable DNA binding, and RAD50 dimerization tethers the two DNA ends together. NBS1 interacts with MRE11 and associates with ATM via its C-terminal domain, promoting the recruitment of the kinase to the DSB, where ATM gets activated. The MRN complex, together with CtIP, has also a role in the first step of DNA end processing that leads to resection.

### *1.2.2 DNA damage signaling*

The DDR cascade is dependent on a broad variety of post-translational modifications such as phosphorylation, ubiquitination, sumoylation, poly(ADP-ribosylation), acetylation and

methylation (Ciccia and Elledge, 2010; Jackson and Durocher, 2013; Polo and Jackson, 2011). These modifications are recognized by specific protein domains, mediating the recruitment of DDR factors to the DNA damage sites. Here I will depict some of the main players and their post-translational modifications involved in the DDR cascade.

In the absence of DNA damage, ATM is maintained in an inactive, probably dimeric, structure in which the kinase domain is hidden (Shiloh and Ziv, 2013). Upon DNA damage, by still unclear mechanisms, a conformational change in the ATM protein stimulates the auto-phosphorylation on serine 1981 and ATM becomes an active monomer. However, *in vitro* as well as *in vivo* studies have argued that the auto-phosphorylation may not be required for ATM monomerization and activation (Lee and Paull, 2005; Pellegrini et al., 2006). Monomeric ATM is recruited to DSBs via interaction with the MRN complex, where it phosphorylates many substrates, including H2AX on Ser139 (γH2AX), NBS1 and the DDR mediators like the mediator of DNA damage checkpoint 1 (MDC1), which directly binds γH2AX, p53 binding protein 1 (53BP1) and breast cancer 1 E3 ubiquitin ligase (BRCA1). These phosphorylation events fuel a positive feedback loop facilitating the recruitment of additional ATM molecules to the DSB site (Bekker-Jensen et al., 2005; Stucki et al., 2005). It has been proposed that 53BP1 serves more to amplify ATM signaling than to initiate it: indeed, 53BP1 is known to localize at the DSBs after MRN and MDC1 initial recruitment, promoting progressive MRN-ATM concentration at foci via interaction with RAD50 (Lee et al., 2010).

ATR exists in a complex with the ATR-interacting protein (ATRIP), both before and after exposure to stress such as UV irradiation. Exposure of single-strand DNA, mainly upon DNA ends resection, triggers rapid coating of the DNA filament by replication protein A (RPA), which in turn directs the recruitment of the RAD9-RAD1-HUS1 (9-1-1) complex and ATR kinase via ATRIP. ATR kinase activity is then boosted by the 9-1-1 complex and by topoisomerase II binding protein 1 (TopBP1) (Nam and Cortez, 2011).

Therefore, DSBs such as those generated by IR, primarily activate ATM, while RPA-coated ssDNA triggers ATR activity. However, during S and G2 phases, resection activity at DNA double-stranded ends generates ssDNA, that provides a suitable substrate for ATR activation (Jazayeri et al., 2006).

Increase of local ATM and ATR activity determines phosphorylation of downstream protein kinases CHK2 and CHK1 respectively, although ATM can also phosphorylate CHK1 (Bekker-Jensen et al., 2006; Buscemi et al., 2004; Lukas et al., 2003). Activated CHK1 and CHK2 diffuse in the nucleoplasm, spreading the signal by phosphorylating their substrates throughout the nuclear space.

### *1.2.3 Crosstalk between chromatin and DDR*

It is known that chromatin structure affects DDR signaling around the site of DNA damage (Sulli et al., 2012). For example, heterochromatin appears to be resistant to H2AX phosphorylation and to restrain DDR spreading (Kim et al., 2007). The use of histone deacetylase (HDAC) inhibitors enhances DDR activation by relaxing chromatin compaction (Murga et al., 2007). ATM-dependent phosphorylation of KRAB-associated protein 1 (KAP1) reduces its association with chromatin, allowing DDR repair machinery to access DNA lesions (Goodarzi et al., 2011). In mammals, heterochromatin proteins HP1α, HP1β and HP1γ bind to methylated histone H3 mediating chromatin condensation and senescence-associated heterocromatic foci (SAHF, see Introduction, section 1.4) formation (Sulli et al., 2012). Interestingly, it has been observed that the binding of HP1 proteins to centromeric heterochromatin requires an RNA component (Maison et al., 2002). HP1 proteins have been involved in the modulation of DDR and they localize at the site of damage in a dynamic, and partially contradictory, manner. HP1β is immediately displaced upon damage, promoting H2AX phosphorylation. However, it has been shown that HP1α, HP1β and HP1γ can be instead recruited at the site of break; in particular HP1α is necessary for 53BP1 and RAD50 foci formation (Ayoub et al., 2009; Luijsterburg

et al., 2009; Zarebski et al., 2009). These apparently inconsistent observations can be reconciled considering that HP1 proteins might be immediately displaced from the site of damage and slowly recruited again to the DSB (Sulli et al., 2012).

An increasing number of histone modifications and related enzymes have been observed to play a role in DDR signaling. For example, H2AX is constitutively phosphorylated on Tyr142 in undamaged cells by WSTF (Williams-Beuren syndrome transcription factor). Upon DNA damage, and concurrent with phosphorylation of Ser139, Tyr142 is dephosphorylated by EYA1 and EYA3 phosphatases (Cook et al., 2009). Phosphorylation of H2AX at Tyr142 inhibits the recruitment of MDC1 and DNA repair proteins and promotes the binding of pro-apoptotic factors such as JNK1 (Cook et al., 2009). Thus, the balance of H2AX Tyr142 phosphorylation and dephosphorylation provides a switch mechanism to determine cell fate after DNA damage. Recently, a pathway relying on ubiquitination has been described involving the RNF8/RNF168 E3 ubiquitin ligases (Panier et al., 2012). The ubiquitin ligase RNF8 is recruited to sites of DNA damage via interaction with ATM-phosphorylated MDC1 (Huen et al., 2007; Kolas et al., 2007; Mailand et al., 2007). RNF8-interacting Ubc13 (a E2 ubiquitin conjugating enzyme) modifies histone H2AX, favoring the recruitment of DDR factors at sites of DNA damage. RNF168 is additionally involved in sustaining DDR foci assembly downstream of RNF8 and MDC1 by favouring 53BP1 and BRCA1 foci formation (Al-Hakim et al., 2010). Accumulation of 53BP1 at sites of DNA damage depends on the phosphorylation of H2AX by the ATM/ATR or DNA-PK kinases, binding of MDC1 to γ-H2AX and ubiquitination of histone H2A and H2AX by MDC1-dependent RNF8/RNF168 ubiquitin ligases. 53BP1 does not bind directly to MDC1 or other DDR factors, instead it interacts with histone H4 through an association of its tandem Tudor domain with the dimethylated form of H4 lysine 20 (H4K20Me2). H4K20Me2 is a constitutive modification that has been proposed to become more accessible near the sites of DNA damage, due to ubiquitin-dependent removal of H4K20Me2 binding proteins like Jumonji domain 2 A (JMJD2A) (Mallette et

al., 2012). This explains the dependency of 53BP1 accumulation on γ-H2AX, MDC1 and ubiquitin ligases. An alternative model is suggested by the observation that MDC1-dependent MMSET histone methyltransferase activity is increased at sites of DNA damage, enabling 53BP1 foci formation via de novo histone H4K20 methylation (Pei et al., 2011). Moreover, a recent paper has shown that 53BP1 recognizes histone H2A (and H2AX) when it is ubiquitinated on Lys 15 by RNF168 in response to DNA damage, through its ubiquitination-dependent recruitment (UDR) motif located close to the tandem Tudor domain (Fradet-Turcotte et al., 2013). Thus, the stable accumulation of 53BP1 at sites of DNA damage requires the recognition of two histone modifications, one that is constitutive and one that is DNA-damage inducible.

### *1.3 The DNA damage checkpoints*

In response to DNA damage, cells activate a transient proliferative arrest in order to fix the break before the next cell division. ATM and ATR target the downstream CHK1 and CHK2 kinases, and in turn the cyclin-dependent kinases (CDKs), responsible for progression at key stages of the cell cycle. There are three DNA damage checkpoints: between the G1 and S phases (G1/S checkpoint), within S phase (intra-S phase checkpoint) and between G2 and M phase (G2/M checkpoint) (Branzei and Foiani, 2008; Malumbres and Barbacid, 2009).

*The G1/S checkpoint*. Cell cycle progression is driven by phosphorylation events mediated by CDK4-CyclinD, CDK2-CyclinE, and CDK2-CyclinA complexes that sequentially phosphorylate pRb. These complexes are maintained active through dephosphorylation by CDC25A phosphatase. In the presence of DNA damage, entry into S phase is prevented by the phosphorylation of CDC25A phosphatase by CHK1 and CHK2, resulting in its inactivation by both nuclear exclusion and ubiquitin-mediated proteolytic degradation. The inactivation of CDC25A leads to the inhibition of the cyclinE(A)CDK2 complexes, delaying the G1/S transition for few hours, unless a sustained p53-dependent

mechanism prolongs the arrest. In addition, ATM and ATR directly phosphorylate serine 15 of p53, while the neighboring serine 20 residue is phosphorylated by activated CHK1 and CHK2. Furthermore, the ubiquitin ligase MDM2, that normally binds p53 and ensures its rapid turnover, is targeted by ATM and ATR upon DNA damage. The phosphorylation of p53 and MDM2 inhibits p53 nuclear export and degradation, allowing its protein levels to greatly increase. The accumulated p53 activates its target genes, including the gene encoding the CDK inhibitor p21, which specifically binds to and inhibits the S-phase-promoting CDK2-CyclinE complex, thereby maintaining the G1/S arrest.

*The intra-S-phase checkpoint*. The intra-S-phase checkpoint is activated by stalled replication forks during the S phase or by unrepaired damage that escaped the G1/S checkpoint and causes a reversible inhibition of the firing of those DNA replication origins that have not yet been initiated. It can be triggered either by the ATM/ATR-CHK2/CHK1-CDC25A-CDK2 pathway (very similar to the G1/S checkpoint), or by a second pathway that requires the phosphorylation of the cohesin protein SMC1 by ATM with the aid of BRCA1, FANCD2 and NBS1. Recent work demonstrated the presence of the so-called 53BP1 “nuclear bodies” as marks of DNA fragile sites and DNA lesions that arise during DNA replication stress. 53BP1 nuclear bodies are inherited by the daughter cell, shielding these regions of unrepaired damage into nuclear compartments that might enable repair before the subsequent S phase (Lukas et al., 2011).

*The G2/M checkpoint.* The G2/M checkpoint prevents cells from entering into mitosis when they experience DNA damage during G2, or when they progress into G2 with unrepaired lesions inflicted during the previous S or G1 phases. ATM and ATR, through phosphorylation of CHK2 and CHK1, inhibit the progression to mitosis by down-regulating CDC25A and up-regulating Wee1, controlling CDC2/Cyclin B1 activity. 53BP1 and BRCA1 are also involved in the regulation of the G2-checkpoint responses.

If the DNA lesion cannot be repaired, persistent DDR activation may induce cell death by apoptosis or a permanent cell cycle arrest called cellular senescence.

*1.4 DNA damage induced senescence*

Cellular senescence is a condition initially described by Hayflick as a permanent loss of proliferative capacity, despite viability and metabolic activity of the cell (Hayflick and Moorhead, 1961). It is characterized by growth arrest, changes in cell morphology, increase of senescence-associated-β-galactosidase (SA-β-gal) activity, appearance of senescence-associated heterochromatin foci (SAHFs), senescence-associated DNA damage foci (SDFs) and senescent-associated secretory phenotype (SASP) (d'Adda di Fagagna, 2008). Cellular senescence can occur in response to different types of stresses like dysfunctional telomeres, DNA damage, and oncogene activation (d'Adda di Fagagna et al., 2003; Di Micco et al., 2006; Herbig et al., 2004). A unifying concept that possibly reconciles all the different types of senescence has been recently proposed by our group: cellular senescence is triggered by persistent DDR at special genomic regions that, once damaged, cannot be repaired: the telomeres (Fumagalli et al., 2012).

Following the activation of an oncogene, checkpoint-proficient cells undergo a specific type of senescence called oncogene-induced senescence (OIS). OIS has been considered a natural barrier against tumorigenesis and it is now appreciated that OIS occurs *in vivo* and contributes to tumour suppression by preventing the expansion of oncogene-expressing cells (Evan and d'Adda di Fagagna, 2009; Jackson and Bartek, 2009). The activation of DDR pathways is causally involved in the establishment of OIS, and although it is still a matter of intense investigation, both altered DNA replication (Bartkova et al., 2006; Di Micco et al., 2006) and oxidative stress (Ogrunc and d'Adda di Fagagna, 2011) have been proposed to be the mechanisms responsible for the activation of DDR signaling following oncogene activation.

*1.5 The DNA repair pathways*

Unrepaired lesions may lead to genomic instability and chromosomal aberrations. Therefore, multiple repair pathways have evolved to maintain the continuity and integrity of the genome. Modified bases, such as products of spontaneous hydrolysis, alkylation and oxidative lesions, are repaired by base excision repair (BER) throughout the cell cycle (Wilson and Bohr, 2007). Nucleotide excision repair (NER) (Gillet and Scharer, 2006) plays an important role during G1 phase to remove bulky lesions, such as those caused by UV irradiation and chemicals. Mismatch repair (MMR) (Li, 2008) is fundamental during replication to remove mismatches, small insertion or deletion loops, which are generated by faulty replication. BER, NER and MMR share a similar repair procedure that includes lesion recognition and excision. The strand containing the lesion is cleaved to remove 1-2 nucleotides in BER, 12-30 nucleotides in NER or hundreds nucleotides in MMR. New DNA is synthesized to replace the removed nucleotides and the single-strand nick is sealed (Altieri et al., 2008).

There are two major pathways to repair DSBs by either homology-dependent or independent mechanisms: the homologous recombination (HR) and the non-homologous end joining (NHEJ) (Figure 3) (Chapman et al., 2012; Helleday et al., 2007).

The HR is an error-free mechanism that requires a homologous template, usually a sister chromatid, which allows accurate repair of post-replicative DSBs during S and G2 phases of the cell cycle (Karpenshif and Bernstein, 2012). In contrast, NHEJ is active throughout the entire cell cycle, but is the only mode of repair during G0, G1 and early S phase when sister chromatids are unavailable. Although highly efficient, its very simple mechanism of basic re-ligation, without proof-reading, makes NHEJ prone to mutations (Lieber, 2010).

An important regulatory step that determines the choice between the two main DSB repair pathways is the resection of the DNA ends, that is required for HR but not for NHEJ. Resection of the DSB in the 5'-to-3' direction is initiated by the MRN complex, together with the auxiliary protein CtIP, the helicase BLM and the exonuclease EXO1. RPA then

coats the growing 3'-ended single-stranded overhang, before being substituted by the RAD51 recombinase, which mediates homology search and DNA strand invasion. Subsequently, a DNA polymerase extends the 3' terminus of the damaged molecule, DNA ligation takes place and RECQ helicases, such as the BLM and WRN proteins, resolve the HR intermediates, like the Holliday junctions, to obtain two intact DNA molecules (Chapman et al., 2012).

In NHEJ, the DNA ends are first recognized by KU70/80 heterodimeric complex, followed by recruitment of DNA-PK catalytic subunit (DNA-PKcs) that phosphorylates itself and other targets, among which the nuclease ARTEMIS. DNA ligase IV, in association with its binding partners XRCC4 and XRCC4-like factor (XLF), finally ligates the DNA ends. It has been proposed that 53BP1 inhibits DSB resection through RIF1 (Zimmermann et al., 2013), promoting NHEJ by increasing the stability and mobility of DSBs to find each other (Difilippantonio et al., 2008; Dimitrova et al., 2008).

In the absence of protein machinery involved in classical NHEJ, another pathway can contribute to DSB repair, the so-called alternative NHEJ, also known as microhomology-mediated end joining (MMEJ), because it exploits microhomology regions during joining (McVey and Lee, 2008; Nussenzweig and Nussenzweig, 2007; Wang et al., 2003). The mechanisms of alternative NHEJ are not fully understood, however DNA ligase III, XRCC1 and PARP-1 seem to play a major role, whereas KU inhibits it and promotes the canonical NHEJ (Fattah et al., 2010).

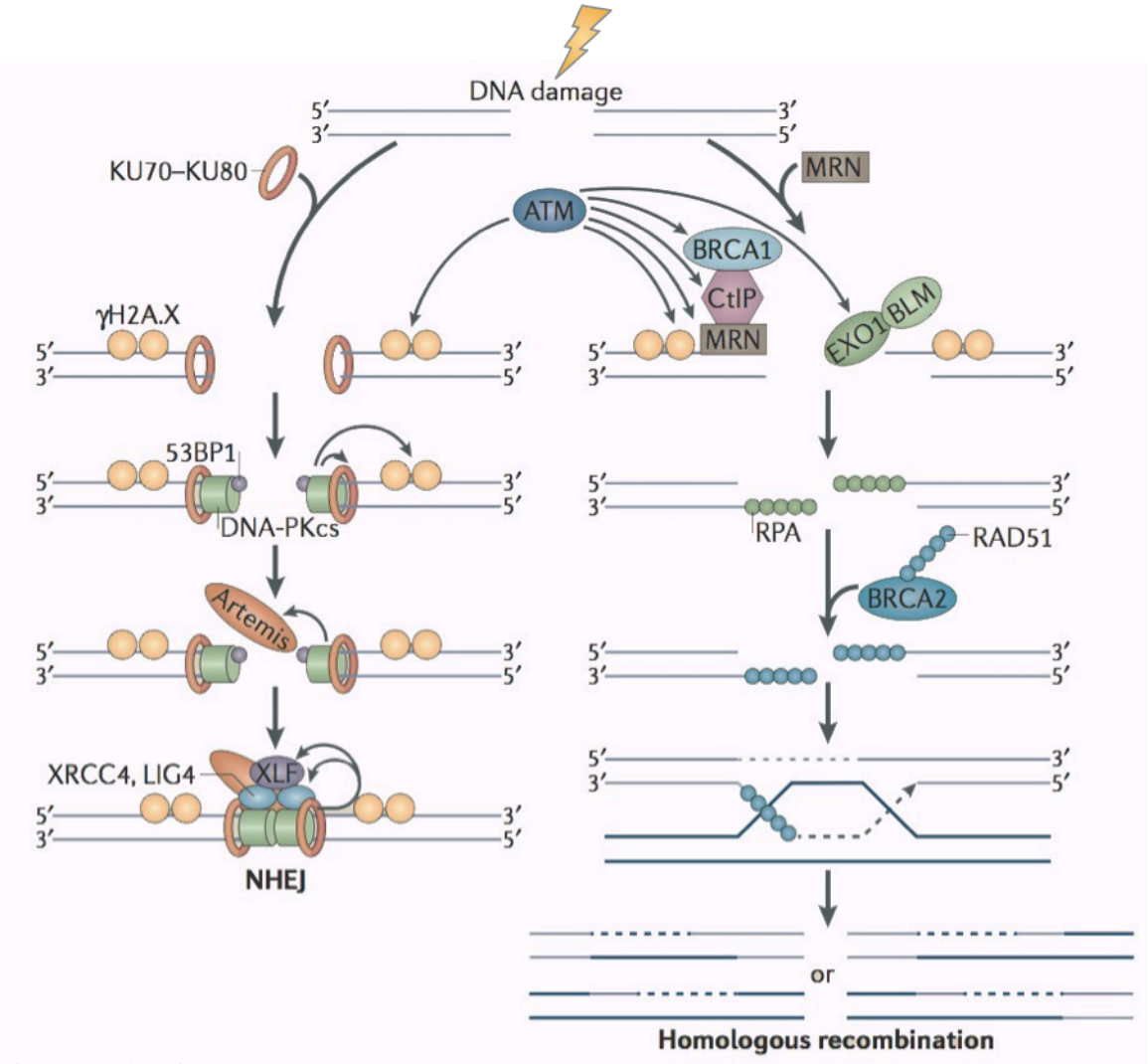


adapted from Chowdhury et al., 2013

**Figure 3. The DNA damage repair pathways.**

In the first steps of NHEJ, the KU70/80 heterodimer is loaded onto DSB ends and recruits the catalytic subunit of DNA-PK (DNA-PKcs) and 53BP1. ATM-mediated phosphorylation of histone H2AX (γH2AX) and the recruitment of 53BP1 protect DSB ends from being resected. DNA-PKcs regulates the stability of DSB ends through phosphorylation of Artemis and other substrates. Artemis facilitates end processing and, subsequently, DNA ligase IV (LIG4), XRCC4 and XLF ligate the broken ends to complete repair.

HR begins with the DNA lesions being recognized by the MRN complex and the activation of the apical kinases ATM and ATR that rapidly phosphorylate multiple DNA repair factors including H2AX, CtIP, BRCA1 and EXO1. HR pathway needs DNA end resection, which is mediated by MRE11 together with CtIP and EXO1 in the presence of BRCA1 and BLM helicase. The single-stranded DNA generated by resection is rapidly coated by RPA and subsequently replaced by RAD51 in the presence of BRCA2. RAD51 mediates invasion of the sister chromatid to search for homology. The invading strand is extended by DNA polymerase and then ligated. The final product of the homologous recombination-mediated repair is then determined by the resolution of Holliday junctions.

The choice between these two pathways is determined by the DNA end resection, required for HR but not for NHEJ, and by the cell cycle phase.

*1.6 Defects in DNA repair and checkpoint pathways*

The importance of the DDR signaling and DNA repair is indicated by the broad spectrum of defects displayed by individuals carrying mutations in DDR genes, primarily affecting the nervous, immune and reproductive systems but also leading to premature aging and cancer (Jackson and Bartek, 2009). For example, mutations in the *ATM* gene results in the inherited syndrome ataxia-telangiectasia (A-T), a rare human disease characterized by ataxia (dysfunction in movement coordination by the nervous system), telangiectasia (dilated blood vessels), immune defects, increased sensitivity towards IR, and cancer predisposition (Shiloh and Ziv, 2013). In patients with A-T-like disorders, mutations in the *MRE11* gene were identified, consistent with the described role of MRE11 in activating ATM (Biton et al., 2008). Mutations in the *NBS1* gene cause the Nijmegen breakage syndrome (NBS), whose main symptoms (microcephaly, growth retardation and "bird-like" face) are different from the A-T phenotypes, reflecting the complex functions of MRN (Ciccia and Elledge, 2010). Disruption of both alleles of ATR causes embryonic lethality in mice. However, hypomorphic mutations in ATR cause the Seckel syndrome in humans, characterized by growth retardation, dwarfism, microcephaly and mental retardation (Kerzendorfer and O'Driscoll, 2009). The human syndrome called RIDDLE (Radiosensitivity, Immunodeficiency, Dysmorphic features and LEarning difficulties) is due to the inability to recruit 53BP1 to sites of damage (Stewart et al., 2007), caused by mutations in the RNF168 gene (Stewart et al., 2009). Haploinsufficiency for H2AX results in detectable genomic instability and enhanced tumor susceptibility in the absence of p53 (Celeste et al., 2003). Homozygous loss of CHK1 is lethal, whereas heterozygosity impacts mildly on tumorigenesis (Liu et al., 2000). Lack of CHK2 enhances skin tumorigenesis induced by carcinogen exposure and increases tumour susceptibility in mouse models in combination with mutations in other genes like BRCA1, NBS1 and MRE11 (Cao et al., 2006; Hirao et al., 2002; McPherson et al., 2004; Stracker et al., 2008). The inheritance of a single mutated allele of either BRCA1 or BRCA2 markedly increases the incidence of

breast and ovarian cancers in women (O'Donovan and Livingston, 2010). A broad spectrum of malignancies is displayed by the DDR disorders Bloom syndrome and Li-Fraumeni syndrome, caused by mutations in *BLM* or *TP53* genes respectively (Ciccia and Elledge, 2010). Accumulation of DNA damage can also lead to many different progeroid syndromes in humans, as for example the Cockayne syndrome, which is associated with defects in NER pathway, and the Werner syndrome in WRN helicase-deficient patients, or it can lead to accelerated aging phenotypes in mouse models defective for DDR components (Ciccia and Elledge, 2010).

Given the elevated levels of DNA damage in cancer cells (Bartek et al., 2007), it has been proposed that inhibiting DDR components in combination with chemotherapeutic drugs could lead to the selective death of cancerous cells. Indeed, ATM, DNA-PK and CHK1 inhibitors show preferential toxicity towards cancer cells following treatment with genotoxic agents (Bolderson et al., 2009). Moreover, PARP-1 inhibitors have been successfully used to treat tumors with mutations in BRCA1 and BRCA2 genes (Ciccia and Elledge, 2010; Jackson and Bartek, 2009). Thus, elucidating the molecular mechanisms through which DDR pathways operate will provide novel therapeutic opportunities for cancer and many other human diseases.

# 2. The RNA world

## *2.1 Different RNAs from different RNA polymerases*

Over four decades ago, biochemical studies identified three multi-subunit RNA polymerase (RNA pol) enzyme complexes, RNA pol I, II, and III, transcribing the eukaryotic genome. The differential sensitivity of the enzymes to the mushroom toxin α-amanitin revealed that the polymerases synthesize different classes of cellular RNA. RNA pol I synthesizes the 47S ribosomal RNA (rRNA) precursor, that is subsequently cleaved into 18S, 5.8S, and 28S RNA molecules of the ribosome in eukaryotes; RNA pol II is responsible for the synthesis of protein-coding messenger RNA (mRNA), but also non-coding RNA such as most small nuclear RNA (snRNA) and microRNA (miRNA); RNA pol III synthesizes transfer RNA (tRNA), 5S rRNA but also U6 spliceosomal RNA, several small nucleolar RNAs (snoRNAs), regulatory ncRNA such as 7SK RNA, short interspersed elements (SINE) like Alu elements, and a subset of miRNAs (Bensaude, 2011; Borchert et al., 2006; Vannini and Cramer, 2012).

RNA pol II holoenzyme, the most studied RNA polymerase, is composed of 12 subunits and additional factors important for transcription initiation, elongation, and termination (Shandilya and Roberts, 2012). The template DNA is "read" in the 3'-to-5' direction during transcription and the complementary RNA is polymerized from the 5' to the 3' end. Transcription initiation begins with the formation of a closed promoter complex, which contains DNA, the 10 subunits of RNA pol II core, the RNA pol II sub-complex Rpb4/7, and the transcription factors TFIID (which includes the TATA-box binding protein TBP and TBP-associated factors), TFIIB, TFIIE, TFIIF, and TFIIH. DNA strands are then separated to form the transcription "bubble", allowing RNA synthesis to initiate from the transcription start site. The initially transcribing complex is unstable and releases short RNAs during abortive initiation (Margeat et al., 2006). When the RNA reaches a critical length (10-12 nucleotides), initiation factors are released, and a stable elongation complex

is formed. During this early elongation step, the transcript can be extended up to around 60 nucleotides, till RNA pol II pauses; escape from this pause into productive elongation is highly regulated (Kwak and Lis, 2013). Elongation can also transiently pause at certain DNA sequences (Landick, 2006), backtrack and arrest (Cheung and Cramer, 2011) when encounters a DNA lesion in the template strand (Damsma and Cramer, 2009) or in the presence of misincorporated non-complementary nucleotides (Sydow and Cramer, 2009). It has been proposed that the RNA/DNA helicase Sen1 in *Saccharomyces cerevisiae* would be relevant to protect genome integrity from DNA damage, resulting from the collision between transcription and replication proceeding from opposite directions. Sen1 association with DNA replication forks is crucial to protect fork integrity across RNA polymerase II-transcribed genes (Alzu et al., 2012). A similar role in preventing replication-transcription conflicts was proposed for the human ortholog Senataxin (Yuce and West, 2013). Elongation factors are required to reactivate an arrested elongation complex by stimulating RNA cleavage and RNA pol II processivity. The carboxy-terminal domain of RNA pol II (CTD) is a long flexible tail subjected to a number of post-translational modifications and involved in the regulation of the activity, initiation of transcription, capping of the RNA transcript, and attachment of spliceosome components. CTD can be highly phosphorylated, mainly at serine 2 (S2) and serine 5 (S5) residues. S5 phosphorylation marks the initiation complex, since it occurs in promoter-proximal regions, and leads to recruitment of the capping enzyme. S2 phosphorylation instead is a mark of elongating RNA pol II and predominates in regions that are more distal from the promoter, triggering the binding of the 3'-RNA processing machinery (Hsin and Manley, 2012).

The other two RNA polymerases, RNA pol I and RNA pol III, share many subunits with the RNA pol II holoenzyme but contain additional factors that are not present, although related to parts of the RNA pol II complex (Vannini and Cramer, 2012; White, 2011).

*2.2 The RNA "dark matter"*

Current estimates indicate that only about 2% of the mammalian genome codes for proteins (Kapranov and St Laurent, 2012). However, thanks to high-resolution new technologies in the field of RNA sequencing, mounting evidence over the past decade has suggested that the vast majority of the genome is transcribed, also in regions previously thought to be silent, a phenomenon known as "pervasive transcription" (Birney et al., 2007; Clark et al., 2011; Kapranov and St Laurent, 2012). Formerly annotated as junk or selfish DNA, this non-coding portion of the genome is now starting to become biologically relevant and it has been proposed to be the source of evolutional and developmental complexity (Dinger et al., 2009; Mattick, 2003).

Consistent with the idea of pervasive transcription, RNA polymerase II can be found at almost any genomic location, such as intergenic regions or heterochromatin domains in *Saccharomyces cerevisiae* (Steinmetz et al., 2006), and at previously not annotated regions of the human genome (Kim et al., 2005).

The definition of RNA "dark matter" includes not only non-protein coding RNA, but any RNA molecule whose function is not yet fully understood such as transcripts arising from intronic and intergenic regions, transcripts arising from known genes either in the same orientation (sense) or in opposite orientation (antisense) to the coding transcript, excised introns, alternative exons, non-protein coding isoforms of known transcripts, repetitive regions like retrotrasposons, long intergenic non-coding RNA, small non-coding RNA, products of the cleavage of protein coding messenger RNA and so on (Berretta and Morillon, 2009; Kapranov and St Laurent, 2012). Some of these transcripts can have very low abundance in RNA preparations from a cell population or a tissue, but probably this low abundance is the result of developmental-specific, tissue-specific or even cell-specific and stimuli-dependent expression of these transcripts rather than their actual concentration within the cell (Carninci et al., 2005; Kapranov and St Laurent, 2012). Otherwise the expression of these transcripts can be masked by an active RNA degradation, as in the case

of XUTs (Xrn1-sensitive unstable transcripts) in *Saccharomyces cerevisiae* (van Dijk et al., 2011). XUTs are constantly degraded by the cytoplasmic RNA decay machinery and become detectable only when the exonuclease Xrn1 is absent.

Although the functions of these transcripts are largely unknown, it is likely that they play an active role in different biological processes. For example, an increasing number of observations correlate the aberrant expression of non-coding RNAs with diseases like cancer and neurological disorders (Askarian-Amiri et al., 2011; Gupta et al., 2010; Kapranov and St Laurent, 2012; Karreth et al., 2011; Khaitan et al., 2011; Tay et al., 2011). Moreover, an association of "dark matter" transcripts, emerging from a family of repetitive regions, with a particular type of pancreatic cancer has been recently provided (Clark et al., 2011).

### *2.3 Non-coding RNA*

Non-coding RNAs (ncRNAs) are defined as RNA species that do not have protein coding potential. Several distinct classes of ncRNAs, some newly identified, have been discovered to play important regulatory roles in diverse cellular processes, among which transcriptional and post-transcriptional gene silencing, splicing, chromatin regulation, X inactivation, dosage compensation, imprinting, genome surveillance and Polycomb-mediated chromatin remodeling (Farazi et al., 2008). Except for ncRNAs as ribosomal RNA, small nuclear RNAs, small nucleolar RNAs and transfer RNA, the remaining ncRNAs can be divided, based on their length, into long non-coding RNAs and small non-coding RNAs (typically below 200 nucleotide in length). The latter can be further classified as miRNAs, siRNAs, repeat associated small interfering RNAs (rasiRNAs) and PIWI-interacting RNAs (piRNAs) (Castel and Martienssen, 2013; Krol et al., 2010).

Long non-coding RNA (lncRNAs) have been shown to play functional roles in a number of diverse biological processes, ranging from cell cycle control and pluripotency to differentiation and epigenetic regulation both *in cis* and *in trans* (Rinn and Chang, 2012).

The molecular mechanism by which lncRNAs exert their function is poorly understood, but it is known that they can associate with proteins and act as guides, scaffold, decoys or signal for the correct function of these proteins on the chromatin and the genome (Rinn and Chang, 2012).

For example, in the process of X-chromosome inactivation, the 17 Kb long non-coding X-inactivation specific transcript (XIST) recruits the Polycomb repressive complex to silence the X-chromosome from which it is transcribed. From the same region, an antisense lncRNA called TSIX is generated to repress *in cis* the expression of XIST (Deuve and Avner, 2011). Polycomb proteins are a family of chromatin remodeling factors that transcriptionally repress genes by favoring the formation of closed chromatin structures. Also the long intergenic non-coding RNA (lincRNA) HOTAIR, which originates from the HOXC locus, represses transcription of the HOXD locus *in trans*, by recruiting Polycomb complex and altering the chromatin state (Spitale et al., 2011). Moreover, a number of studies identify lncRNAs with enhancer like functions, arising from genomic regions previously classified as enhancers or from other intergenic regions, in a stimulus-dependent manner, regulating the neighboring protein-coding genes mainly through changes in the three-dimensional chromosome architecture (Orom and Shiekhattar, 2013).

Despite their heterochromatic structure, telomeres from yeast to humans are transcribed into telomeric repeat-containing RNA called TERRA (Azzalin et al., 2007; Schoeftner and Blasco, 2008). TERRAs are transcribed by RNA polymerase II starting from promoters located in the sub-telomeric regions through the telomeric repeats, they are polyadenylated, contain the G-rich telomeric sequence and are heterogeneous in size, ranging from around 0.1 to 9 Kb. The physiological functions of TERRA have not been completely elucidated yet, but some evidences suggest that they are involved in telomere end protection. They can also negatively regulate telomere length, in fact it has been shown that long telomeres inhibit TERRA expression by promoting heterochromatin formation (Arnoult et al., 2012; Flynn et al., 2011).

Small ncRNAs have many different biological functions such as translation and transcription regulation, transposon repression, DNA methylation and chromatin remodelling. miRNAs and siRNAs belong to the most studied class of small ncRNAs, they are 20-23 nucleotide in length and mediate the post-transcriptional control of gene expression. miRNAs are produced by the sequential cleavages by the two ribonucleases DROSHA and DICER and associate with Argonaute proteins (AGO) to exert their function (for a more detailed description of miRNA, siRNA and RNA interference see Introduction, section 3.2). PIWI-interacting RNAs (piRNAs) form RNA-protein complexes through interactions with PIWI (P-element induced wimpy testis) proteins, which are a clade of the Argonaute family of proteins. piRNA have been linked to both epigenetic and post-transcriptional gene silencing of retrotransposons and other genetic elements in germ line cells, particularly in spermatogenesis. They are distinct from miRNAs in size (26–31 nucleotides), lack of sequence conservation, and increased complexity (Siomi et al., 2011). Among different species (from *Drosophila* to mammals) they share a 5' monophosphate and a 2'-O-methylation at the 3' end; the reason for this modification by HEN1 methyltransferase is not clear, but it has been suggested to increase piRNA stability and to be important for piRNA recognition by PIWI proteins (Ji and Chen, 2012). The biogenesis of piRNAs also has not been well elucidated yet, but it appears to be different from the biogenesis of miRNAs, being DICER-independent. It has been proposed a 'ping pong' mechanism according to which the piRNA precursor from the so-called "piRNA cluster" is cleaved by the nuclease Zucchini and then somehow processed to generate the primary mature sense piRNA, which guides PIWI clade proteins to complementary sequence on the antisense transcript from the same piRNA cluster. This causes the cleavage and trimming of the transcript, resulting in the production of a mature antisense secondary piRNA, which can now target sense transcripts transcribed from the piRNA cluster (Meister, 2013; Siomi et al., 2011).

Repeat associated small interfering RNAs (rasiRNAs) were identified by cloning small RNA libraries from *Drosophila melanogaster* and *Danio rerio* (Zebrafish) (Aravin et al., 2003; Chen et al., 2005), but they have not been observed in mammals. Given their association with the PIWI protein family, they are also known as piRNAs. In fact in the germline, rasiRNAs are involved in establishing and maintaining heterochromatin structure, controlling transcripts that emerge from repeat sequences, and silencing transposons and retrotransposons.

In the fission yeast *Schizosaccharomyces pombe* DICER-independent primal small RNAs (priRNAs) are derived from sense and antisense transcripts of heterochromatin-associated repeats. priRNAs associate with Argonaute 1 and target complementary RNA transcripts initiating the amplification of small interfering RNAs, thus promoting heterochromatin formation and silencing of the repeats (Halic and Moazed, 2010). In euchromatic DNA, priRNAs are believed to have a different function, namely RNA surveillance, binding primarily to the 3' UTRs of mRNAs and possibly suppressing the read-through of antisense transcripts. Moreover, in mouse embryonic stem cells a positive correlation has been found between the heterochromatin status at telomeres and the level of telomere specific small RNAs (tel-sRNAs), that are different from TERRA and are DICER-independent (Cao et al., 2009).

### *2.4 Non-coding RNA in human diseases*

The crucial importance of ncRNAs has become increasingly apparent, since dysregulation of ncRNA homeostasis has been associated to cancer and other human diseases such as neurological, cardiovascular, autoimmune and developmental disorders (Esteller, 2011). LncRNA, snoRNA, but especially miRNA expression has been found altered in cancer (for miRNA and cancer see Introduction, section 3.4). For example, the lincRNA HOTAIR is increasingly transcribed in transformed cells and is involved in retargeting Polycomb proteins across the genome (Gupta et al., 2010). Strikingly, piRNAs have been found to be

aberrantly expressed in human somatic tumors, suggesting that the PIWI pathway can have other important functions outside the germline tissue (Cheng et al., 2011). Apart from cancer, disruption of miRNA biogenesis has been shown to cause hallmarks of many neurological disorders, like multiple sclerosis and Alzheimer's disease (Esteller, 2011). A lncRNA targeting the β-secretase 1 mRNA has been characterized to increase the production of β-amyloid peptide in Alzheimer's disease (Esteller, 2011).

The increasing awareness of the crucial function of ncRNAs in human physiology, and consequently diseases, will bring about the production of new therapeutic approaches targeting expression, stability and function of ncRNAs in the very near future (Esteller, 2011).

# 3. RNA interference

## *3.1 The discovery of RNA interference*

The idea that RNA is not just a copy of a DNA gene but can also have regulatory roles is not new and originates in the earliest days of molecular biology, when it was proposed that sequence-specific non-coding RNA might interact with gene's promoters (Jacob and Monod, 1961). Nowadays, after forty years of studies, our understanding of RNA functions and complexity has undergone a sort of revolution. A turning point in this field was achieved with the discovery of RNA interference (RNAi). It all started with a test for the efficacy of messenger-RNA downregulation by an antisense RNA in *Caenorhabditis elegans*. Sense RNA was a necessary negative control in that experiment but, unexpectedly, antisense and sense RNAs both caused silencing of the targeted gene with a comparable extent (Guo and Kemphues, 1995). What might have been considered a failed experiment, built the foundation of a new field in gene expression regulation. Few years later, it was proposed that the *in vitro* transcribed RNA preparations used by Guo et al. in their studies were not purely single-stranded RNA and that contaminating dsRNA might have been the key trigger of target gene silencing. Indeed, dsRNA was a much more potent silencing trigger than either strand alone (Fire et al., 1998). This silencing mechanism mediated by dsRNA has been subsequently found in other eukaryotes from the fission yeast *Schizosaccharomyces pombe* (but not the budding yeast *Saccharomyces cerevisiae*) to mammals (Hannon, 2002). Named RNAi for its ability to interfere with protein expression at the mRNA level, it has been used in science for over two decades as a tool to understand gene function.

*3.2 miRNA, siRNA and the RNAi pathway*

miRNAs are the most abundant class of small RNAs in animals. They play important roles in almost every cellular process investigated, from cell fate determination, proliferation and cell-death to immune response, gene expression, circadian rhythms, and cancer (Krol et al., 2010; Sayed and Abdellatif, 2011).

The biogenesis of miRNAs begins with the synthesis of a long transcript known as a pri-miRNA, generally transcribed by RNA polymerase II, with mRNA features such as 5'cap structure and 3'poly(A) tail (Figure 4). However, other pathways generate a minor set of miRNAs. For example, RNA polymerase III is responsible for transcription of miRNAs from Alu repeats (Borchert et al., 2006). An alternative miRNA biogenesis mechanism relies on intronic miRNAs, named mirtrons, generated as a result of splicing and debranching of very short introns, thereby bypassing the DROSHA step (see below) (Berezikov et al., 2007). pri-miRNAs fold into a hairpin structure becoming suitable substrates for the RNase III enzyme DROSHA. The microprocessor complex, formed by DROSHA together with the double-stranded-RNA-binding protein DGCR8 (DiGeorge syndrome critical region 8), cleaves the precursor transcript into a 70-nucleotide pre-miRNA. The pre-miRNA is actively transported to the cytoplasm in a GTP-dependent manner by an export protein complex containing a Ran GTPase and a dsRNA-binding export receptor, such as mammalian Exportin 5 (XPO5) (Kohler and Hurt, 2007). In the cytoplasm, the pre-miRNA is further processed by another RNase III enzyme called DICER, together with its partner TRBP (transactivation-responsive RNA binding protein), to form the mature double-stranded miRNA with a 2-nucleotide 3' overhang. DICER-TRBP complex has not only a role in miRNA processing but it is also a platform for the RNA-induced silencing complex (RISC) assembly (Krol et al., 2010). Mature miRNAs are on average 20 to 23 nucleotides in length and usually have a uridine at their 5' end, a feature that is likely determined by the structure of the 5' binding pocket of Argonaute proteins (Frank et al., 2012). Moreover, both DROSHA and DICER enzymes generate 5′

ends that contain a monophosphate (5' monophosphate), important for the binding by specific positively charged pockets in DICER and AGO2 (Frank et al., 2010; Kawamata et al., 2011; Park et al., 2011). The so-called 'guide strand' of the duplex is the one whose 5' end is less thermodynamically stable and is favored for incorporation into the miRNA-induced silencing complex, miRISC (Krol et al., 2010). The specific helicase that separates the two strands is still unknown, even if DDX5 RNA helicase is known to unwind human Let-7 miRNA duplex precursor and to be required for Let-7-directed silencing of gene expression (Salzman et al., 2007). The other strand, referred to as miRNA* (the so-called 'passenger strand'), is generally degraded, but can also be loaded into the RISC complex (Krol et al., 2010).

The main components of RISC are Argonaute proteins, the direct binding partners of small RNAs. The eukaryotic Argonaute family can be divided into AGO proteins, which are similar to *Arabidopsis thaliana* Ago1, and PIWI proteins, which are homologous to *Drosophila melanogaster* Piwi. The PIWI domain, present in all Argonaute proteins, is structurally similar to RNase H. Indeed it has been shown that Argonaute proteins can function as endonucleases and cleave target RNA that is fully complementary to the bound small RNA. In mammals, there are four AGO proteins, but only AGO2 is catalytically active and functions as an endonuclease (Meister, 2013). Direct interactors of AGO are the GW182 (glycine–tryptophan proteins of 182 KDa) family members, required for the efficient assembly and function of the miRISC. When the miRNA finds its target, miRISC can induce translational repression or deadenylation and degradation of the mRNA (Krol et al., 2010). Efficient mRNA targeting requires base-pairing of nucleotides 2 to 8 at the 5' end of the miRNA, the so-called 'seed region'. Many miRNAs are represented as families that are defined by the conservation of the seed region. In general, if a perfectly matched target RNA sequence is present, AGO2 can induce target cleavage. miRISC with a greater degree of mismatches, instead, inhibits translation and/or triggers the transport of the mRNA to the mRNA-processing bodies (P-bodies). Components of the RNAi machinery

localize to the P-bodies, including members of the AGO/PIWI family, RNA helicases, mRNA translation repression and mRNA decay machinery proteins, mRNA decapping proteins, translational repressors, deadenylase complexes and RNA-binding proteins (Eulalio et al., 2007). Surprisingly, in some cases, miRNAs may also activate, instead of repress, the translation of target mRNA in cells arrested in the G0/G1 stage (Vasudevan et al., 2007). Recently, miRNA activity has been shown to be affected by the presence of miRNA sponges, in mouse and in human, harbouring several binding sites for specific miRNAs. These sponges can be either linear transcripts, the so-called "competing endogenous RNA" (ceRNA) (Karreth et al., 2011; Tay et al., 2011) or circular RNA (circRNA) (Hansen et al., 2013; Memczak et al., 2013).

siRNAs are double-stranded RNA molecules, 20-25 base pairs in length, known to interfere with the expression of specific genes with complementary nucleotide sequence. siRNAs can be produced from RNA transcribed in the nucleus (endogenous siRNAs), or can be virally derived or experimentally introduced as chemically synthesized dsRNA (exogenous siRNAs). Endogenous siRNAs have been described in plants and in *C. elegans*. They can originate from overlapping sense and antisense transcripts (Borsani et al., 2005), or from repeat-associated genomic regions (Buker et al., 2007). So far, endogenous siRNAs have not been identified in mammals. In cultured mammalian cells, siRNAs have been successfully used to analyze gene function.

siRNA are unwound and loaded into RISC, where they guide the siRISC complex to a perfectly complementary target mRNA. AGO2 then cleaves a single site within the target mRNA which is consequently degraded (Carthew and Sontheimer, 2009). In *C. elegans* and plants, secondary siRNAs participate in a signal amplification loop (Pak and Fire, 2007). The cleaved mRNA is converted into dsRNA by RNA-dependent RNA polymerases (RdRP) and it is further processed by DICER. Secondary siRNAs associate with AGO/PIWI protein members, leading to other target mRNA cleavage (Pak and Fire, 2007).

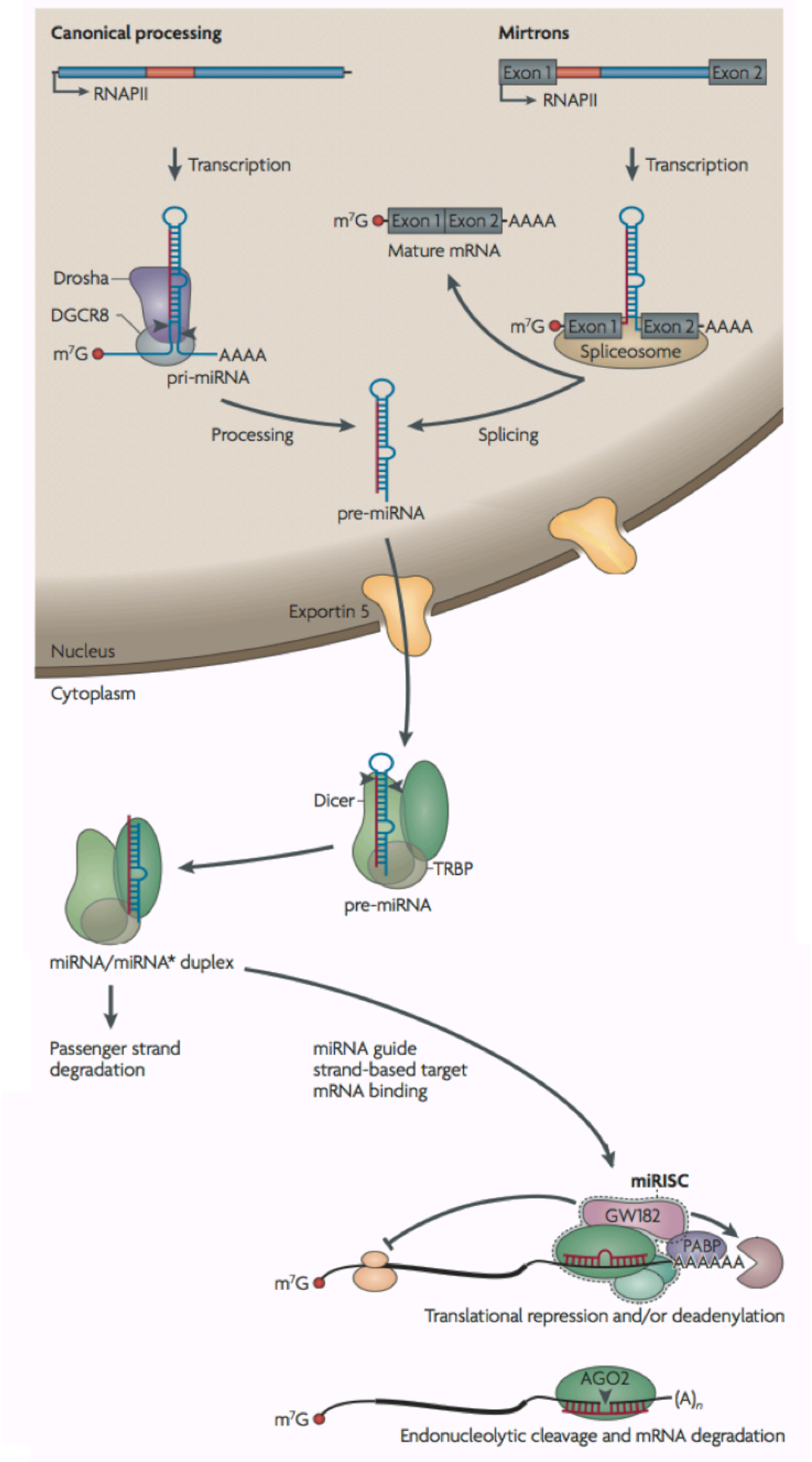


adapted from Krol et al., 2010

**Figure 4. Biogenesis and function of miRNA.**
In the canonical pathway for miRNA biogenesis, RNA polymerase II-dependent, capped, primary precursor (pri-miRNA) is first processed by DROSHA/DGCR8 complex in the nucleus into an ~70-nucleotide precursor hairpin (pre-miRNA), which is exported to the cytoplasm via Exportin 5. Some pre-miRNAs are produced from very short introns (mirtrons) as a result of splicing and debranching, thereby bypassing the DROSHA–DGCR8 step. In the cytoplasm, cleavage by DICER, together with TRBP, results in a ~20 bp miRNA/miRNA* duplex. Due to thermodynamic features, just one strand of the miRNA/miRNA* duplex (the guide strand or miRNA) is preferentially incorporated into the miRNA-induced silencing complex (miRISC), whereas the other strand (passenger or miRNA*) is released and generally degraded. In some cases miRNA* can also be loaded into miRISC to function as miRNA. The miRISC complex is mainly composed by Argonaute proteins bound to miRNA and GW182 (glycine-tryptophan protein of 182 kDa) proteins, important for the silencing function of the miRISC. In mammals, Argonaute 2 (AGO2) is the only Argonaute protein that possesses an endonuclease activity. miRISC binds to the correct mRNA via miRNA-target complementarity, determining either target translational repression and deadenylation (in case of imperfect complementarity) or target cleavage (in case of perfect complementarity).

Endogenous siRNAs and RNAi are thought to play an important role in defending genomes against transposable elements, as well as foreign nucleic acids, such as viruses. The random integration of new DNA or the rearrangement of existing sequences, for example by transposons, might trigger the formation of dsRNA.

Human siRISC and miRISC are thought to localize and function in the cytoplasm, where the mature mRNA is translated. However, in human cells RNAi has been demonstrated to mediate repression of target RNAs also in the nucleus (Castel and Martienssen, 2013). In plants, nuclear-localized DICER is responsible for pri-miRNA processing to miRNA (Vazquez, 2006).

### *3.3 DROSHA and DICER*

DROSHA and DICER are members of the RNase III family of nucleases that specifically cleave double-stranded RNAs and are evolutionarily conserved in plants, fungi, worms, flies and mammals. DROSHA is responsible to convert pri-miRNAs into pre-miRNAs, which are ~70 nucleotide stem–loop structures. DROSHA acts as a component of a complex named the microprocessor. This nuclear complex, that possesses a robust pri-miRNA processing activity, is minimally composed of two proteins: the dsRNA-binding protein DGCR8/Pasha and DROSHA. DROSHA and DGCR8 are known to regulate each

other's function and mRNA levels, in order to maintain a balance that may be important for the cell (Krol et al., 2010). A second, larger complex containing DROSHA and multiple accessory proteins is also present in the nucleus, but its function is still unknown. The accessory proteins include the RNA binding proteins Ewing sarcoma breakpoint region 1 (EWSR1), Fused in sarcoma (FUS), numerous heterogeneous nuclear ribonucleoproteins (hnRNPs) and the DEAD-box helicases DDX5 and DDX17 (Ameres and Zamore, 2013; Newman and Hammond, 2010).

DICER is a large (200 KDa) multi-domain protein including two RNase III motifs, an RNA helicase domain, a double-stranded RNA binding domain (dsRBD) and a PAZ domain, responsible for dsRNA end recognition (Jaskiewicz and Filipowicz, 2008). The helicase domain has an autoregulatory function, likely disrupting the functionality of the DICER active site until a structural rearrangement occurs, perhaps upon assembly with its molecular partners (Ma et al., 2008). It has been proposed that the two RNase III domains associate with each other to form an 'internal dimer' and that the distance between the PAZ domain and the catalytic active site closely matches miRNA length, acting as molecular ruler (MacRae et al., 2007). Interestingly, it has been shown that proteolysis can modulate DICER activity (Lugli et al., 2005; Zhang et al., 2002) or even converting its specificity towards DNA, as it was observed for *Caenorhabditis elegans* Dcr-1, which has a role in DNA fragmentation during apoptosis (Nakagawa et al., 2010). Although recombinant DICER is active *in vitro*, it generally functions in association with other proteins *in vivo*. In mammalian cells, DICER associates with its partner TRBP (TARBP-2 in human cells) that stimulates DICER activity. Decrease of TRBP levels leads to DICER destabilization and defects in pre-miRNA processing (Krol et al., 2010).

In invertebrates such as *A. thaliana*, *S. pombe*, *D. melanogaster* and *C. elegans* DICER, in addition to its cytoplasmic function, has been shown to localize in the nucleus and to have a role in epigenetic regulation through RNA-directed DNA methylation, in heterochromatin formation and in RNA polymerase II positioning at promoters and

transcription (Cernilogar et al., 2011; Lejeune et al., 2010). Moreover, recent work in *S. pombe* demonstrated that fission yeast DICER is a shuttling protein between cytosol and nucleus and that the C-terminal dsRDB is responsible for its nuclear retention (Barraud et al., 2011; Emmerth et al., 2010). Increasing evidence supporting the possibility that also mammalian DICER can transiently translocate and function in the nucleus emerged recently. For example, DICER has been found associated with ribosomal DNA in mammalian cells (Sinkkonen et al., 2010), probably to preserve the stability of the repetitive rDNA locus. Using advanced microscopy technologies DICER can be detected in the nucleus of mammalian cells (Ohrt et al., 2012). Furthermore, a recent study proposed that mammalian DICER is involved in the transcriptional silencing of genes expressing convergent transcripts in the nucleus (Gullerova and Proudfoot, 2012). Finally, it has been demonstrated that the dsRBD domain of human DICER functions as non-canonical nuclear localization signal and that human DICER is a shuttling protein, whose steady state localization resides in the cytoplasm (Doyle et al., 2013).

DICER activity is strictly required for life and it is essential for development of healthy organisms. In fact, DICER-deficient mice die very early in development, around embryonic day 7.5, with a complete loss of pluripotent stem cells (Bernstein et al., 2003). Indeed DICER is required for proliferation and differentiation of ES cells (Kanellopoulou et al., 2005), spermatogenesis and female germline lineage maintenance (Murchison et al., 2007; Papaioannou et al., 2009), cardiac functionality (da Costa Martins et al., 2008), skeletal muscles development (O'Rourke et al., 2007), angiogenesis (Suarez et al., 2008), brain functionality (Davis et al., 2008), cell survival in B lymphocyte (Koralov et al., 2008) and morphogenesis of hair follicles (Andl et al., 2006).

### *3.4 miRNA in cancer and diseases*

miRNAs can act as oncogenes or tumor suppressors and they can have key functions in tumorigenesis. One of the best-characterized example is the case of miR-200 family

alteration involved in epithelial-to-mesenchimal transition (EMT), a key step towards malignancy and metastatization. Silencing of miR-200 locus in human tumours causes up-regulation of ZEB1 and ZEB2 transcriptional repressor which, in turn, leads to the down-regulation of E-cadherin, promoting EMT (Davalos et al., 2012). Other miRNAs have been found to be deregulated in leukaemias, colon, ovarian and breast cancers and melanomas (Esteller, 2011). However, the miRNA expression profile of human tumours is generally characterized by a defect in miRNA production that results in global miRNA reduction (Carninci et al., 2005). In fact, alterations in the RNAi machinery factors such as TARBP2 (Melo et al., 2009), DICER1 (Hill et al., 2009) and XPO5 (Melo et al., 2010) has been reported to be tumour-specific defects, contributing to explain the global miRNA dysregulation in cancer.

Aberrant miRNA signatures have been observed also in other diseases such as neurodegenerative, inflammatory and cardiovascular disorders (Esteller, 2011).

Given their importance in human cancer and many other diseases, miRNAs and components of RNAi machinery have become targets of novel therapeutic approaches. Taking advantage of miRNA base-pair complementarity mechanism of action, antisense oligonucleotide (ASO) strategies have been developed. The main classes of ASOs are locked nucleic acids (LNAs), which are modified (an extra bridge connects the 2' oxygen and 4' carbon) DNA oligonucleotides, anti-miRNA oligonucleotides (AMOs) and antagomirs, which harbor different chemical modifications to increase stability and efficacy. The efficacy of AMOs has been demonstrated in different cases, both in mouse and humans (Stenvang et al., 2012). Excitingly, Miravirsen from Santaris Pharma, an LNA targeting a specific miRNA required for the replication of hepatitis C virus, has now successfully passed phase 2 of a clinical trial for the treatment of hepatitis C (Janssen et al., 2013).

# 4. DDR and RNA

## *4.1 DDR and RNA transcription*

The interplay between transcription and DDR has been intensely studied by several groups, but the debate remains open and controversial.

It has been shown that the transcription by elongating RNA polymerase II of a reporter gene is repressed *in cis* by ATM-dependent regulation of chromatin condensation in response to a cluster of DSBs upstream of the reporter (Shanbhag et al., 2010). Consistently, MDC1 has been described to play a role in silencing of sex chromosomes during meiosis (Ichijima et al., 2011) and the repressive complexes Polycomb and NuRD have been found at the sites of breakage in a PARP1-dependent manner (Chou et al., 2010). The recruitment of Polycomb proteins at the DSBs and the histone methylation associated to Polycomb activity have been reported by several other groups (Hong et al., 2008; O'Hagan et al., 2011; Seiler et al., 2011; Sustackova et al., 2012), however Polycomb role in RNA polymerase II transcriptional arrest was not investigated. Immunofluorescence studies have shown that RNA polymerase II, both in the initiating and the elongating forms, is depleted from the sites of microirradiation (Beli et al., 2012; Miller et al., 2010). Moreover, it has been observed that the E3 ubiquitin ligase BRCA1 interacts with elongating RNA pol II via BRCA1 associated RING protein 1 (BARD1) (Bennett et al., 2008; Starita et al., 2005) and ubiquitinates the largest RNA pol II subunit, triggering its degradation upon UV exposure (Kleiman et al., 2005). Additionally, transcription of rDNA locus by RNA polymerase I is inhibited by the ATM-NBS1-MDC1 pathway and by coilin, the Cajal body marker protein, in response to DNA damage (Gilder et al., 2011; Kruhlak et al., 2007). However, a recent work using a cell system in which discrete DSBs can be induced at individual endogenous loci indicated that a break does not affect the transcription of adjacent genes, but inhibits it only if occurring within a transcriptional unit and in a DNA-PK-dependent manner (Pankotai et al., 2012). Upon

DNA-PKcs inhibition, RNA pol II is able to bypass the break and to continue transcription elongation (Pankotai et al., 2012). Supporting the observation that a break next to a gene may not reduce transcription, it has been found that DNA-damage induced γH2AX spreading is discontinuous and "holes" have been observed in actively transcribing, RNA pol II-enriched, regions inside the γH2AX domains (Iacovoni et al., 2010). In particular, cohesin has been proposed to be an insulator of γH2AX spreading along the active genes (Caron et al., 2012). Similarly, in yeast, transcription is inhibited only when a DSB occurs within a gene, but no change of expression was observed for genes surrounding the DSB, where γH2AX was present (Kim et al., 2007).

### *4.2 DDR proteins and RNA*

There are scattered observations suggesting an interaction of specific RNA molecules with DDR components. It has been shown that KU impacts both telomere-length maintenance and DNA repair, by binding the RNA component of telomerase in *Saccharomyces cerevisiae* (Stellwagen et al., 2003). The same direct interaction has been found also in human cells (Ting et al., 2005). In addition, the human telomerase RNA seems to restrain ATR activity and participates in the recovery of cells from UV (Kedde et al., 2006). Moreover, it has been shown recently that treating cells with RNase A increases the detection of KU and other DNA repair proteins at DSBs, suggesting that a large fraction of these factors is bound to chromatin via RNA (Britton et al., 2013).

53BP1, a protein mediator of the DDR, contains two Tudor domains (Charier et al., 2004), that are usually found in RNA-binding proteins. In fact, it has been observed that 53BP1 can be immunoprecipitated with RNA molecules (the snoRNAs U1 and U2, the RNase MRP RNA and the signal recognition particle RNA 7SL) and that RNase A treatment dissociates 53BP1 from IR-induced foci (Pryde et al., 2005). Moreover, 53BP1 foci re-assembly can be triggered by re-addition of nuclear RNA in RNase A treated, irradiated

HeLa cells (Pryde et al., 2005). These results suggest a possible involvement of RNA in the binding of 53BP1 to damaged chromatin. Another DDR protein, BRCA1, associates with XIST and is involved in the X chromosome inactivation process (Ganesan et al., 2002).

The list of factors that participate to maintain genome integrity has expanded, starting to include many proteins involved in RNA binding and processing. For example, the RNA binding protein FUS has been demonstrated to localize at the site of laser-induced DNA damage, in a PARP-dependent but ATM-independent manner, and to be critical for DNA repair (Mastrocola et al., 2013). Defects in FUS recruitment to DNA lesions has been associated and may contribute to Amyotrophic lateral sclerosis (Rulten et al., 2013). Like FUS, also the RNA binding protein NONO binds to the poly(ADP-ribose) (PAR) chains and it is recruited to the site of DNA lesions, stimulating NHEJ and repressing HR (Krietsch et al., 2012). High-throughput approaches, such as genome-wide siRNA-based or mass-spectrometry-based screenings, revealed the involvement of splicing-regulating proteins like RBMX (Adamson et al., 2012), or PPM1G and THRAP3 (Beli et al., 2012), respectively in DNA damage response and repair. The ribonucleoprotein RBMX is recruited at the site of breakage dependently on PARP-1 and facilitates BRCA2 expression (Adamson et al., 2012). While the phosphatase PPM1G localize at the damaged sites, both THRAP3 and elongating RNA polymerase II are excluded (Beli et al., 2012). Finally heterogeneous nuclear ribonucleoprotein U-like (hnRNPUL) proteins 1 and 2 are engaged at the site of DSB, following MRN and CtIP binding to DNA ends, and contribute to resection stimulating BLM recruitment (Polo et al., 2012).

### *4.3 DDR and miRNA*

There are many observations of interplay between the RNAi machinery, miRNA and DDR (Figure 5) (Chowdhury et al., 2013). ATM plays an essential role in regulating miRNA expression through several mechanisms (Wang and Taniguchi, 2013). One way is the

ATM-dependent phosphorylation of KH-type splicing regulatory protein (KSRP) (Zhang et al., 2011), a protein that interacts with both DROSHA and DICER stimulating the maturation of a subset of miRNAs (Trabucchi et al., 2009). ATM phosphorylation of KSRP increases its interaction with pri-miRNAs and its processing activity (Zhang et al., 2011). Another mechanism of ATM-mediated miRNA regulation is through its downstream target p53, acting both at transcriptional and post-transcriptional levels. For example, p53 promotes the expression of miR-34 family that regulates the G1/S and the S checkpoints, in a DNA damage dependent manner (He et al., 2007); p53 also interacts with DDX5 RNA helicase stimulating the processing of a class of miRNAs (Suzuki et al., 2009) and, in turn, DDX5 is required for the p53-induced transcription of the cell cycle regulator p21 and growth arrest upon DNA damage (Nicol et al., 2013). ATM phosphorylation of Delta Np63alpha, a splice variant of the p53-homolog called p63, alters the transcription of some miRNAs and up-regulates DICER expression, stimulating miRNA processing after cisplatin treatment (Huang et al., 2013b). Recently it has been shown that ATM controls also pre-miRNA nuclear export upon DNA damage, by phosphorylating Nup153, a component of the nucleopore, and increasing its interaction with Exportin 5 (Wan et al., 2013).

The MAPK ERK is also phosphorylated after DNA damage and, in turn, it phosphorylates TRBP, stabilizing the TRBP–DICER complex to promote pre-miRNA processing (Paroo et al., 2009). Moreover, it has been shown that BRCA1 facilitates the processing of some miRNAs via its direct interaction with DROSHA, DDX5 and pri-miRNAs (Kawai and Amano, 2012), and that also DNA-PKcs and ATR can modulate the cellular miRNome upon DNA damage (Wang and Taniguchi, 2013).

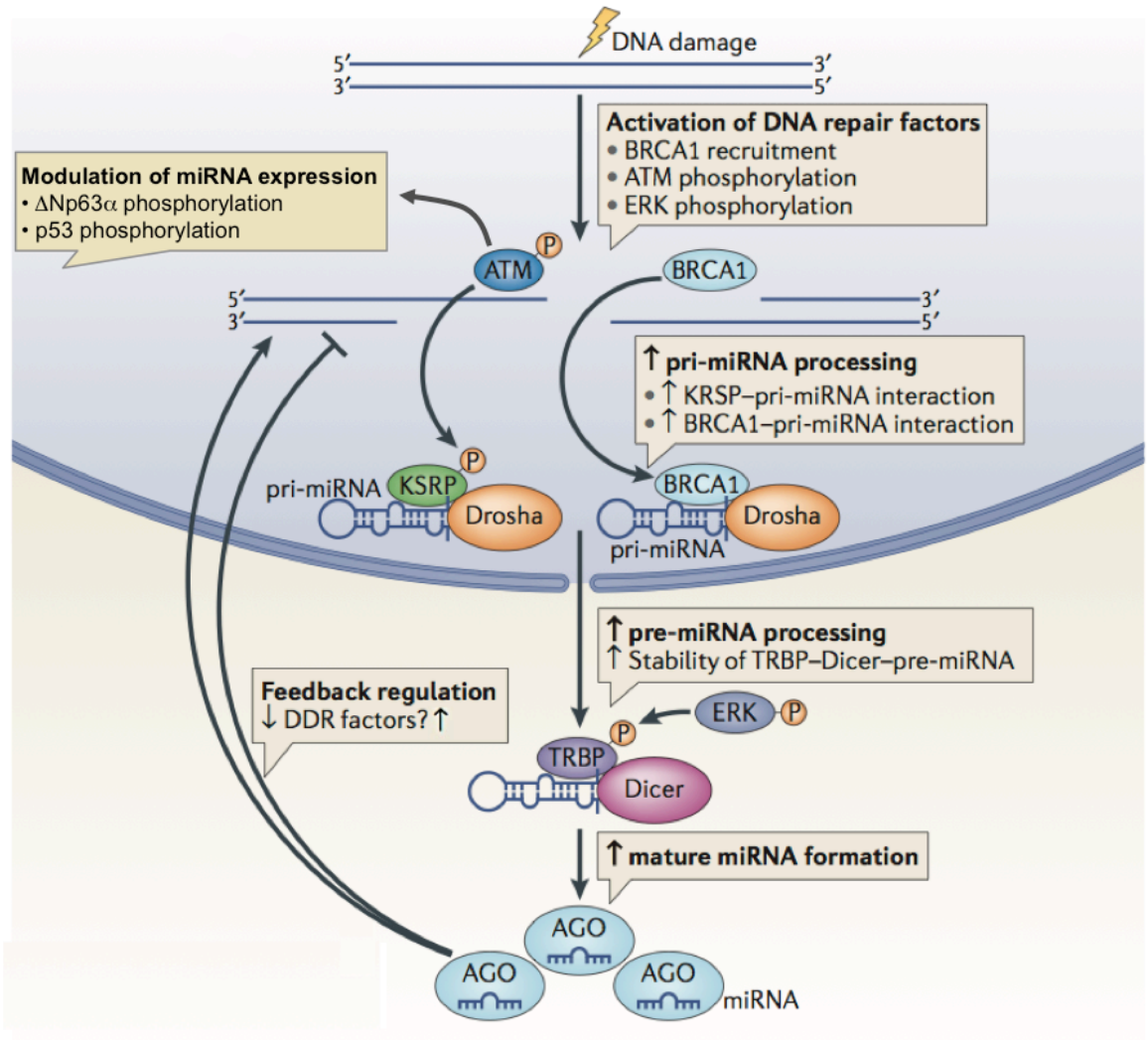


adapted from Chowdhury et al., 2013

**Figure 5. Interplay between DDR and miRNA.**

DNA damage response and miRNA biogenesis have been recently connected. ATM-dependent phosphorylation of the splicing factor KSRP – a protein that interacts both with DROSHA and with DICER – enhances its interaction with primary miRNAs (pri-miRNAs) and stimulates DROSHA processing. ATM phosphorylation of p53 and ΔNp63alpha, a splice variant of the p53-homolog called p63, alters the transcription of some miRNAs. BRCA1 directly interacts with both pri-miRNAs and DROSHA complex, facilitating pri-miRNA processing by the DROSHA complex. The MAPK ERK is phosphorylated after DNA damage and in turn it phosphorylates TRBP, stabilizing the TRBP–DICER complex to promote pre-miRNA processing in the cytoplasm. Increased levels of mature miRNAs might affect the DNA damage response (DDR) protein levels. For example, miR-421, miR-100 and miR-101 suppress ATM expression; miR-24 and miR-138 directly target histone H2AX; miR-355 reduces CtIP expression; DNA-PKcs is another target of miR-101; BRCA1 is under the control of miR-182 and miR-146a/b; miR-96 suppresses RAD51 expression and RPA is repressed by CU1276, a particular miRNA derived from a tRNA.

While DDR proteins appear to regulate miRNAs, miRNAs in turn can influence the expression of key DDR factors. For example, miR-421, miR-100 and miR-101 suppress ATM expression; miR-24 and miR-138 directly target histone H2AX; DNA-PKcs is another target of miR-101; BRCA1 is under the control of miR-182 and miR-146a/b; miR-96 suppresses RAD51 expression and RPA is repressed by CU1276, a particular miRNA derived from a tRNA (Sharma and Misteli, 2013). Recently, it has been shown that ATM-dependent expression of miR-355 reduces CtIP expression, thus influencing the DSB repair pathway choice (Martin et al., 2013). Loss of miRNA biogenesis, by DICER inactivation, induces p19Arf-p53 signaling, DNA damage and premature senescence in primary cells (Mudhasani et al., 2008). Moreover, in human cells it has been observed that knockdown of DICER by siRNA elicits DNA damage and ATR/CHK1 checkpoint pathway activation (Tang et al., 2008).

### *4.4 DDR and lncRNA*

The first lncRNA discovered to be induced in response to DDR is a low copy number, RNA pol II regulated, polyadenylated, uncapped transcript, generated upstream of the cyclin D1 (CCND1) promoter (Wang et al., 2008). Upon DNA damage, this transcript binds to the RNA-binding protein TLS (translated in liposarcoma), which inhibits the histone acetyltransferases, resulting in CCND1 silencing *in cis*. There are several lncRNAs induced by p53 upon DNA damage. Among them lincRNAp21, located 15 Kb upstream of the cell cycle regulator p21, binds to the transcription and RNA-processing factor hnRNP-K and this interaction is required for the proper silencing of p53-repressed genes, *in trans* (Huarte et al., 2010). Another p53-dependent lncRNA named PANDA (p21 associated ncRNA DNA damage activated) is located 5 Kb upstream of p21 and interacts with the transcription factor NF-YA to limit apoptosis, while p21 induces cell cycle arrest upon DNA damage (Hung et al., 2011).

*4.5 Non-canonical small RNA in DDR and DNA repair*

miRNAs modulate DDR through an indirect mechanism, for example by targeting the mRNA of DDR factors. However, recent studies suggest a direct involvement of non-canonical small ncRNAs in the modulation of DDR and DNA repair events.

In the yeast *Saccharomyces cerevisiae* RNA was shown to mediate homologous recombination (Derr and Strathern, 1993). Moreover, pairing between broken DNA ends and complementary single-stranded RNA occurs *in vitro* and RNA can serve as a template for DNA synthesis during repair of a chromosomal DSB in fission yeast (Storici et al., 2007). In the protozoa *Tetrahymena*, the development of the somatic macronucleus from germ micronucleus involves chromosome rearrangements that lead to the elimination of specific sequences, among which repetitive elements with transposon features. This DNA elimination requires an Argonaute homolog and the presence of small 28-nucleotide RNAs, complementary to the regions that are lost (Mochizuki et al., 2002). A similar mechanism has just been discovered for the Argonaute protein of *Rhodobacter sphaeroides* (RsAgo). RsAgo has been found associated with small RNAs but also with complementary small DNA molecules, mainly derived from exogenous sequences like plasmids, transposons and phage genes, suggesting that RNA works as a guide to destroy foreign DNA (Olovnikov et al., 2013).

Recently, it has been shown in *Arabidopsis thaliana* and in human cells that small RNAs of 21-24 nucleotides in length, named DSB-induced RNAs (diRNAs), are involved in DNA repair by HR (Wei et al., 2012). diRNAs are induced in an ATR-dependent manner upon DNA damage and are transcribed by plant RNA polymerase IV from sites in the immediate vicinity of the DSB. Their biogenesis involves RNA-dependent RNA polymerases and components of the RNAi machinery, such as Dicer-like proteins and Ago2. In human cells, diRNAs are generated from sense and antisense strands in the region surrounding the DSB and appear to regulate DNA repair in a DICER- and AGO2-dependent manner. In *Drosophila* endogenous small interfering RNAs (endo-RNAs) are

produced from a transfected linearized plasmid, mimicking DNA ends. These small RNAs require Dcr-2 and are able to silence transcription of homologous DNA sequences *in trans* (Michalik et al., 2012). Finally, in *Neurospora crassa* small RNAs termed qiRNAs are transcribed from the rDNA locus in response to DNA damage (Lee et al., 2009). Although the mechanism of action of these RNAs is not clear yet, depletion of proteins involved in their biogenesis increases the sensitivity to DNA damage.

Thus, induction of small RNAs upon DNA damage seems to be conserved among species, still their possible roles in DNA damage activation and DNA repair events remain to be fully understood.

# Materials and Methods

## Cell culture

HeLa (The American Type Culture Collection, ATCC), HEK293T (ATCC) and NIH3T3 (ATCC) cell lines were grown under standard tissue culture conditions (37°C, 5% $CO_2$) in DMEM, supplemented with 10% fetal bovine serum, 1% L-glutamine, 1% penicillin/streptomycin. Early-passage WI-38 cells (ATCC) were grown under standard tissue culture conditions (37°C, 5% CO2) in MEM supplemented with 10% fetal bovine serum, 1% L-glutamine, 1% non-essential aminoacids, 1% Na pyruvate. Adeno-293 (Stratagene) cells were grown in DMEM, supplemented with 10% fetal bovine serum and 1% L-glutamine. $DICER^{exon5}$ colon cancer cell lines (Cummins et al., 2006) were cultured in Mc'Coy 5A medium supplemented with 10% fetal calf serum, 1% penicillin/streptomycin. H-RasV12 overexpressing senescent BJ cells were generated as in (Di Micco et al., 2006).

NIH2/4 cells (Soutoglou et al., 2007) where grown in DMEM, supplemented with 10% fetal bovine serum, 1% L-glutamine, 1% penicillin/streptomycin, and hygromycin (400 μg/ml). NIH2/4 are a NIH3T3-derived cell line co-transfected with the Lac-I-SceI-Tet plasmid together with a vector containing the resistance to hygromycin.

## Ionizing radiation (IR)

Ionizing radiation (IR) at different doses was used to generate acute DNA damage exogenously. IR refers to highly energetic particles or waves that can detach (ionize) at least one electron from an atom or molecule. IR-induced lesions include base damage, SSBs, DSBs and DNA cross-links. DNA damage can be generated directly by IR or as secondary hits by free radical species. Examples of IR are energetic beta particles, neutrons, alpha particles, X- and gamma-rays. X-rays are photons (electromagnetic radiations) emitted from electron orbits, such as when an excited orbital electron "falls" back to a lower energy orbit. The Gray (Gy) is the International System of Units of

absorbed radiation dose, where 1 Gy is the absorption of 1 joule of radiation energy by 1 kilogram of matter. Ionizing radiation was induced by a high-voltage X-rays generator tube (Faxitron X-Ray Corporation). HeLa and DICER$^{exon5}$ cells were exposed to 2Gy for the DDR foci formation studies, and 5Gy were used for the G2/M checkpoint assays.

## Plasmid transfection

Cells were plated into 6 multi-well plates so that they were at around 90% confluency the day of the transfection. For each transfection reaction 250 µl of serum-free medium (Opti-MEM) were mixed with plasmidic DNA (usually 1 µg final concentration) and 250 µl of Opti-MEM were mixed with 6 µl Lipofectamine 2000 transfection reagent (Life Technologies). The two solutions were incubated 5 minutes at RT, then mixed and incubated for 20 minutes at RT to allow the formation of lipid complexes. The growth medium was removed from the cells and substituted with 1.5 ml of Opti-MEM. The mix was added to the cells that were left in the incubator for 6 hours, then transfection reaction was removed and fresh culture medium was added.

Cherry-Lac and I-Sce I-restriction endonuclease expressing vectors were transfected in NIH2/4 cells by Lipofectamine 2000 (Life Technologies) in a ratio of 3:1. 16h post transfection around 70% of the cells was scored positive for DDR markers at the Lac array. For the DNA repair assay, NIH2/4 were transfected with YFP-TetR (2 µg) and RFP-I-SceI-GR (2 µg) expressing vectors by Lipofectamine 2000 (Life Technologies). To induce YFP-TetR binding to the TetO array, doxycycline (1 µg/ml) was added to the culture medium for 3 hours. To induce RFP-I-SceI-GR translocation to the nucleus, 16 hours post transfection Triamcinolone Acetonide (Sigma-Aldrich, 0.1 nM) was added to culture medium. 3 hours after treatment, cells were fixed for immunostaining (I-Sce I ON) or washed with PBS to inactivate the endonuclease and fixed for immunostaining 24 hours later (I-Sce I OFF).

DICER-flag, DICER44ab-flag were a kind gift of R. Shiekhattar, at the Wistar Institute, Philadelphia, USA. DICER44ab-flag double mutant carries two amino acid substitutions in the RNase III domains of DICER (Asp1320->Ala and Asp1709->Ala), reported to be deficient in endonuclease activity (Zhang et al., 2004). Cherry-LacR, YFP-TetR, and I-Sce I-restriction endonuclease expressing vectors were kind gifts of E. Soutoglou, National Cancer Institute, NIH, Bethesda, USA (Soutoglou et al., 2007). pLKO.1, shRNA against mouse DICER and DROSHA expressing vectors were a kind gift of W.C. Hahn, Dana-Farber Cancer Institute, Boston, USA. shRNA for mouse DICER: CCG GGC CTC ACT TGA CCT GAA GTA TCT CGA GAT ACT TCA GGTCAA GTG AGG CTT TTT. shRNA for mouse DROSHA: CCG GCC TGG AAT ATG TCC ACA CTT TCT CGA GAA AGT GTG GAC ATA TTC CAG GTT TTT G.

## RNA interference

In the cell, the RNA interference pathway is responsible for post-transcriptional regulation of endogenous genes and is crucial against viral invasion and transposon expansion. Short interfering RNAs (siRNAs) are commonly used to knockdown a specific gene of interest. Alternatively, short hairpin RNA (shRNA) inserted into vectors are designed to form hairpins and loops of variable length, which are then processed to siRNAs by the cellular RNA machinery, and to produce stable gene silencing. For siRNA transfection, cells were plated in 6 multi-well plates so that they were at around 30-50% confluency the day of the transfection. For each transfection reaction 250 µl of serum-free medium (Opti-MEM) were mixed with siRNA oligo (usually 20nM final concentration) and 250 µl of Opti-MEM were mixed with 4 µl Lipofectamine RNAiMAX transfection reagent (Life Technologies). The two solutions were mixed and incubated for 20 minutes at RT to allow the formation of lipid complexes. The growth medium was removed from the cells and substituted with 1.5 ml of fresh culture medium. The mix was added to the cells that were

left in the incubator until the analysis. Knockdown by siRNA transfection is transient and usually biological effects are studied within 72 hours post transfection.

The DHARMACON siGENOME *SMARTpool* siRNA oligonucleotide sequences for human DICER, DROSHA were:

DICER: UAA AGU AGC UGG AAU GAU G; GGA AGA GGC UGA CUA UGA A; GAA UAU CGA UCC UAU GUU C; GAU CCU AUG UUC AAU CUA A.

DROSHA: CAA CAU AGA CUA CAC GAU U; CCA ACU CCC UCG AGG AUU A; GGC CAA CUG UUA UAG AAU A; GAG UAG GCU UCG UGA CUU A.

siRNA against human DICER 3' UTR: CCG UGA AAG UUU AAC GUU U.

siRNA against GFP: AAC ACU UGU CAC UAC UUU CUC.

siRNAs were transfected at a final concentration of 50 nM for OIS cells and 20 nM for the other cell lines. The siRNA against human DICER 3'UTR was used at a final concentration of 100 nM.

## LNA transfection

NIH2/4 cells were transfected by Lipofectamine 2000 (Life Technologies) with Cherry-LacR and I-Sce I-restriction endonuclease expressing vectors in a ratio of 3:1. LNA were first boiled at 90°C for 5 minutes and immediately transferred into ice for 5 minutes and then added in different combinations to the Cherry-LacR and I-Sce I transfection mix, at the final concentration of 200 pM. 24h post transfection cells were scored for DDR markers at the Lac array. For the DNA repair assay, LNA were first boiled at 90°C for 5 minutes and immediately transferred into ice for 5 minutes and then added in different combinations to the transfection mix containing YFP-TetR (2 μg) and RFP-I-SceI-GR (2 μg), at the final concentration of 200 pM. NIH2/4 cells were then transfected by Lipofectamine 2000 (Life Technologies). To induce YFP-TetR binding to the TetO array, doxycycline (1 μg/ml) was added to the culture medium for 3 hours. To induce RFP-I-

SceI-GR translocation to the nucleus, 16 hours post transfection Triamcinolone Acetonide (Sigma-Aldrich, 0.1 nM) was added to culture medium. 3 hours after treatment, cells were fixed for immunostaining (I-Sce I ON) or washed with PBS to inactivate the endonuclease and fixed for immunostaining 24 hours later (I-Sce I OFF). The Exiqon LNA sequences used were:

Control LNA: CCC TAA CCC TAA CCC TAA CCC; Lac upper strand: TTA TCC GCT CAC AAT TCC ACA T; Lac lower strand: ATG TGG AAT TGT GAG CGG ATA A; Tet upper strand: ACT GAT AGG GAG TGG TAA ACT; Tet lower strand: AGA GAA AAG TGA AAG TCG AGT

## Lentiviral infection

Lentiviruses are a subclass of retroviruses with the ability to integrate into the genome of non-dividing as well as dividing cells. Lentiviruses were produced by transfecting HEK 293T by calcium phosphate method with the vector expressing the gene of interest (10 μg for each plate of HEK 293T cells) together with the second-generation packaging vectors expressing the gag, pol, rev and envelope genes. The day after the transfection the growth medium was replaced with 5 ml of fresh medium to concentrate viral particles in the supernatants. 48 hours post-transfection, viral supernatants were collected, filtered with 0.45 μm filter, to remove cells that were dead or detached from the plate, and supplemented with 8 μg/ml polybrene. Target cells were incubated with the supernatant for 8-16 hours. After infection, cells were selected with the appropriate antibiotic.

For generation of DICER and DROSHA knockdown, NIH2/4 cells were infected with lentiviral particles carrying pLKO.1, shDICER or shDROSHA vectors and collected 48 hours later.

## Adenoviral infection

Adenoviruses are non-enveloped viruses with a dsDNA genome that does not integrate into the genome of the infected cells, thus it is not replicated during cell division. The recombinant adenoviral vectors are replication deficient and Adeno-293 cells, which express genes for viral particle assembly, are used to amplify viral particles. Adeno-293 cells were plated so they were at around 80% confluency the day of the infection and infected with the adenoviral particles (2 plaque forming units/cell) in medium without serum for 1 hour and 30 minutes. Infection medium was replaced with DMEM supplemented with 5% horse serum. 2-4 days later, cells were lysed by the virus and detached from the plate. Supernatant medium was treated with 3 cycles of freezing and thawing (putting it in liquid nitrogen and then in 37°C waterbath) to complete lysis of cells. After being centrifuged to eliminate cell debris, supernatant was stored as intermediate stock at -80°C. The intermediate stock was used for a second round of Adeno-293 infection to obtain the final stock. 1 ml of final stock was used to infect 1 well of 6 multi-well plates of target cells for 16 hours.

To produce the RNA for the deep sequencing, NIH2/4 cells were first infected with lentiviral particles carrying pLKO.1, shDICER or shDROSHA vectors. After 48h cells were superinfected with Adeno Empty Vector (kind gift of Elisabetta Dejana, IFOM, Milan, Italy) or Adeno I-Sce I (kind gift of Philip Ng, Baylor College of Medicine, Houston, Texas). Nuclei were isolated the day after the adenoviral infection.

## G2/M checkpoint assay

HEK 293 were co-transfected with siRNA (100nM) and plasmids (1μg) using Lipofectamine RNAi Max (Life Technologies). 48h later cells were irradiated with 5Gy and allowed to respond to IR-induced DNA damage in a cell culture incubator for 12, 24 or 36 hours. Then, at these three time points post irradiation, together with not irradiated

cells, $1X10^6$ cells were collected for Fluorescence Activated Cell Sorting (FACS) analysis, fixed in 75% ethanol in PBS, 30 minutes on ice. Afterwards, cells were treated 12h with 250 μg/ml of RNase A and incubated at least 1h with propidium iodide (PI). FACS profiles were obtained by the analysis of at least $5X10^5$ cells, acquired on FACS Calibur and analyzed using Flow Jo software. FACS is a specialized type of flow cytometry and provides a method for analyzing and sorting a heterogeneous mixture of biological cells, based upon the specific light scattering and fluorescent characteristics of each cell.

## Inhibition of RNA transcription

To inhibit RNA transcription I made use of several drugs that, at the appropriate concentrations, specifically blocked only one of the three RNA polymerases. Actinomycin D -a polypeptide antibiotic isolated from *Streptomyces* bacteria that intercalates in double-stranded DNA (Bensaude, 2011)- at low doses (0.05 μg/ml) and CX-5461 -a small molecule that selectively inhibits RNA pol I, shown to be effective against lymphoma and solid tumor xenografts (Bywater et al., 2012; Drygin et al., 2011)- are specific inhibitors of RNA polymerase I; actinomycin D at high doses (2 μg/ml) and α-amanitin (20 or 50 μg/ml) -a toxin extracted from the mushroom *Amanita phalloides* that binds to RNA pol II blocking RNA synthesis and triggering RNA pol II degradation (Bushnell et al., 2002; Nguyen et al., 1996)- are specific inhibitors of RNA polymerase II; ML-60218 -a small compund shown to inibit RNA pol III in yeast and human cells (Castelnuovo et al., 2010; Wu et al., 2003) is a specific inhibitor of RNA polymerase III. Specificity and efficacy of the drugs were monitored analyzing by qRT-PCR the levels of short-lived RNAs that are specifically transcribed by one of the different RNA polymerases: *47S* RNA (ribosomal RNA precursor) for RNA polymerase I; *fos* RNA for RNA polymerase II; *7SK* and *5S* RNAs for RNA polymerase III.

## RNase A treatment and RNA complementation experiments

Cells were plated on poly-D-lysinated coverslips and irradiated (2Gy) or cut by a restriction enzyme. 1 hour later HeLa cells were permeabilized with 2% Tween 20 in PBS for 10 minutes at RT while I-Sce I-transfected NIH2/4 cells were permeabilized 24 h post transfection in 0.5% Tween 20 in PBS for 10 minutes at RT. RNase A treatment was carried out in 1 ml of 1 mg/ml Ribonuclease A from bovine pancreas (Sigma-Aldrich) in PBS for 25 minutes at room temperature. Acetylated BSA in PBS (1 mg/ml) was used in parallel as negative control. After RNase A digestion, samples were washed with PBS, treated with 80 units of RNase inhibitor (RNaseOUT Life Technologies 40 units/ml) and 20 μg/ml of α-amanitin (Sigma-Aldrich) for 15 minutes in a total volume of 70 μl. For experiments with mirin, NIH2/4 cells were incubated at this step also with 100 μM mirin (Sigma-Aldrich) or DMSO for 15 minutes. For experiments with cycloheximide, NIH2/4 cells were incubated at this step also with 50 μg/ml cycloheximide (Sigma-Aldrich) or DMSO for 15 minutes. Then, RNase A-treated cells were incubated with total, small or gel-extracted RNA, or the same amount of tRNA, for additional 25 minutes at room temperature. If using mirin, NIH2/4 cells were incubated with total RNA in the presence of 100 μM mirin or DMSO for 25 minutes at room temperature. If using cycloheximide, NIH2/4 cells were incubated with total RNA in the presence of 50 μg/ml cycloheximide or DMSO for 25 minutes at room temperature. Cell were then fixed with 4% paraformaldehyde (NIH2/4 cells) or methanol:acetone 1:1 (HeLa cells).

In complementation experiments with synthetic labeled and unlabeled RNA oligonucleotides, eight RNA oligonucleotides with the potential to form four pairs were chosen among the sequences that map at the integrated locus in NIH2/4 cells, obtained by deep sequencing. Synthetic unlabeled RNA oligonucleotides were generated by Sigma-Aldrich. Synthetic cy5-RNA oligonucleotides were generated by Integrated DNA Technology, having the same sequences of the unlabeled synthetic RNA generated by

Sigma-Aldrich, but harboring a cy5 fluorophore at the 3' end and a monophosphate modification at the 5' end. Sequences map to different regions of the integrated locus: two pairs map to a unique sequence flanking the I-Sce I restriction site, one to the Lac-operator and one to the Tet-operator repetitive sequences. Two paired RNA oligonucleotides with the sequences of Let7a1 miRNA or anti-CXCR4 miRNA were used as negative control. RNAs were resuspended in 60 mM KCl, 6 mM HEPES-pH 7.5, 0.2 mM MgCl2, at the stock concentration of 12 μM, denatured at 70°C for 10 minutes and annealed for at room temperature. The synthetic cy5-RNAs (1 ng/μl) were mixed to tRNA (800 ng) and used to complement DDR focus formation in NIH2/4 uncut or cut cells. Sequences and position of the fluorophore are reported below:

Unique 1 (U1): 5' AUA ACA AUU UGU GGA AUU CGG CGC-cy5 3', Unique 2 (U2): 5' CGA AUU CCA CAA AUU GUU AUC C-cy5 3', Unique 3 (U3): 5' AUU UGU GGA AUU CGG CGC CUC UAG AGU CGA GG-cy5 3', Unique 4 (U4): 5' CCU CGA CUC UAG AGG CG-cy5 3', Lac 1 (L1): 5' AGC GGA UAA CAA UUU GUG GCC ACA UGU GGA-cy5 3', Lac 2 (L2): 5' UGU GGC CAC AAA UUG UU-cy5 3', Tet 1 (T1): 5' ACU CCC UAU CAG UGA UAG AGA AAA GUG AAA GU-cy5 3', Tet 2 (T2): 5' CUU UCA CUU UUC UCU AUC ACU GAU AGG GAG UG-cy5 3'

Negative control sequences and position of the fluorophore are reported below:

GFP 1: 5' GUU CAG CGU GUC CGG CGA GUU 3'; GFP 2: 5' CUC GCC GGA CAC GCU GAA CUU 3'; Let7a1 miRNA: 5' UGA GGU AGU AGG UUG UAU AGU U-cy5 3'; 5' CUA UAC AAU CUA CUG UCU UUC 3'; anti-CXCR4 miRNA: 5' UGU UAG CUG GAG UGA AAA CUU-cy5 3'; 5' GUU UUC ACA AAG CUA ACA CA 3'

DICER RNA products were generated as follows. A 550 bp DNA fragment carrying the central portion of the genomic locus studied (three Lac repeats, the I-Sce I site and two Tet repeats) was flanked by T7 promoters at both ends and was used as a template for *in vitro* transcription with the TurboScript T7 transcription kit (AMSBIO). The 500 nt long RNAs obtained were purified and incubated with human recombinant DICER enzyme (AMSBIO)

to generate 22-23 nt RNAs. RNA products were purified, quantified and checked on gel. As a control, the same procedure was followed with a 700 bp construct containing the RFP DNA sequence. Equal amounts of DICER RNA products were used in complementation experiment in NIH2/4 cells following RNase A treatment.

## Antibodies

Anti-γH2AX (mouse, Millipore 05-636, 1:300 for immunofluorescence); anti-ATM pS1981 (mouse, Rockland 200-301-400, 1:400 for immunofluorescence); mouse monoclonal anti-ATM (Sigma-Aldrich, 1:1000 for immunoblotting) anti-pS/TQ (Cell Signalling 2851, 1:200 for immunofluorescence); anti-53BP1 (rabbit, Novus NB100-304, 1:200 for immunofluorescence; 1:1000 for immunoblotting); anti-MDC1 (a gift from Jiri Bartek, IMG, Prague, Czech Republic, 1:20 for immunofluorescence); anti MRE11 rabbit polyclonal raised against recombinant MRE11 (1:200 for immunofluorescence); anti-RAD50 (mouse, Abcam, 1:200 for immunofluorescence); anti-NBS1 (rabbit, Novus, 1:200 for immunofluorescence); anti-β-tubulin (Sigma-Aldrich T5168, 1:2000 for immunoblotting).

As secondary antibodies for immunofluorescence goat anti-rabbit Alexa 405 IgG (Life Technologies, 1:100, excitation wavelength 401 nm, emission wavelength 421 nm); donkey anti-mouse or anti-rabbit Alexa 488 IgG (Life Technologies, 1:100, excitation wavelength 495 nm, emission wavelength 519 nm); donkey anti-mouse or anti-rabbit Cy3 IgG (Jackson Immuno Research, 1:400, excitation wavelength 550 nm, emission wavelength 570 nm), donkey anti-mouse or anti-rabbit Alexa 647 IgG (Life Technologies, 1:100, excitation wavelength 650 nm, emission wavelength 665 nm) were used.

## Immunofluorescence

To study protein sub-cellular localization at the single cell level immunofluorescence techniques were used. Cells were grown on coverslips, washed twice for 5 minutes with

PBS and fixed with either 1:1 methanol/acetone solution for 2 minutes at RT or with 4% PFA for 10 minutes at RT. In case of PFA fixation, cells were permeabilized with 0.2% Triton X-100 for 10 minutes at RT. Cells were incubated for 1 hour in blocking solution (PBG, 0.5% BSA, 0.2% gelatin from cold water fish skin) and then stained with primary antibodies diluted in PBG for 1 hour at RT in a humidified chamber. Cells were washed 3 times for 5 minutes with PBG and incubated with secondary antibodies diluted in PBG for 1 hour at RT in a dark humidified chamber. Cells were washed twice for 5 minutes with PBG, twice for 5 minutes with PBS and incubated with 4'-6-Diamidino-2-phenylindole (DAPI, 1 μg/ml, Sigma-Aldrich, excitation wavelength 358 nm, emission wavelength 461 nm) for 2 minutes at RT. DAPI binds preferentially to AT clusters of DNA minor groove and it was used to visualize nuclei. Cells were briefly washed with PBS and water and coverslips were then mounted with mowiol mounting medium (Calbiochem), which is a polyvinyl alcohol solution containing an "anti fade" agent, capable of reducing light-induced fading (photobleaching) of the fluorophore. Coverslips were air dried before microscope analysis.

## Imaging

Immunofluorescence images were acquired using a widefield Olympus Biosystems Microscope BX71 and the MetaMorph software (Soft Imaging System GmbH). Comparative immunofluorescence analyses were performed in parallel with identical acquisition parameters using ImageJ software; at least 100 cells were screened for each antigen. Cells with more than two DDR foci were scored positive. Confocal sections were obtained with a Leica TCS SP2 or AOBS confocal laser microscope by sequential scanning. For the experiments with cy5-DDRNAs, sections were obtained at the DeltaVision microscope (Applied Precision) by acquisition of 40 optical z-sections at different levels along the optical axis to allow a more accurate signal discrimination and

detection of co-localization events. Each image was automatically subjected to deconvolution by the softWoRx software (Applied Precision). The 40 z-sections were then loaded onto ImageJ software to reconstruct a 3D projection image. Cells were considered positive when there was an overlapping signal between cy5-DDRNAs and YFP-TetR in the three dimensional reconstruction.

## Immunoblotting

Cells were lysed in Laemmli sample buffer (2% sodium dodecyl sulphate (SDS), 10% glycerol, 60 mM Tris HCl pH 6.8). SDS is an anionic detergent, which denatures secondary and tertiary structures providing a uniform negative charge along the length of the polypeptide, thus allowing separation by electrophoresis only by molecular weight. The amount of proteins in the samples was measured by the biochemical Lowry protein assay. Copper (II) ions in alkaline solution react with protein to form complexes, and with the Folin-phenol reagent, a mixture of phosphotungstic acid and phosphomolybdic acid in phenol. The product becomes reduced to molybdenum/tungsten blue and can be detected colorimetrically by absorbance at 750 nm. A tracking dye, bromophenol blue, is added to the protein solution to allow the tracking of the proteins through the gel during the electrophoretic run. Disulfide linkages were reduced by adding β-mercaptoethanol and proteins were further denatured by heating at 95°C for 5 minutes. 50 μg of whole cell extracts were resolved by SDS polyacrylamide gel electrophoresis (SDS-PAGE). Protein solution run is performed in two layers of gel, namely stacking or spacer gel and resolving or separating gel. The stacking gel is a large pore 4% polyacrylamide gel in which proteins are concentrated. It is prepared with Tris HCl buffer at pH 6.8. This gel is cast over the resolving gel, which is a small pore polyacrylamide gel. The Tris HCl buffer used is of pH 8.8. Resolving gel is used for separating different range of proteins. Commonly 6% gel was used for > 100 kDa proteins, 10% gel for 40-100 kDa proteins and 15% gel for < 40

kDa proteins, in running buffer (25 mM Tris HCl, 0.2 M glycine, 0.1% SDS, pH 8.3). After running, the proteins were transferred to nitrocellulose membrane by a wet electroblotting transfer method with transfer buffer (25 mM Tris HCl, 0.2 M Glycine, 20% methanol). Following protein transfer, membranes were temporarily stained with Ponceau to assess the transfer efficiency. Ponceau is a negative stain, which binds to the positively charged amino groups of the protein and it also binds non-covalently to non-polar regions of the protein. Blocking of unspecific sites and primary and secondary antibody incubations were carried out in 5% milk in TBST (0.1% Tween in Tris-Buffered Saline). All the washes between incubations were performed in TBST. The primary antibody is specific for the protein of interest, whereas the secondary antibody is a modified antibody, which is linked to the horseradish peroxidase enzyme that, in the presence of the acridan-based substrate, produces localized light in the region where the antibody is bound to the membrane. The localized light, which is emitted from the bands, was detected by photosensitive photographic film. This method of detection is called chemiluminescence.

## Real-time quantitative reverse transcription PCR (qRT-PCR)

Total RNA was isolated from cells using RNAeasy kit (Qiagen) according to the manufacturer's instructions, and treated with DNase before reverse transcription. For small RNA isolation we used *mir*Vana™ miRNA Isolation Kit (Ambion). cDNA was generated using the Superscript II Reverse Transcriptase (Life Technologies) and used as template in real-time quantitative PCR analysis.

The Real Time PCR Instrument allows real time detection of PCR products as they accumulate during PCR cycles. In the initial cycles of PCR, the low fluorescence defines the baseline for the plot of fluorescence signal *vs* cycle number. A fixed fluorescence threshold can be set above the baseline. The parameter Ct (threshold cycle) is defined as the cycle number at which the fluorescence becomes higher than the fixed threshold. So,

the higher the initial amount of the sample, the sooner accumulated product is detected in the PCR process as a significant increase in fluorescence, and the lower the Ct value. Ct values are very reproducible in replicates because the threshold is picked to be in the exponential phase of the PCR, where there is a linear relation between log of the change in fluorescence and cycle number. When the Ct values were higher than 35, PCR result was classified as undetermined.

The Sybr Green-based qRT-PCR experiments were performed on a Roche LightCycler 480 sequence detection system in triplicate. Sybr Green binds to all double-stranded DNA species present in the sample, thus during the reaction the fluorescence intensity increases proportionally to the amount of PCR product produced. The Taqman-based qPCR experiments and the following analyses were carried in triplicate by the Real Time PCR unit (Cogentech) at the IFOM-IEO Campus, Milan, Italy, using the ABI 7900HT sequence detection system and 7500 Real-Time PCR system (Life Technologies). The detection of the amplified products involves the 5'-3' nuclease activity of Taq DNA polymerase. A gene-specific probe carrying two dyes, the fluorescent reporter and the quencher, hybridizes to the amplicon during the PCR reaction. The two fluorescent dyes interact whenever the probe is intact, causing the quencher dye to quench the reporter dye. During the amplification, the Taq DNA polymerase cleaves the 5' end of the probe, releasing the quencher dye resulting in an increase in fluorescence. The change in reporter dye fluorescence is quantitative for the amount of PCR product produced.

TaqMan MicroRNA Assays (Applied Biosystems) were used for the evaluation of mature miR-21 and rnu44 and rnu19 expression levels (Assay ID: 000397, 001094 and 001003). For TaqMan reactions, 18S was used as a control gene for normalization. For Sybr Green reactions, ribosomal protein P0 (RPP0) was used as a human and mouse control gene for normalization.

Primer sequences for real-time quantitative PCR were:

RPP0: TTC ATT GTG GGA GCA GAC (Forward), CAG CAG TTT CTC CAG AGC

(Reverse); human endogenous DICER: AGC AAC ACA GAG ATC TCA AAC ATT (Forward), GCA AAG CAG GGC TTT TCA T (Reverse); human endogenous and overexpressed DICER: TGT TCC AGG AAG ACC AGG TT (Forward), ACT ATC CCT CAA ACA CTC TGG AA (Reverse); human DROSHA: GGC CCG AGA GCC TTT TAT AG (Forward), TGC ACA CGT CTA ACT CTT CCA C (Reverse); mouse Dicer: GCA AGG AAT GGA CTC TGA GC (Forward), GGG GAC TTC GAT ATC CTC TTC (Reverse); mouse Drosha: CGT CTC TAG AAA GGT CCT ACA AGA A (Forward), GGC TCA GGA GCA ACT GGT AA (Reverse).

## Small RNA preparation

To generate small RNA-enriched fraction and small RNA-devoid fraction *mir*Vana™ microRNA Isolation Kit (Ambion) was used according to the manufacturer's instructions. The *mir*Vana microRNA isolation kit employs an organic extraction followed by immobilization of RNA on glass-fiber (silica-fibers) filters to purify either total RNA, or RNA enriched for small species. For total RNA extraction ethanol is added to samples, and they are passed through a Filter Cartridge containing a glass-fiber filter, which immobilizes the RNA. The filter is then washed a few times, and finally the RNA is eluted with a low ionic-strength solution. To isolate RNA that is highly enriched for small RNA species, ethanol is added to bring the samples to 25% ethanol. When this lysate/ethanol mixture is passed through a glass-fiber filter, large RNAs are immobilized, and the small RNA species are collected in the filtrate. The ethanol concentration of the filtrate is then increased to 55%, and it is passed through a second glass-fiber filter where the small RNAs become immobilized. This RNA is washed a few times, and eluted in a low ionic strength solution. Using this approach consisting of two sequential filtrations with different ethanol concentrations, an RNA fraction highly enriched in RNA species ≤200nt can be obtained (Cummins et al., 2006).

## RNA extraction from gel

In order to obtain the size separation of interest, total RNA samples (15 ng) were heat-denatured, loaded and resolved on a 15% denaturing acrylamide gel [1X TBE, 7 M urea, 15% acrylamide (29:1 acryl:bis-acryl)]. Gel was run for 1 h at 180 V and stained in GelRed solution. Gel slices were excised according to the RNA molecular weight marker, moved to a 2 ml clean tube, smashed and RNA was eluted in 2 ml of ammonium acetate 0.5 M, EDTA 0.1 M in RNase-free water, rocking overnight at 4°C. Tubes were then centrifuged 5 minutes at top speed, the acqueous phase was recovered and RNA was precipitated and resuspended in RNase free water.

## Northern blotting

Northern blotting or is a technique for detection of specific RNA sequences in a sample. Northern blotting was developed in 1977 by James Alwine and George Stark at Stanford University (Alwine et al., 1977). Northern blotting takes its name from its similarity to the first blotting technique, the Southern blot, named for biologist Edwin Southern. Northern blotting involves the following steps: cellular RNA is size-separated by denaturing polyacrylamide or agarose gel electrophoresis; the gel-resolved RNA is transferred onto a nylon membrane; the RNA is then detected with a radioactively labeled complementary DNA probe.

To generate the probe for DDRNA detection, the entire ~14 Kb Lac-I-SceI-Tet locus was cut out from the same plasmid used to derive NIH2/4 cells (Soutoglou et al., 2007). The restriction enzymes used were SacII and KpnI (New England BioLabs). The reaction product was run on an agarose gel and the ~14 Kb band was recovered from the gel and eluted using the QIAquick PCR Purification Kit (Qiagen).

Total RNA and small (< 200 nt) RNA were extracted from parental cells untransfected and from parental and NIH2/4 cells transfected with Cherry-Lac vector alone (uncut) or Cherry-Lac and I-Sce I expressing vectors (cut). 20 μg of total RNA and 8 μg of small RNA were loaded on a denaturing 12% 1X TBE-polyacrylamide (29:1) gel containing Urea (7 M) in the large vertical apparatus for Northern blot (Bio-Rad). Equal volumes of 2X loading buffer containing formamide (Thermo Scientific) were added to the adjusted volumes of samples. The mixture was then heated to 95°C for 5 minutes, chilled on ice and centrifuged prior loading. The gel was pre-run in 1X TBE at 250V for 10 minutes. Wells were cleaned from Urea and polyacrylamide before loading. After loading, gel was run in 1X TBE at 250V for 3 hours and then stained with 0.5 μg/ml of GelRed (Biotium) in 1X TBE for 10 minutes to visualize the RNA samples. RNA was electrically transferred in 0.5X TBE to a Hybond-N membrane at 80V for 1 hour at 4°C. To immobilize the RNA on the membrane, UV crosslinking with 254 nm light was performed at 1200 joules, equivalent to the "auto-crosslink" feature of the instrument. In addition, the membrane was also baked in an oven for 30 minutes at 80°C. Pre-hybridization of the membrane was performed in PerfectHyb Plus hybridization buffer (Sigma-Aldrich) for 1 hour at 37°C. To generate the radioactive Lac-I-SceI-Tet and U6 probes, 25 ng of the DNA template was heated for 5 minutes at 95°C, chilled in ice and added to a solution containing (α-32P)dATP (50 μCi) and 5 units of DNA Polymerase I large (Klenow) Fragment (Promega). The reaction was incubated for 1 hour at room temperature and then centrifuged in a MicroSpin G-25 column (GE Healthcare) to remove unincorporated radioactive nucleotides. To generate the radioactive Let7a probe, 5 pmol of template were incubated with (γ−32P)dATP (50 μCi) and 10 units of T4 Polynucleotide Kinase (Promega). The reaction was incubated for for 30 minutes at 37°C and then centrifuged in a MicroSpin G-25 column (GE Healthcare) to remove unincorporated radioactive nucleotides. The membrane was soaked over night at 37°C in PerfectHyb Plus hybridization buffer (Sigma-Aldrich) supplemented with the radioactive probe of interest

and salmon sperm DNA (10 mg/ml) (Sigma-Aldrich) as blocking agent, both previously heated for 5 minutes at 95°C. 16 hours later, the membrane was washed twice in a low stringency wash buffer (2X SSC, 0.2% SDS) for 10 minutes at room temperature and once for 2 minutes at 37°C (this step was avoided when less stringent washing conditions were used). The membrane was exposed first to the PhosphorImager (Molecular Dynamics) for 1 hour and then to a radiographic film overnight at -80°C.

## RNA sequencing

Nuclear RNA shorter than 200 nt was purified using *mir*Vana™ microRNA Isolation Kit. RNA quality was checked on a small RNA chip (Agilent) before library preparation. For Illumina hi Seq Version3 sequencing, spike RNA was added to each RNA sample in the RNA:spike ratio of 10000:1 before library preparation and libraries for Illumina GA IIX were prepared without spike. An improved small RNA library preparation protocol was used to prepare libraries (Kawano et al., 2010). In brief, adenylated 3' adapters were ligated to 3' ends of 3'-OH small RNAs using a truncated RNA ligase enzyme followed by 5' adapter ligation to 5'-monophosphate ends using RNA ligase enzyme, ensuring specific ligation of non-degraded small RNAs. cDNA was prepared using a primer specific to the 3'adapter in the presence of Dimer eliminator and amplified for 12-15 PCR cycles using a special forward primer targeting the 5' adapter containing additional sequence for sequencing and a reverse primer targeting the 3' adapter. The amplified cDNA library was run on a 6% polyacrylamide gel and the 100 bp band containing cDNAs up to 33 nt was extracted using standard extraction protocols. Libraries were sequenced after quality check on a DNA high sensitivity chip (Agilent). Multiplexed barcode sequencing was performed on Illumina GA-IIX (35 bp Single end reads) and Illumina Hi seq version3 (51 bp single end reads). Sequence data have been deposited in the DNA Data Bank of Japan under accession code DRA000540.

## Microinjection

NIH2/4 cells were microinjected in the nucleus using a Femtojet pump (Eppendorf) and a microscope mounted Injectman NI2 micromanipulator (Eppendorf). Solutions to be microinjected were centrifuged at 16.000 g for 15 min at 4°C just prior to microinjection. The micropipette (Femtotips, Eppendorf) was loaded with with plasmids expressing EGFP-LacR (65 ng/µl) for the uncut sample or EGFP-LacR (65 ng/µl) and I-Sce I (100 ng/µl) for the cut sample, together with the four annealed couples of cy5-RNAs (2 µM or 100nM) or cy5-CXCR4 as negative control (2 µM) and Alexa555 Dextran (0.1 mg/ml) in PBS. Alexa555 Dextran, which is spectrally distinct from cy5, served as a marker to locate microinjected cells. All of the microinjections were performed at 100 hPa microinjection pressure for 0.5 s with 40 hPa compensation pressure. Using these conditions, microinjection volume was estimated to be ~0.02 pl or ~0.5-5% of the total cell volume, which translates to ~24.000 molecules of cy5-RNAs (at 2 µM working concentration).

24 hours later cells were first washed five times with PBS, fixed using 4% (w/v) paraformaldehyde in PBS for 20 min, washed five times with PBS after fixing and imaged in an antioxidant mix (PBS-OSS). Imaging was performed using a cell-TIRF system based on an Olympus IX81 microscope equipped with a 60x 1.45 NA oil-immersion objective (Olympus), nanometer-precision motorized stage (ASI Imaging), focal drift control module (zero drift control, Olympus), 1x-4x magnification changer (Olympus) and an EM-CCD camera (Evolve, Photometrics). Stack images were acquired (<10x100 nm stacks) at 120x magnification and 100 ms exposure time, and subsequently processed to subtract the background. Signals where the pixel bearing maximum intensity of EGFP-LacR particle was the same as the maximum intensity pixel of cy5-RNA particle were considered as perfectly overlapping. Signals where the pixel bearing maximum intensity of EGFP-LacR particle was < 5 pixels (~600 nm) from the maximum intensity pixel of cy5-RNA particle were considered as partially overlapping. Peaks of particles were identified based on an algorithm similar to Simonson et al., 2010.

## Single step photobleaching

Photobleaching of a single fluorophore is characterized by sudden decrease of fluorescence intensity. The number of photobleaching steps indicates the number of incorporated fluorophores. By measuring the discrete decreases in fluorescence intensity as incorporated fluorophores bleach over time, this technique permits a direct measure of the number of fluorophores, and thus the number of molecules, in multi-component nanoparticles.

Microinjected NIH2/4 cells were first washed five times with PBS, fixed using 4% (w/v) paraformaldehyde in PBS for 20 min, washed five times with PBS after fixing and imaged in an antioxidant mix (PBS-OSS). Single-molecule high-resolution imaging with photobleaching was performed as in Pitchiaya et al., 2012. Intensity analysis to determine number of photobleaching steps was performed using a custom written LabView (National Instruments) code (Ding et al., 2009). A Chung-Kennedy non-linear filter was used (Chung and Kennedy, 1991) to effectively average out the noise within intensity traces, yet preserving fast and sudden transitions, which aided in better visualization of photobleaching steps. The number of fluorophores per spot was estimated based on the number of photobleaching steps. The density of spots within cells was low enough (~0.1 - 0.25 spots/μm2) to be confident that single particles were discerned. The uncut sample always had < 5 cy5 labeled molecules at the locus, whereas the cut sample contained a significant fraction of larger aggregates at the locus.

## Statistical analyses

Results are shown as means plus/minus standard error (s.e.m.). *p-value* was calculated by Chi-squared test. qRT-PCR results are shown as means of a triplicate plus/minus standard deviation (s.d.) and *p-value* was calculated by Student's t-test as indicated. * indicates *p-value<0.05*. n stands for number of independent biological experiments.

# Results

The work I am going to illustrate in this section comes from the collaborative efforts of Sofia Francia, a postdoc in the laboratory when I joined it, and mine. A large portion, but not all, of this work has been published in Nature, in May 2012 (Francia et al., 2012). In this section I describe my results, published and unpublished, and summarize Sofia's data when necessary, making reference to the figures of the published paper. For crucial experiments, important for the reader to understand my data, I also show Sofia's figures and data from our collaborators Alka Saxena and Sethu Pitchiaya.

## 1. IR-induced DDR foci are sensitive to RNase A treatment, are rescued by total RNA re-addition and are RNA polymerase II dependent

### *1.1 IR-induced DDR foci are sensitive to RNase A treatment*

It has been shown that mammalian cells can tolerate a transient membrane permeabilization followed by RNase treatment. This approach allowed the study of the contribution of RNA to heterochromatin structure (Maison et al., 2002) and to the assembly of ionizing radiation (IR)-triggered 53BP1 foci (Pryde et al., 2005). 53BP1 contains two Tudor domains (Charier et al., 2004), usually found in RNA-binding proteins, and it immunoprecipitates with some RNA molecules (Pryde, 2005 #222). Treating irradiated HeLa cells with RNase A dissociates 53BP1-GFP IR-induced foci. Moreover, 53BP1 foci re-assembly can be triggered by re-addition of nuclear RNA in RNase A-treated, irradiated HeLa cells (Pryde et al., 2005). These results suggested a possible involvement of RNA in the binding of 53BP1 to damaged chromatin. Therefore, when I joined the laboratory, this technique was utilized to test the potential contribution of RNA in DDR activation. IR-exposed human cells (HeLa) were permeabilized with a mild detergent, treated with the broad specificity RNA nuclease RNase A, fixed and stained for different DDR markers (Figure 6).

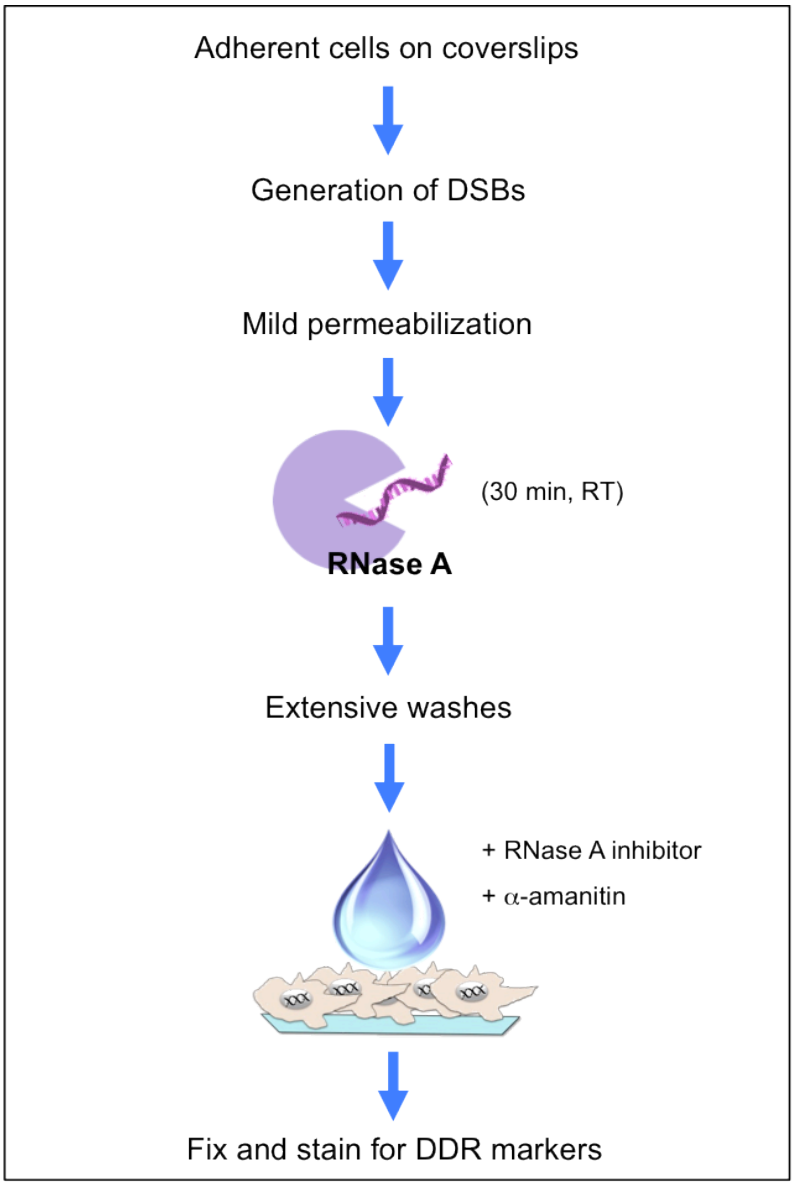


**Figure 6. Scheme of RNase A treatment.**
Cells are plated on glass coverslips and DSBs are induced by exposing them to IR or the expression of restriction enzymes. Cells membrane is then permeabilized with a mild detergent (Tween 20) for 15 minutes at RT. RNase A (1mg/ml in PBS) treatment is carried out for 30 minutes at RT. Acetylated BSA (1mg/ml in PBS) is used in parallel as negative control. After RNase A digestion, samples are washed extensively with PBS, further treated with RNase inhibitor and with α-amanitin (20µg/ml) to prevent endogenous transcription, for 10 minutes at RT. In complementation experiments, RNase A-treated cells are incubated with total RNA, or the same amount of tRNA, in the presence of RNase inhibitor and α-amanitin for additional 25 minutes at RT. Cell are then fixed and stained for DDR markers.

Upon IR, factors involved in the DNA damage response are normally recruited to DNA lesions forming structures called DDR foci. It is important to mention that the whole procedure, from the permeabilization step till the cell fixation, lasts less then 1 hour at room temperature. The RNase A treatment led to the degradation of both messenger RNAs

and miRNAs, including the mRNAs of DDR genes, without however significantly affecting DDR protein levels (Francia et al., 2012, Supplementary Fig. 16a). Irradiated HeLa cells, RNase A-treated or incubated with BSA (-), were stained for markers of DDR activation such as the phosphorylated histone H2AX (γH2AX), its direct interactor MDC1, the phosphorylated, and thus activated, form of ATM (pATM) and proteins phosphorylated by ATM, ATR and DNA-PK (pS/TQ). RNA degradation strongly impaired 53BP1, pATM, pS/TQ and MDC1 foci formation (Figure 7). This result is consistent with the reported sensitivity of 53BP1-GFP to ribonuclease treatment (Pryde et al., 2005). γH2AX accumulation was instead only marginally affected by RNase A. Thus not only 53BP1, but also other DDR mediators and downstream factors are sensitive to the removal of cellular RNA.

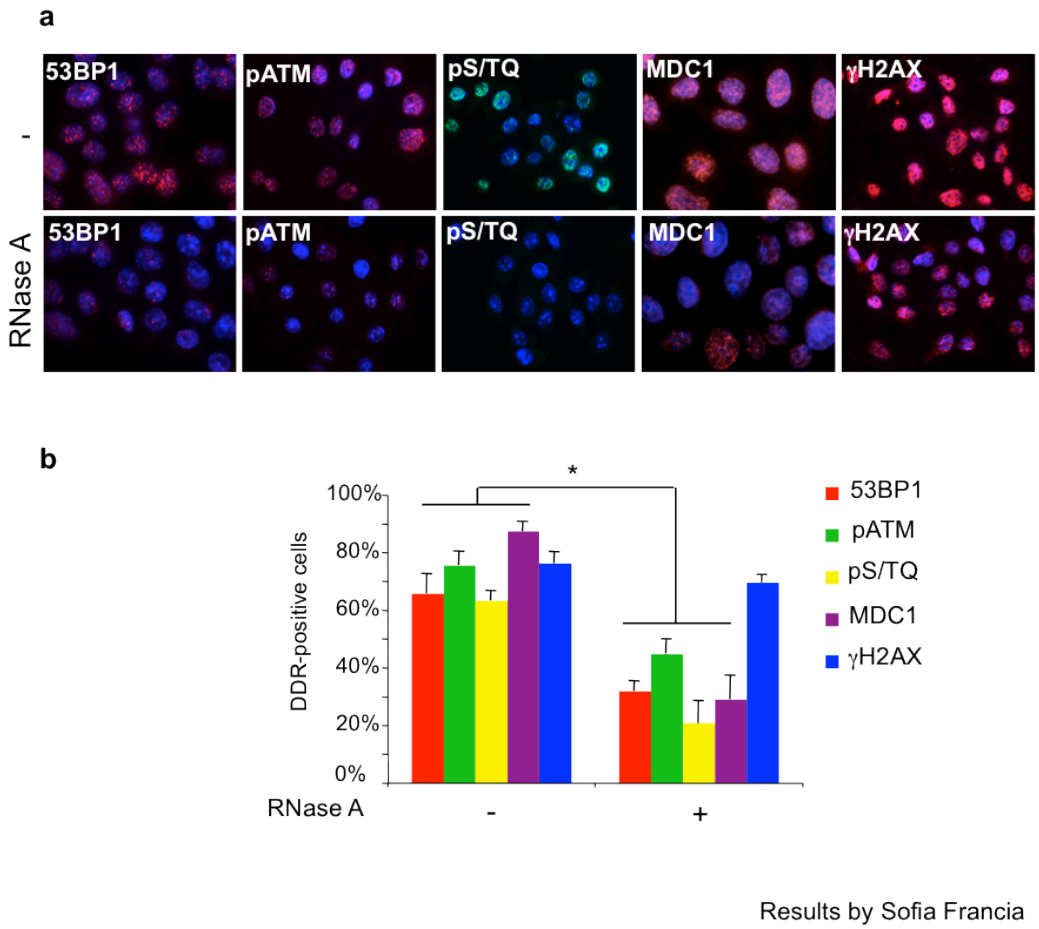


**Figure 7. IR-induced DDR foci are sensitive to RNase A treatment.**
**a.** Irradiated HeLa cells (2 Gy) were treated with acetylated BSA (-) or RNase A (+), fixed and probed for 53BP1, pATM, pS/TQ, MDC1 and γH2AX foci. **b.** Histogram shows the percentage of cells positive for DDR foci. Error bars indicate s.e.m. (n=3). Differences are statistically significant (*p-value<0.01).

*1.2 Total RNA addition restores DDR foci in RNase A-treated cells*

Next, as it was shown for 53BP1 (Pryde et al., 2005), the reformation of DDR foci, lost after RNase A treatment, was attempted by the incubation of RNase A-treated cells with their own RNA. Therefore, irradiated RNase A-treated cells were incubated with purified total RNA in the presence of an RNase A inhibitor and the RNA polymerase II-specific inhibitor α-amanitin, a toxin extracted from the mushroom *Amanita phalloides* that binds to RNA pol II blocking RNA synthesis and triggering RNA pol II degradation (Bushnell et al., 2002; Nguyen et al., 1996), to prevent the synthesis of endogenous transcripts. In fact, when DMSO instead of α-amanitin was added to RNase A-treated cells, DDR foci progressively reappeared within minutes, suggesting that DDR foci formation was dependent on ongoing RNA polymerase II transcription in our experimental setup (Francia et al., 2012, Supplementary Fig. 17a, b). Strikingly, addition of total RNA, but not tRNA used as control, to RNase A-treated and transcription-impaired cells robustly restored focal accumulation of all DDR factors tested (Francia et al., 2012, Fig. 2a and Supplementary Fig. 16b) within a relatively short time (20 minutes) at room temperature.

*1.3 IR-induced DDR foci are RNA polymerase II dependent*

As mentioned above, previous work in the laboratory showed that the RNA polymerase II inhibitor α-amanitin prevents DDR foci reformation in RNase A-treated irradiated cells. Prompted by this observation, I decided to further study the dependency of DDR activation on RNA synthesis, by testing the impact of the selective inhibition of RNA polymerase I, II or III on IR-induced DDR foci formation and re-formation following RNase-A treatment. To this aim, I used several drugs that, at the appropriate concentrations, specifically inhibit only one of the three enzymes. Actinomycin D, a polypeptide antibiotic isolated from *Streptomyces* bacteria that intercalates in double-stranded DNA (Bensaude, 2011), at low dose (0.05 μg/ml) and CX-5461, a small molecule that selectively inhibits

RNA pol I (Bywater et al., 2012; Drygin et al., 2011), are specific inhibitors of RNA polymerase I; actinomycin D at high dose (2 μg/ml) and α-amanitin are specific inhibitors of RNA polymerase II; ML-60218, a small compound shown to inhibit RNA pol III in yeast and human cells (Castelnuovo et al., 2010; Wu et al., 2003), is a specific inhibitor of RNA polymerase III. In all setup used, I monitored the specificity and efficacy of the drugs by analyzing by qRT-PCR the levels of short-lived RNAs that are specifically transcribed by one of the different RNA polymerases: *47S* RNA (ribosomal RNA precursor) for RNA pol I; *fos* RNA for RNA pol II; *7SK* and *5S* RNAs for RNA pol III.

To test the impact of α-amanitin on IR-induced DDR foci formation, I treated HeLa cells with the inhibitor (20 μg/ml) for 24 hours before irradiation. Given that impairing RNA transcription can elicits DNA breaks and genome instability (Dominguez-Sanchez et al., 2011; Stirling et al., 2012), I first checked if α-amanitin by itself was not causing DDR activation in not irradiated cells. The percentage of 53BP1 foci was comparable between α-amanitin and DMSO treatments in not irradiated cells, whereas a decreased amount of 53BP1 signal became apparent in irradiated α-amanitin-treated cells fixed 10' post IR, as compared to DMSO (Figure 8a). However, the qRT-PCR analysis revealed that not only the short lived RNA *fos* was affected by α-amanitin treatment for 24 hours, but also *53BP1* mRNA levels were reduced (Figure 8b). This data were confirmed by western blot, in which I observed a reduction both in 53BP1 and in ATM total protein levels, either in not irradiated or in irradiated cells (Figure 8c).

In order to avoid this issue, I decided to use a higher dose of α-amanitin (50 μg/ml) for a shorter incubation time before irradiation. Since α-amanitin is poorly permeable to the cell membrane (Khidir et al., 1995), I permeabilized cells with a mild detergent before adding the drug to the medium. Also under this condition, α-amanitin was not triggering DDR activation in not irradiated cells, as confirmed by 53BP1, γH2AX and pATM stainings (Figure 9a, b). Interestingly, in irradiated cells I could observe a reduction of 53BP1 and pATM, but not γH2AX, foci dependent on the incubation time, reaching a maximum at 8

hours treatment before IR (Figure 9a, b). The efficacy and specificity of the drug as well as the stability of *53BP1* and *ATM* mRNAs at each time point were evaluated by qRT-PCR (Figure 9c) and demonstrated that α-amanitin, under this condition, is able to specifically inhibit RNA pol II without altering the mRNA levels of the DDR factors tested. Thus, these results suggest that blocking RNA pol II transcription before DNA damage reduces DDR foci formation.

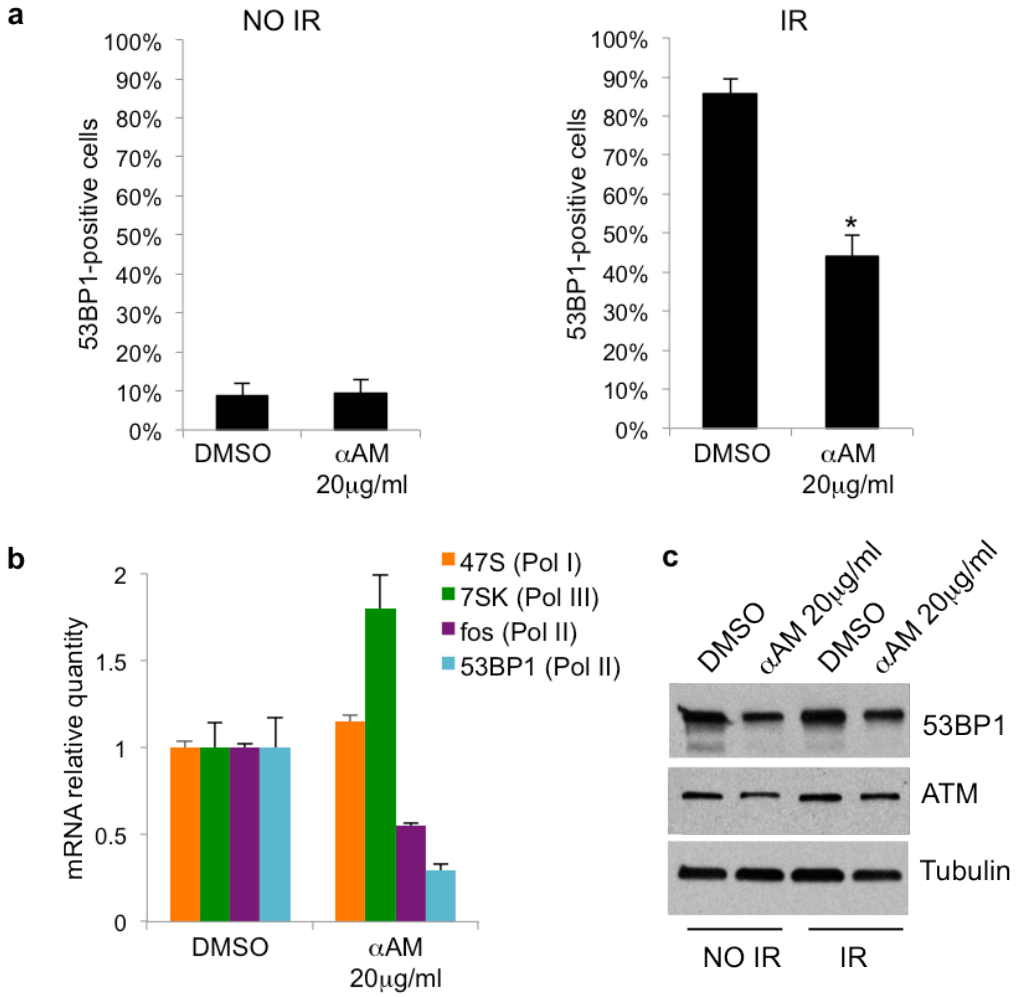


**Figure 8. RNA polymerase II inhibition for 24 hours leads to an impairment in DDR foci formation but also to a decrease of DDR protein and mRNA levels.**
**a.** HeLa cells were treated with 20μg/ml of α-amanitin (to specifically inhibit RNA polymerase II) or DMSO, as negative control, for 24 hours before irradiation (IR, 2Gy) or not (NO IR). Histogram shows the percentage of cells positive for DDR foci. Error bars indicate s.e.m. (n=2). For the quantification shown around 300 cells were analyzed. Differences are statistically significant (*p-value<0.01). **b.** Efficiency as well as specificity of α-amanitin treatment were evaluated by qRT-PCR by analyzing the levels of short-lived RNAs that are specifically transcribed by the different RNA polymerases as indicated. Also 53BP1 mRNA level (RNA polymerase II transcript) was evaluated by qRT-PCR and it decreases after 24 hours of treatment with α-amanitin. **c.** Immunoblot analysis of 53BP1 and total ATM in HeLa cells irradiated (IR) or not irradiated (NO IR). Tubulin was used as loading control.

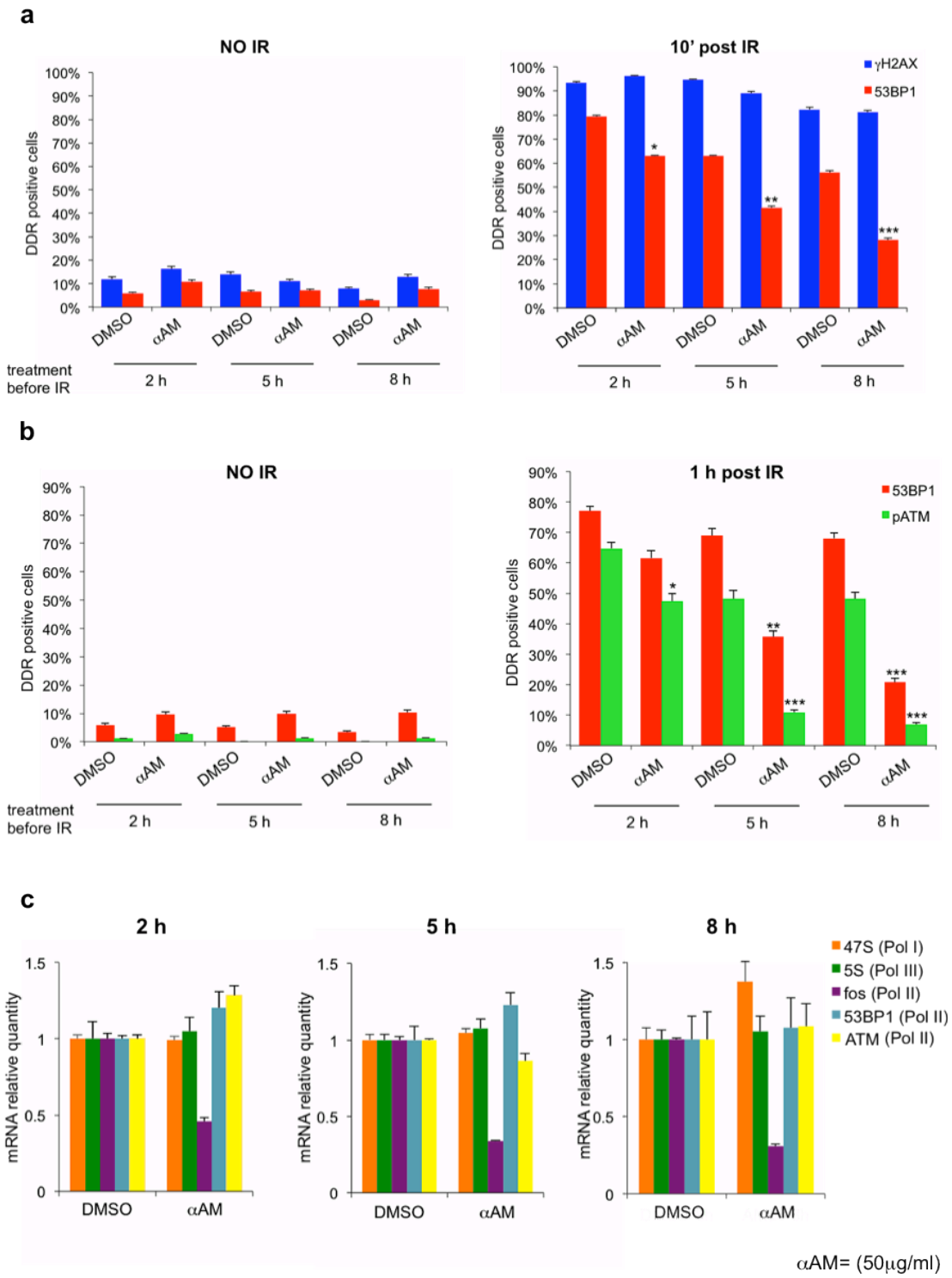


**Figure 9. RNA polymerase II inhibition for 8 hours in permeabilized cells leads to an impairment in DDR foci formation without detectably altering mRNA levels of DDR proteins.** HeLa cells were permeabilized with a mild detergent (Tween 20) for 15 minutes at RT, then cultured in their growth medium supplemented with 50μg/ml of α-amanitin (to specifically inhibit RNA polymerase II) or DMSO, as negative control, for the time indicated before irradiation (IR 2Gy) or not (NO IR). Histogram shows the percentage of cells positive for DDR foci 10 minutes post IR (**a**) or 1 h post IR (**b**). Error bars indicate s.e.m. For the quantification shown around 200 cells were analyzed. Differences are statistically significant (*p-value<0.01, **p-value<0.001, ***p-value<0.0001). **c.** Efficiency as well as specificity of the drug were evaluated by qRT-PCR, by analyzing the levels of short-lived RNAs that are specifically transcribed by the different RNA polymerases. Also 53BP1 and ATM mRNA levels (RNA polymerase II transcripts) were evaluated by qRT-PCR and they were stable after 8 h of α-amanitin treatment.

I next tested if RNA polymerase I could have a role in DDR foci formation, by either treating HeLa cells with actinomycin D both at low (0.05 μg/ml) and high doses (2 μg/ml) for 5 hours before IR or with CX-5461 (5 μM) for 24 hours before IR. I used actinomycin D at high concentration, which inhibits RNA pol I but also RNA pol II transcription, as positive control.

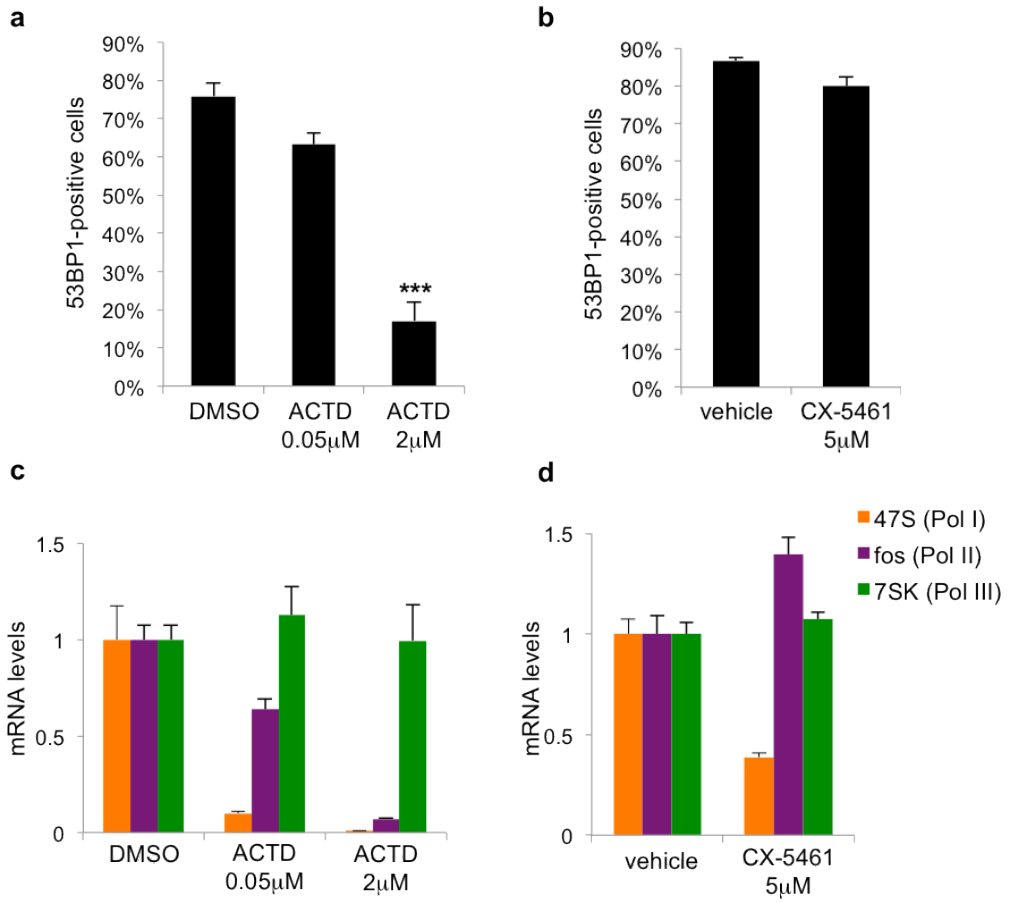


**Figure 10. RNA polymerase I is not involved in DDR foci formation.**
**a.** HeLa cells were treated with 0.05μM (to inhibit specifically RNA polymerase I) or 2 μM (to inhibit RNA polymerase I and II) of actinomycin D or DMSO as negative control for 5 hours before irradiation (2Gy). Histogram shows the percentage of cells positive for 53BP1 foci. Error bars indicate s.e.m. (n=3). For the quantification shown around 300 cells were analyzed. Differences are statistically significant (***p-value<0.0001). **b.** HeLa cells were treated with 5μM of CX-5461 (to inhibit specifically RNA polymerase I) or vehicle (50 mM NaH2PO4, pH 4.5) as negative control for 24 hours before irradiation (2Gy). Histogram shows the percentage of cells positive for 53BP1 foci. Error bars indicate s.e.m. For the quantification shown around 100 cells were analyzed. **c.** Efficiency as well as specificity of the drugs were evaluated by qRT-PCR, by analyzing the levels of short-lived RNAs that are specifically transcribed by the different RNA polymerases.

Strikingly, a reduction in 53BP1 foci formation was only present when cells were pre-treated with actinomycin D at high dose compared to DMSO, confirming the results obtained with α-amanitin and suggesting that RNA polymerase I inhibition has no impact on DDR activation (Figure 10a, b). The efficacy and specificity of the drugs were confirmed by qRT-PCR (Figure 10c). Unfortunately, I observed that both actinomycin D and CX-5461 treatments caused DNA damage in not irradiated cells (data not shown), complicating the interpretation of these data.

The incubation with the RNA polymerase III inhibitor ML-60218 (30 μM) for 24 hours before IR did not trigger DDR per se in not irradiated cells (data not shown) and did not have an impact on 53BP1 foci formation in irradiated cells (Figure 11a), suggesting that RNA polymerase III may not be involved in DDR. However, compared to the other drugs I used, ML-60218 was less specific and less efficient (Figure 11b).

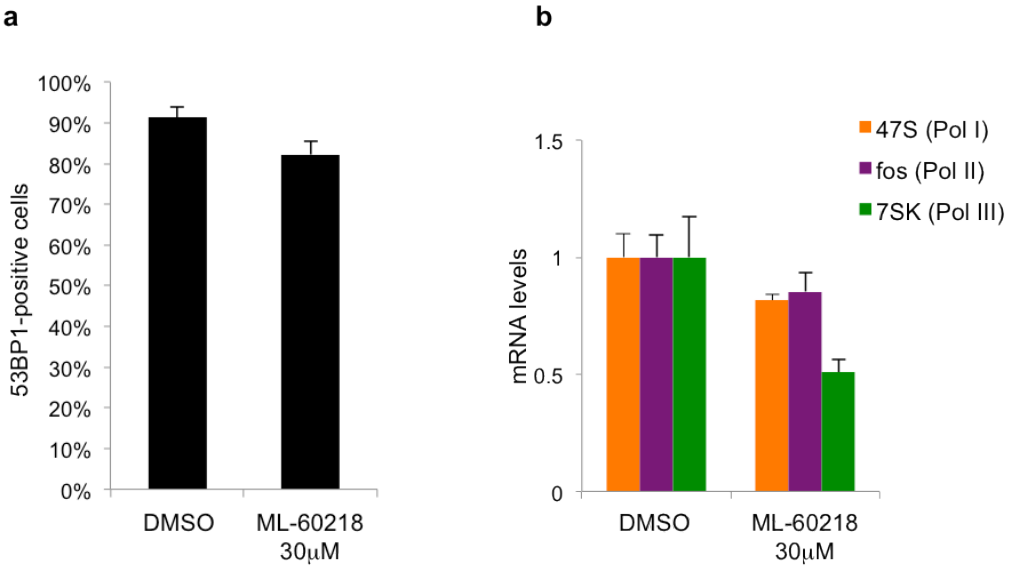


**Figure 11. RNA polymerase III is not involved in DDR foci formation.**
**a.** HeLa cells were treated with 30μM of ML-60218 (to inhibit specifically RNA polymerase III) or DMSO, as negative control, for 24 hours before irradiation (2Gy). Histogram shows the percentage of cells positive for 53BP1 foci. Error bars indicate s.e.m. For the quantification shown around 100 cells were analyzed. **b.** Efficiency as well as specificity of the drug were evaluated by qRT-PCR, by analyzing the levels of short-lived RNAs that are specifically transcribed by the different RNA polymerases.

To assess the contribution of different RNA polymerases in DDR foci reformation post RNase A, I irradiated HeLa cells, permeabilized them, treated them with RNase A and incubated with different RNA polymerase inhibitors.

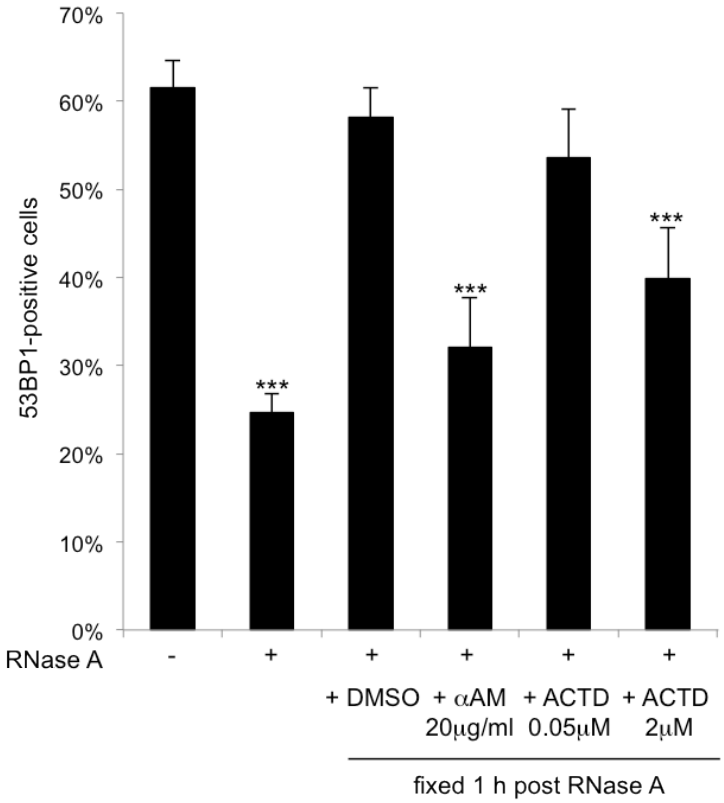


**Figure 12. RNA polymerase II but not RNA polymerase I inhibition prevents DDR foci reformation after RNase A treatment.**
HeLa cells were irradiated (2Gy), permeabilized and incubated with BSA (-) or RNase A (+) for 30 minutes at RT. Cells treated with RNase A were then washed and incubated with 20μg/ml of α-amanitin (to inhibit specifically RNA polymerase II), 0.05μM (to inhibit specifically RNA polymerase I) or 2 μM (to inhibit RNA polymerase I and II) of actinomycin D or DMSO, as negative control, for 1 hour. Histogram shows the percentage of cells positive for 53BP1 foci. Error bars indicate s.e.m. (n=4). For the quantification shown around 400 cells were analyzed. Differences are statistically significant (***p-value<0.0001).

After RNase A treatment, control cells incubated with DMSO reformed DDR foci (Figure 12), confirming the previous observation (Francia et al., 2012, Supplementary Fig. 17a, b). Also under these conditions I could not see an impact of RNA polymerase I inhibitors in DDR foci reformation, whereas inhibiting RNA polymerase II, both using α-amanitin and

actinomycin D at high dose, impaired DDR foci reformation, compared to DMSO-treated cells (Figure 12). The RNA polymerase III inhibitor showed an even stronger effect on DDR foci reformation (data not shown), but cells looked very sick after the treatment and the analysis of the unstable RNAs by RT-qPCR revealed that, when used in permeabilized cells, this drug become a non-specific inhibitor of transcription, an effect that is maybe due to its increased intracellular concentration.

Collectively these results indicate that RNA polymerase II is the main player involved in the biogenesis of the RNA species necessary for DDR activation.

## 2. The RNA species involved in DDR activation are in the size range of DROSHA and DICER products

In order to characterize the RNA species involved in DDR-foci reformation I incubated RNase A-treated HeLa cells with different RNA populations. I resolved total RNA from irradiated HeLa cells on a 15% polyacrylamide gel and recovered RNAs of different lengths: longer than 100 nt, between 100 nt and 35 nt and between 35 nt and 20 nt (Figure 13a). I also recovered the so-called gel-purified total RNA, which represents a mixture of the three fractions above mentioned. I then used total RNA not gel-purified as positive control and tRNA as negative control. To check for the quality and the enrichment of the three preparations, I performed a qRT-PCR analysis of different RNAs representing the three size ranges (Figure 13b) and I confirmed that each gel-purified RNA fraction was enriched for the RNA of the specific length: RNU19 (200 nt) was present only in the >100nt fraction; RNU44 (61 nt) was observed specifically in the 35-100 nt fraction; miR-21 (22 nt) was enriched just in the 20-35 nt fraction. Following RNase A treatment, I incubated irradiated HeLa cells with either tRNA (200 ng), total RNA (200 ng), various amounts (100, 50 or 20 ng) of gel-purified total RNA or equal quantities (50 ng) of RNA from the three fractions. I observed that 20-35 nt size range was the most effective in restoring 53BP1 foci formation, compared to the other two longer fractions (Figure 13c). These size-separation experiments indicate that the RNA components required for DDR foci assembly are small, ranging from 20 to 35 nucleotides in length.

The size range of the RNA components necessary for DDR activation was compatible with the length of DROSHA and DICER RNA products (see Introduction, sections 3.2 and 3.3). Thus, I decided to investigate the possible role of DROSHA and DICER in DDR activation and checkpoint establishment following IR, and in DDR foci reformation following RNase A treatment.

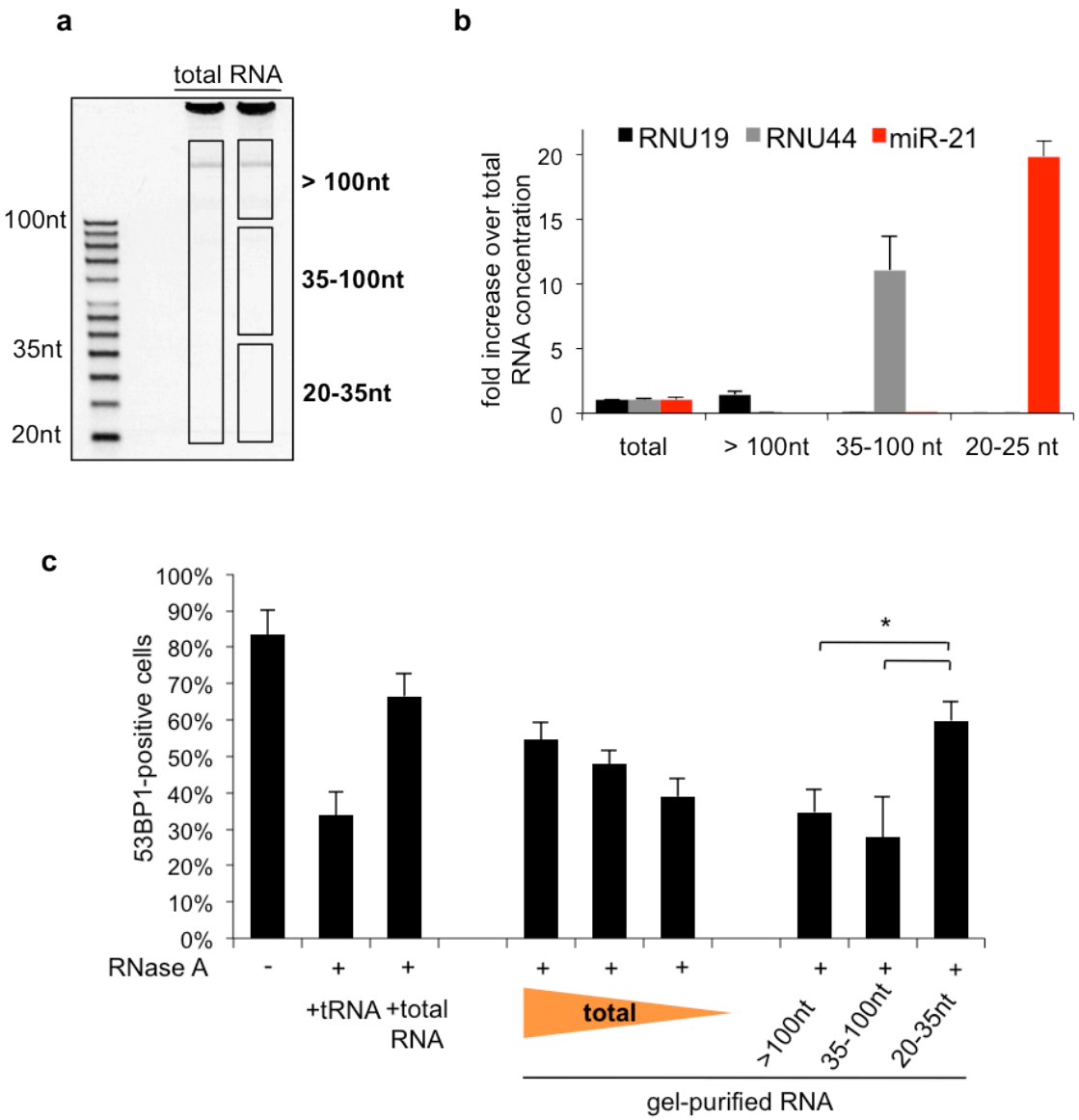


**Figure 13. Incubation with 20-35nt long RNAs is sufficient to restore DDR foci formation in RNase-treated cells.**

**a.** HeLa cells were irradiated (2Gy), permeabilized and incubated with BSA (-) or RNase A (+) for 30 minutes at RT. 100, 50 or 20 ng of gel-extracted total RNA and 50 ng of RNA extracted from each gel slice (longer than 100 nt, 35–100 nt and 20–35 nt size ranges) were used for DDR foci reconstitution after RNase treatment. Histogram shows the percentage of cells positive for 53BP1 foci. Error bars indicate s.e.m. (n=3). Differences are statistically significant (*p-value<0.01). **b.** Total RNA was separated by polyacrylamide gel electrophoresis and gel-extracted. 100, 50 or 20ng of gel extracted total RNA and 50ng of RNA extracted from each gel fraction (>100nt, 35-100nt and 20-35nt) were used for DDR foci reconstitution in HeLa cells. **c.** qRT-PCR analysis of RNU19 (200 nt), RNU44 (61 nt) and miR-21 (22 nt) in the indicated RNA fractions extracted from gel. The enrichment was evaluated as the ratio between PCR cycles (ct values) of the small RNAs analyzed and ct values of β-actin mRNA in each fraction, after normalization over the total RNA. Error bars indicate s.d.

## 3. DICER or DROSHA inactivation impairs IR-induced DDR foci formation and establishment of cell cycle checkpoints

*3.1 IR-induced DDR foci are sensitive to DICER or DROSHA knockdown independently from the canonical RNAi pathway*

The DNA damage response is an evolutionary-conserved mechanism, essential to preserve genome integrity (Jackson and Bartek, 2009). Components of the RNAi machinery are thought to have evolved to preserve genome stability from the attacks of viruses and mobile genetic elements (Hannon, 2002). However, RNAi and DDR pathways had not been demonstrated to directly interact. DICER and DROSHA are crucial ribonucleases of the RNAi machinery (Krol et al., 2010) and their RNA products have been involved in important cellular processes such as gene silencing, chromatin assembly, cell fate determination, transformation, proliferation and cell death (Farazi et al., 2008; Sayed and Abdellatif, 2011).

When I joined, ongoing research in the laboratory already suggested that DICER and DROSHA are necessary for the DNA damage response activation upon exogenous DNA damage. DICER or DROSHA were transiently inactivated by siRNA in human normal fibroblasts (HNF), subsequently exposed to IR. To study DDR activation upon DICER or DROSHA knockdown, cells were fixed few hours post irradiation and stained for nuclear foci containing γH2AX, MDC1, pATM and pS/TQ. Despite similar levels of protein expression (Francia et al., 2012, Supplementary Fig. 5), the formation of pATM, pS/TQ, MDC1, but not γH2AX foci, as observed in the RNase A treatment, was reduced in DICER- or DROSHA-inactivated HNF (Figure 14a, b). Under these conditions, no impairment in 53BP1 foci formation was observed. Since 53BP1, like MDC1, is a DDR mediator protein that assembles at DSBs in an ATM-dependent manner, this result was unexpected.

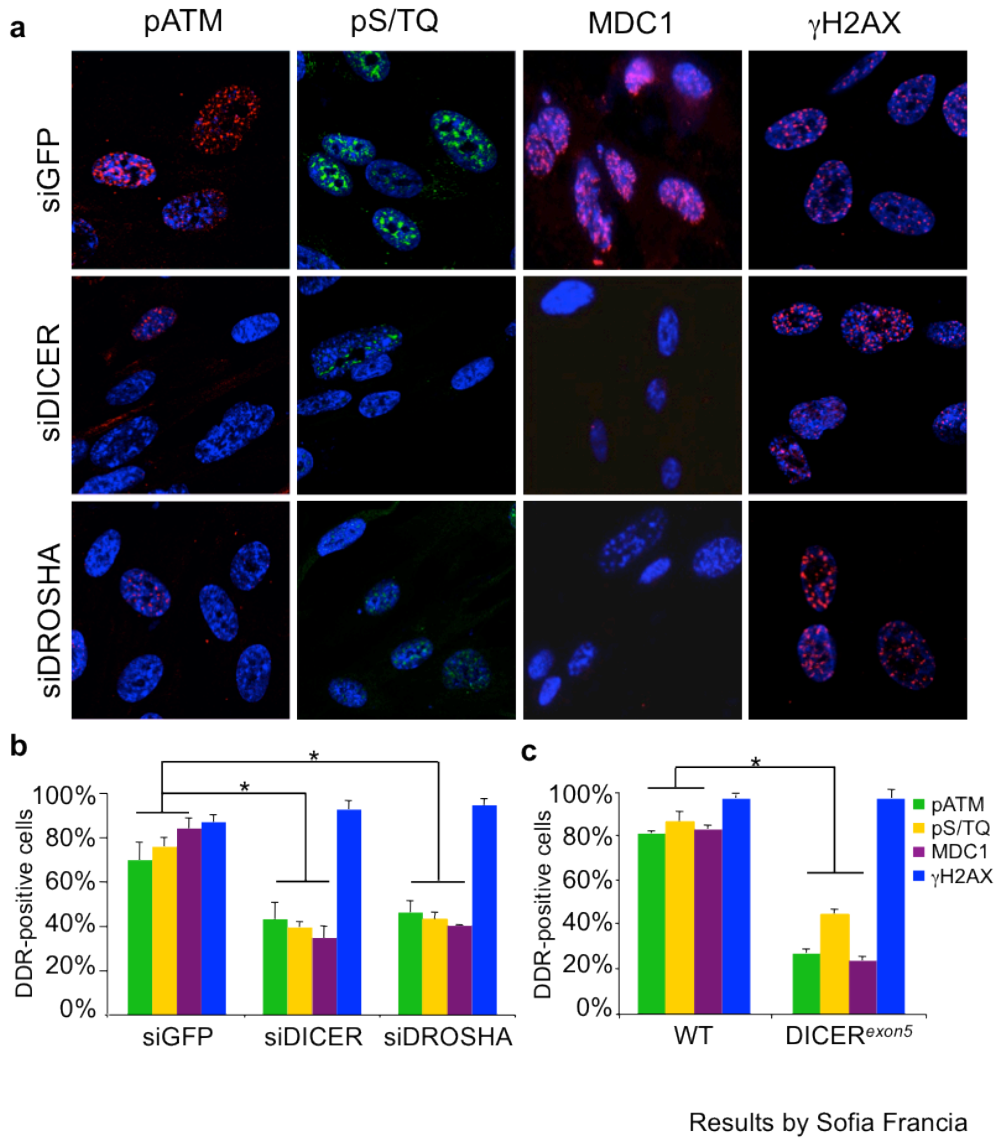


**Figure 14. DICER or DROSHA inactivation impairs DDR foci formation in irradiated cells.** **a.** WI-38 normal human fibroblasts knocked-down for DICER or DROSHA were irradiated (10 Gy), fixed 7 h later and stained for DDR markers. **b.** Histogram shows the percentage of cells positive for pATM, pS/TQ, MDC1 and γH2AX foci. **c.** Wildtype (WT) and DICER$^{exon5}$ cells were irradiated (2 Gy) and fixed 2 h later. Histogram shows the percentage of cells positive for pATM, pS/TQ, MDC1 and γH2AX foci. Error bars indicate s.e.m. (n=3). Differences are statistically significant (*p-value<0.01).

Thus, to better investigate 53BP1 behavior in the absence of DICER or DROSHA, a time course analysis was performed. At 10' post IR, a significant reduction of 53BP1 foci formation in DICER- or DROSHA-inactivated HNF became apparent (Francia et al., 2012, Supplementary Fig. 6a), suggesting that the lack of DICER or DROSHA causes a delay in 53BP1 foci formation. Similar conclusions were drawn upon the analyses of a colon cancer cell line (RKO), carrying a hypomorphic allele of DICER due to the homozygotic genetic

deletion of exon 5 in DICER (DICER$^{exon5}$), and reportedly defective in miRNA maturation (Cummins et al., 2006). Also in DICER$^{exon5}$-irradiated cells, pATM, pS/TQ and MDC1, but not γH2AX foci formation was impaired (Figure 14c), despite unaltered levels in their protein (Francia et al., 2012, Supplementary Fig. 8d). In addition, 53BP1 foci formation was delayed compared to the DICER wildtype parental cell line (Francia et al., 2012, Supplementary Fig. 8b, c).

Since inactivation of DICER and DROSHA inevitably impacts on the translational control exerted by miRNAs, it was important to distinguish the role of the two ribonucleases in DDR from their canonical function in gene expression regulation. To this aim, all the three GW182 family members, key components of the RNAi machinery involved downstream of DICER and DROSHA in mRNA translational control (Tritschler et al., 2010), were simultaneously knocked-down in HNF. Differently from DICER and DROSHA knockdown, inactivation of GW182 proteins did not impact on DDR foci formation (Francia et al., 2012, Supplementary Fig. 7).

Combined, these results reveal that DICER or DROSHA depletion impairs DDR activation induced by exogenous sources of DNA damage in a manner independent from canonical RNAi translational repression.

### *3.2 DNA damage recognition by MRE11–RAD50–NBS1 complex is affected by the lack of DICER or DROSHA*

The MRE11–RAD50–NBS1 (MRN) complex plays an important role in the initial steps of DNA damage recognition and it is necessary for ATM activation (Stracker and Petrini, 2011). To better investigate the mechanism of action of DICER and DROSHA in DNA damage detection by DDR sensors, I decided to test if the recruitment of the MRN complex to DDR foci was affected in DICER- or DROSHA-depleted cells. For this aim, I used oncogene-induced senescent (OIS) cells, because their persistent DNA damage

activation (Bartkova et al., 2006; Di Micco et al., 2006) allowed me to better visualize the association of the MRN complex to DNA lesions. I thus inactivated DICER or DROSHA by siRNA in OIS cells and 48 hours later I stained the cells for RAD50 and NBS1 subunits of the MRN complex. I observed that both RAD50 and NBS1 recruitment to DDR foci was impaired in DICER- or DROSHA-inactivated OIS cells (Figure 15). In a similar experiment, I was able to show that RAD50 recruitment to IR-induced DSBs was also weakened in irradiated HeLa cells lacking DICER (Figure 16). These data suggest that DNA damage recognition by DDR sensors, such as the MRN complex, is affected by the absence of DICER or DROSHA.

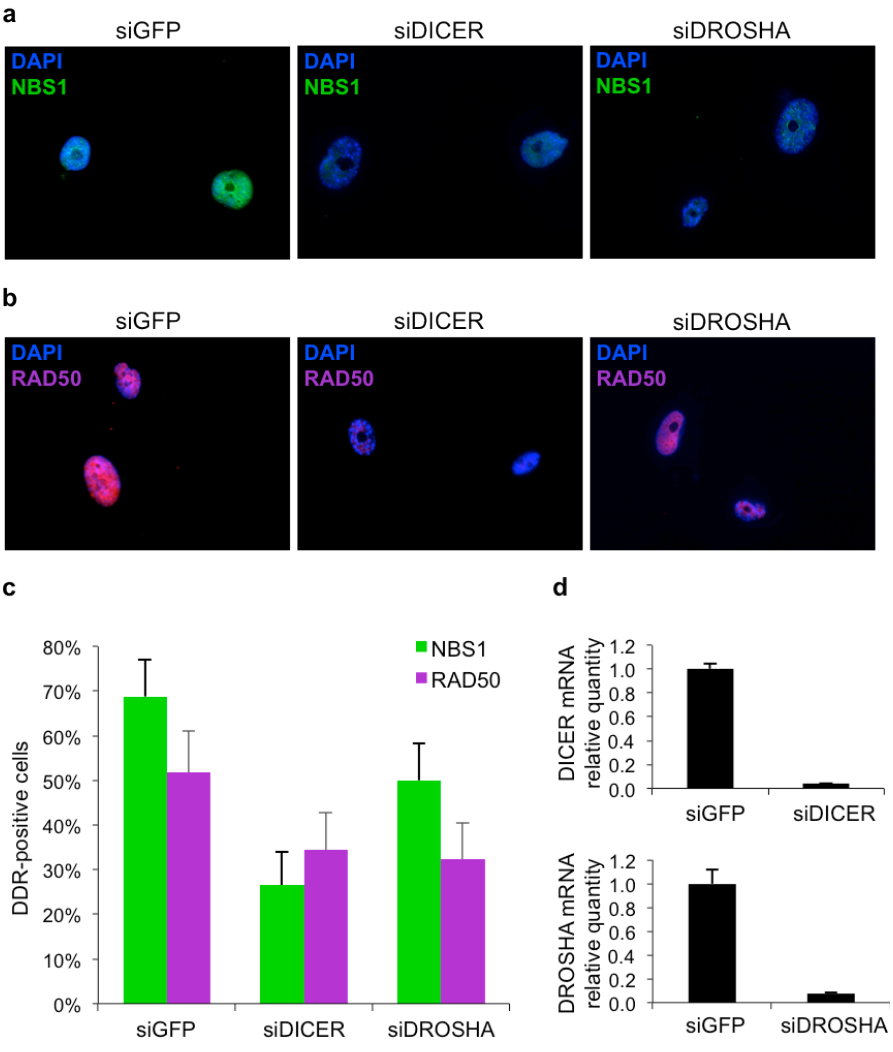


**Figure 15. DICER or DROSHA knockdown in OIS cells impairs RAD50 and NBS1 foci formation.**

**a.** OIS cells were transfected with siGFP, siDICER and siDROSHA. 48 hours later cells were fixed and stained for RAD50 and NBS1. **b**. Histogram shows the percentage of cells positive for RAD50 and NBS1 foci. Error bars indicate s.e.m. For the quantification shown around 100 cells were analyzed. **c**. Knockdown was evaluated by qRT-PCR.

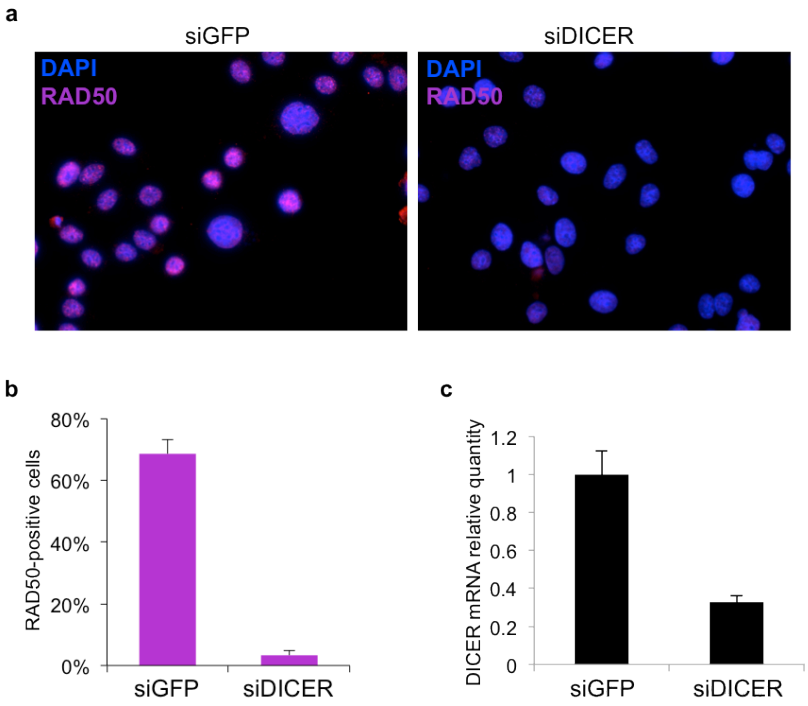


**Figure 16. DICER knockdown impairs RAD50 foci formation in HeLa cells.**
**a.** HeLa cells were transfected with siGFP or siDICER and 48 hours later were fixed and stained for RAD50. **b**. Histogram shows the percentage of cells positive for RAD50 foci. Error bars indicate s.e.m. For the quantification shown around 100 cells were analyzed. **c**. Knockdown was evaluated by qRT-PCR.

*3.3 IR-induced DDR foci are dependent on the ribonuclease activity of DICER*

To further prove the involvement of DICER in DDR activation, I transfected two different RNAi-resistant forms of DICER in DICER-depleted HeLa cells, which were subsequently irradiated (2Gy). I observed that re-expression of wildtype DICER, but not of a mutant allele (DICER*44ab*) previously shown to abolish its RNA endonuclease activity (Zhang et al., 2004), was able to rescue 53BP1 (studied at 10' post IR), MDC1 and pATM (studied at 1 h post IR) foci formation (Figure 17a, b). The efficacy of the knockdown as well as the level of re-expressed DICER cDNA were evaluated by qRT-PCR, taking advantage of 3'UTR-specific pair of primers that could discriminate between endogenous and exogenous DICER mRNA (Figure 17c). Moreover, I performed a similar experiment in DICER$^{exon5}$ cells, where the transfection of wildtype DICER, but not of the endonuclease-mutant allele DICER*44ab*, restored the DDR foci formation defects observed (Figure 14c),

making DICER$^{exon5}$ cells behave like wildtype paretal cells (Figure 18). Collectively, these data further confirm that the effects on DDR foci observed are indeed DICER dependent, but also indicate that DICER controls DDR through its capacity to process RNA.

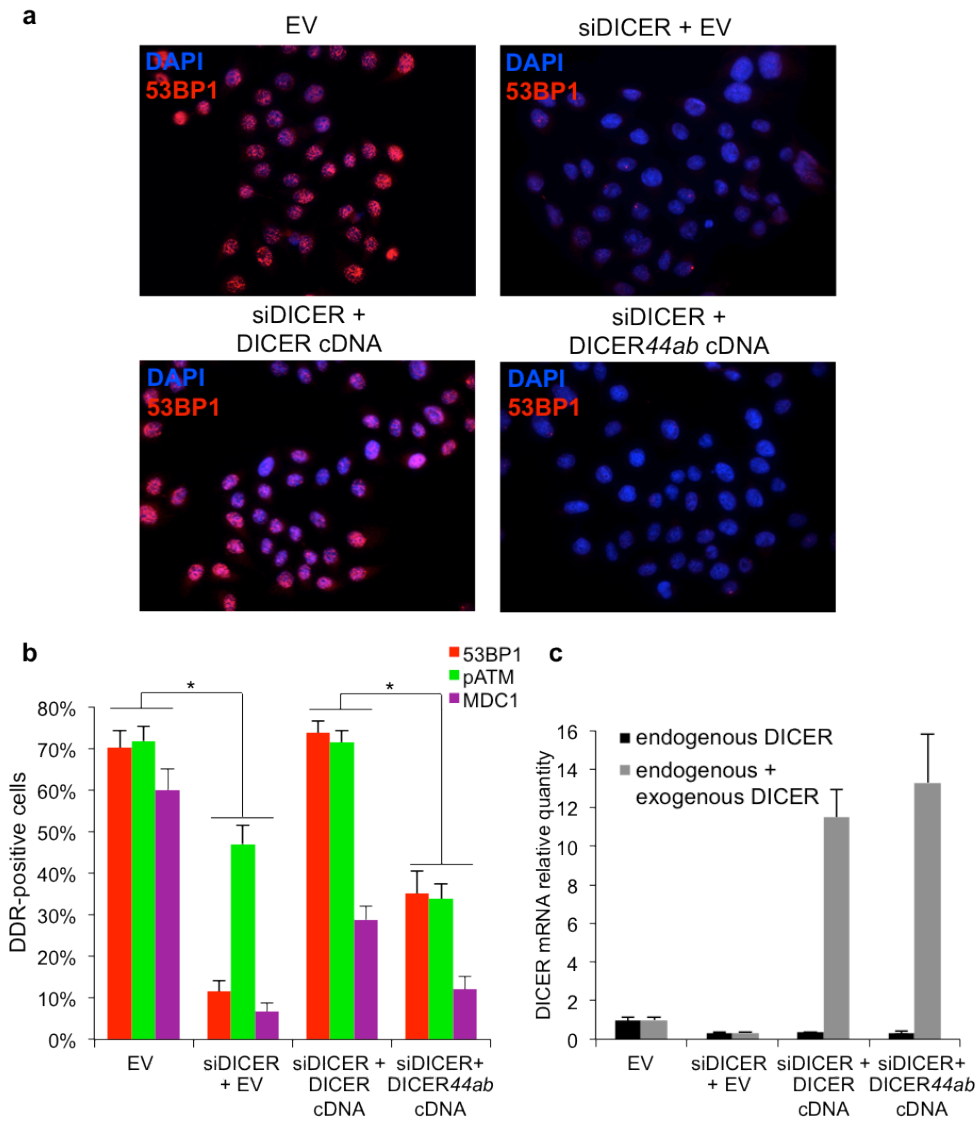


**Figure 17. DDR foci are sensitive to DICER or DROSHA knockdown and DDR foci formation is rescued by wildtype but not mutant DICER.**
HeLa cells were co-transfected with siRNA targeting the 3' UTR of DICER and either siRNA-resistant wildtype DICER or the endonuclease-mutant allele DICER*44ab* expressing plasmids. 48 hours later cells were irradiated (2Gy), fixed and stained for DDR markers. **a.** Expression of siRNA-resistant wildtype DICER, but not of the mutant allele DICER44ab lacking endonuclease activity, rescues 53BP1 foci formation defect in DICER knocked-down HeLa cells. **b.** Histogram shows the percentage of cells positive for DDR foci. 53BP1 foci formation was studied 10' post IR, pATM and MDC1 1 hour post IR. Error bars indicate s.e.m. Differences are statistically significant (*p-value<0.05). For the quantification shown around 100 cells were analyzed. **c.** Endogenous DICER knockdown and exogenous DICER overexpression were evaluated by qRT-PCR using distinct sets of primers.

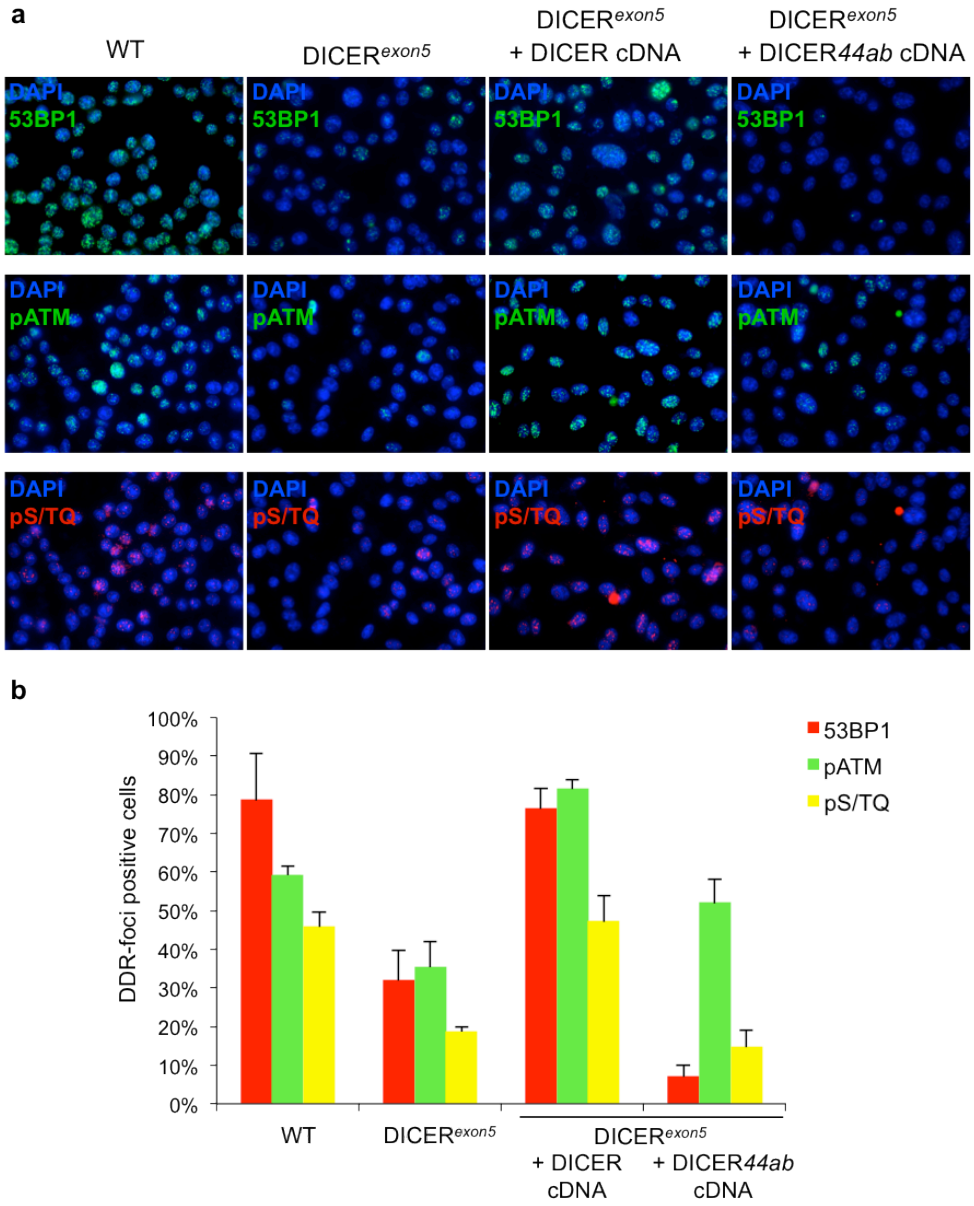


**Figure 18. Impaired DDR foci formation in *DICER*$^{exon5}$ cells is rescued by wildtype but not mutant DICER.**

*DICER*$^{exon5}$ cells were transfected either with wildtype DICER or the endonuclease-defective mutant allele DICER*44ab* expressing vectors, while parental cells were mock transfected (WT). 24 hours later cells were irradiated (2Gy), fixed and stained for DDR markers. **a.** Expression of wildtype DICER, but not the mutant allele DICER44ab, restores DDR foci formation defects in *DICER*$^{exon5}$ cells compared to parental cells (WT). 53BP1 foci formation was studied 10' after IR (2 Gy), pATM and pS/TQ 1 hour afterward. **b**. Histograms show the percentage of cells positive for the indicated DDR foci. Error bars indicate s.e.m. For the quantification shown around 200 cells were analyzed.

*3.4 DICER RNA products are required for DDR foci reformation in RNase A-treated cells*

To test if DICER enzymatic activity, and thus its RNA products, directly contributed to DDR foci formation, I extracted total RNA from wildtype and DICER$^{exon5}$-hypomorphic cells and I used these two RNA preparations to restore DDR foci in RNase A-treated irradiated cells. Total RNA preparations from the two cell lines are expected to have the same RNA molecules composition apart from the population of DICER RNA products. Strikingly, while RNA extracted from wildtype cells restored 53BP1 or pS/TQ foci, RNA extracted from DICER$^{exon5}$ cells did not (Figure 19). Importantly, RNA from DICER$^{exon5}$ cells transfected with a vector expressing wildtype DICER allowed DDR foci reformation, whereas RNA from DICER$^{exon5}$ cells transfected with a vector expressing the endonuclease-mutated form (DICER*44ab*) was unable to rescue the phenotype.

Thus, DICER involvement in DDR activation and DDR foci re-formation following RNase A treatment likely relies on its capacity to produce small RNAs necessary to control the DNA damage response.

*3.5 DICER or DROSHA inactivation impairs G1/S and G2/M DNA damage checkpoints and allows senescent cells to re-enter into cell cycle*

DNA damage elicits a DDR signal transduction, leading to checkpoint-dependent cell cycle arrest at two critical transition steps: the G1/S and the G2/M checkpoints (Jackson and Bartek, 2009). Previous work in the laboratory showed that G1/S checkpoint arrest was impaired in DICER- and DROSHA-inactivated HNF and that it was dependent on the enzymatic activity of DICER (Francia et al., 2012, Supplementary Figs. 11, 12).

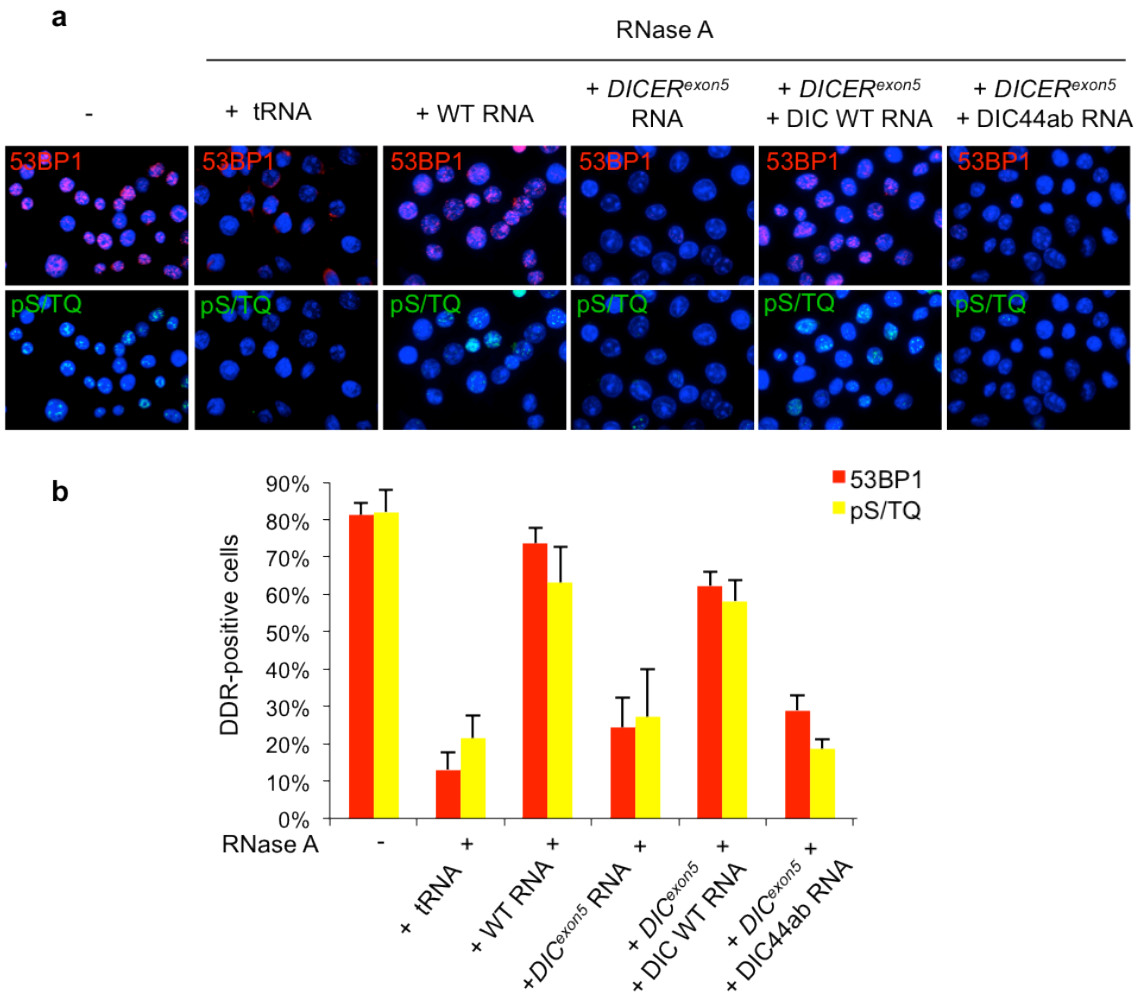


**Figure 19. DICER RNA products are required for DDR foci reformation.**
**a.** Irradiated HeLa cells were RNase A-treated and incubated with RNA extracted from the indicated cells. RNA from wildtype cells (WT RNA) or from DICER$^{exon5}$ cells transfected with WT DICER (DICER$^{exon5}$ + DIC WT RNA) allows 53BP1 foci reformation, while RNA from mock transfected DICER$^{exon5}$ cells (DICER$^{exon5}$ RNA) or from the same cells transfected with mutant DICER (DICER$^{exon5}$ + DIC 44ab RNA) does not. **b.** Histograms show the percentage of cells positive for the indicated DDR markers. Error bars indicate s.e.m. For the quantification shown more than 100 cells were analyzed.

In order to study the potential contribution of DICER activity also in G2/M checkpoint, I knocked-down its expression by siRNA transfection in HEK293 cells, in which I co-transfected an siRNA-resistant wildtype DICER. I performed a time course analysis post IR by monitoring by Fluorescence-Activated Cell Sorting (FACS) the cell cycle profiles of the different populations at the indicated time points (Figure 20a, b). As expected,

irradiated mock-transfected cells progressively accumulated in the G2 phase of the cell cycle, as a consequence of checkpoint enforcement. Differently, DICER-depleted cells did not arrest upon DNA damage and passed through the G2/M transition. The defect in G2/M checkpoint activation in DICER-knocked-down cells could be rescued by the expression of the siRNA-resistant wildtype DICER construct. Importantly, the cell cycle profiles of not-irradiated cells were similar in all the three conditions (Figure 20a, NO IR). The efficacy of the knockdown as well as the level of re-expressed DICER cDNA were evaluated by qRT-PCR (Figure 20c). Consistent with the observed G1/S checkpoint impairment, these results suggest that DICER activity is necessary also to enforce the G2/M checkpoint upon DNA damage.

OIS is a non-proliferative state, triggered by oncogene activation and characterized by a sustained DDR. It is generally understood to act as a barrier against tumorigenesis, imposed by DNA damage checkpoints (Bartkova et al., 2006; Di Micco et al., 2006). Given the results obtained in G1/S and G2/M checkpoint studies, DICER and DROSHA contribution in OIS cell cycle arrest was examined. It was observed that senescent cells require DICER and DROSHA to maintain DDR activation and cell cycle arrest: the lack of one of the two enzymes was sufficient to reduce DDR foci and to push senescent cells into S-phase (Francia et al., 2012, Supplementary Figs. 1, 2).

Overall, these observations are consistent with a model in which small RNA molecules, that from now on I will call DDR-regulating RNA or DDRNAs, are generated by DROSHA and DICER and are necessary to form IR-induced DDR foci and to establish DDR-dependent checkpoints.

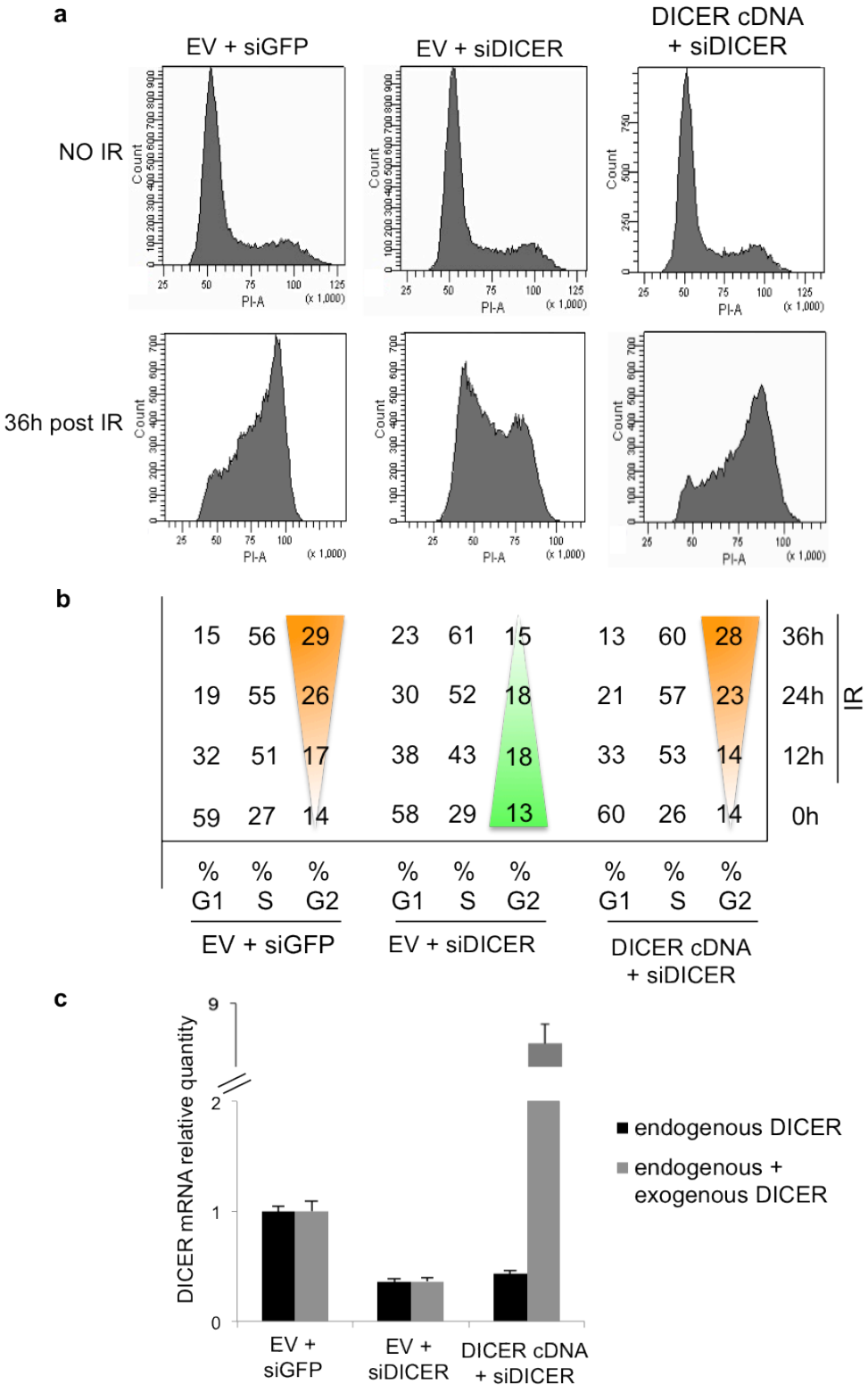


**Figure 20. Loss of G2/M checkpoint activation in DICER-inactivated cells is rescued by wildtype DICER re-expression.**

**a.** The image shows the cell cycle profiles by FACS of HEK293 cells co-transfected with the indicated combinations of siRNA and vectors (EV stands for empty vector), in not irradiated cells (NO IR) or in cells 36 hours post IR (5Gy). **b.** DICER knocked-down cells have an impaired G2/M checkpoint that can be restored upon transfection of siRNA-resistant DICER. The table shows the percentage of cells in G1, S and G2 phase of the cell cycle at different time points post IR. **c**. Endogenous DICER knockdown and exogenous DICER overexpression were evaluated by qRT-PCR using distinct sets of primers.

# 4. DDR focus formation at a defined genomic site requires damage site-specific DDRNAs that act in a translation-independent, MRN-dependent, manner

*4.1 An inducible DDR focus can disappear and reform in a RNA-dependent manner at a unique and traceable locus*

IR induces the formation of DNA lesions that are heterogeneous and randomly located in the genome. To reduce this diversity, experiments were performed in a model system in which a single DSB at a unique, defined and traceable genomic locus can be generated, a cell line named NIH2/4. NIH2/4 are NIH3T3-derived mouse cells carrying an integrated copy of the I-Sce I restriction site flanked by an array of Lac-repressor (LacR) binding sites and an array of Tet-repressor (TetR) binding sites, so that the cut consensus is in the middle between Lac and Tet elements (Soutoglou et al., 2007). In this system, the expression of the I-Sce I restriction enzyme, together with the fluorescent protein Cherry-Lac-repressor (Cherry-LacR) or YFP-Tet-repressor (YFP-TetR), allows the visualization in the nucleus of the site-specific DSB generated by the nuclease (Figure 21).

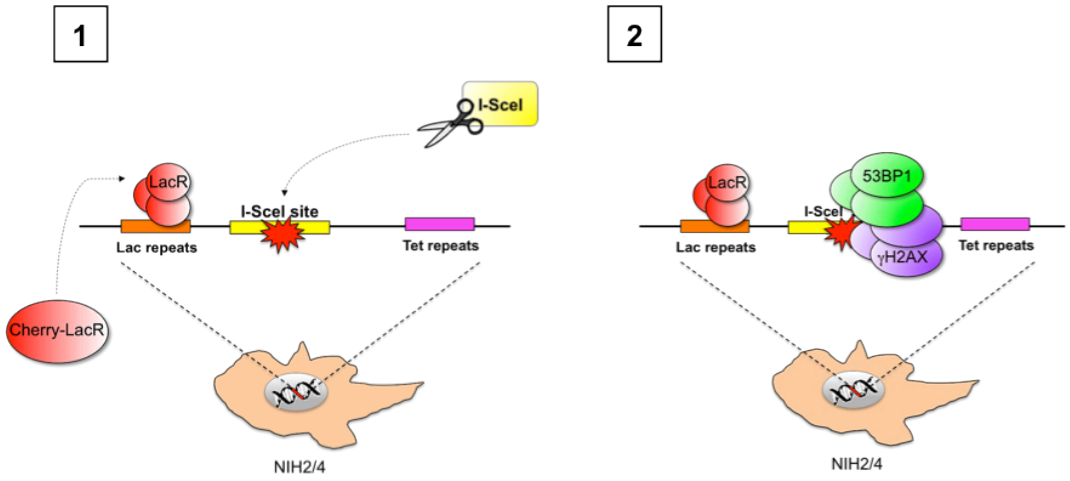


**Figure 21. An inducible DSB system at a unique and traceable locus.**
NIH2/4 are NIH3T3 cells carrying an integrated copy of the I-Sce I restriction site, flanked by an array of Lac and Tet repeats. Expression of the I-Sce I restriction enzyme and the fluorescent protein Cherry-Lac repressor (Cherry-LacR) allows the visualization in the nucleus of the locus at which the site-specific DSB is generated by the nuclease (1). After the induction of the I-Sce I cut, DDR factors accumulate at the site of damage, co-localizing with the Cherry-LacR signal (2).

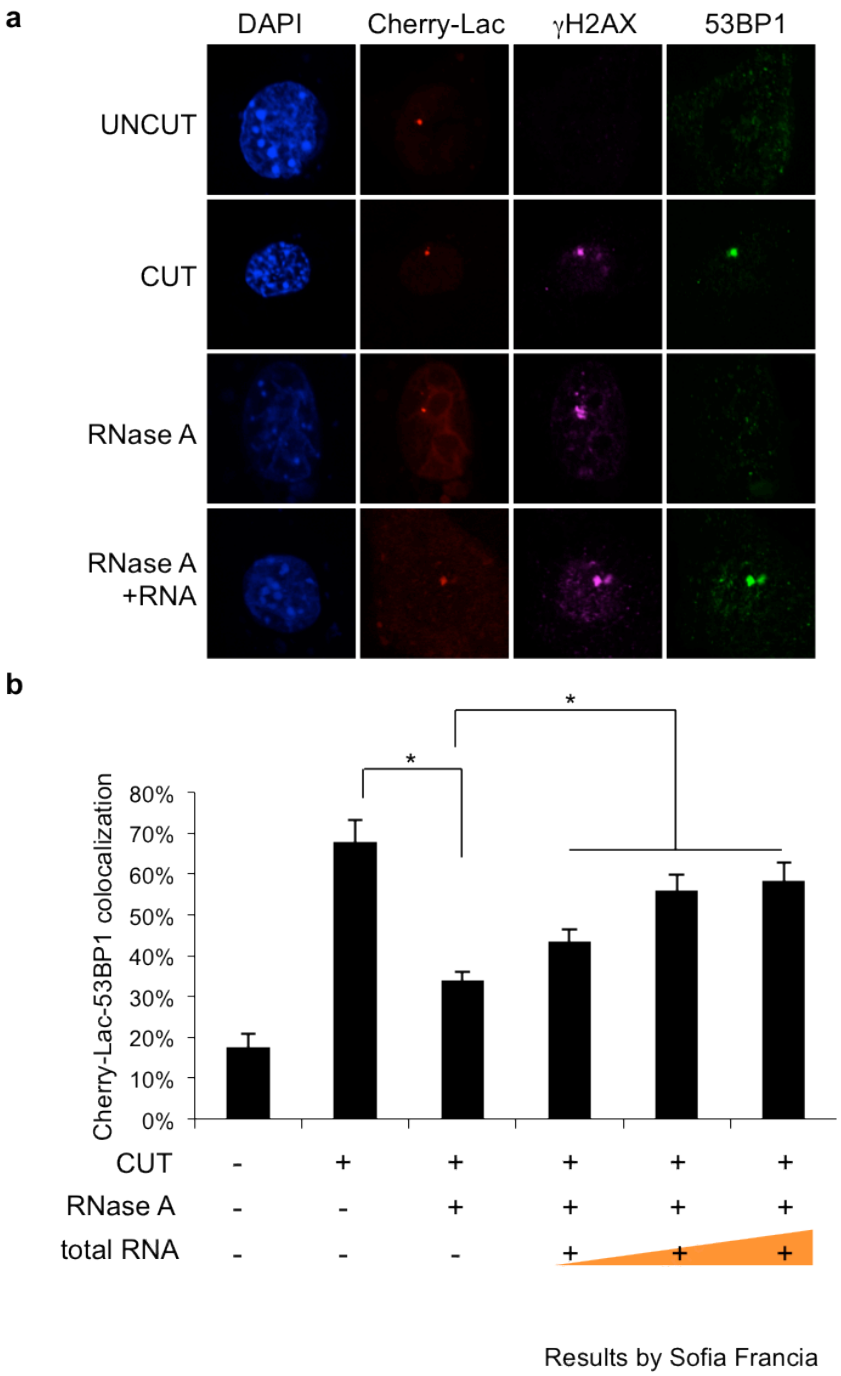


**Figure 22. A single DDR focus at a defined locus can disappear and reappear in an RNA dependent manner.**

**a.** Cut NIH2/4 cells display a 53BP1 and γH2AX focus co-localizing with the Cherry-LacR focal signal. 53BP1, but not γH2AX, focus is sensitive to RNase A and it is restored upon incubation of permeabilized cells with total RNA. **b.** Histogram shows the percentage of cells in which 53BP1 and Cherry-Lac foci co-localize. Addition of 50, 200 or 800 ng of RNA purified from cut NIH2/4 rescues 53BP1 foci formation in a dose-dependent manner.

Indeed, co-expression of I-Sce I and Cherry-LacR in NIH2/4 cells induces a 53BP1 and γH2AX focus that overlaps with a focal Cherry-LacR signal (Figure 22a). Also in this

system, RNase A treatment caused the disappearance of the 53BP1, but not γH2AX, focus at the cut site (Figure 22a). Next it was tested if total RNA re-addition, following RNase A treatment, could restore DDR focus at the I-Sce I-induced DNA lesion. Therefore, RNase A-treated NIH2/4 cells were incubated with increasing amounts of total RNA extracted from cells treated in parallel. When RNA was added to the RNase A-treated samples, NIH2/4 cells re-acquired a bright 53BP1 focus co-localizing with the Cherry-LacR, in a linear manner dependent on the RNA amount (Figure 22a, b). Therefore, the same DDR focus generated at a unique DSB can disassemble and reassemble in an RNA-dependent manner.

*4.2 DDR-regulating RNAs are site-specific*

I next investigated the origin of DDRNAs necessary for DDR focus formation. DDR-regulating RNAs may either be DDR co-factors, generated *in trans* from a distinct genomic locus or they may be generated *in cis* using the damaged genomic locus as a template (Figure 23). To discriminate between these two possibilities, NIH2/4 cells and parental cells, that do not have any exogenous sequence, were transfected with I-Sce I and the Cherry-LacR expressing vectors and RNA extracted from the two cell lines was used to attempt to restore 53BP1 focus formation in RNase A-treated NIH2/4 cells, that had experienced the I-Sce I-induced DSB. The two RNA preparations were expected only to differ in the presence of RNA transcripts potentially generated from the exogenous integrated construct, carrying the Lac and Tet repeats and the I-Sce I site (Figure 24). Excitingly, 53BP1-focus assembly on the I-Sce I-induced DSB, labeled by Cherry-LacR, was efficiently recovered only by the addition of RNA purified from NIH2/4 cells and not by RNA extracted from the NIH3T3 parental cell line (Figure 25). This result indicates that DDR-focus formation requires an RNA component, which originates from the damaged genomic locus.

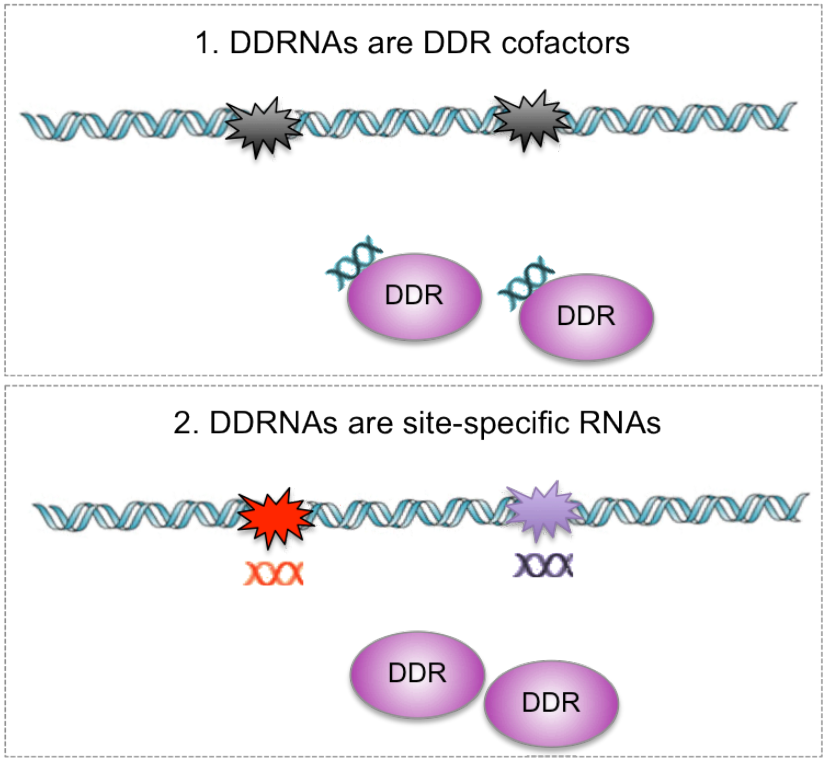


**Figure 23. Molecular mechanisms of action of DDRNAs: two alternative models.**
According to the first model shown, DDRNAs are DDR cofactors, transcribed from their genetic locus, that, upon DNA damage, associate with DDR proteins and help to DDR focus formation and DDR signaling. According to the second model, DDRNAs are site-specific RNAs, originating from the damaged sites and act locally to help DDR focus formation and DDR signaling.

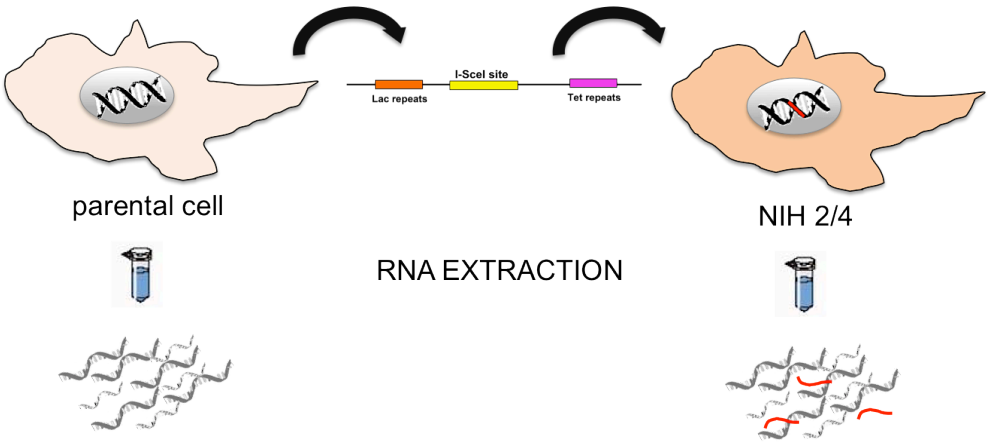


**Figure 24. Two isogenic cell lines that differ only for an integrated exogenous sequence.**
NIH2/4 cells differ from parental cells only for the presence of the Lac-I-SceI-Tet exogenous sequence. Thus the two cell lines share the same genome and the same RNA content, apart from the potential synthesis of RNAs originating from the exogenous locus (shown in red).

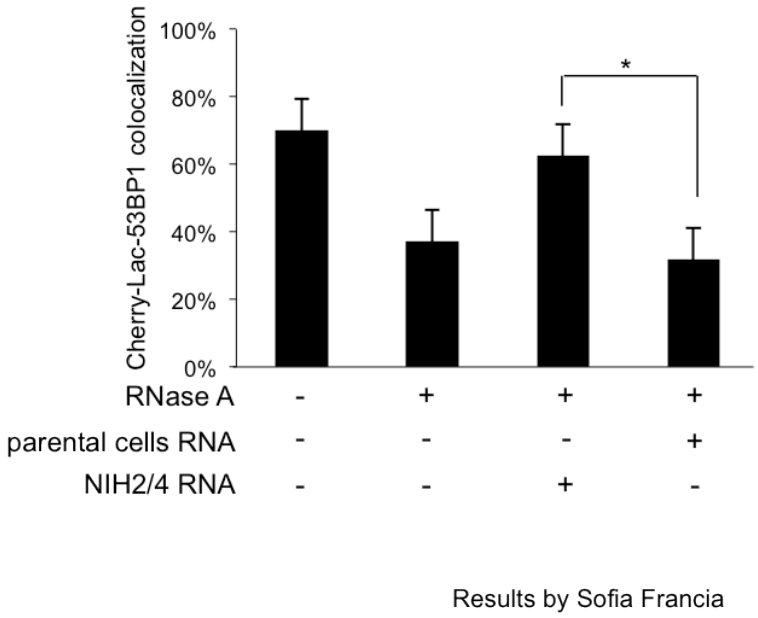


**Figure 25. DDR-regulating RNAs are site-specific.**
RNase A-treated cut NIH2/4 cells were incubated with RNA from cut NIH2/4 cells, or parental ones, to test 53BP1 focus restoration. Histogram shows the percentage of cells in which 53BP1 and Cherry-Lac foci co-localize. RNA purified from cut NIH2/4 restores 53BP1 focus, whereas RNA from parental cells expressing I-Sce I does not.

*4.3 DDR-regulating RNAs act in a translation independent manner*

Although an implication of the canonical miRNA pathway was excluded by the observation that knockdown of GW182-like proteins did not impact on DDR (Francia et al., 2012, Supplementary Fig. 7), there was still the necessity to formally reject a contribution of translation in DDRNA activity. DDRNAs, for example, could somehow impede the translation of a DDR inhibitor, thus allowing DDR foci to reform after RNase A treatment. To clearly address this issue, I complemented 53BP1 focus reformation in the presence of the translation inhibitor cycloheximide (Schneider-Poetsch et al., 2010). I observed that, although translation was inhibited by cycloheximide, the rescue of site-specific DDR focus formation still occurred, specifically by the addition of RNA from cells carrying the integrated locus and not the parental strain (Figure 26). Thus, locus-specific DDRNAs directly control DDR focus formation, independently from protein translation in the recipient cell.

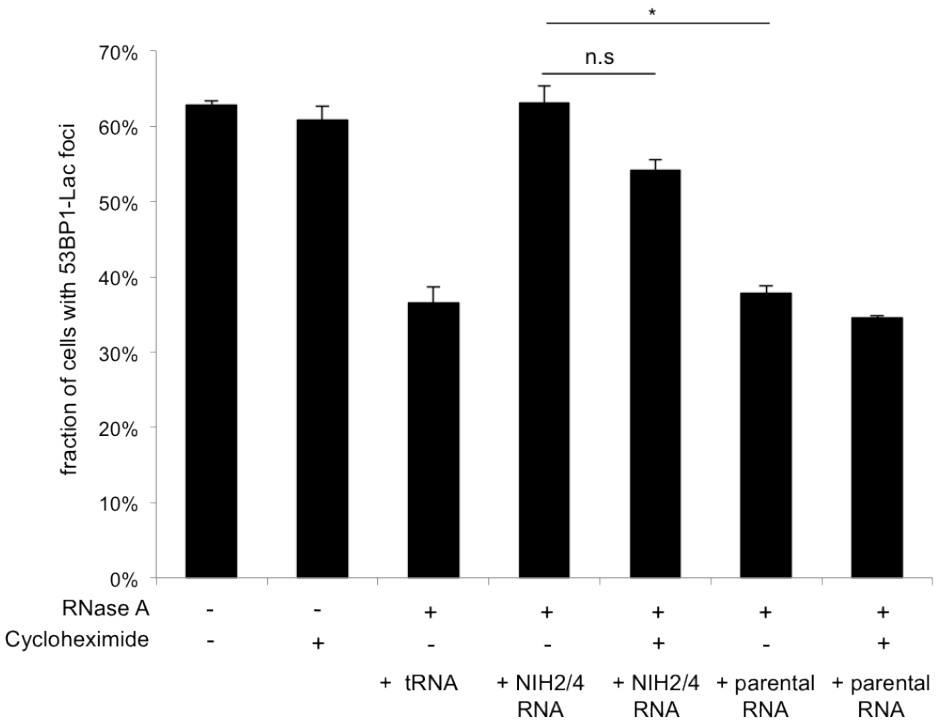


**Figure 26. The mechanism of DDR focus reformation triggered by DDRNAs is not affected by modulation of translation.**
RNase A-treated cut NIH2/4 cells were incubated with RNA from cut NIH2/4 cells, or parental ones, to test 53BP1 focus reformation in the presence of the translation inhibitor cycloheximide (50μg/ml) or DMSO. Histogram shows the percentage of cells positive for a DDR focus. Error bars indicate s.e.m. Differences labeled with * are statistically significant (*p-value<0.05; n.s. not significant).

*4.4 DDR-regulating RNAs act in an MRN-dependent manner*

In order to elucidate the possible molecular mechanism of action of DDRNAs in the DDR cascade, I decided to understand if DDRNAs were needed for full ATM activation upon DNA damage. Thus, I investigated the possible relationship between DDRNAs and the MRN complex, a key DNA damage sensor and a necessary cofactor of ATM (Stracker and Petrini, 2011). Also MRE11 focus formation upon I-Sce I induction was sensitive to RNase A-treatment, as well as ATM and 53BP1 (Figure 27). This result was in agreement with my previous observation that DICER and DROSHA knockdown reduced MRN foci in OIS and irradiated HeLa cells (Figures 15, 16). To probe the molecular mechanisms of action of RNAs at sites of DNA damage, I used mirin, a specific small molecule inhibitor of MRN (Dupre et al., 2008) that, as expected, prevented ATM activation also following I-

Sce I induction (Figure 28c). I therefore tested whether RNAs involved in DDR modulation engaged MRN: I observed that in the presence of mirin, NIH2/4 RNA was unable to induce 53BP1 or pATM focus reformation (Figure 28a, b). This result demonstrates that RNAs at sites of DNA damage modulate DDR in an MRN-dependent manner.

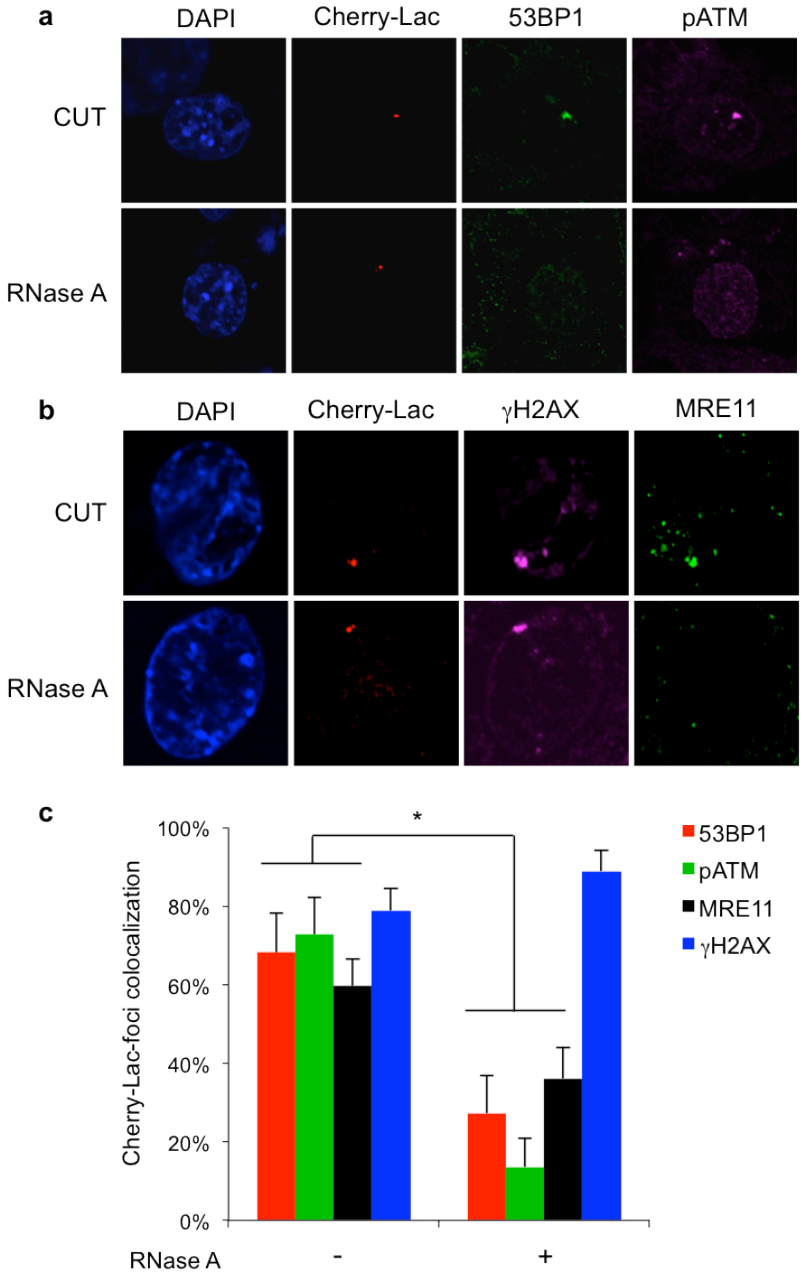


**Figure 27. pATM and MRE11 foci in cut NIH2/4 cells are sensitive to RNase A treatment.**
**a**. 53BP1 and pATM foci are lost in RNase A-treated cut NIH2/4 cells. **b**. MRE11 foci, but not γH2AX foci, are lost in RNase A-treated cut NIH2/4 cells. Error bars indicate s.e.m. (n=3). Differences are statistically significant (*p-value<0.05). **c**. Histograms show the percentage of cells in which 53BP1, pATM, MRE11 or γH2AX foci co-localize with the Cherry-Lac focus.

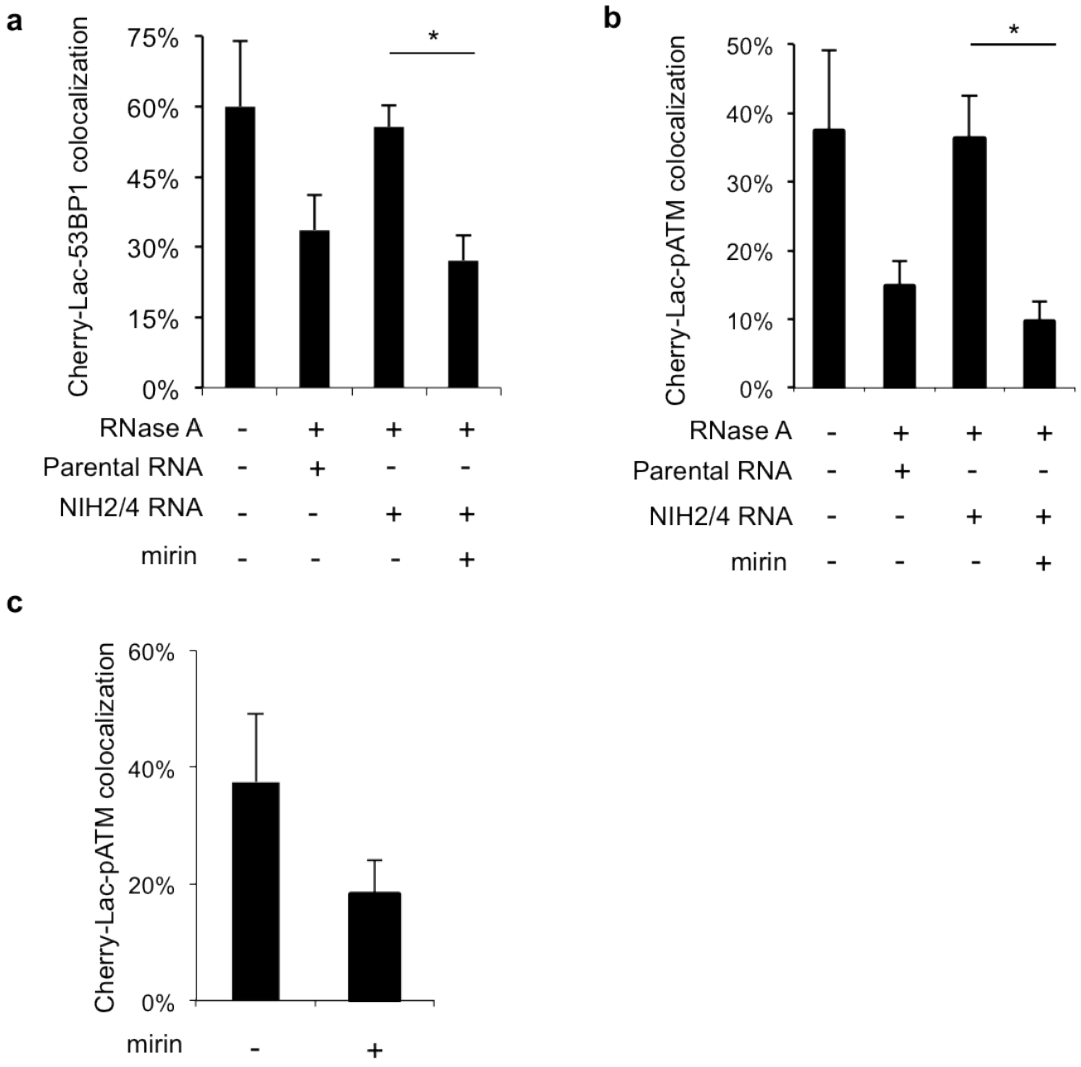


**Figure 28. Site-specific DDRNAs act in a MRN-dependent manner.**

**a, b.** RNase A-treated cut NIH2/4 cells were incubated with RNA from cut NIH2/4 cells, or parental cells, to test 53BP1 or pATM focus reformation in the presence of the MRN inhibitor mirin (100 μM). Histogram shows the percentage of cells positive for a DDR focus. Error bars indicate s.e.m. (n=3). Differences are statistically significant (*p-value<0.05). **c**. Mirin (100 μM) impairs pATM activation at the I-Sce I-induced DSB. Histogram shows the percentage of cells in which pATM focus co-localized with the Cherry-Lac focus. For the quantification shown around 50 cells from two independent experiments were analyzed.

## 5. DDR-regulating RNAs are DNA damage site-specific DICER and DROSHA products

*5.1 DICER and DROSHA are necessary for the generation of DDRNAs in NIH2/4 cells*

I next proceeded to demonstrate a direct role for DICER and DROSHA in generating the active RNA species, trying to uncouple this new DDR-regulating activity from their well-known function in the modulation of mRNA translation. I extracted total RNA from NIH2/4 cells expressing the I-Sce I enzyme and an empty vector (EV) or plasmids carrying short hairpin RNA against mouse DICER (shDICER) or DROSHA (shDROSHA). These different RNA preparations were used to rescue RNase A-driven disappearance of the site-specific focus in NIH2/4 cells, expressing I-Sce I together with Cherry-LacR. As expected, tRNA and RNA purified from parental cells failed to restore 53BP1 and pATM foci at the DSB site, while RNA extracted from cut NIH2/4 succeeded (Figure 29). Interestingly, RNA extracted from NIH2/4 cells lacking DICER or DROSHA was unable to allow focus reformation, strongly suggesting a direct role for the two ribonucleases in the generation of the active molecules that regulate DDR. Importantly, this phenotype could not be due to the lack of miRNA in the RNA preparations coming from DICER- or DROSHA-depleted cells, since the recipient RNase-treated cells had no target mRNAs. Thus, under these conditions I could uncouple DICER and DROSHA role in translational repression from their function in DDR activation.

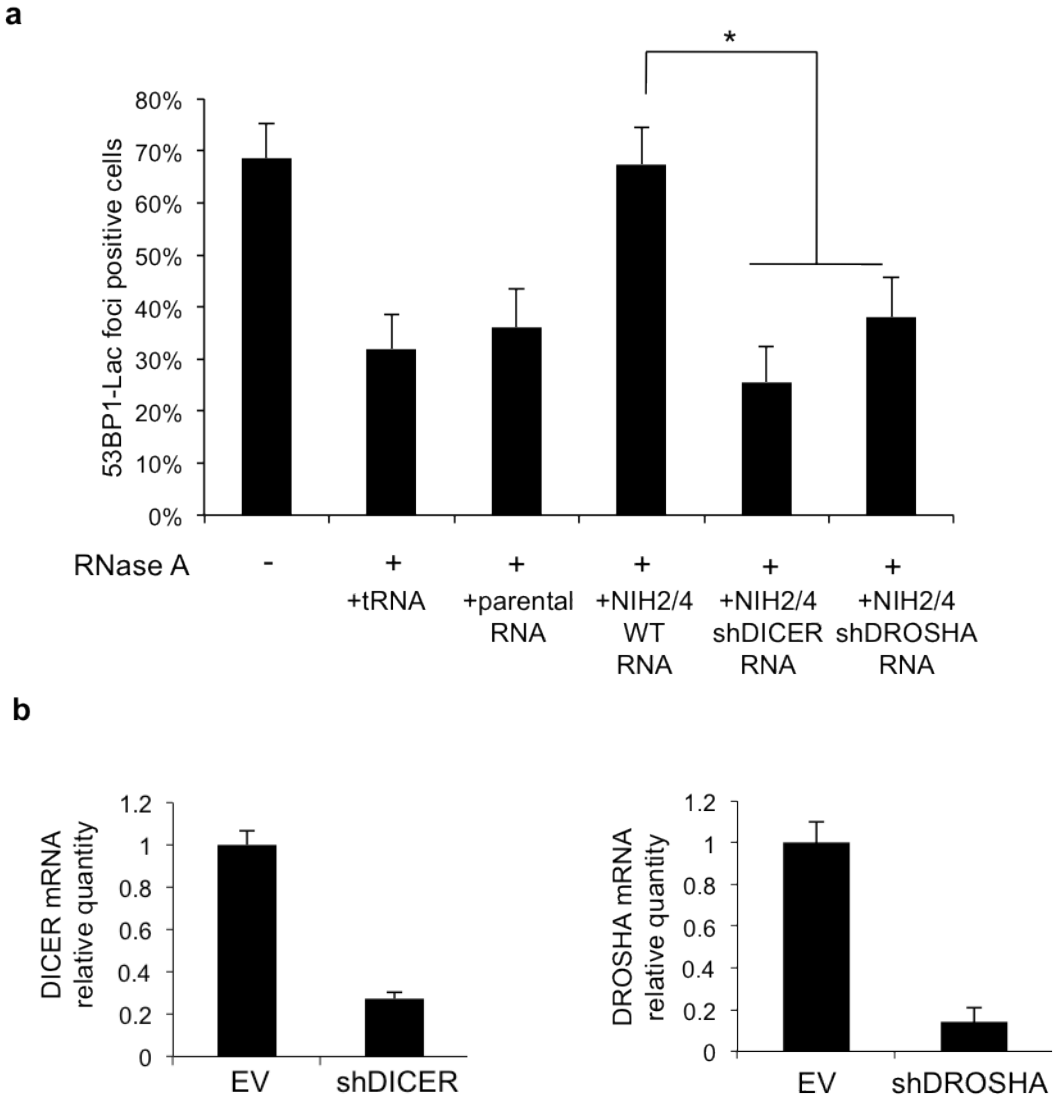


**Figure 29. Site-specific RNAs that allow reformation of DDR foci in RNase A-treated cells are DICER and DROSHA dependent.**

**a.** NIH2/4 cells were transfected with either an empty vector (EV) or shDICER and shDROSHA expressing vectors. After 48 hours, the I-Sce I endonuclease was expressed and 24 additional hours later total RNA was extracted. Cells co-transfected with Cherry-Lac and I-Sce I were treated (+) or not (-) with RNase A, incubated with different RNA preparations, fixed and stained for 53BP1. Histogram represents the quantification of 53BP1 focus co-localizing with Cherry-Lac focus in the indicated conditions. Error bars indicate s.e.m. (n=2). Differences are statistically significant (*p-value<0.02). **c.** qRT-PCR analysis of NIH2/4 transfected with an empty vector (EV) or shDICER and shDROSHA expressing vectors, 48h post transfection.

*5.2 DDRNAs are not detectable by Northern blot analysis*

In order to actually visualize DDRNAs, I decided to perform a Northern blot analysis of RNA extracted from NIH2/4 cells. Given that DDRNAs in NIH2/4 have the sequence of the exogenous locus, I used the entire Lac-I-SceI-Tet locus as probe for Northern blot (Figure 30a). I first controlled that my total RNA preparations, both from parental and NIH2/4 cells uncut or cut, were DNA-free by PCR (Figure 30b), and then I loaded 20 μg of total RNA on a denaturing 12% polyacrylamide gel (Figure 31a). The RNA was electrically transferred on a membrane which was then incubated overnight with ($\alpha$-$^{32}$P)ATP-labeled Lac-I-SceI-Tet probe, washed and then exposed to a radiographic film. Unfortunately, I could not observe any specific signal in the NIH2/4 samples compared to the parental ones (Figure 31b), whereas the positive control probes for U6 snRNA (107 nt) and Let7a miRNA (22 nt) gave a clearly visible signal at the correct height (Figure 31c).

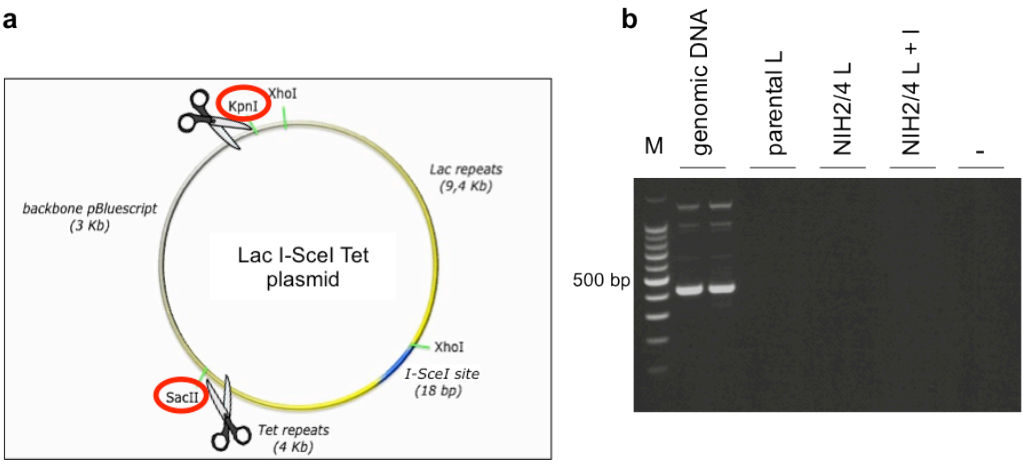


**Figure 30. Probe generation for Northern blot and testing for DNA contamination of RNA preparations.**

**a.** The ~14Kb probe for Northern blot was generated by cutting out the entire Lac-I-SceI-Tet locus from the same plasmid used to derive NIH2/4 cells. The restriction enzymes used are highlighted with red circles. **b.** Total RNA was extracted from parental cells transfected with Cherry-Lac vector (L) and from NIH2/4 cells transfected with Cherry-Lac vector alone (L) or Cherry-Lac and I-Sce I expressing vectors (L+I). DNA contamination of the RNA preparations was evaluated by PCR using primers for the mouse genomic locus *Rosa26* and the amplification products were run on agarose gel. 50ng of genomic DNA were used as positive control. Buffer alone was used as negative control (-).

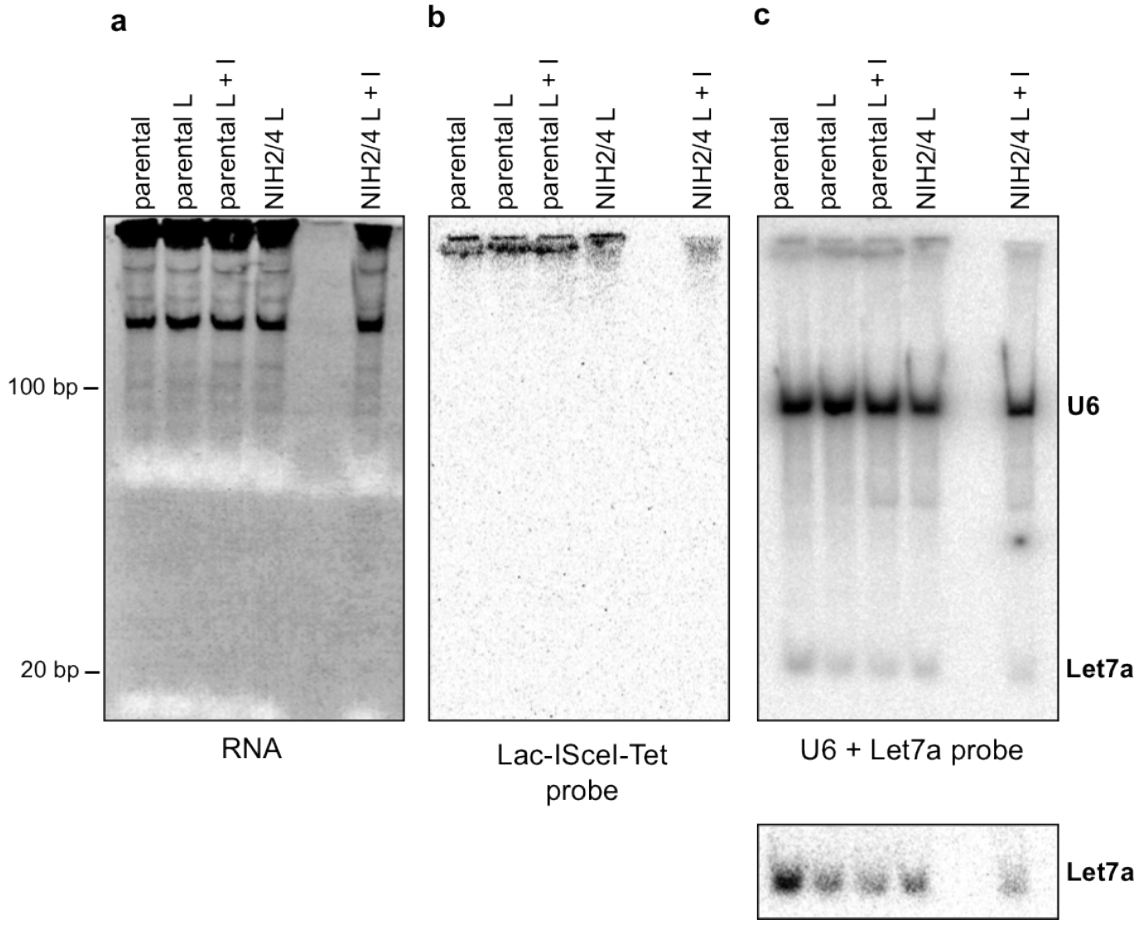


**Figure 31. Northern blot analysis of total RNA from NIH24 cells does not show any specific signal of RNA transcripts at the locus upon cut.**

Total RNA was extracted from parental cells untransfected and from parental and NIH2/4 cells transfected with Cherry-Lac vector alone (L) or Cherry-Lac and I-Sce I expressing vectors (L+I). 20μg of total RNA were loaded on a denaturing 12% polyacrylamide gel. **a.** The image shows the gel analysis of RNA stained with GelRed. **b.** The RNA was electrically transferred to a Hybond-N membrane and incubated with a radioactively-labeled ($\alpha$–$^{32}$P)dATP Lac-I-SceI-Tet DNA probe and, after washing, exposed to a radiographic film overnight at -80°C. **c.** The membrane was incubated with radioactively-labeled probes for control small RNAs, ($\alpha$–$^{32}$P)dATP U6 RNA (107nt) and ($\gamma$–$^{32}$P)dATP Let7a miRNA (22nt), and then exposed to a radiographic film overnight at -80°C. The lower panel shows a longer exposure of the Let7a-probed membrane.

To enrich for DDRNAs, I decided to use small RNA preparations (< 200nt), selected by chromatography. I first checked the purity of my small RNA by running in parallel 20 μg of total RNA and 2 μg of small RNA on a 3% agarose gel, blotting and probing for U6 snRNA, as control for small RNA, and β-actin mRNA, as control for long RNA (Figure 32a). The U6 signal was twice as strong in the small RNA fraction compared to the total

RNA fraction (Figure 32b). Since I loaded 10 times less small RNA on the gel, I concluded that, by this chromatographic procedure, small RNAs were enriched 20 times and that they were effectively devoid of long RNAs, as shown by hybridization with a β-actin probe (Figure 32c). I then resolved in parallel 20 μg of total RNA and 8 μg of small RNA (corresponding to 160 μg of total RNA) of parental and NIH2/4 cells uncut or cut on a denaturing 12% polyacrylamide gel (Figure 33a). After blotting, I incubated the membrane overnight with ($\alpha$-$^{32}$P)ATP labeled Lac-I-Sce-I-Tet probe in less stringent washing conditions (see Materials and Methods). Also in this case I could not see a specific signal in the NIH2/4 samples compared to the parental ones (Figure 33b). Thus, Northern blot technique is not sensitive enough to visualize DDRNAs, probably because they are low abundance RNA species.

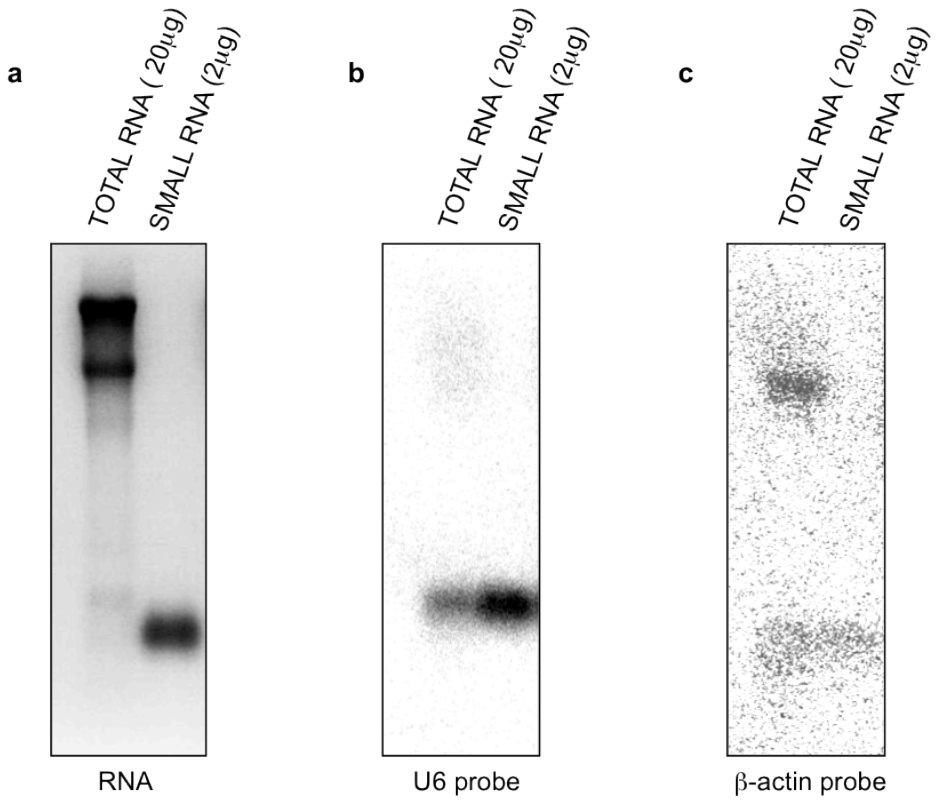


**Figure 32. Small RNA fraction is enriched for RNAs below 200nt in length and it is devoid of longer RNA.**

20μg of total RNA and 2μg of small (<200nt) RNA were loaded on a 3% agarose gel. **a.** The image shows the gel analysis of RNA stained with GelRed. **b, c.** The RNA was transferred by capillarity to a Hybond-N membrane and incubated with radioactive ($\alpha$–$^{32}$P)dATP probe for U6 RNA or ($\alpha$–$^{32}$P)dATP probe for β-actin and then exposed to a radiographic film overnight at -80°C.

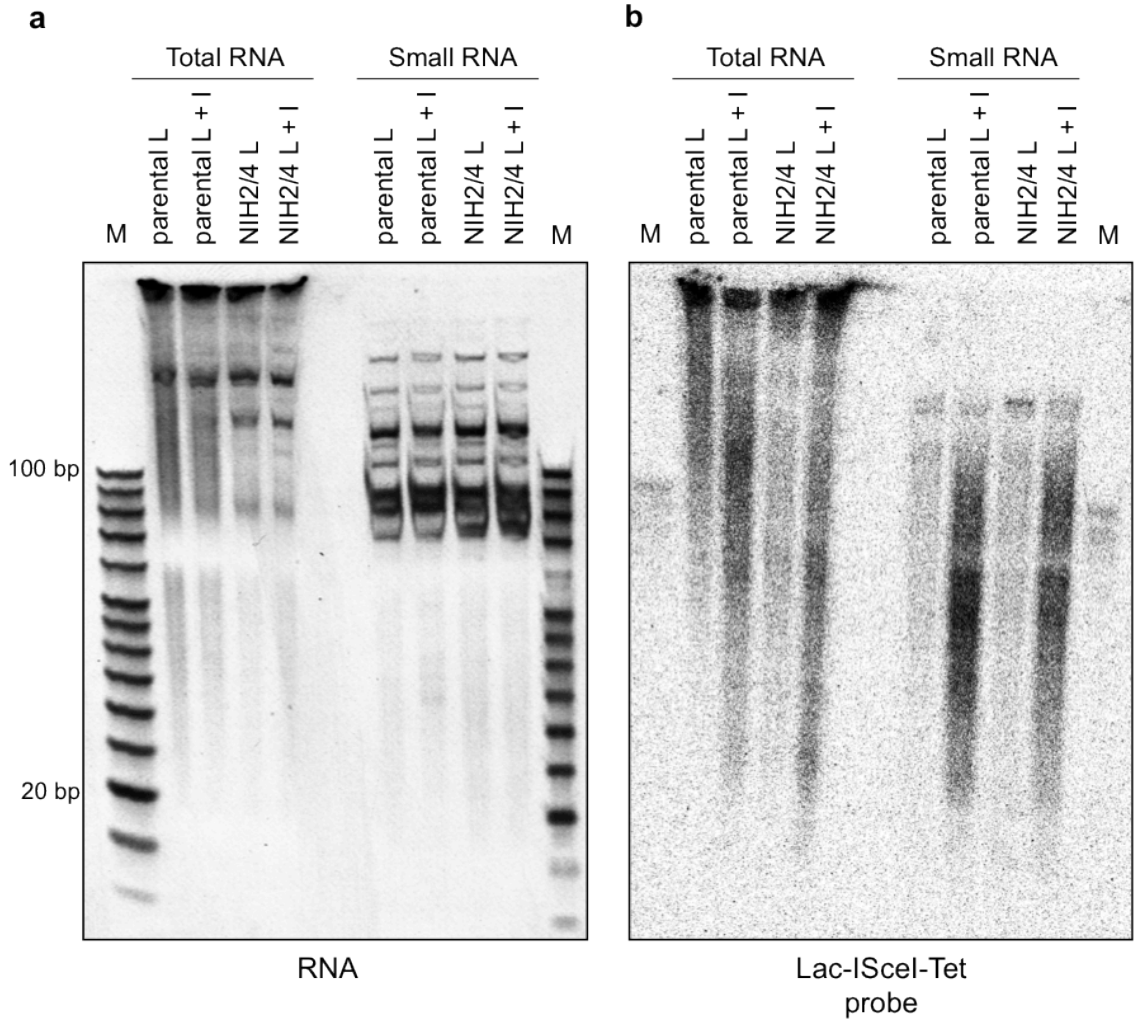


**Figure 33. Northern blot analysis of small RNA from NIH2/4 cells does not identify any specific signal of DDRNAs upon cut.**
Total and small (<200 nt) RNA fractions were extracted from parental and NIH2/4 cells transfected with Cherry-Lac vector alone (L) or Cherry-Lac and I-Sce I expressing vectors (L+I). 20μg of total RNA and 8μg of small RNA were loaded on a denaturing 12% polyacrylamide gel. **a.** The image shows the gel analysis of RNA stained with GelRed. **b.** The RNA was electrically transferred on a Hybond-N membrane and incubated with a radioactively-labeled ($\alpha$–$^{32}$P)dATP Lac-I-SceI-Tet probe under low stringency conditions and then exposed to a radiographic film overnight at -80°C.

*5.3 Deep sequencing of nuclear small RNA reveals a peak of DDRNAs around 22-23 nt that is DICER dependent*

To better characterize DDRNAs I decided to use a technique that can reveal also low abundant RNA species: next generation sequencing (NGS). To obtain the maximum DDRNA enrichment, I extracted small RNAs from the nucleus of parental cells transfected

with I-Sce I (mock) and NIH2/4 cells transfected with Cherry-LacR (uncut) or I-Sce I (cut) (Figure 34).

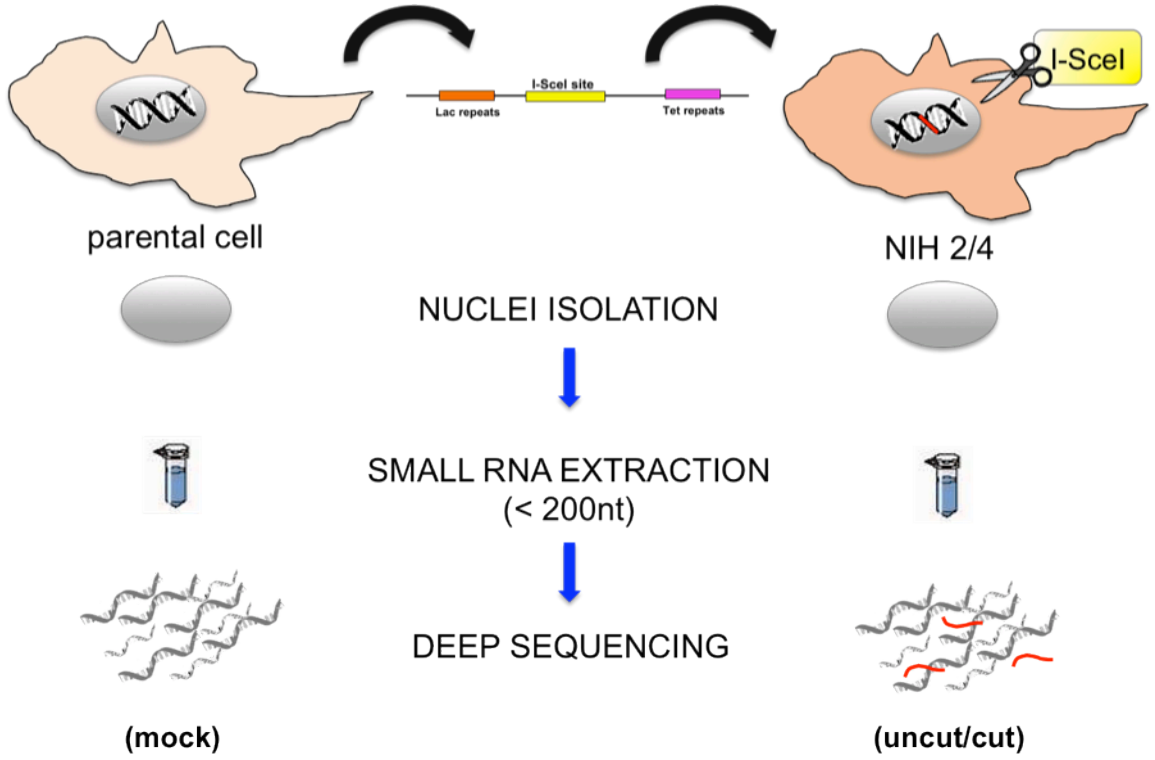


**Figure 34. Small nuclear RNA preparation for next generation sequencing.**
**a.** NIH2/4 cells were infected with lentiviral particles carrying pLKO (empty vector), shDICER or shDROSHA vectors. After 48 hours cells were superinfected with Adeno Empty Vector or Adeno I-Sce I. Nuclei were isolated the day after the adenoviral infection. Nuclear RNA shorter than 200 nt was purified from parental and either wildtype or DICER/DROSHA-depleted NIH2/4 cells, cut or uncut, by the use of the mirVanaTM microRNA Isolation Kit. High quality RNA and cDNA libraries were prepared and sequencing was performed on Illumina Hiseq Version 3.

Before NGS nuclear small RNAs were tested for activity in RNase A treated NIH2/4 cut cells. I observed that just 20 ng of the small nuclear RNA fraction were sufficient to restore DDR focus formation, while 800 ng of total RNA were necessary to restore it to the same extent (Figure 35). On the contrary, 800 ng of parental RNA were not able to rescue 53BP1 focus formation. On the ground of these results, I estimated that the small nuclear RNA fraction was enriched 40 folds for active RNAs in comparison with total RNA.

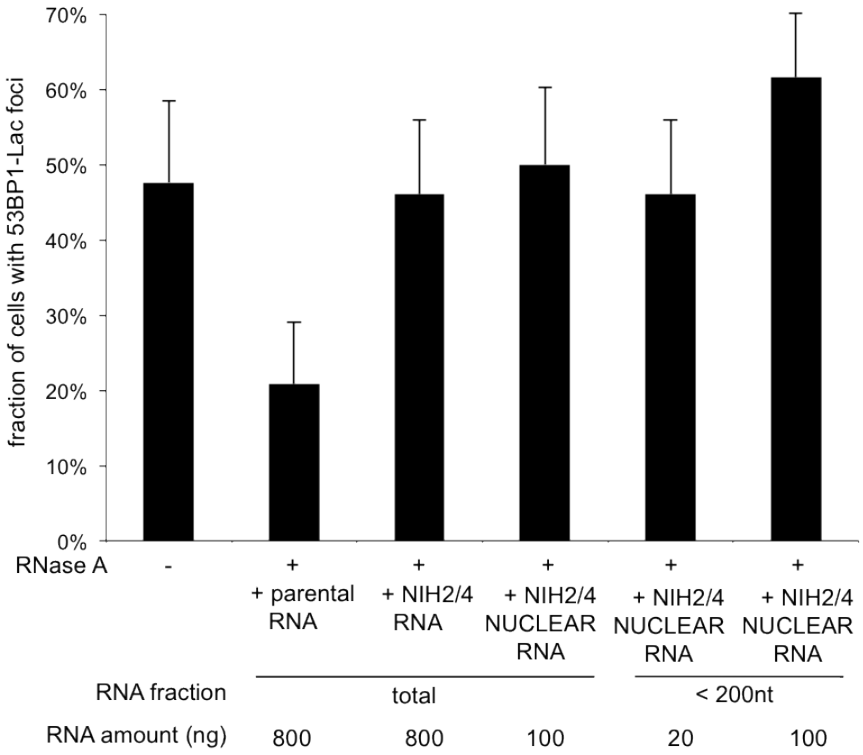


**Figure 35. Small nuclear RNA fraction is more active in restoring 53BP1 focus formation compared to total RNA in RNase-treated cells.**

**a.** Cellular and nuclear RNA, either the total or the small (<200 nt) fractions were extracted from NIH2/4 wildtype cut cells and used at the indicated amounts to allow 53BP1 focus re-formation after RNase A treatment in NIH2/4 cut cells. 20ng of the small nuclear RNA fraction were sufficient to allow DDR focus reformation, while 800ng of total RNA were necessary to restore it to the same extent. Thus, selecting small RNA from nuclei enriches 40 fold for RNAs active in DDR foci reformation compared to total RNA.

I sent these small nuclear RNAs from the parental and uncut or cut NIH2/4 cells to our collaborator Piero Carninci at RIKEN Institute in Japan for deep sequencing. Libraries prepared from these samples were sequenced by Illumina GAII-X to obtain 15-32 nt reads. Analysis of the libraries revealed 47 reads arising from the exogenous locus in cut cells, 20 reads in uncut cells and none in the parental cells (Figure 36). Moreover, a slight strand bias in the abundance of DDRNAs was observed: the majority of the reads were present in the Tet upper strand and in the Lac lower strand (Figure 36). Finally, DDRNAs showed a significant nucleotide bias for A/U at the 5' start site (80%) and G at the 3' end site (55%) distinct from the base composition of the locus (data not shown). Thus, although low abundant, DDRNAs can be detected by deep sequencing.

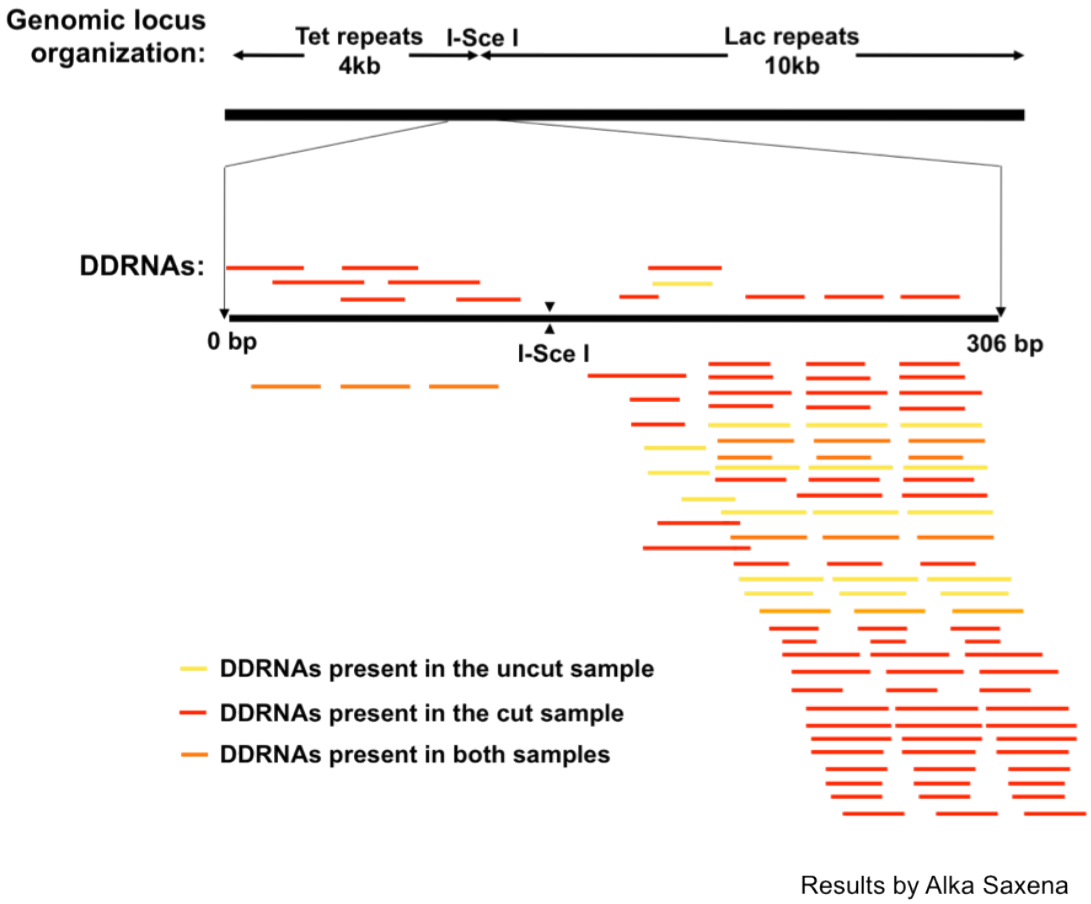


**Figure 36. Distribution of DDRNA reads along the locus sequence.**
The organization of the entire 14 Kb locus is shown in the top panel and a zoom-in view of the distribution of sequenced tags along the region around the I-Sce I recognition site is shown in the bottom panel. RNAs from the uncut sample are in yellow, those from the cut sample are in red and those present in both samples are in orange.

Taking advantage of the NGS approach, I tried to shed light onto DDRNAs biogenesis. I extracted small nuclear RNA from cut and uncut wildtype as well as DICER or DROSHA knocked-down NIH2/4 cells and I sent these samples to our collaborators for a novel round of deeper sequencing with Illumina HiSeq V3. For the generation of DICER and DROSHA knockdown, NIH2/4 cells were infected with lentiviral particles carrying pLKO.1 (wildtype), shDICER or shDROSHA vectors. 48 hours later cells were superinfected with Adeno Empty Vector (uncut) or Adeno I-Sce I (cut) and nuclei were isolated the day after the adenoviral infection. DICER or DROSHA knockdown (Figure 37a) as well as the percentage of I-Sce I cut cells (Figure 37b) were checked before NGS.

As expected, DICER or DROSHA knockdown significantly reduced reads mapping to the known miRNAs (Francia et al., 2012, Supplementary Fig. 22).

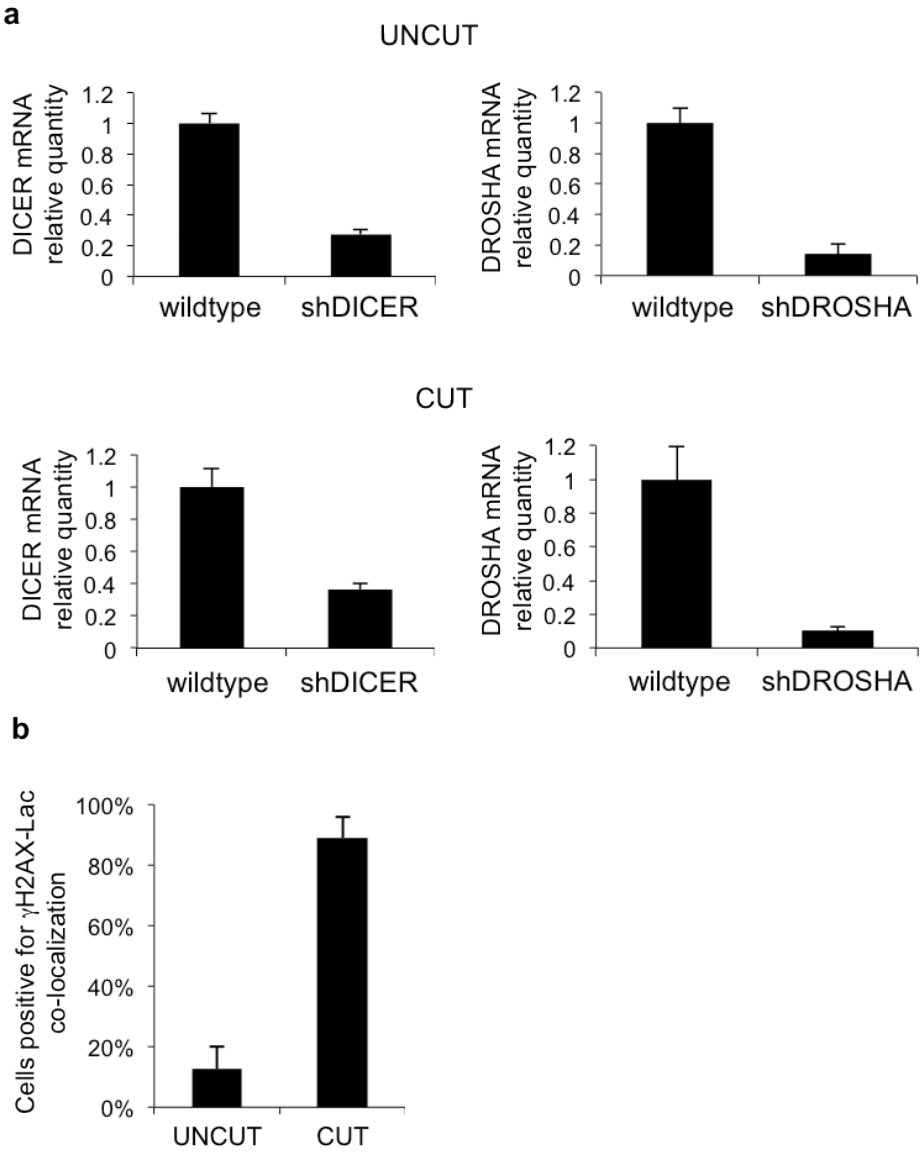


**Figure 37. DICER and DROSHA knockdown and I-Sce I cut controls.**
**a.** NIH2/4 cells were infected with lentiviral particles carrying pLKO (wildtype), shDICER or shDROSHA vectors. After 48 hours cells were superinfected with Adeno Empty Vector or Adeno I-Sce I. RNA was isolated the day after the adenoviral infection. DICER and DROSHA knockdown with respect to pLKO-infected cells (wildtype) by shRNA in uncut and cut samples was evaluated by qRT-PCR. **b.** Histogram shows the percentage of pLKO-infected NIH2/4 cells (wildtype), superinfected with Adeno Empty Vector (uncut) or Adeno I-Sce I (cut), in which γH2AX focus co-localized with the Cherry-LacR signal. For the quantification shown around 30 cells were analyzed.

The statistical analyses revealed that the percentage of 22-23 nt RNAs arising from the locus significantly increased in the wildtype cut sample compared to the uncut one (Figure 38a, b). Moreover, DICER inactivation significantly reduced the peak of 22-23 nt tags mapping to the locus in both cut and uncut samples; the detectable decrease in DROSHA-inactivated cells did not reach statistical significance (Figure 38a, b). Confirming the data of the previous deep sequencing, 22–23-nucleotide RNAs at the locus showed a clear nucleotide bias toward A or U at their 5' and a G at their 3' end (Figure 38c). These results clearly demonstrate that 22-23nt site-specific DDRNAs increase upon cut and are generated by DICER.

*5.4 DDRNAs generated in vitro by a recombinant DICER are sufficient to restore DDR foci*

In order to prove the biological activity of locally generated DICER RNA products, I cloned the Lac-I-SceI-Tet locus, and an unrelated control DNA, in a plasmid to allow transcription of both strands by T7 polymerase (Figure 39a), and I processed the resulting double-stranded RNAs with commercially available recombinant DICER protein, *in vitro*. The resulting small RNAs (Figure 39b) were purified and tested in RNase A-treated NIH2/4 cells, mixed with an inert RNA such as tRNA or with RNA from parental cells. I observed that locus-specific DICER-generated RNAs, but not equal amounts of control RNAs, allowed DDR focus reformation, both when mixed with RNA from parental cells (Figure 39c) or yeast tRNA (Figure 39d). Thus, *in vitro*-generated DICER RNA products are sufficient to allow DDR focus reformation in a sequence-specific manner, in absence of any other transcript in the recipient cell.

Overall, these results indicate that DDRNAs are DICER RNA products, 22-23 nucleotides in length, with the sequence of the damaged locus and that they play a direct role in DDR activation.

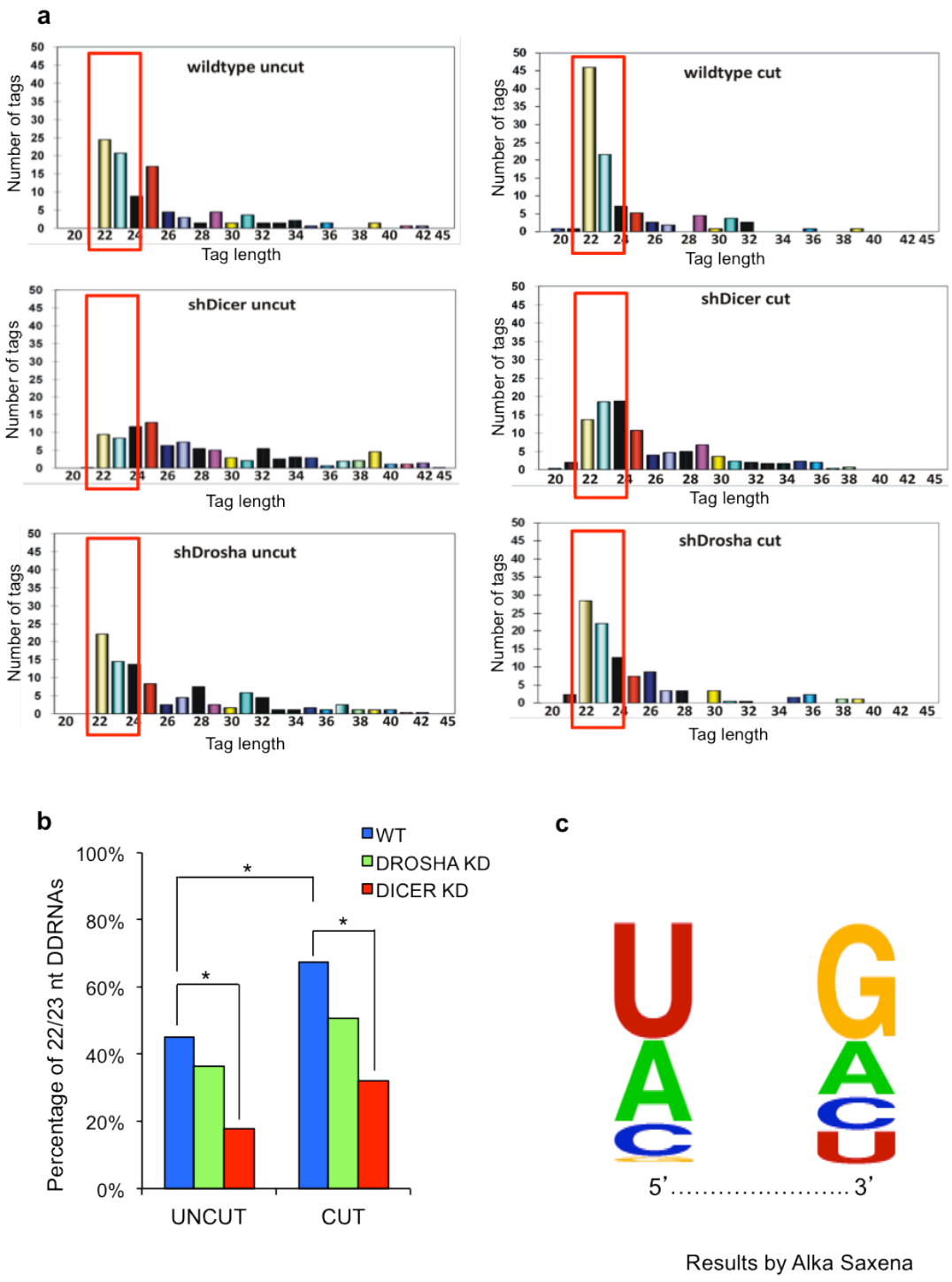


**Figure 38. DDRNAs arising from the locus are DICER (and DROSHA) dependent and show a 5' and 3' base bias.**

**a.** Length of tags arising from the locus before and after cut. The bulk of small RNAs in wildtype samples before and after cut is in the 22-23 nt size range. The fraction of 22-23 nt decreases in DICER and DROSHA knockdown samples both in UNCUT and CUT conditions. **b.** The fraction of 22-23 nt vs total small RNAs at the locus increases in the wildtype upon cutting (p=0.02). In DICER knockdown samples, the decrease is statistically significant (in the UNCUT samples p = 4.8e-7, in the CUT samples p=0.029). The reduction of 22-23 nt small RNAs in DROSHA knockdown samples do not reach statistical significance. **c.** The distribution of nucleotides at the 5' and the 3' end of RNA sequences from the locus is significantly different from both the genomic background nucleotide distribution (p=0.012 at the 5' end and 0.008 at the 3' end) as well as the background nucleotide distribution at the locus (p=0.014 at the 5' end and 1.2e-6 at the 3' end). Specifically, 82.9% sequences start with an A/U and 48.6% sequences end with a G.

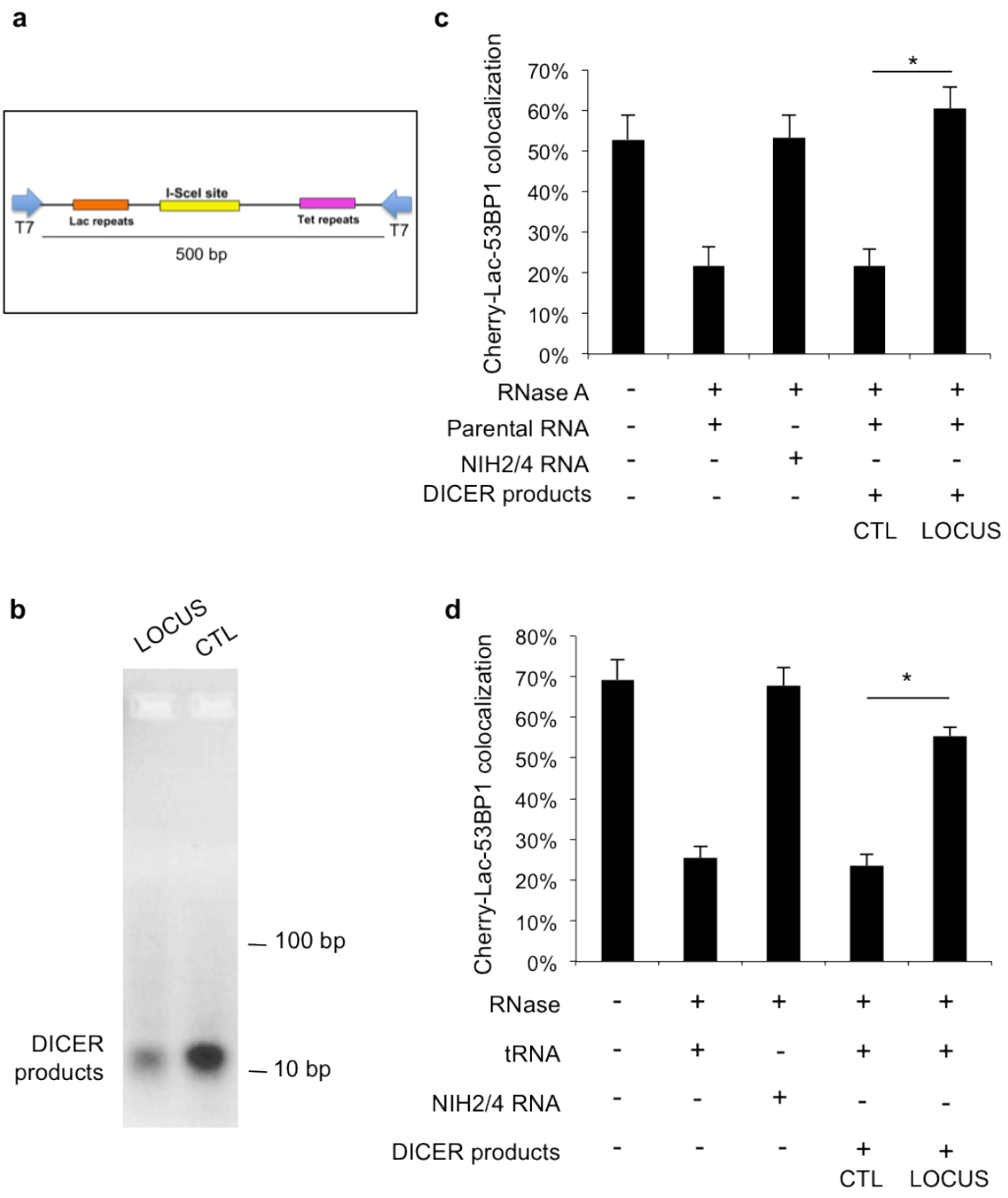


**Figure 39. In vitro-generated DICER RNA products are sufficient to restore DDR focus formation in RNase-A-treated cells in a sequence-specific manner.**

**a**. The minimal Lac-I-SceI-Tet containing locus (500bp in length) was cloned between T7 promoters, in order to allow transcription of both strands in vitro and the generation of a long double-stranded RNA spanning the entire locus. **b.** DICER processing of the long RNA precursor was evaluated by running DICER RNA-products on a 3% agarose gel. **c,d**. Small double-stranded RNAs generated by recombinant DICER were tested to restore DDR focus formation in RNase-A-treated cut NIH2/4 cells. 1ng/μl RNA was tested mixed with 800ng of parental cell RNA or tRNA. Locus-specific DICER RNAs, but not control RNAs, allow site-specific DDR activation. Histograms show the percentage of cells positive for 53BP1 focus at the Cherry-Lac locus. Error bars indicate s.e.m. (n=3). Differences are statistically significant (*p-value<0.05).

# 6. Synthetic biologically active DDRNAs and DDRNA antagonists modulate the DDR activation at the damaged locus

*6.1 Synthetic DDRNAs are sufficient to restore 53BP1 focus after RNase A treatment in NIH2/4 cells*

To test whether the identified locus-specific small RNAs were biologically active molecules with a causal role in DDR activation, four potential pairs among the RNAs identified by deep sequencing were chemically synthesized. These eight RNA oligonucleotides matched the Lac repeats, the Tet repeats or the unique sequences close to the cut site (Figure 40) and had a monophosphate at the 5' end.

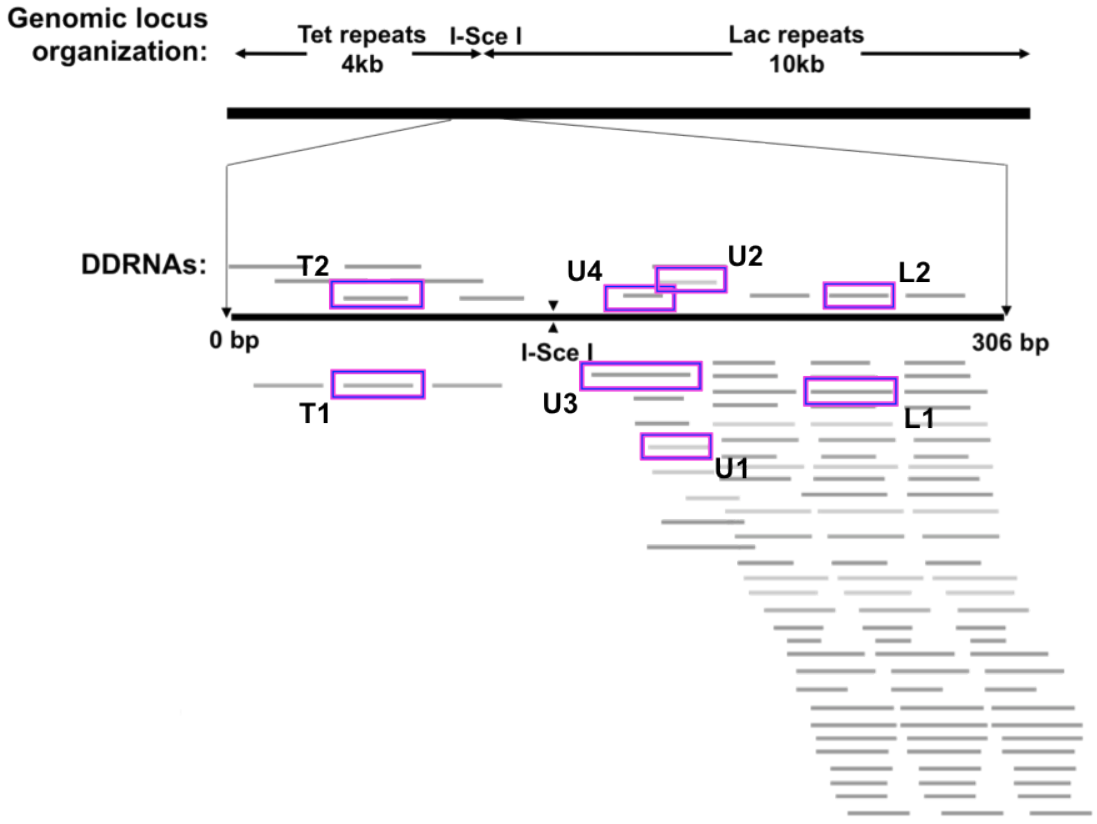


**Figure 40. Synthetic DDRNAs map.**
Eight DDRNAs mapping to different positions of the Lac-I-SceI-Tet locus (as shown in the map) were synthesized with a cy5 fluorophore at the 3' ends of each molecule. The sequences chosen are complementary and can be annealed in vitro. The four pairs match to the Tet repeats (T1T2 pair), to the Lac repeats (L1L2 pair) and to the unique sequence close to the cut site (U1U2 and U3U4 pairs).

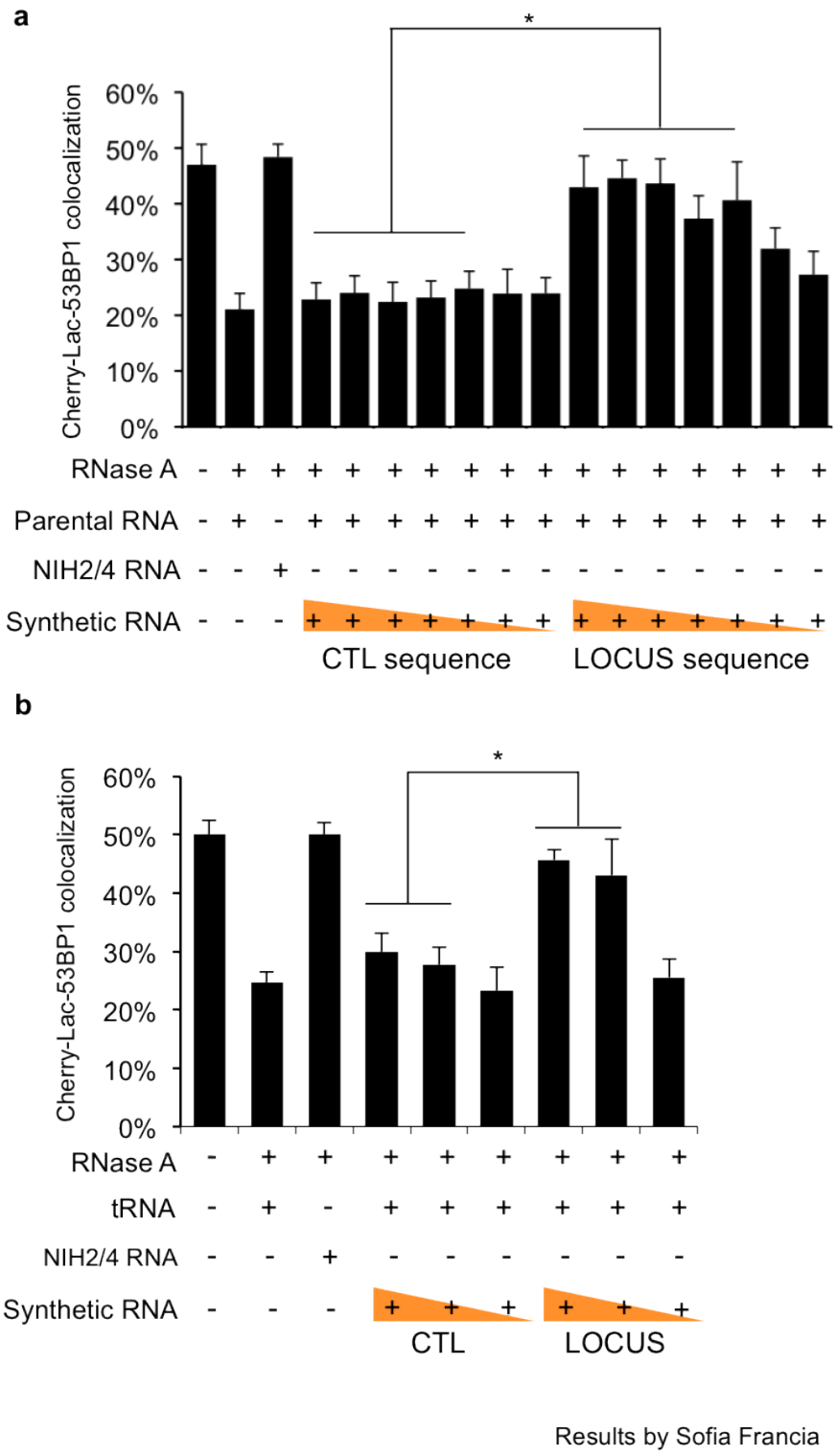


**Figure 41. Synthetic DDRNAs are sufficient to restore 53BP1 focus formation after RNase A treatment.**

**a,b.** A pool of chemically synthesized oligonucleotides mapping flanking to the DSB induced in the exogenous integrated locus was tested to restore DDR focus formation in RNase A-treated NIH2/4 cells. Mixed with a constant amount of either parental RNA or tRNA, a wide range of concentrations (1ng/µl to 1fg/µl, tenfold dilution steps for the parental-mixed; or 0.1ng/µl, 0.1pg/µl and 1fg/µl for the tRNA-mixed) of locus-specific or control (GFP) RNAs, was used. Site-specific synthetic RNAs, but not control RNAs, induce site-specific DDR activation (up to the concentration of 0.1pg/µl). Histogram shows the percentage of cells in which 53BP1 focus co-localizes with the Cherry-Lac focus. Error bars indicate s.e.m. (n=3). Differences are statistically significant (*p-value<0.05).

The RNA pairs were annealed, pooled and used to attempt DDR focus reformation in RNase-A-treated NIH2/4 cut cells. Excitingly, addition of locus-specific synthetic RNAs, but not equal amounts of control RNAs, triggered 53BP1 focus reformation at the site of damage. This was observed over a large range of concentrations both in the presence of total RNA from parental cells (Figure 41a) and tRNA (Figure 41b).

*6.2 Locked Nucleic Acids block DDRNAs function in living cells*

Having established that DDRNAs, in the form of sequence-specific synthetic oligonucleotides, were sufficient for DDR focus reformation in RNase A-treated NIH2/4 cut cells, I then tested if they were also necessary for DDR activation. Thus four Locked Nucleic Acids (LNA, modified RNA oligonucleotides avidly binding and inactivating complementary RNA species) (Jepsen et al., 2004; Machlin et al., 2012) were synthesized against individual DDRNA species, having the sequence of both DNA strands of Lac and Tet repeats (Lac upper and lower strands, Tet upper and lower strands; Figure 42). If DDRNAs were necessary for DDR activation at a damaged locus, inhibiting their action by transfection of complementary LNAs could suppress DDR activation. To do so, NIH2/4 cells were co-transfected with Cherry-LacR and I-Sce I expressing vectors together with no LNA, control LNA with telomeric sequence or LNA matching the DDRNAs in different combinations. More specifically, I combined the four LNAs in four different couples (Lac and Tet upper strand; Lac and Tet lower strand; Lac upper strand and Tet lower strand; Lac lower strand and Tet upper strand), in order to block simultaneously DDRNAs generated upstream and downstream of the DSB. I observed that, whereas γH2AX did not change upon LNA transfection (Figure 43a), 53BP1 accumulation at the locus was significantly reduced upon transfection of LNA matching the DDRNAs, compared to the control LNA, to an extent comparable to RNase A-treated cells or upon DICER e DROSHA inactivation (Figure 43b).

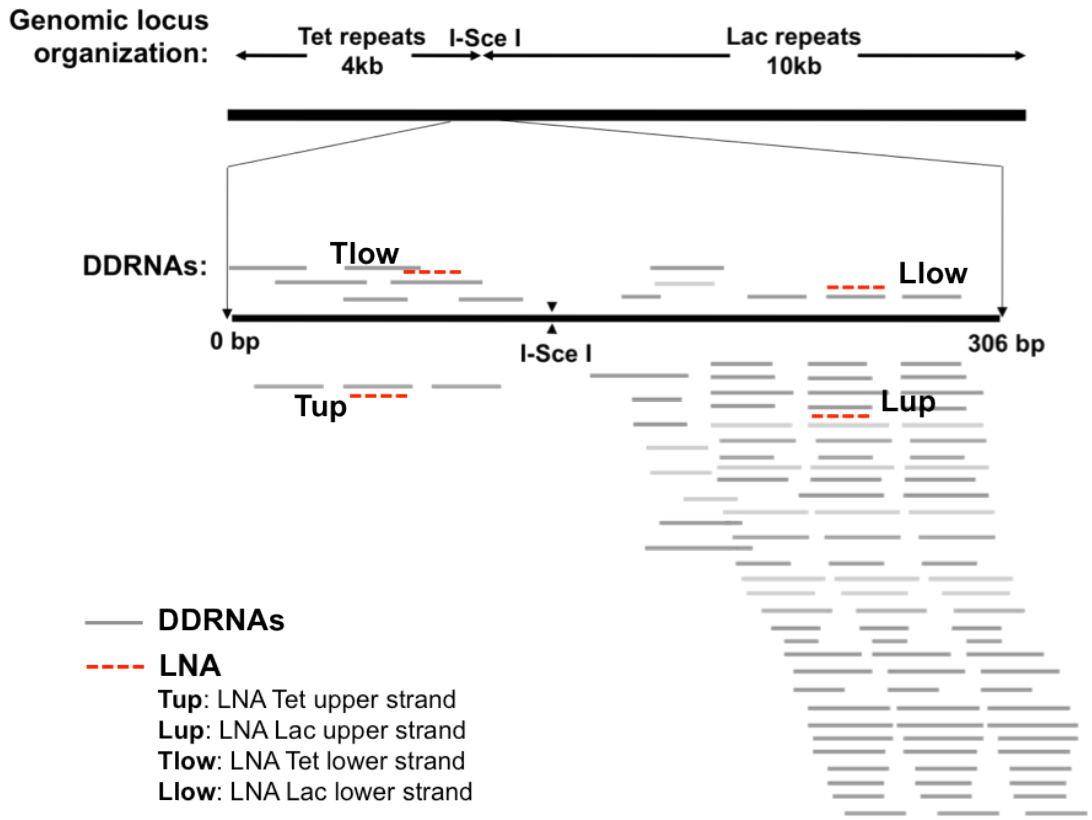


**Figure 42. LNA map.**
Four Locked Nucleic Acids (LNAs) having the sequence of both DNA strands of Lac and Tet repeats (Lac upper and lower strands, Tet upper and lower strands) were synthesized. The four LNA sequences were chosen in order to match the majority of DDRNA transcripts.

This significant decrease was observed, to different extents, with all the LNA couples used, although the most effective one was the combination Lac upper strand and Tet lower strand (number 5). Notably this couple directly targeted the strands that gave rise to the more abundant DDRNA reads (Figure 42). Addition of all the four LNA transfected together did not affect 53BP1 accumulation at the locus, most probably because they annealed during the transfection procedure, in this way neutralizing each other. From these results I concluded that LNA can block DDRNAs in living cells and can modulate DDR focus formation in a sequence-specific manner. I believe there is no precedent for that in the published scientific literature.

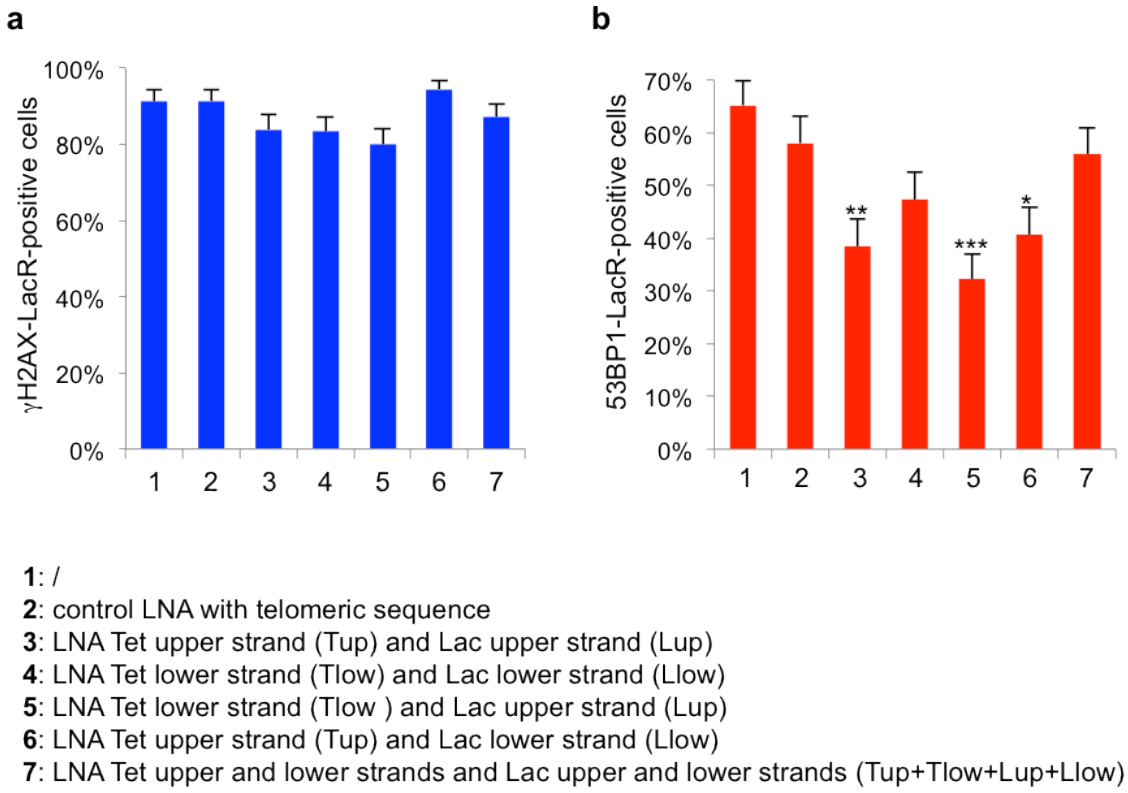


**1**: /
**2**: control LNA with telomeric sequence
**3**: LNA Tet upper strand (Tup) and Lac upper strand (Lup)
**4**: LNA Tet lower strand (Tlow) and Lac lower strand (Llow)
**5**: LNA Tet lower strand (Tlow ) and Lac upper strand (Lup)
**6**: LNA Tet upper strand (Tup) and Lac lower strand (Llow)
**7**: LNA Tet upper and lower strands and Lac upper and lower strands (Tup+Tlow+Lup+Llow)

**Figure 43. LNA transfection impairs DDR at the locus in cut NIH2/4 cells.**
NIH2/4 cells were co-transfected with Cherry-Lac and I-Sce I restriction endonuclease expressing vectors and LNA matching individual strands of the locus (200pM) in different combinations as shown in the legend. LNA matching telomere sequence was used as control. 24h post transfection cells were scored for DDR markers at the Lac array. **a, b.** Histograms show the percentage of cells positive for the DDR markers analyzed: γH2AX is unaffected, whereas 53BP1 accumulation at the locus is significantly reduced upon LNA treatment. For the quantifications shown around 100 cells from three independent experiments were scored. Error bars indicate s.e.m. * p-value<0.05, ** p-value<0.01, *** p-value<0.005.

# 7. DDRNAs and DNA damage repair

*7.1 DICER knockdown impairs DNA damage repair in NIH2/4*

In a recently published paper (Wei et al., 2012) DICER- and AGO2-dependent small RNAs of 21-24 nucleotides in length, called DSB-induced RNAs (diRNAs), were demonstrated to be involved in DNA damage repair by HR. This work, carried out mainly in *Arabidopsis thaliana* but also in human cells, prompted me to investigate the role of DDRNAs in DNA damage repair. To address this, I first checked the involvement of DICER in DNA damage repair, taking advantage of an inducible I-Sce I system: upon addition of triamcinolone acetonide (TA), I-Sce I fused to the glucocorticoid receptor (I-SceI-GR) translocates to the nucleus, generating a DSB that can be detected by a γH2AX focus co-localizing with the YFP-TetR signal (Figure 44, ON).

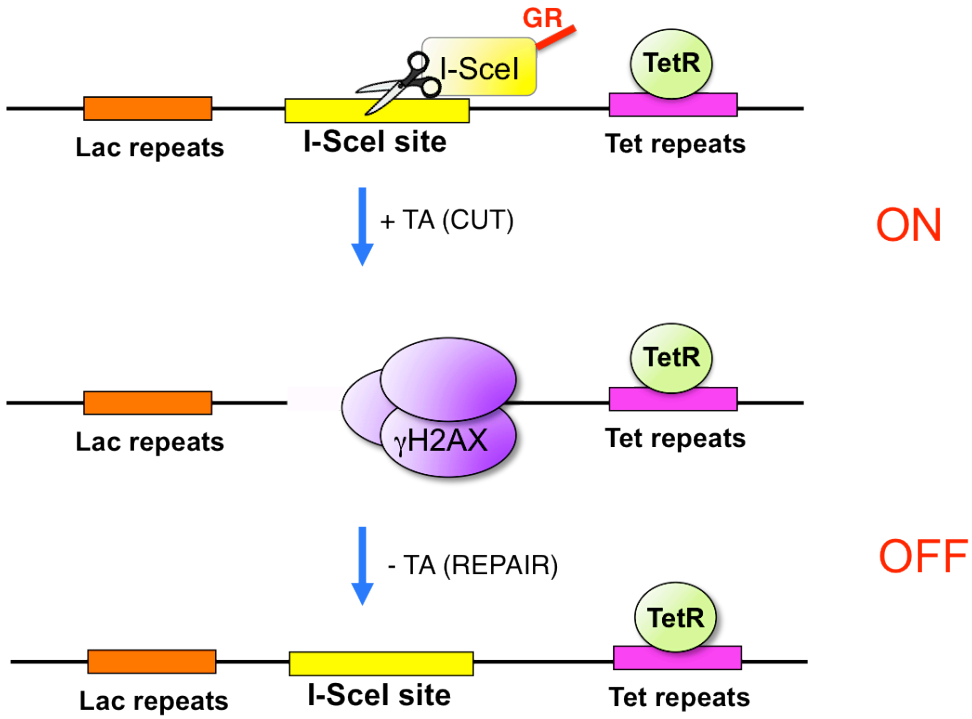


**Figure 44. An inducible I-Sce I to study DNA repair in NIH2/4 cells.**
To study DNA repair in NIH2/4 cells, an inducible I-Sce I fused to the glucocorticoid receptor (I-SceI-GR) was used. When transfected, the enzyme is retained in the cytoplasm and it translocates into the nucleus upon Triamcinolone Acetonide (TA) addition, generating a DSB (ON). Once the drug is removed from the medium, the I-SceI-GR construct returns to the cytoplasm (OFF), allowing the repair of the DSB. In order to visualize the locus, a Tet-On system is used: the Tet repressor fused to YFP (YFP-TetR) binds the corresponding array in the presence of doxycycline.

The removal of the inducing agent restricts I-Sce I again to the cytoplasm, allowing DNA repair that can be monitored by the reduction of γH2AX signal at the locus (Figure 44, OFF). I thus transfected YFP-TetR and I-SceI-GR in wildtype and DICER-knocked-down NIH2/4 cells (shDICER) and followed DNA damage activation and repair (Figure 45). I observed that, upon cut, the percentage of γH2AX accumulation was comparable in both wildtype and DICER-inactivated NIH2/4 cells (Figure 45, ON). However, after I-Sce I inactivation, only cells proficient for DICER could efficiently repair the damaged site, suggesting an involvement of DICER also in DNA repair (Figure 45, OFF).

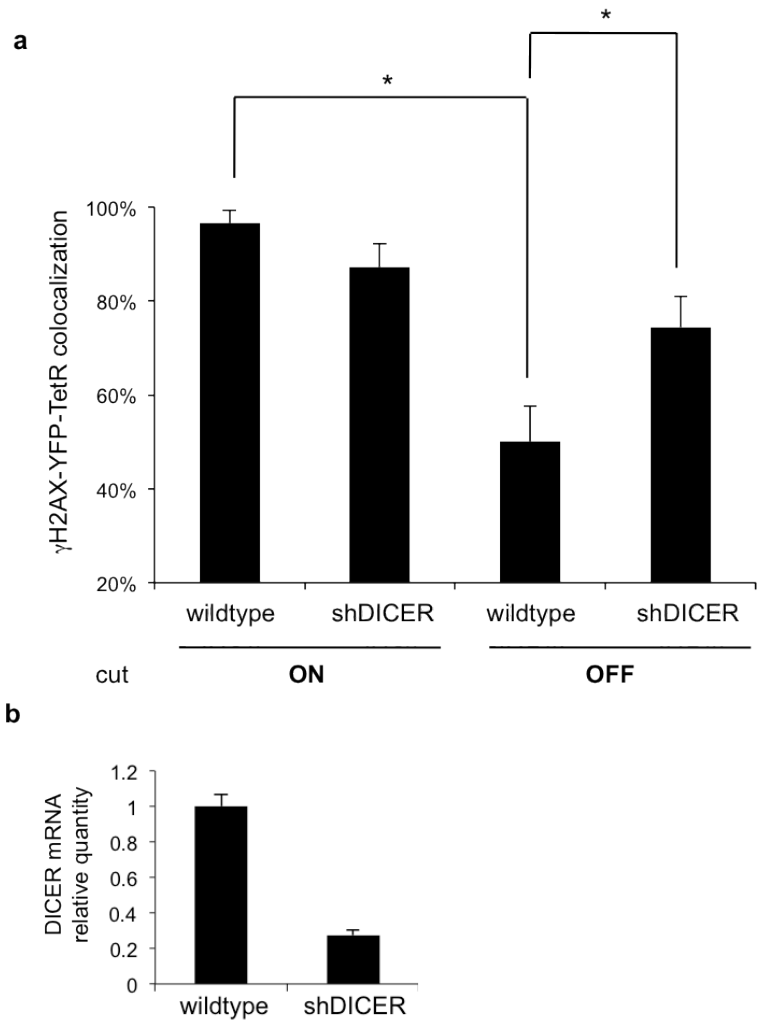


**Figure 45. DICER knockdown impairs DNA repair.**

**a.** NIH2/4 cells were transfected with pLKO (wildtype) or shDICER vectors. After 48 hours cells were transfected with YFP-TetR and I-SceI-GR vectors. 24 hours later, doxycycline (1μg/ml) to visualize the locus and TA (10pM) to induce the cut were added to the medium. 3 hours post induction cells were fixed and stained for γH2AX to evaluate the amount of acute damage (ON). The drug was then removed with extensive washes in PBS and fresh medium with doxycycline was added to the cells. 24 hours later cells were fixed and stained for γH2AX to evaluate the amount of DNA repair (OFF).

*7.2 Locked Nucleic Acids block DDRNAs function in DNA damage repair*

Having established that DICER knockdown impaired DNA damage repair, I then tested whether this effect was direct and DDRNA-dependent. To this aim, I co-transfected NIH2/4 cells with YFP-TetR and I-SceI-GR expressing vectors, together with no LNA, control LNA or LNA matching DDRNAs in different combinations (see Figure 42 for a schematic view of the LNA used). I monitored DNA damage activation and repair by γH2AX and 53BP1 accumulation.

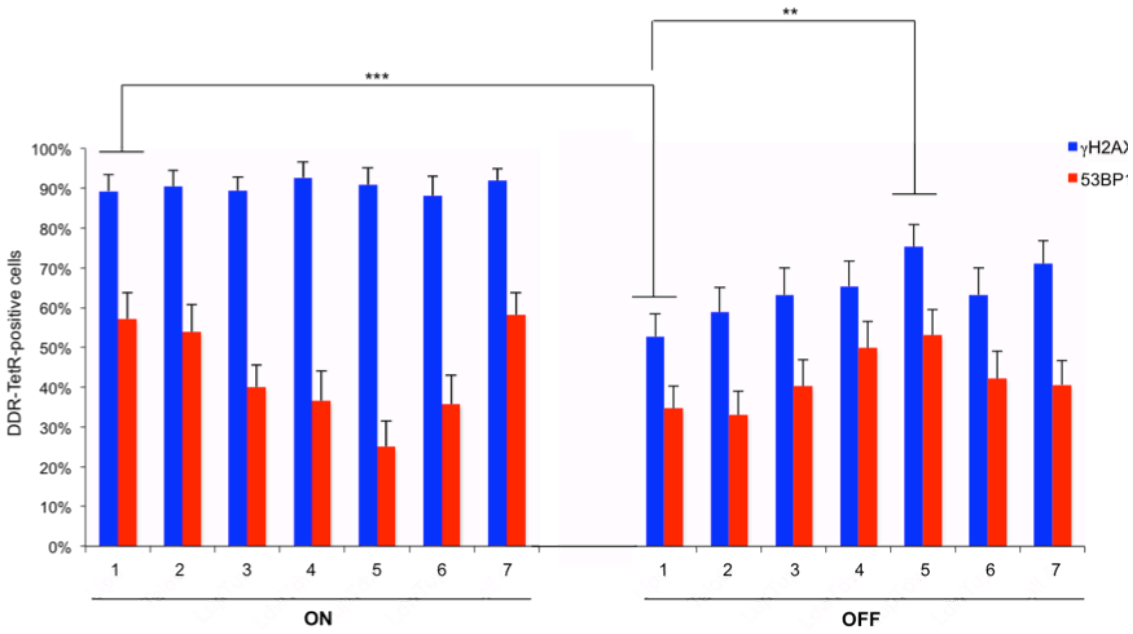


**1**: /
**2**: control LNA with telomeric sequence
**3**: LNA Tet upper strand (Tup) and Lac upper strand (Lup)
**4**: LNA Tet lower strand (Tlow) and Lac lower strand (Llow)
**5**: LNA Tet lower strand (Tlow ) and Lac upper strand (Lup)
**6**: LNA Tet upper strand (Tup) and Lac lower strand (Llow)
**7**: LNA Tet upper and lower strands and Lac upper and lower strands (Tup+Tlow+Lup+Llow)

**Figure 46. LNA transfection impairs DNA repair at the locus in cut NIH24 cells.**
NIH2/4 cells were co-transfected with YFP-TetR and RFP-I-SceI-GR vectors and LNA matching individual strands of the locus (200pM) in different combinations (as shown in the legend). 24 hours later doxycycline (1μg/ml) to visualize the locus and TA (10pM) to induce the cut were added to the medium. At 3 hours post induction cells were fixed and stained for γH2AX and 53BP1 to evaluate the amount of acute damage (ON). The drug was then removed with extensive washes in PBS and fresh medium with doxycycline was added to the cells. 24 hours later cells were fixed and stained for γH2AX and 53BP1 to evaluate the amount of DNA repair (OFF).

As expected, at three hours post I-Sce I induction (Figure 46, ON), γH2AX levels were very similar in all the samples, whereas 53BP1 was reduced by the LNA combinations that were matching the DDRNAs (numbers 3, 4, 5 and 6), compared to the sample with no LNA or with control LNA (numbers 1 and 2). This result confirmed the one obtained in Figure 43, with the most effective LNA couple being Lac upper strand and Tet lower strand (number 5). 24 hours after TA removal (Figure 46, OFF), control cells were able to repair as shown by γH2AX reduction (numbers 1 and 2), whereas LNA transfection, especially the most effective couple (number 5), caused an increase in γH2AX and 53BP1 signals at the locus. On the contrary, addition of all the four LNA transfected together (number 7) did not affect DDR activation or DNA damage repair.

Collectively, these data suggest a possible role of DDRNAs also in DNA damage repair, in addition to DDR signaling.

## 8. DDR foci contain RNA molecules

*8.1 Synthetic cy5-DDRNAs rescue 53BP1 focus in RNase A-treated NIH2/4 cells*

Small RNA molecules arising from a damaged site control DDR activation in the nucleus. However, the mechanisms by which DDRNAs control DDR focus formation in a sequence-specific manner are elusive. One possibility is that RNA has an architectural role guiding and retaining DDR proteins at the specific DNA damaged site. One example of ncRNA having an architectural role is the lncRNA NEAT1, shown to be an essential structural component of paraspeckles, nuclear domains implicated in mRNA nuclear retention (Clemson et al., 2009).

To test whether DDRNAs can function as scaffold for DDR proteins acting locally in close proximity to the DNA damage site and DDR focus, I got the eight synthetic DDRNAs used in the previous experiments (Figure 40) synthesized with a cy5 fluorophore at their 3' ends (cy5-DDRNAs). First, I tested whether cy5-DDRNAs were biological active by using them to attempt to restore the DDR focus in RNase-A-treated cells. NIH2/4 cells were transfected with YFP-TetR and I-Sce I expressing vectors, treated with RNase A and complemented with either synthetic not fluorescent or fluorescent DDRNAs, at two different concentrations, mixed with tRNA. Both concentrations of cy5-DDRNAs were able to restore DDR focus formation to the same extent of the not labeled ones (Figure 47), while the control sequence did not, thus demonstrating that the addition of the cy5 modification did not alter the biological functions of DDRNAs.

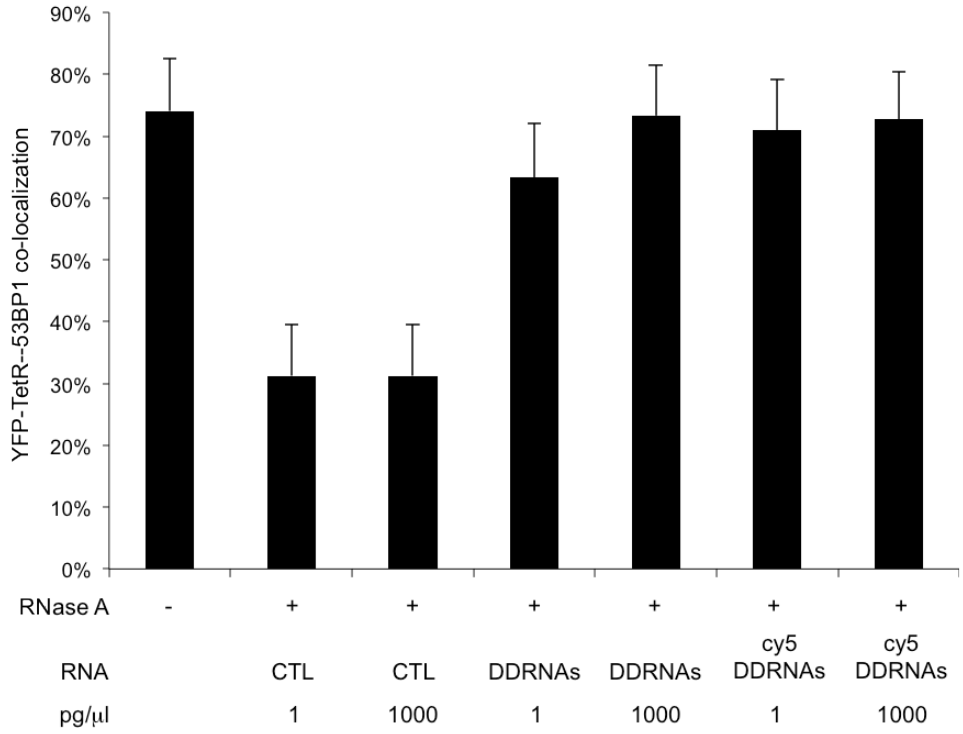


**Figure 47. Synthetic cy5-DDRNAs are able to restore 53BP1 focus formation in RNase A-treated cells as unlabelled ones.**
NIH2/4 cells were co-transfected with YFP-TetR and I-Sce I expressing vectors. 24 hours later doxycycline (1μg/ml) was added to the medium to visualize the locus and after 3 hours cells were permeabilized and treated with RNase A. The four couples of annealed synthetic DDRNAs (1ng/μl), both cy5-labeled (cy5-DDRNAs) and unlabeled (DDRNAs), were mixed to tRNA (800ng) and used to complement 53BP1 focus formation at the locus at the concentrations indicated. An unrelated double-stranded unlabeled oligonucleotide was used as negative control (CTL). Histogram shows the percentage of cells in which 53BP1 focus co-localized with the YFP-TetR focus. For the quantification shown around 30 cells were analyzed.

*8.2 cy5-DDRNAs localize at the damaged site and co-localize with the 53BP1 focus*

The use of colors with distant and separated excitation and emission wavelengths, such as YFP-TetR to visualize the locus, Alexa-405 secondary antibody to visualize 53BP1, and cy5 to visualize the DDRNAs, prevented any "bleed through" towards the cy5 channel, allowing me to perform a co-localization analysis between the locus, the DDR marker and DDRNAs. Images were captured by DeltaVision microscope and deconvolved by the softWoRx software (Applied Precision). I observed that cy5-DDRNAs were able to enter the nucleus of permeabilized and RNase A-treated cells to different extent, that I empirically categorized according to their nuclear patterns, in cells with less then 5 spots

per nucleus, between 5 and 20 spots and more than 20 spots (Figure 48). To reduce the number of potential false positives, I did not consider in my analyses cells with more than 20 spots per nucleus (8% of the total cells positive for cy5-DDRNAs signal). Excitingly, I could often observe a signal of cy5-DDRNAs completely or partially overlapping with the YFP-TetR locus or in its close vicinity, but still co-localizing with the 53BP1 focus (Figure 49).

Thus, cy5-DDRNAs are able to enter the nucleus of permebilized RNAse A-treated cells and to reach the specific locus.

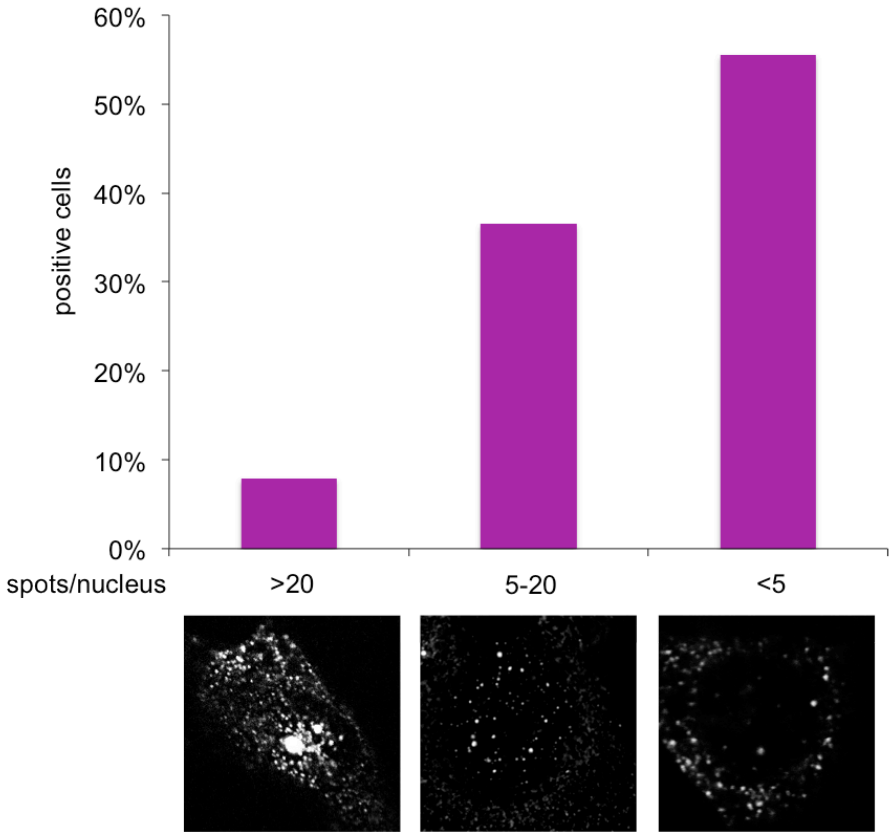


**Figure 48. Cy5-DDRNAs patterns in the nucleus of NIH24 cells.**
NIH2/4 cells were co-transfected with YFP-TetR and I-Sce I expressing vectors. 24 hours later, doxycycline (1μg/ml) was added to the medium to visualize the locus and after 3 hours cells were permeabilized and treated with RNase A. Cell were then incubated with the four couples of annealed synthetic cy5-DDRNAs (1ng/μl) mixed to tRNA (800ng). Histogram shows the percentage of cells with the indicated number of cy5-DDRNA spots per nucleus. Representative images for each pattern are displayed below.

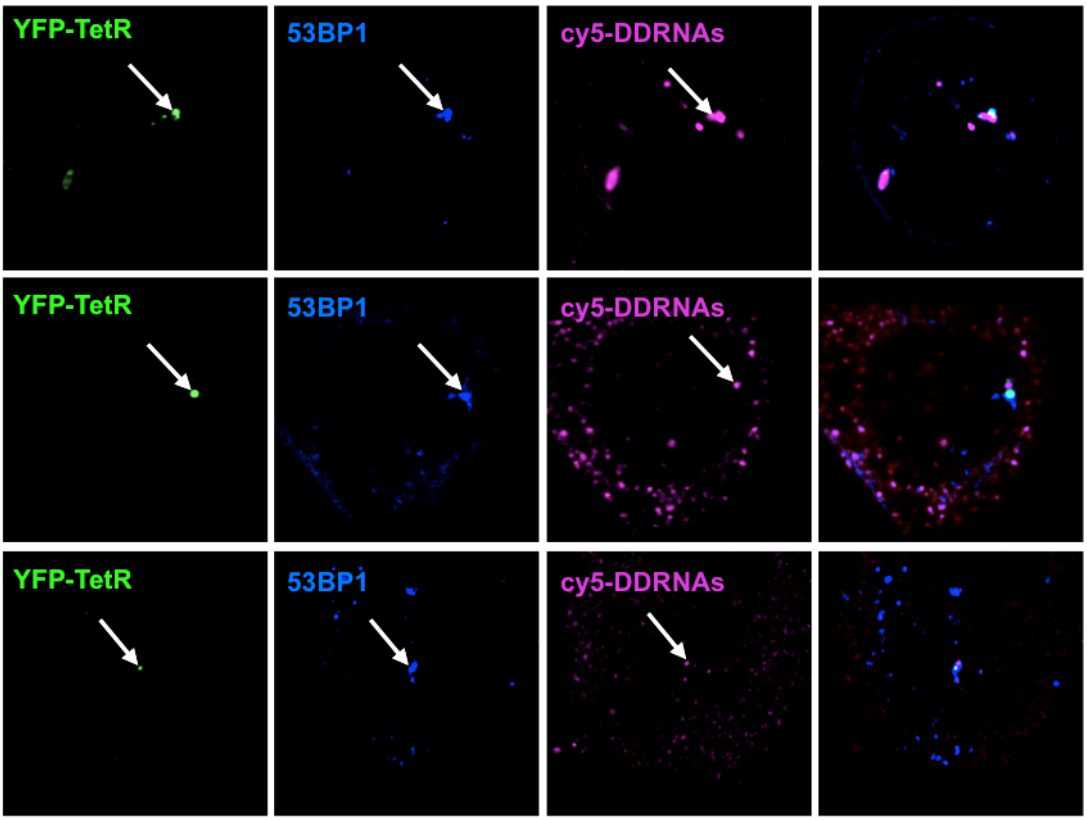


**Figure 49. Cy5-DDRNAs localize at the locus in RNase A-treated cells.**
NIH2/4 cells were co-transfected with YFP-TetR and I-Sce I expressing vectors. 24 hours later, doxycycline (1μg/ml) was added to the medium to visualize the locus and after 3 hours cells were permeabilized and treated with RNase A. The four couples of annealed synthetic cy5-DDRNAs were mixed with tRNA (800ng) and used to complement 53BP1 focus formation at the locus. Images were captured by DeltaVision microscope and deconvolved by the softWoRx software (Applied Precision). Arrows indicate the locus.

*8.3 cy5-DDRNAs but not an unrelated cy5-RNA localize at the locus*

In order to understand if cy5-DDRNAs localization at the locus was specific, I treated permeabilized NIH2/4 cut cells with RNase A and I incubated with cy5-DDRNAs or fluorescent Let7a miRNA (cy5-Let7), as a small RNA with a sequence unrelated to the locus. To perform a precise analysis of DDRNAs spatial distribution in the nucleus with respect to the YFP-TetR and to the 53BP1 signals, I decided to acquire 40 stacks per cell at the DeltaVision microscope and to reconstruct three-dimensionally the 53BP1-TetR-DDRNAs image (Figure 50).

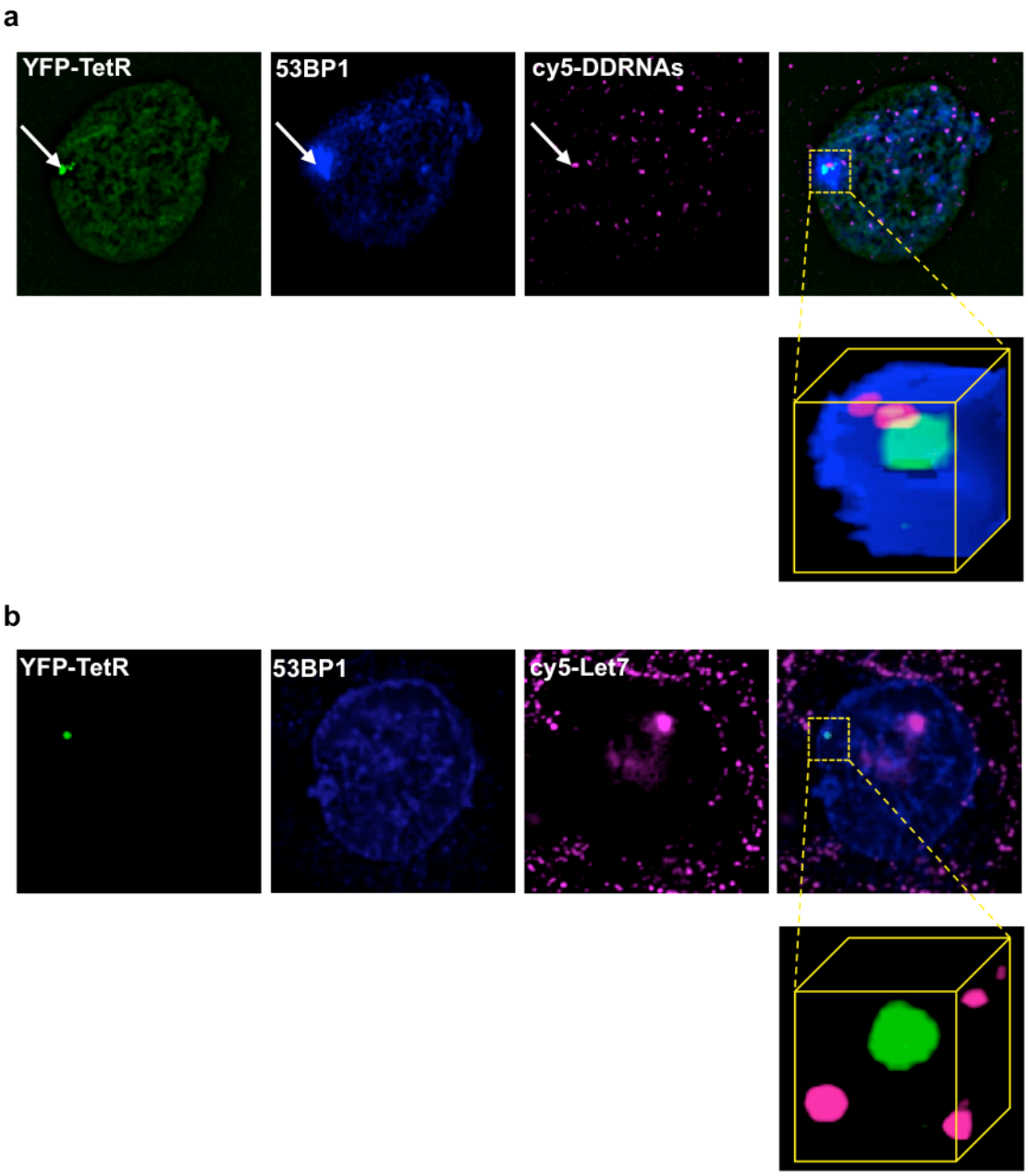


**Figure 50. 3D reconstruction of cy5-DDRNAs at the damaged locus.**
For each cell 40 stacks were captured at the DeltaVision microscope and deconvolved images of the focus were three-dimensionally reconstructed with ImageJ software.

Analyzing the 3D reconstructions, I quantified the percentage of cy5-DDRNAs and cy5-Let7 localizing at the locus (Figure 51, magenta bar) and the percentage of 53BP1 focus reformation (Figure 51, blu bar). I considered as positive those images in which the signals of cy5-DDRNAs and YFP-TetR were at least overlapping in the three dimensional space. In addition, I also calculated the frequency with which a positive localization between

cy5DDRNAs and YFP-TetR corresponded to a 53BP1 focus (Figure 51, yellow bar). I observed that, while cy5-DDRNAs localized at the locus and rescued 53BP1 focus formation, cy5-Let7 failed to do so.

Collectively, these results demonstrate that only cy5-RNAs with the sequence of the damaged locus can localize at the YFP-TetR signal, triggering DDR activation.

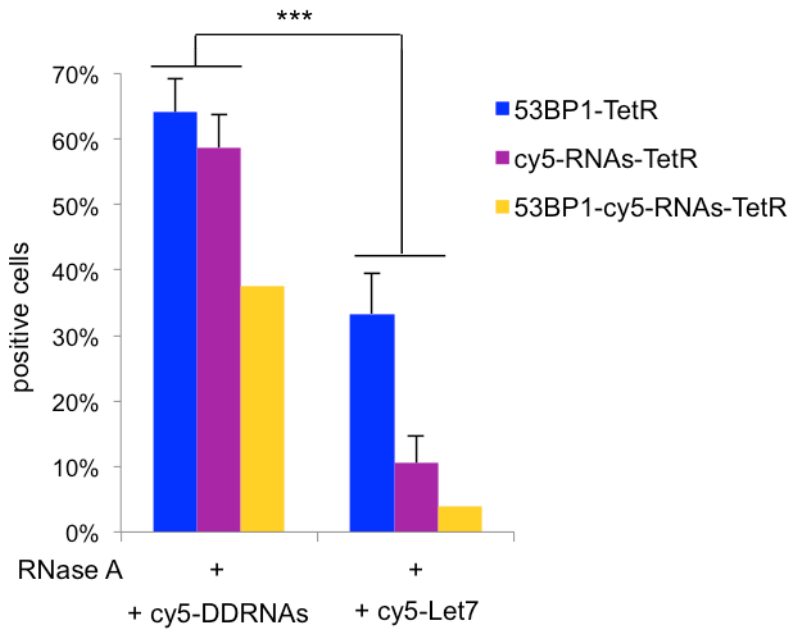


**Figure 51. Cy5-DDRNAs but not an unrelated cy5-RNA co-localize with the locus.**
NIH2/4 cells were co-transfected with YFP-TetR and I-Sce I expressing vectors. 24 hours later doxycycline (1μg/ml) was added to the medium to visualize the locus and after 3 hours cells were permeabilized and treated with RNase A. The four couples of annealed synthetic cy5-DDRNAs (1ng/μl) were mixed to tRNA (800ng) and used to restore 53BP1 focus formation at the locus. cy5-Let7 was used as negative control. Histogram shows the percentage of positive cells for the co-localization of 53BP1 with the locus, of cy5-DDRNAs with the locus and the triple co-localization of 53BP1, cy5DDRNAs and the locus. Error bars indicate s.e.m. (n=4). Differences are statistically significant (***p<0.0005). For the quantification shown around 90 cells were analyzed.

*8.4 cy5-DDRNAs localize more at the damaged than the undamaged locus*

Next I aimed to assess if cy5-DDRNAs localization at the locus was DNA damage dependent. Thus I transfected NIH2/4 cells with YFP-TetR only (uncut) or with YFP-TetR and I-Sce I expressing vectors (cut), I treated them with RNase A and I incubated with cy5-DDRNAs. I then fixed and stained cells for 53BP1 marker and I acquired images at

the DeltaVision microscope. Interestingly, I found a basal level of cy5-DDRNAs localizing at the uncut locus (30% of localization) that was doubled when the locus was cut (60% of localization) (Figure 52).

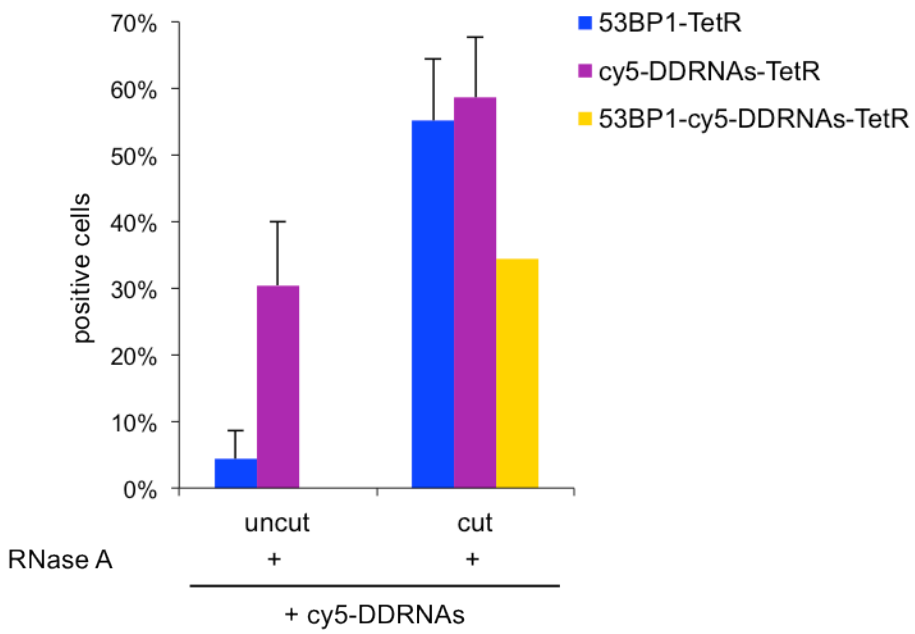


**Figure 52. Cy5-DDRNAs co-localize with the locus more in cut then in uncut RNase A-treated cells.**
NIH2/4 cells were either transfected with YFP-TetR alone (uncut) or co-transfected with YFP-TetR and I-Sce I expressing vectors (cut). 24 hours later, doxycycline (1μg/ml) was added to the medium to visualize the locus and after 3 hours cells were permeabilized and treated with RNase A. The four couples of annealed synthetic cy5-DDRNAs (1ng/μl) were mixed with tRNA (800ng) and used to complement 53BP1 focus formation at the locus. Histogram shows the percentage of positive cells for the co-localization of 53BP1 with the locus, of cy5-DDRNAs with the locus and the triple co-localization of 53BP1, cy5DDRNAs and the locus. For the quantification shown around 20 cells were analyzed.

Our collaborators Nils Walter and Sethu Pitchiaya at the University of Michigan performed a similar experiment but in a different setting. They microinjected in the nuclei of NIH2/4 cells EGFP-LacR expressing vector (uncut) or EGFP-LacR and I-Sce I expressing vectors (cut) together with cy5-DDRNAs at the indicated concentrations (2 μM and 100 nM) (Figure 53a, b). 24 hours post injection they acquired images and they counted the localization of cy5-DDRNAs at the EGFP-LacR locus. Consistently with my results, they observed a basal level of RNA localization at the uncut locus (40% of

localization) that increased about two fold when the locus was cut (80% of localization). The same ratio was maintained also at lower concentration (100 nM) of cy5-DDRNAs. On the contrary, the negative control cy5-siRNA against the CXCR4 gene (cy5-CXCR4), used at the higher concentration (2 μM), did not localize at the cut locus (Figure 53b).

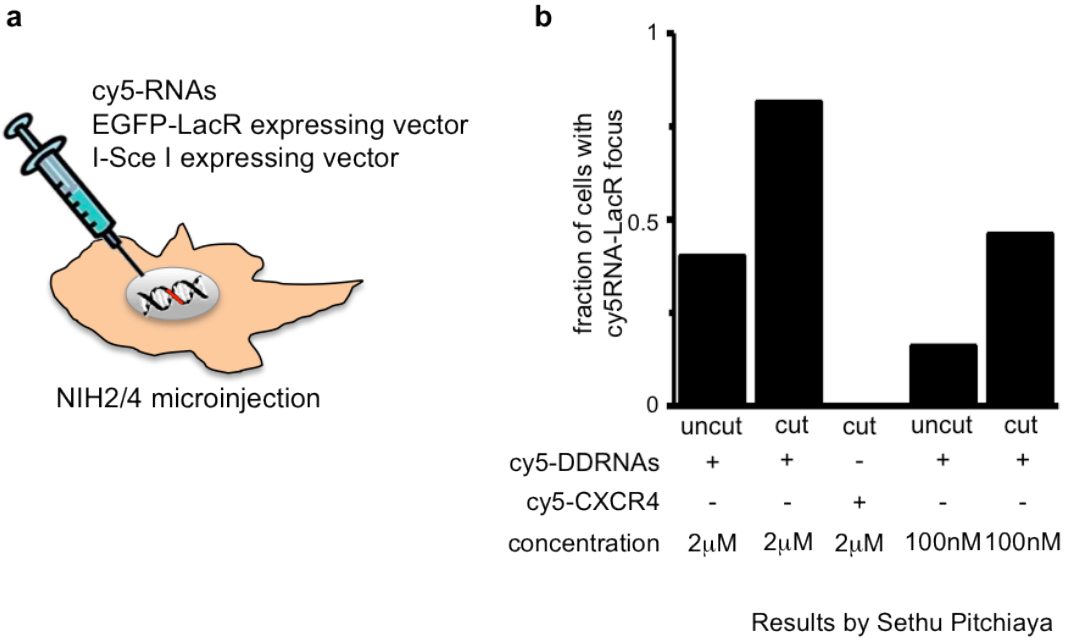


**Figure 53. Synthetic cy5-DDRNAs co-localize with the locus in microinjected NIH24 cells at different concentrations.**
**a.** NIH2/4 cells were microinjected in the nucleus with plasmids expressing EGFP-LacR (65 ng/μl) for the uncut sample or EGFP-LacR (65 ng/μl) and I-Sce I (100 ng/μl) for the cut sample, together with the four annealed couples of cy5-RNAs (2 μM or 100nM) and Alexa555 Dextran (0.1 mg/ml) in PBS. 24 hours later cells were fixed and stack images were acquired (<10x100 nm stacks), and subsequently processed to subtract the background. **b.** Histogram shows the quantification of perfectly and partially overlapping signals between EGFP-LacR and cy5-RNAs (cy5-DDRNAs or cy5-CXCR4). Signals where the pixel bearing maximum intensity of EGFP-LacR particle was the same as the maximum intensity pixel of cy5-RNA particle were considered as perfectly overlapping. Signals where the pixel bearing maximum intensity of EGFP-LacR particle was <5 pixels (~600nm) from the maximum intensity pixel of cy5-RNA particle were considered as partially overlapping. Peaks of particles were identified based on an algorithm similar to Simonson et al., 2010. A basal level of cy5-DDRNA localization at the uncut locus (40% of localization) was observed and increased about two fold when the locus was cut (80% of localization). The same ratio was maintained also at lower concentration of cy5-DDRNAs. The negative control used (cy5-CXCR4), instead, did not localize at the cut locus.

By an accurate analysis performed by single-step photobleaching of labeled RNA molecules (Pitchiaya et al., 2012), our collaborators were able to quantify the number of

cy5-DDRNA molecules at the uncut or cut site. They observed that ~ 2 cy5-DDRNA molecules (< 5 photobleaching steps) localized at the uncut site, whereas larger aggregates of ~20 cy5-DDRNA molecules (> 5 photobleaching steps) formed at the cut site (Figure 54).

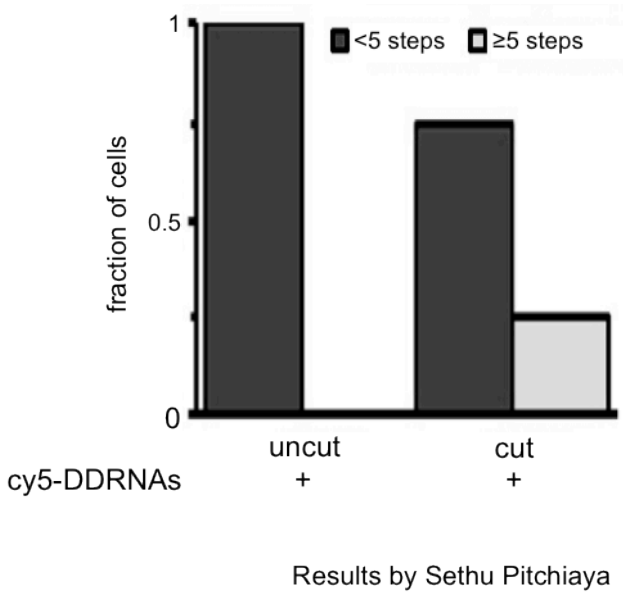


**Figure 54. Larger aggregates of cy5-DDRNAs co-localize with the locus upon induction of DNA damage.**
NIH2/4 cells were microinjected in the nucleus with plasmids expressing EGFP-LacR (65 ng/µl) for the uncut sample or EGFP-LacR (65 ng/µl) and I-Sce I (100 ng/µl) for the cut sample, together with the four annealed couples of cy5-DDRNAs (2 µM) and Alexa555 Dextran (0.1 mg/ml) in PBS. 24 hours later cells were fixed and single-molecule high-resolution imaging with photobleaching was performed as in Pitchiaya et al., 2012. In the uncut sample ~2 cy5-DDRNA molecules (<5 photobleaching steps) localized at the locus, whereas in the cut sample larger aggregates of ~20 cy5-DDRNA molecules (>5 photobleaching steps) formed at the locus.

Collectively these results obtained in two different settings, RNase A treatment and microinjection, demonstrate that cy5-DDRNAs actively localize to the locus, compared to negative controls. Moreover cy5-DDRNAs localization at the locus increases upon DNA damage induction, both in percentage of positive cells and in number of molecules.

*8.5 Deconvolved cy5-DDRNAs localize at the locus*

To understand if all four couples of cy5-DDRNAs were able to localize at the locus and to trigger 53BP1 focus reformation, I incubated RNase A-treated NIH24 cut cells with individual pairs of labeled DDRNAs (see Figure 40 for a schematic view of the cy5-DDRNAs used), with the four pairs in a pool as positive control, or cy5-Let7 and cy5-CXCR4 as negative controls. I observed that every annealed pair is able to localize at the locus, compared to the negative controls, and to be biologically active in activating DDR, although at different extents (Figure 55).

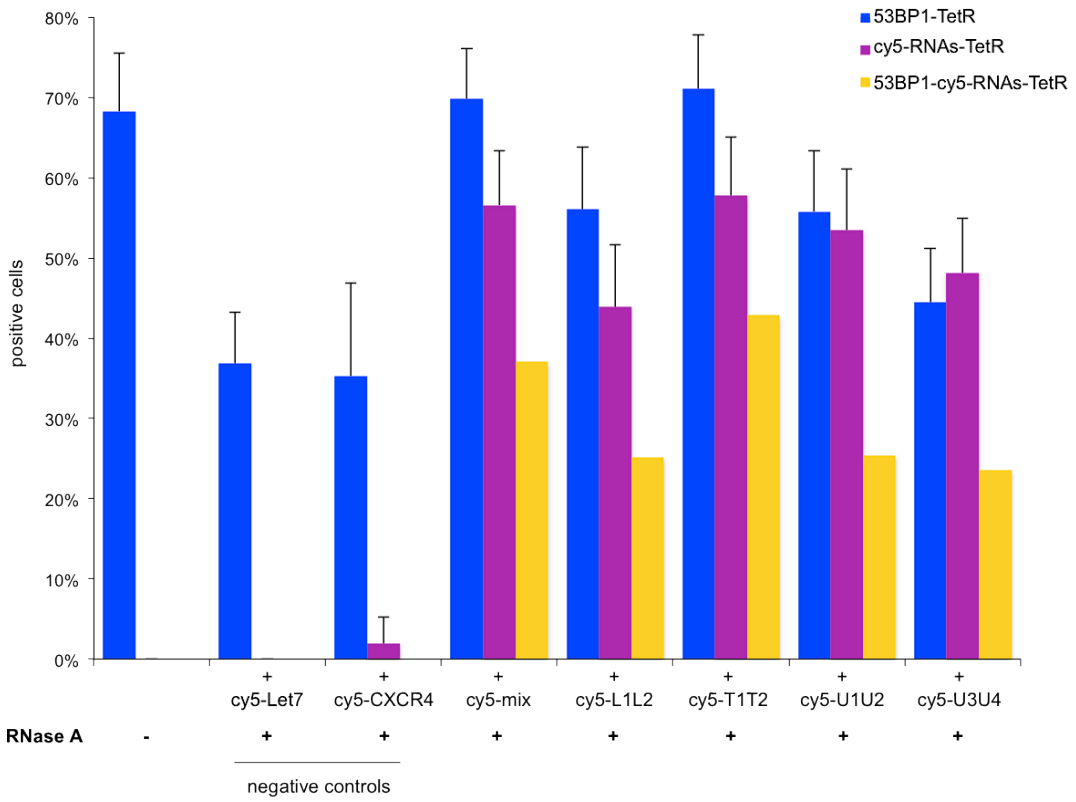


**Figure 55. Deconvolved synthetic cy5-DDRNAs pairs co-localize with the locus.**
NIH2/4 cells were co-transfected with YFP-TetR and I-Sce I expressing vectors. 24 hours later doxycycline (1μg/ml) was added to the medium to visualize the locus and after 3 hours cells were permeabilized and treated with RNase A (+) or not (-). The four pairs of annealed synthetic cy5-DDRNAs were pooled (cy5-mix, 1ng/μl) or kept separated (0.25ng/μl), mixed with tRNA (800ng), and used to restore 53BP1 focus formation at the locus. cy5-Let7 and cy5-CXCR4 (1ng/μl) were used as negative controls. Histogram shows the percentage of positive cells for the co-localization of 53BP1 with the locus, of cy5-DDRNAs with the locus and the triple co-localization of 53BP1, cy5DDRNAs and the locus. For the quantification shown around 50 cells from two independent experiments were analyzed.

In conclusion, making use of a fluorescent tag I could demonstrate for the first time that small RNA molecules are able to scan the genome and find the exact location of their complementary sequence, to actively accumulate if the matching DNA is damaged and to trigger the reformation of the DDR focus.

# Discussion

# 1. DNA makes RNA protects DNA

*1.1 A novel class of non-coding RNA regulates the DNA damage response*

DNA is the most precious molecule in our cells, thus it has to be protected from damage and alterations. Yet, DNA lesions are events that occur frequently in our body and, if damaged, DNA has to be repaired efficiently. The DNA damage response (DDR) is a coordinate set of events that follows the generation of a lesion in the DNA double helix, in order to promptly arrest the cell cycle and attempt DNA repair, thus avoiding the dangerous replication of a damaged template (Polo and Jackson, 2011). Up to now DDR was considered a protein-based signaling cascade, however I contributed to uncover an unexpected layer of DDR regulation. For the first time, a new class of DICER- and DROSHA-dependent small non-coding RNA, named DDRNA, has shown to be necessary for DDR activation at the sites of damage (Francia et al., 2012).

In particular, I showed that DDR foci stability is sensitive to RNA polymerase II inhibition and to RNase A treatment. Incubation of RNase A-treated cells with total cellular RNA, but not tRNA, restores focal accumulation of all DDR factors tested within minutes at room temperature. Importantly, RNA extracted from cells lacking DICER or DROSHA is not able to restore DDR foci formation in RNA-add-back experiments, suggesting that the two ribonucleases are needed to produce the active DDRNA molecules. Fractionating mammalian RNA on a polyacrylamide gel, I was able to show that DDRNAs are in the size range of DROSHA and DICER products. DICER and DROSHA are indeed necessary to trigger DDR upon exogenous DNA damage in human cells and the expression of a siRNA-resistant wildtype DICER cDNA, but not its endonuclease-mutated version, in DICER knockdown or knockout cells is able to rescue DDR foci formation, indicating that DICER controls DDR through its capacity to process RNA. Moreover, DICER and DROSHA knockdown impacts on checkpoint activation and allows senescent cells to re-enter S-phase. Differently, inactivation of GW182, a component of the RNAi machinery

involved downstream of DICER and DROSHA in mRNA translational control, does not impact on DDR foci formation and detection. Exploiting a mammalian cell system in which a single DNA double-strand break can be generated at a defined exogenous integrated locus, I revealed that DDR focus formation requires site-specific RNA molecules. NGS confirmed the presence of 22-23-nucleotide sequence-specific transcripts arising from the exogenous integrated locus, whose abundance significantly increases upon damage. Furthermore, the fraction of 22-23-nucleotide RNAs at the locus shows a peculiar nucleotide bias and decreases upon DICER knockdown, suggesting that DDRNAs are DICER-dependent. Importantly DDRNAs, both chemically synthesized or generated *in vitro* by DICER cleavage, are biologically active even at very low concentrations and LNA, that selectively target DDRNAs, antagonize their action in activating DDR in living cells. In addition, by the use of LNA I also showed that DDRNAs impact not only on DDR signaling, but also on DNA damage repair. Moreover, I shed light on the possible biological mechanism, demonstrating that DDRNAs act at the first steps of the DDR cascade, in an MRN-dependent manner. Finally, employing fluorescently labeled molecules, I could indeed prove that DDRNAs localize at the site-specific damaged locus.

*1.2 RNA-dependent DDR foci assembly and maintenance: the imperturbable γH2AX and the strange case of 53BP1*

In the literature, more and more indications of interplay between DDR proteins and RNA molecules are emerging (see Introduction, section 4.2). In agreement with that, in this thesis I showed that both IR- and endonuclease-induced assembly of DDR factors at DSBs is sensitive to RNase A treatment, and can be restored by exogenous RNA supply (see Results, Figures 13 and 22). In particular, RNA degradation causes the disassembly of MRN, MDC1, 53BP1 and activated ATM (pATM) foci and also of foci of the phosphorylated substrates of ATM, ATR and DNA-PK (pS/TQ). A similar behavior was observed in DICER and DROSHA knockdown experiments, where the focal accumulation

of same DDR factors, although with different kinetics, was affected (see Results, Figure 14). Indeed, in light of all these results a unifying model can be proposed: DICER and DROSHA products, called DDRNAs, are the RNA molecules necessary for DDR foci formation. In other words, the conclusions inferred from RNase A experiments are consistent with those drawn from DICER and DROSHA knockdown experiments.

In apparent contrast to all the other DDR members tested, γH2AX was instead only marginally affected, both by RNase A treatment and by DICER and DROSHA knockdown (see Results, Figures 7 and 14). The persistence of γH2AX accumulation in cells where ATM activation is impaired (pATM and pS/TQ foci are reduced in RNase A-treated and in DICER- and DROSHA-depleted cells) suggests the presence of redundant mechanisms for H2AX phosphorylation, likely being DNA-PKcs dependent (An et al., 2010). This hypothesis could be tested by incubating cells with a DNA-PKcs inhibitor. The contribution of ATR on H2AX phosphorylation has not been investigated, since the kinase is mainly activated upon exposure of ssDNA. However, it would be very interesting to assess if DDRNAs have also a role in the ATR pathway.

It has to be considered that, unlike all the other markers tested whose focal accumulation is RNA-dependent, H2AX is an histone, thus difficult to mobilize. DDRNAs are maybe needed to retain DDR factors at breakage sites, already positive for γH2AX. In any case, the detection of γH2AX upon RNA degradation provides a convenient control, indicating that the mild permeabilization used and the RNase A treatment do not dramatically alter chromatin structure or nucleus integrity. Consistent with my results, γH2AX is unaffected in diRNA-deficient plant mutants (Wei et al., 2012), demonstrating that, similarly to DDRNAs, diRNAs are most likely involved in events that are downstream of H2AX phosphorylation.

At present, it is unclear if the absence of DDRNAs can prevent H2AX phosphorylation. A hint against this hypothesis comes from my data in cells pre-treated with α-amanitin: while 53BP1 foci formation is affected by RNA polymerase II inhibition, γH2AX levels remain

unaltered (see Results, Figure 9), suggesting that, at least under these conditions, DDRNAs do not control the phosphorylation of the histone.

It is worth noticing that γH2AX accumulation was uncoupled from MDC1 recruitment in cells lacking DDRNAs, meaning in RNase A-treated and DICER- or DROSHA-knocked-down cells. This observation is unexpected because it is generally accepted that MDC1 directly binds to the phosphorylated histone tail (Stucki et al., 2005). Additional data are needed to understand where and when DDRNAs exert their role in DDR.

There are two possible explanations for the loss of DDR foci in cells treated with RNase A or depleted of DICER or DROSHA: either DDRNAs affect the initial recruitment of the DNA damage sensors to the lesion, or, if the initial recognition of the break is RNA-independent, DDRNAs are specifically involved in fuelling the positive feedback loop that leads to the amplification of the signal and to the formation of cytologically visible DDR foci. The experimental settings used in this project (IR and a restriction enzyme) cannot distinguish between these two phases of DDR activation: at individual DNA lesions generated randomly in the genome by IR and at the single-cut site it is only possible to detect a fully activated DDR focus, a relatively big structure formed by multiple copies of the same proteins. Therefore, with the results so far described, a conclusion cannot be drawn. However, the use of laser microirradiation technique, which generates high-density DNA lesions in close vicinity allowing the detection of even few DDR proteins at the DSBs (Bekker-Jensen et al., 2006; Bekker-Jensen et al., 2005; Doil et al., 2009), will make it possible to understand if DDRNAs are required in the initial recognition of the lesion or in the subsequent accumulation of DDR factors. In this regard, preliminary results obtained in our laboratory seem to point to a role of DDRNAs in the secondary recruitment, while the initial phase of lesion recognition seems to be RNA-independent.

Consistent with a previous report (Pryde et al., 2005), I observed that 53BP1 foci are disrupted by RNase A-dependent total RNA degradation (see Results, Figures 7 and 13). In the same report, IR-driven 53BP1 foci determined solely by the tandem Tudor domains

(usually found in RNA-binding proteins) have been shown to be sensitive to RNase A treatment, specifically at early stages of the post-IR period (in particular, foci are lost within 20 minutes post IR, start to be less sensitive at 1 hour post IR and are not sensitive anymore at 2 hours post IR). In my experiments this phenomenon has not been studied, since irradiated cells are RNase A-treated within 1 hour from IR and endonuclease cut cells are constitutively damaged. However, in HeLa cells lacking DICER and DROSHA a similar phenotype has been observed: differently from the other DDR markers tested, 53BP1 foci formation is affected by DICER or DROSHA knockdown only at early time points post IR (10-30 minutes), suggesting that DDRNAs are necessary to the assembly process of 53BP1 foci and, once the association is established, they are not required for 53BP1 foci maintenance. The situation is different in NIH2/4 cut cells, in which this time-dependent sensitivity of 53BP1 to DICER and DROSHA knockdown cannot be observed, due to the constitutive damage generated by the activity of the I-Sce I enzyme, which cuts the DNA and will cut it again as soon as it is repaired. The idiosyncrasy of 53BP1 behavior with respect to the other DDR markers analyzed, in particular MDC1, can probably be ascribed to different ways of recruitment to the DSB. It is tempting to speculate that once the DNA lesion is sensed in the first steps of the DDR cascade, the *in situ* generated DDRNAs interact directly with the Tudor domains of 53BP1, which in turn recruit more MRN complex to the DSB, boosting ATM activation in a positive feedback loop. Once the secondary recruitment is established and the DDR focus has become a complex multiprotein structure, DDRNAs are not needed anymore for 53BP1 retention to the DSB. Indeed, the supposed RNA-binding domains of 53BP1, the tandem Tudor domains, are also responsible for its association to H4K20Me2 histone mark surrounding the break (Mallette et al., 2012; Pei et al., 2011). Therefore, a competition hypothesis can be proposed, in which 53BP1 first recognizes the DNA lesion through the binding to DDRNAs via its Tudor domains, and to ubiquitinated Lys 15 on histone H2A (and H2AX) via its ubiquitination-dependent recruitment (UDR) motif (Fradet-Turcotte et al., 2013).

Then, once H4K20Me2 is unmasked, 53BP1 affinity changes towards the methylated histone, becoming independent from RNA. To prove this hypothesis it would be crucial to perform a time-course crosslinking immunoprecipitation (CLIP) experiment, followed by high-throughput sequencing of the RNA bound to 53BP1 in cut and uncut NIH2/4 cells. This technique is more sensitive and accurate with respect to the immunoprecipitation followed by RNA radiolabeling performed previously (Pryde et al., 2005), by which, probably, just the most abundant RNA were observed.

*1.3 RNA polymerase II transcription at the DSB: a possible reconciliation?*

The issue of transcription at DSBs has been intensely studied by several groups and it is still a matter of debate. The discovery of DDRNAs and diRNAs (Wei et al., 2012), having the sequence of the DNA next to the DSB, and the involvement of DICER (and DROSHA for DDRNAs) in their biogenesis indicate that transcription near the cut site and synthesis of a long RNA precursor must occur. Of note, the observation that even an exogenous bacterial sequence lacking any mammalian promoter, such as the Lac-I-SceI-Tet locus, can give rise to RNA transcripts is in agreement with the current model of "pervasive transcription" (see Introduction, section 2.2). Moreover, the dependency of DDR focus formation upon IR and reformation after RNase A treatment on RNA polymerase II, showed by my experiments with transcription inhibitors (see Results, Figures 9 and 12), suggests that RNA pol II can be considered as a member of the DDR cascade. However, some observations seem to argue against these hypotheses. For example, it has been shown that RNA polymerase II, both the initiating and the elongating forms, is depleted from the sites of microirradiation (Beli et al., 2012; Miller et al., 2010), that Polycomb repressive complexes have been found to the sites of breakage (Chou et al., 2010) and that transcription of a reporter gene close to a cluster of DSBs is repressed by ATM-dependent regulation of chromatin condensation in response to DNA damage (Shanbhag et al., 2010).

The fact that RNA polymerase II has not been found at the sites of DNA damage can be due to the low sensitivity and resolution of the techniques used (immunofluorescence), not enough powerful to detect a possibly transient and/or weak association of the enzyme with the DNA around the break. It is conceivable that differential amounts of RNA pol II are engaged at the transcribing genes (most of the enzyme) and at the DNA lesions (few molecules). The generation of a long RNA precursor can, in fact, occur at a specific time point upon DNA damage and maybe just few molecules of RNA pol II are needed for its transcription, making it difficult to visualize this transient interaction. Another explanation could be that the post-transcriptional modifications of RNA pol II CTD, recognized by the antibodies that discriminate between specific forms of the enzyme (initiating or elongating), are not the same in a context of DNA damage. Maybe there are new DDR-dependent modifications of the C terminal tail of RNA pol II still to be discovered.

Supporting the idea of RNA generation at the site of DNA damage, it has been demonstrated that transcription can occur in DNA-damage induced γH2AX domains, specifically in discontinuities of the histone mark spreading, that are occupied by RNA pol II (Iacovoni et al., 2010). Moreover, high-resolution ChIP experiments have shown that γH2AX is depleted from the regions surrounding the break (on average 2 Kb at each end of the break are γH2AX-free), similarly to what happens at the transcription start sites of neighboring genes (Iacovoni et al., 2010). Since RNA pol II can transcribe within gaps of γH2AX signal, it is tempting to speculate that transcription can occur at the very near regions, γH2AX-free, around the cut site. In accordance with this model, DDRNAs and diRNAs map on sequences next to the DSB (see Results, Figure 36; (Wei et al., 2012)).

RNA pol II has also been shown to be able to bypass a break within a gene and to continue transcription elongation if DNA-PKcs is inhibited (Pankotai et al., 2012). Of course, this phenomenon can be dangerous for the cell, leading to mutations in the RNA transcript. Further studies are needed to better understand this intriguing but potentially hazardous ability of RNA pol II and how it is regulated by the DNA damage response.

Regarding the reports showing transcriptional silencing associated with DSB generation, in apparent discordance with my results, a possible reconciliation can be found. It is well known, in fact, that transcriptional silencing is induced by products of the RNAi machinery. The best examples are *Schizosaccharomyces pombe* centromeric locus, where transcriptional repression is enforced by DICER small RNA products, and the siRNA-directed DNA methylation coupled with gene silencing in *Arabidopsis thaliana* (Verdel et al., 2009). Moreover, the Polycomb repressive complex, shown to localize at the damaged sites (Chou et al., 2010), needs a lncRNA platform, to be recruited to the correct DNA sequence (Gupta et al., 2010; Spitale et al., 2011). Thus the presence of RNA, in particular small RNAs, at sites of DNA damage associated with transcriptional repression is not unusual and could have, on the contrary, an evolutionary conserved biological relevance.

## 2. Biogenesis and features of DDRNAs

*2.1 DICER and DROSHA direct involvement in DDR: differences between DDRNAs and miRNAs*

Although generated by DROSHA and DICER, DDRNAs do not act as miRNAs (Figure 56). First of all, miRNAs exert their function by targeting mRNAs, while DDRNAs are active also in the absence of any cellular RNA. In fact, chemically synthesized DDRNAs, specifically with the sequence of the damaged site, allow DDR focus reformation in RNase A-treated cells devoid of any RNA (see Results, Figure 41). Given that DDRNAs in NIH2/4 cells are not generated by the mouse genome, but they originate instead from the exogenous integrated sequence, DDR modulation by DDRNAs cannot be due to a translation-dependent mechanism. Indeed, DDRNAs in NIH2/4 cells do not match any endogenous transcript and the translation inhibitor cycloheximide does not impact on DDRNA activity (see Results, Figure 26). Moreover miRNA function is necessarily slow, since miRNAs modulate cellular events indirectly, by regulating protein levels. On the contrary, DDRNAs exert their role very quickly since they regulate DDR activation directly at the site of damage. Reconstitution with DDRNAs after RNase A treatment lasts, in fact, just 20 minutes at room temperature, arguing against an involvement of translation mechanisms. Finally, knockdown of GW182-like proteins does not impact on DDR foci formation, meaning that the canonical miRNA pathway is not involved in the accumulation of DDR factors under these experimental conditions; GW182-like proteins are instead necessary component of the miRISC complex (Tritschler et al., 2010).

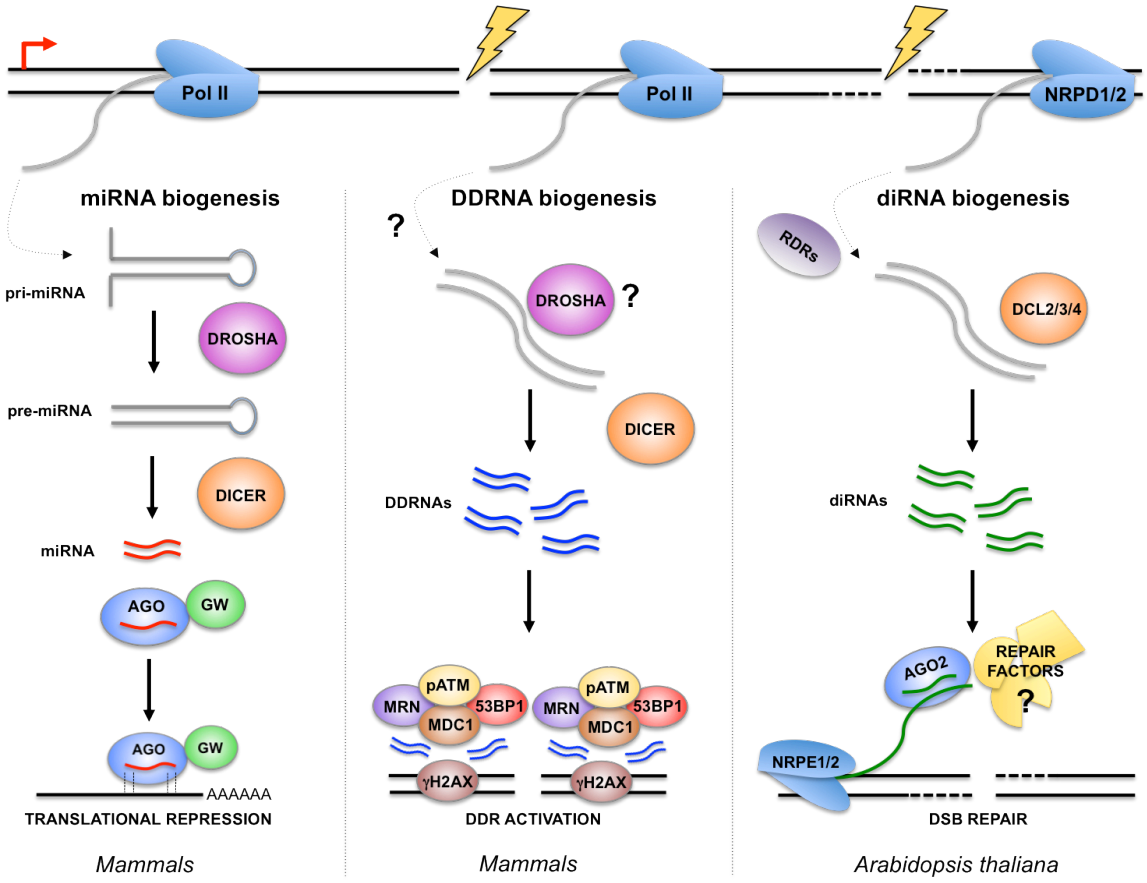


**Figure 56. Differences and similarities between DDRNAs, miRNAs and diRNAs.**
In mammals miRNA biogenesis starts with the transcription by the RNA polymerase II of a miRNA locus. The single-stranded RNA precursor, the pri-miRNA, folds into a hairpin which is recognized and processed by DROSHA. The resultant pre-miRNA is then further cut by DICER to form a double-strand ~22-nucleotide mature miRNA, whose guide strand is incorporated in the RISC complex (composed mainly by AGO and GW proteins) and mediates the translational repression of the mRNA target.
In mammalian cells upon DNA damage DDRNAs arise from the regions surrounding the break. RNA polymerase II is involved in their generation, although the exact biogenesis remains to be elucidated. The requirement for DROSHA is still controversial, but DICER activity is necessary for the production of possibly double-stranded, ~22-nucleotide DDRNAs. DDRNAs localize at the site of damage and are necessary to mount the DDR signaling cascade.
In plants ~21-nucleotide single-stranded RNA transcripts are generated by RNA polymerases IV (NRPD1/2) from the sequences in the vicinity of a DSB. RNA-dependent RNA polymerases (RDRs) convert these transcripts into double-stranded RNAs, which are processed into diRNAs by Dicer-like proteins (DCL2/3/4). diRNAs are then incorporated into Argonaute 2 (AGO2) and are localized to the DSB site through interaction with scaffold transcripts probably produced by RNA polymerases V (NRPE1/2). AGO2/diRNA complexes may recruit DSB repair proteins to facilitate DSB repair.

*2.2 Biogenesis of DDRNAs by DROSHA and DICER: a hypothetical model*

To justify the involvement of DICER and DROSHA ribonucleases in DDRNA biogenesis, a double-stranded precursor transcript must be generated at DNA lesions (Figure 56). Supporting this concept, I demonstrated that an *in vitro*-generated long fully double-stranded transcript spanning the Lac-I-SceI-Tet locus can be processed by recombinant human DICER and that DICER products are able to rescue 53BP1 focus formation in NIH2/4, in the absence of any cellular RNA (see Results, Figure 39). These data, together with the observation that DDRNA (but also diRNA) sequence reads from both strands are detectable by deep sequencing (see Results, Figure 36; (Wei et al., 2012)) suggest that either both DNA strands are transcribed or a still unknown mammalian RNA-dependent RNA polymerase produces a long dsRNA starting from a ssRNA transcript, as in the case of diRNA biogenesis in plants (Figure 56). In a recent paper, it has been shown that human RNA polymerase II can act as an RNA-dependent RNA polymerase, using an internal sequence of the murine ncRNA B2 (analogue to human Alu repeats) as template to extend B2 3' end by 18 nucleotides and to control its cellular metabolism (Wagner et al., 2013). Given the strong dependency of DDR activation specifically on RNA polymerase II (see Results, Figures 9-12), and not on other RNA polymerases, the synthesis of the double-stranded precursor RNA may rely entirely on the multiple functions of this enzyme.

The involvement of DROSHA in DDRNA biogenesis remains to be clarified. The deep sequencing results showed just a mild dependency of DDRNA production on DROSHA activity compared to DICER (see Results, Figure 38), in contrast with the observed alteration of DDR foci formation upon IR in DROSHA-depleted cells (see Results, Figure 14). Mirroring the deep sequencing trend, I observed that RNA coming from NIH2/4 cells lacking DROSHA was able to rescue 53BP1 focus formation in the single-cut system, although not to the same extent of RNA prepared from NIH2/4 cells lacking DICER (see Results, Figure 29). This behavior of DROSHA suggests that different situations can occur. For example, DROSHA can be dispensable if the double-stranded DDRNA

precursor is perfectly linear, generated by pairing of convergent transcripts or by the action of an RNA-dependent RNA polymerase. Conversely, DROSHA can be required if the damage happens in a genomic sequence that has the potential to internally anneal and fold into a double stranded-RNA with a stem-loop structure. This ribonuclease, in fact, is known to selectively process RNAs with double-stranded features and a hairpin structure, like pri-miRNAs. However, these are non-stringent rules because DROSHA seems to require also single-stranded extensions on the RNA substrate for an efficient processing, but it can also cut circular pri-miRNAs (Zeng and Cullen, 2005).

One additional question that remains to be elucidated is whether the generation of the RNA precursor precedes the occurrence of a break (and then DDRNAs are promptly processed or modified in response to DNA damage), or it is induced upon DNA damage. The detection of sequence reads from the uncut locus (although less then the cut locus) by both deep sequencings of NIH2/4 RNA (see Results, Figures 36 and 38) is not sufficient to support the first hypothesis. The locus studied in NIH2/4 cells contains Lac repeats that have been shown to be prone to a basal level of spontaneous DNA damage (Jacome and Fernandez-Capetillo, 2011). Thus, DDRNA reads detected in uncut cells may belong instead to a fraction of damaged cells. Regarding the second hypothesis, meaning the generation of the RNA precursor after the cut, the observation that DDR foci of senescent cells are indefinitely persistent suggests that a constant synthesis of RNA at the damaged sites must occur. Furthermore, in RNase A-treated cells DDR foci rapidly reform if RNA neo-synthesis is allowed (see Results, Figure 12), indicating that at sites of DNA damage RNA is constantly synthesized, processed and, likely, degraded.

Finally, it has to be determined if the processing of a precursor RNA into DDRNAs occurs at the DNA lesion sites, thus in the nucleus, or if a passage into the cytoplasm, where most, but not all (Doyle et al., 2013; Gullerova and Proudfoot, 2012; Ohrt et al., 2012; Sinkkonen et al., 2010), DICER molecules can be found, is needed.

*2.3 Are other components of the RNAi machinery involved in DDRNA generation and function?*

Increasing amounts of data indicate that members of the RNAi pathway, in particular AGO proteins, are engaged in processes different from their canonical cytoplasmic functions. In yeast, plants and mammals, AGO proteins can direct transcriptional silencing of heterochromatic regions, associate with transcriptionally active chromatin, orchestrate alternative splicing and interact with RNA polymerase II (Huang et al., 2013a; Meister, 2013). It has also been demonstrated that AGO2 in plants and human cells is necessary for diRNA functions in DNA repair (Wei et al., 2012). Given the similarities between diRNAs and DDRNAs, it is conceivable that AGO proteins are also involved in DDRNA-directed regulation of DDR activation. Moreover, both RNA deep sequencings of NIH2/4 cells confirmed that DDRNAs share a base bias towards uridine at their 5' end (see Results, Figure 38), compatible with AGO binding.

The proposed model (Figure 57; (Ba and Qi, 2013)) requires the presence of a putative RNA platform generated at the damaged site, that is recognized by the diRNAs/DDRNAs loaded into AGO proteins, similarly of what happens for plant RNA-dependent DNA methylation (Law and Jacobsen, 2010). AGO proteins may in turn recruit DDR and DNA damage repair components, but also chromatin remodeling complexes, in order, for example, to relax local chromatin making it more accessible to DDR factors and to compact neighboring chromatin, thus silencing adjacent genes. This model is supported by the observation that fluorescent DDRNAs promptly localize at the sequence-specific locus, upon DNA damage. It would be interesting to test if this localization can be affected by the absence of AGO proteins.

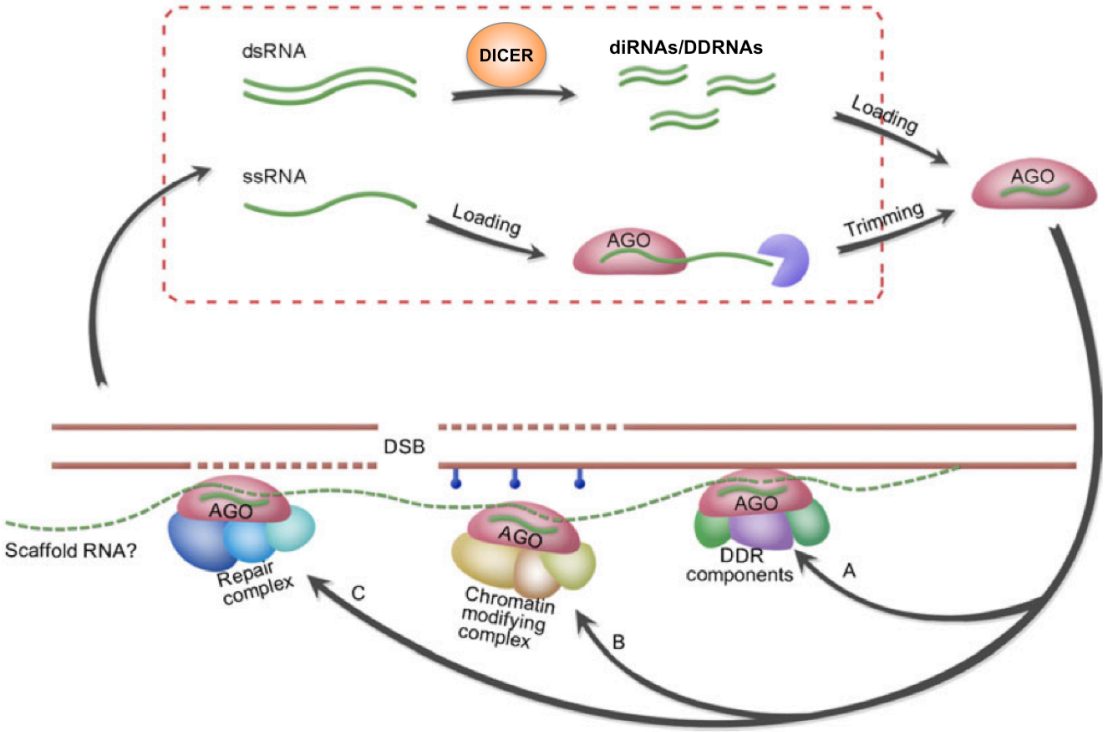


**Figure 57. A possible working model for DDRNAs and diRNAs in DDR and DNA damage repair.**
Upon DNA damage single-stranded RNA transcripts (ssRNAs) are generated by RNA polymerases (RNA polymerase IV in Arabidopsis and RNA polymerase II in mammals) from the regions surrounding the break. ssRNAs are then converted into double-stranded RNAs (dsRNAs) that are processed by DICER into diRNAs and DDRNAs, which can be subsequently incorporated into Argonaute (AGO) proteins. Alternatively, long ssRNAs can be directly loaded into AGO protein and processed by exonucleolytic trimming. In either case, AGO/diRNA or AGO/DDRNA complexes are localized to the DSB site through interaction with putative scaffold RNAs that are produced from the sequences around the DSB site. There, AGO/diRNA or AGO/DDRNA complexes may recruit DNA damage response (DDR) components to activate DDR (A), chromatin modifying complexes to modify local chromatin (B), or directly recruit DSB repair complex to the DSB site (C) to facilitate DSB repair.

### *2.4 DDRNA features and abundance*

In this thesis I have shown that DDRNAs are generated locally at the site of damage and favor the assembly of DDR factors (see Results, Figure 25). Indeed RNA sequencing of NIH2/4 RNA confirmed the presence of small RNAs arising from the integrated exogenous locus, which are induced upon cut (see Results, Figures 36 and 38). Selection for RNA with a 5'-monophosphate modification (as miRNA) and comparison of the reads with small RNAs generated at other genomic loci demonstrate that DDRNAs are distinct

from products of cellular RNA degradation. Furthermore their nucleotide bias at 5' end and 3' end indicates that these RNAs are processed at preferential RNA precursors sites, or that they are cut and subsequently trimmed. At present, it is unknown if DDRNAs harbor other modifications, common in other classes of small RNAs or in lower organisms, such as methylation at the 3' end.

One question still to be elucidated is whether DDRNAs act as single or double-stranded RNA. I have shown that synthetic DDRNAs, both labeled and unlabeled forms, are able to rescue DDR focus reformation, if annealed *in vitro* (see Results, Figures 41 and 47). However, it is still possible that these double-stranded DDRNAs, once in the cell, are unwound becoming single-stranded, just like miRNA. The fact that the deep sequencing data show a slight strand bias in DDRNA composition suggests that one of the two strands is preferentially maintained. Moreover, since a complementarity-based mechanism of action is the most likely, active DDRNAs have to be single-stranded in order to scan for their target. It is still conceivable that, similarly to miRNA and siRNA, DDRNAs arise as double-stranded molecules that have to be unwound to exert their function. Experiments using single-stranded DDRNA oligonucleotides are needed to clarify this important point.

DDRNAs appear to be low abundant, since they are not detectable by Northern blot analysis of samples enriched in small RNA (see Results, Figure 33) and they show a low number of reads (but still hundreds of reads) by deep sequencing. While plant diRNAs are detectable by Northern blot, in the same published report human diRNAs are detected only by deep sequencing (Wei et al., 2012), suggesting that in mammals these small RNA species are difficult to be visualized by Northern blot. One possibility is that DDRNA production is highly regulated, and they are generated, and then degraded, at a specific step of the DDR cascade. Thus, their real abundance within one cell at a given phase of the DDR activation is flattened looking at the cell population. Overcome the detection problem, for example by replacing NGS with less expensive and time-consuming techniques, like qRT-PCR, would be a step-forward for the study of DDRNAs.

# 3. Role of DDRNAs in DDR and DNA damage repair

*3.1 DDRNAs in DDR signaling: a structural component of the focus?*

Although it is unclear how DDRNAs may act to favor DDR activation, several models can be conceived. DDR initiation requires the focal assembly of DDR factors at DNA damage sites and some of these DDR factors such as 53BP1, BRCA1, KU and ATR have been previously reported to bind to RNA (see Introduction, section 4.2). Moreover it has been shown that the local accumulation of DDR proteins can be sufficient to trigger the activation of the signaling cascade even in the absence of DNA lesions (Soutoglou and Misteli, 2008). Thus, it is possible that DDRNAs may provide an opportunity for DDR factors to oligomerize and multimerize, favoring their activation. As it has been demonstrated for Polycomb complex recruitment on chromatin (Gupta et al., 2010; Spitale et al., 2011), DDRNAs can guide DDR components to the correct DNA lesion. It is tempting to speculate that DDR foci, already demonstrated to be dynamic structures (Lukas et al., 2003), may be indeed colloidal structures made of RNA and proteins, displaying liquid-like features, just like it has been validated for germline P-granules in *Caenorhabditis elegans* (Brangwynne et al., 2009).

Indeed experiments with fluorescent synthetic DDRNAs clearly reveal that they localize at the complementary DNA locus, in particular if damaged (see Results, Figures 52 and 53). However, my data and data from collaborators agree on the fact that cy5-DDRNAs do not appear to perfectly co-localize with the Lac and Tet repressor proteins, that bind to the DNA repeats at each side of the cut site. A possible explanation could be the issue of optical resolution: cy5-DDRNAs are in fact sub-resolution molecules (< 200 nm of diameter) and technical limitations can interfere with their correct visualization and, thus, localization. Super-resolution microscopy and/or electron microscopy may shed light on the real structure of DDR-RNA foci.

*3.2 DDRNAs in DDR signaling: a chromatin-mediated mechanism?*

RNA and components of the RNAi machinery have been shown to affect chromatin structure in different organisms (Verdel et al., 2009). Association of HP1 with heterochromatin depends on the RNA binding domain of the protein, and a still uncharacterized RNA component is essential to maintain the high-order chromatin structure (Maison et al., 2002). It has been shown that HP1 mobilization promotes chromatin changes that are essential for DDR initiation (see Introduction, section 1.2.*3*). In a possible working model, DDRNAs act by favoring site-specific chromatin modifications that stimulate DDR factors accumulation and spreading from the break. Interestingly, ATM has been proposed to monitor the presence of DSBs through DSB-induced changes in chromatin structure (Shanbhag et al., 2010). Moreover, ATM signaling is specifically required for DSB repair within heterochromatin and ATM signaling itself reduces KAP-1 association with chromatin, allowing DDR repair machinery to access DNA lesions (Goodarzi et al., 2011). Therefore, it is possible that DDRNAs control the affinity of ATM to DSBs by modulating chromatin changes. ATM association with the DSB could then cooperate in chromatin relaxation at the site of damage, making it more accessible to transcription and establishing a positive feedback loop.

*3.3 DDRNAs and MRN complex: an intimate relationship*

One of the first sensors of DNA damage is the MRN complex, which recognizes DNA ends and triggers the DDR cascade through ATM activation (Stracker and Petrini, 2011). I have shown that the focal accumulation of NBS1 and RAD50 components of the MRN complex is sensitive to DICER and DROSHA knockdown in human cells (see Results, Figures 15 and 16). Moreover, in the murine single-cut system I observed that MRE11 focus is reduced upon RNase A treatment, to an extent comparable to 53BP1 and pATM foci reduction (see Results, Figure 27). If DDRNAs are involved in secondary recruitment (see Discussion, section 1.2), they may control MRN focal stability during the feedback

loop phase, when the complex accumulates at the DSB through 53BP1-RAD50 interaction. The MRN molecules that firstly recognized the break, however, should not be affected. Interestingly I have also demonstrated that the activity of DDRNAs relies on MRN, since the use of mirin impedes the RNA-dependent rescue of DDR foci (see Results, Figure 28). The small molecule mirin has been shown to block 3'-to-5' exonuclease activity of MRE11 and to impair ATM activation without affecting MRN (and ATM) binding to DSBs (Dupre et al., 2008). Collectively these results suggest that the cytologically visible focal accumulation of DDR factors relies both on DDRNA and MRN functions. More specifically it appears that DDRNAs are not anymore able to exert their role when both the nuclease activity of MRE11 and ATM activation are impaired by mirin. It would be interesting to clarify the dependency of DDRNAs on MRE11 or ATM in terms of DDR foci reformation, by knocking-down and/or inhibiting in parallel ATM and MRE11 in NIH2/4 cells, deprived of all endogenous RNA and reconstituted with synthetic DDRNAs. One speculative possibility is that the MRN complex regulates DDRNAs by direct binding, although there is still no evidence in the literature of MRN capability to bind RNA molecules.

*3.4 DDRNAs in DNA damage repair*

A direct role for RNA in DNA damage repair was first shown in *Saccharomyces cerevisiae*, where RNA oligonucleotides were demonstrated to serve as templates for DNA repair via homologous recombination of a site-specific DSB (Derr and Strathern, 1993). This idea is further supported by RNA-mediated DNA rearrangements occurring in the unicellular eukaryotes *Oxytricha trifallax* (Nowacki et al., 2008) and *Tetrahymena thermophila* (Mochizuki et al., 2002). In *Arabidopsis thaliana* and in human cells, reporter-based assays suggest that diRNAs affect homologous recombination-dependent repair of DSBs (Wei et al., 2012). This is consistent with another work in *Drosophila melanogaster* suggesting that transcription at DSB sites requires resection (Michalik et al.,

2012). More recently, it has been shown that the RNA-binding proteins hnRNPUL-1 and -2 are required for effective DSB resection and they contribute to ATR-dependent signaling and DSB repair via HR, acting downstream of MRN (Polo et al., 2012). However, at present it is unclear if also DDRNAs have a role in HR. My experimental evidence indicates that DDRNAs can regulate DNA damage repair in the NIH2/4 cell system, both by DICER knockdown and LNA transfection (see Results, Figures 45 and 46). The principal DNA repair pathway in this case should be NHEJ, since non-synchronized cells are mainly in G1 when damaged. However, I cannot formally exclude an involvement of HR. Of note, I have shown that synthetic small RNAs spanning the locus are able to trigger 53BP1 focal accumulation (see Results, Figures 41 and 47). Although the formation of 53BP1 foci is not a surrogate marker for a specific DNA damage repair pathway, it is known that 53BP1 promotes NHEJ, inhibiting homologous recombination via RIF1 (Zimmermann et al., 2013). Therefore it remains to be clarified whether DDRNAs promote a specific repair pathway.

Taken together all the emerging observations, the possible roles of the small ncRNAs in DNA repair can be: platform to recruit DNA repair factors or chromatin modifying complexes at DSBs, template for DNA polymerase to fill in resected DNA during HR, or guide for the resection itself. It is not a new concept that RNA can direct the site-specific processing of a target DNA. In the protozoa *Tetrahymena*, DNA elimination requires an Argonaute homolog and small RNAs complementary to the regions that are lost (Mochizuki et al., 2002); in *Rhodobacter sphaeroides* RsAgo has been proposed to destroy foreign DNA sequences using small RNAs as a guide (Olovnikov et al., 2013). Another intriguing example is the CRISPR (Clustered Regularly Interspaced Short Palindromic Repeats) prokaryotic immune system. When a bacterium encounters a plasmid or phage for the first time, the exogenous DNA is processed by proteins encoded by CRISPR-associated (Cas) genes into small elements (of ~30bp in length), which are then inserted into the genomic CRISPR loci. RNAs from the CRISPR loci are constitutively expressed and

processed by a different set of Cas proteins (Cas II) into small RNAs. If the bacterium is infected again by the same plasmid or phage, the small RNAs guide additional Cas proteins (Cas III) to silence the exogenous transcripts or to directly eliminate the DNA (Bhaya et al., 2011).

Thus, it is not so unlikely that small RNAs can guide the resection, annealing to the DNA strand that has to be processed and allowing DNA repair via HR. In line with this hypothesis, RAD51, a protein involved in homology search during HR, has been shown in yeast to promote RNA:DNA hybrid formation (Wahba et al., 2013).

## 4. Looking for sequence-specific damaged locus

The reproducible observation that incubating RNase A-treated cells with synthetic DDRNAs rescues foci formation, within minutes at room temperature, has always been a surprisingly efficient process for me and my laboratory. The underlying implication was, in fact, that the synthetic oligonucleotides could scan the genome and find the right genetic locus to act and to reconstitute focal accumulation of DDR factors in a relatively short time (20-30 minutes). The use of fluorescent DDRNAs in RNase A-treated NIH2/4 cells confirmed what was, at the same time, an expected as well as surprising and exciting discovery: small RNA molecules are indeed able to find the exact location of their complementary DNA, in few minutes at room temperature (see Results, Figure 49). To explain this phenomenon, two possible models can be conceived (Figure 58). The first model envisages the presence of a long RNA platform generated at the locus upon DNA damage that is recognized by DDRNAs, similarly to what happens for the formation of heterochromatin in yeast (Verdel et al., 2009). In the second model DDRNAs directly bind the complementary DNA sequence of the locus. Thus, there are at least three possibilities of how RNA can recognize the sequence-specific locus: via an RNA:RNA interaction, via an RNA:DNA interaction or via a triplex RNA:DNA:DNA structure.

The fact that cy5-DDRNAs are able to localize at the locus even in the presence of α-amanitin suggests that either an RNA pol II-dependent platform RNA is bound to chromatin or to proteins, and it is somehow protected from RNase A degradation, or the platform RNA is transcribed by a different RNA polymerase. My data using RNA polymerase inhibitors argue against a possible involvement of RNA polymerase I and III in DDR (see Results, Figures 9-12), however this can be in part due to the experimental setup and to the inhibitory efficacy of the drug used. Reconstitution experiments with cy5-DDRNAs in the presence of specific RNA polymerase inhibitors or in cells knocked-down for the different RNA polymerases are needed to address this point. However, this model

does not explain the lower, but significant, fraction of cells in which cy5-DDRNAs localize at the uncut locus.

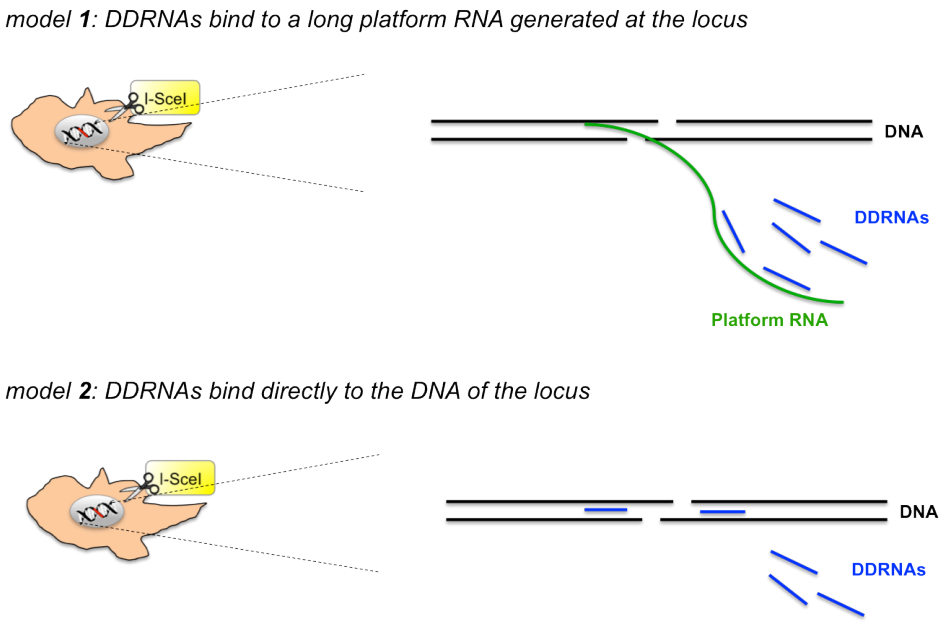


**Figure 58. Two hypothetical models of sequence recognition by DDRNAs.**
There are two conceivable models to explain the localization of DDRNAs at the site of damage. According to the first model, a long RNA platform is generated at the locus upon DNA damage and it is recognized by DDRNAs via an RNA:RNA interaction. In the second model DDRNAs directly bind the complementary DNA sequence of the locus, either via an RNA:DNA interaction or via a triplex RNA:DNA:DNA structure.

Double-stranded DNA is able to form triple-helical structures by accommodating a third DNA or RNA strand in its major groove. The third strand forms Hoogsteen or reverse Hoogsteen hydrogen bonds with the purine(A,G)-rich strand of the duplex. Triplexes have been implicated in a variety of cellular mechanisms (transcriptional regulation, chromatin organization, DNA repair, and RNA processing), however evidence for their existence is predominately based on *in vitro* experiments and computational analysis (Buske et al., 2011). Triplexes have the unique ability to target DNA in a sequence-specific manner, without requiring unwinding of the double helix, and this mechanism could explain how DDRNAs recognize the uncut DNA locus. However, Hoogsteen base pairing is not always granted and seems to occur only to specific stretches of DNA (purine-rich sequences);

differently, DDRNAs seem to have a genome-wide control of DDR foci formation. Alternatively, another possible mechanism that explains how DDRNAs directly bind their DNA target could be strand invasion, similarly to what happens during homologous recombination.

Consistent with a previous report (Pryde et al., 2005), I observed that 53BP1 foci are disrupted by RNase A-dependent total RNA degradation (see Results, Figures 7 and 13). On the contrary, in the same report RNase H treatment, that specifically degrades RNA:DNA hybrids, does not affect IR-dependent 53BP1 foci, suggesting that the RNA component involved in DDR foci formation does not anneal with a homologous DNA molecule. However, a recent work shows that when GFP-tagged RNase H1 is expressed in the cells, 53BP1 foci driven by endogenous replication stress disappear (Yuce and West, 2013). The two apparently contradictory results can reflect two different roles of 53BP1, one in response to DSB and DDR activation, the other in response to replication and transcription problems and to the formation of unresolved R-loop structures created by RNA:DNA hybrids.

In conclusion, both models proposed for the recognition of the locus by DDRNAs can be applied to explain the experimental results. When injected or added to RNase A-treated cells, cy5-DDRNAs scan the genome to find their complementary sequence, by a direct recognition of the DNA. If the DNA is damaged, a long platform RNA spanning the locus may be generated and multiple DDRNAs can be recruited to the lesion. Supporting this model, our collaborators have shown that the uncut sample always have less then 5 cy5-DDRNA molecules localized at the locus, whereas the cut sample contains a significant fraction of larger aggregates of ~20 cy5-DDRNA molecules localized at the locus (see Results, Figure 54). Time-laps experiments upon DNA damage induction and cy5-DDRNAs microinjection should be performed to understand the timing and the mode of recruitment of RNA molecules to the damaged locus, to further enter into the details of the biological mechanism.

# 5. Physiological relevance of DDRNAs

*5.1 DDRNAs as new guardians of the genome*

DNA double-strand breaks are the most dangerous DNA lesions since they may lead to massive loss of genetic information and genomic instability. A cycling cell carrying damaged DNA may run into the risk of replicating and propagating a corrupted DNA template to daughter cells. Thus, cells arrest cell cycle progression as soon as DNA damage is detected. In some cases, DNA damage generation enforces a persistent DDR signaling and a permanent proliferative arrest known as cellular senescence, the natural barrier to tumorigenesis (Jackson and Bartek, 2009). Ageing and cancer are intimately connected with the accumulation of DNA damage and the activation of DDR signaling. The discovery of DDRNAs adds an additional unanticipated level of DDR regulation. The idea that complexes containing DDR factors and small RNA products of DICER and DROSHA may control genome stability and the DNA damage response is radically new. The underlying hypothesis is that the "pervasive transcription" of the genome makes a crucial contribution to the activation and modulation of DDR, the vital process necessary to enforce cell cycle arrest and DNA repair. Thus, it is tempting to speculate that RNA is not only the messenger of genetic information or a byproduct of DNA transcription, but instead it contributes also to the preservation of genome integrity. Given the known tumor suppressive functions of DDR and the implication of its activation in a number of biological relevant processes, such as senescence, the study of the molecular mechanisms of DDRNA action may have a significant impact on our understanding of ageing and cancer. In this regard, it would be intriguing to study if DDRNAs are produced at damaged telomeres, recently shown to be the main cause of cellular senescence (Fumagalli et al., 2012).

*5.2 LNA technology to counteract site-specific DNA damage*

Achieving an effective therapy is a matter of finding the right target. The growing and powerful field of non-coding RNAs, that are now more and more implicated in a variety of diseases, indicates that maybe we have found novel good targets for therapy. Antisense-based new drugs such as Miravirsen from Santaris Pharma, a new treatment for hepatitis C virus (Janssen et al., 2013), and Kynamro from Genzyme, a new adjuvant for the cure of hypercholesterolaemia (Hair et al., 2013), are excellent examples. My experiments with LNA transfection in NIH2/4 cells suggest that also DDRNAs can be successfully targeted by antisense-based strategies (see Results, Figure 43). Specific LNA could then be used in all the conditions in which site-specific DNA damage activation is detrimental for the cell, for example in case of oncogene activation, DNA replication stress, telomere shortening, damaged telomeres or viral integration in the genome. Moreover, the inhibition of DDR activation via DDRNA neutralization can be used to radiosensitize cells harboring peculiar DNA sequences in their genome, such as transformed cells with chromosomal translocations.

*5.3 A new vision of DICER and DROSHA in pathology and cancer*

Inactivation of DICER or various components of DICER and DROSHA complexes enhances cell transformation and tumorigenesis (Kumar et al., 2007; Kumar et al., 2009). Mutations of DICER and its cofactor TARBP2 have been described in human carcinomas (Melo et al., 2009), pointing out a tumor-suppressor role for DICER and other components of the RNAi apparatus. However, individual miRNAs have been reported both to promote and to reduce cell proliferation, by regulating stability and translation of mRNAs encoding proteins with different roles in cell proliferation (Esquela-Kerscher and Slack, 2006). Therefore it is presently unclear how the inactivation of the RNAi machinery favors tumorigenesis. In the light of the novel concept of DDRNAs in DDR control, it is tempting to suggest that, in addition to their well-characterized functions in the modulation of gene

expression, DICER and DROSHA may impede cancerous cell proliferation, by sustaining DDR activation.

In a very recent paper it has been shown that DGCR8 binds to expanded CGG repeats in the 5' UTR of the fragile X mental retardation 1 (FMR1) mRNA, in patients with Fragile X-associated tremor/ataxia syndrome (FXTAS). This binding causes the partial sequestration of both DGCR8 and DROSHA within RNA aggregates, resulting in a reduced miRNA processing, that contributes to the neurodegenerative disease (Sellier et al., 2013). Since DROSHA is involved in controlling a correct DDR activation upon IR, it would be interesting to test if cells derived from those patients are particularly radiosensitive.

Complete genetic ablation of DICER in primary cells has been reported to cause premature senescence (Mudhasani et al., 2008). Conversely, partial down-regulation of DICER causes DNA damage and increases γH2AX foci, without significantly altering cell cycle progression (Tang et al., 2008). One possible explanation is that complete DICER inactivation may dramatically impair the cellular response to DNA damage, resulting in massive DNA-damage accumulation, incompatible with viability. In line with the data presented in this thesis, DICER partial inactivation may, instead, alleviate DDR and allow damaged cells to escape from checkpoint activation, without being detrimental for cell proliferation. In this way partial, but not complete, DICER inactivation can favor genomic instability and tumor progression. This model fits nicely with the observation that DICER haploinsufficiency, but not its homozygous deletion, is frequent in human cancer, and that, in mice, DICER haploinsufficiency promotes cancer, while complete loss of DICER is lethal (Kumar et al., 2009).

To conclude, I contributed to uncover a novel function of DICER and DROSHA in the modulation of the DNA damage response, through the production of genome-guardian small RNA molecules. It is worth noticing that this is consistent with the well-established

and evolutionary-conserved role of the RNAi machinery in preserving genome integrity from the attack of viruses and transposable elements.

# References

Adamson, B., Smogorzewska, A., Sigoillot, F.D., King, R.W., and Elledge, S.J. (2012). A genome-wide homologous recombination screen identifies the RNA-binding protein RBMX as a component of the DNA-damage response. Nat Cell Biol *14*, 318-328.

Al-Hakim, A., Escribano-Diaz, C., Landry, M.C., O'Donnell, L., Panier, S., Szilard, R.K., and Durocher, D. (2010). The ubiquitous role of ubiquitin in the DNA damage response. DNA Repair (Amst) *9*, 1229-1240.

Altieri, F., Grillo, C., Maceroni, M., and Chichiarelli, S. (2008). DNA damage and repair: from molecular mechanisms to health implications. Antioxid Redox Signal *10*, 891-937.

Alwine, J.C., Kemp, D.J., and Stark, G.R. (1977). Method for detection of specific RNAs in agarose gels by transfer to diazobenzyloxymethyl-paper and hybridization with DNA probes. Proceedings of the National Academy of Sciences of the United States of America *74*, 5350-5354.

Alzu, A., Bermejo, R., Begnis, M., Lucca, C., Piccini, D., Carotenuto, W., Saponaro, M., Brambati, A., Cocito, A., Foiani, M.*, et al.* (2012). Senataxin associates with replication forks to protect fork integrity across RNA-polymerase-II-transcribed genes. Cell *151*, 835-846.

Ameres, S.L., and Zamore, P.D. (2013). Diversifying microRNA sequence and function. Nat Rev Mol Cell Biol *14*, 475-488.

An, J., Huang, Y.C., Xu, Q.Z., Zhou, L.J., Shang, Z.F., Huang, B., Wang, Y., Liu, X.D., Wu, D.C., and Zhou, P.K. (2010). DNA-PKcs plays a dominant role in the regulation of H2AX phosphorylation in response to DNA damage and cell cycle progression. BMC Mol Biol *11*, 18.

Andl, T., Murchison, E.P., Liu, F., Zhang, Y., Yunta-Gonzalez, M., Tobias, J.W., Andl, C.D., Seykora, J.T., Hannon, G.J., and Millar, S.E. (2006). The miRNA-processing enzyme dicer is essential for the morphogenesis and maintenance of hair follicles. Curr Biol *16*, 1041-1049.

Aravin, A.A., Lagos-Quintana, M., Yalcin, A., Zavolan, M., Marks, D., Snyder, B., Gaasterland, T., Meyer, J., and Tuschl, T. (2003). The small RNA profile during Drosophila melanogaster development. Developmental cell *5*, 337-350.

Arnoult, N., Van Beneden, A., and Decottignies, A. (2012). Telomere length regulates TERRA levels through increased trimethylation of telomeric H3K9 and HP1alpha. Nat Struct Mol Biol *19*, 948-956.

Askarian-Amiri, M.E., Crawford, J., French, J.D., Smart, C.E., Smith, M.A., Clark, M.B., Ru, K., Mercer, T.R., Thompson, E.R., Lakhani, S.R.*, et al.* (2011). SNORD-host RNA Zfas1 is a regulator of mammary development and a potential marker for breast cancer. RNA *17*, 878-891.

Ayoub, N., Jeyasekharan, A.D., and Venkitaraman, A.R. (2009). Mobilization and recruitment of HP1: a bimodal response to DNA breakage. Cell Cycle *8*, 2945-2950.

Azzalin, C.M., Reichenbach, P., Khoriauli, L., Giulotto, E., and Lingner, J. (2007). Telomeric repeat containing RNA and RNA surveillance factors at mammalian chromosome ends. Science *318*, 798-801.

Ba, Z., and Qi, Y. (2013). Small RNAs: Emerging key players in DNA double-strand break repair. Sci China Life Sci *56*, 933-936.

Barraud, P., Emmerth, S., Shimada, Y., Hotz, H.R., Allain, F.H., and Buhler, M. (2011). An extended dsRBD with a novel zinc-binding motif mediates nuclear retention of fission yeast Dicer. EMBO J *30*, 4223-4235.

Bartek, J., Bartkova, J., and Lukas, J. (2007). DNA damage signalling guards against activated oncogenes and tumour progression. Oncogene *26*, 7773-7779.

Bartkova, J., Rezaei, N., Liontos, M., Karakaidos, P., Kletsas, D., Issaeva, N., Vassiliou, L.V., Kolettas, E., Niforou, K., Zoumpourlis, V.C*., et al.* (2006). Oncogene-induced senescence is part of the tumorigenesis barrier imposed by DNA damage checkpoints. Nature *444*, 633-637.

Bekker-Jensen, S., Lukas, C., Kitagawa, R., Melander, F., Kastan, M.B., Bartek, J., and Lukas, J. (2006). Spatial organization of the mammalian genome surveillance machinery in response to DNA strand breaks. J Cell Biol *173*, 195-206.

Bekker-Jensen, S., Lukas, C., Melander, F., Bartek, J., and Lukas, J. (2005). Dynamic assembly and sustained retention of 53BP1 at the sites of DNA damage are controlled by Mdc1/NFBD1. J Cell Biol *170*, 201-211.

Beli, P., Lukashchuk, N., Wagner, S.A., Weinert, B.T., Olsen, J.V., Baskcomb, L., Mann, M., Jackson, S.P., and Choudhary, C. (2012). Proteomic investigations reveal a role for RNA processing factor THRAP3 in the DNA damage response. Mol Cell *46*, 212-225.

Bennett, C.B., Westmoreland, T.J., Verrier, C.S., Blanchette, C.A., Sabin, T.L., Phatnani, H.P., Mishina, Y.V., Huper, G., Selim, A.L., Madison, E.R*., et al.* (2008). Yeast screens identify the RNA polymerase II CTD and SPT5 as relevant targets of BRCA1 interaction. PLoS One *3*, e1448.

Bensaude, O. (2011). Inhibiting eukaryotic transcription: Which compound to choose? How to evaluate its activity? Transcription *2*, 103-108.

Bensimon, A., Schmidt, A., Ziv, Y., Elkon, R., Wang, S.Y., Chen, D.J., Aebersold, R., and Shiloh, Y. (2010). ATM-dependent and -independent dynamics of the nuclear phosphoproteome after DNA damage. Sci Signal *3*, rs3.

Berezikov, E., Chung, W.J., Willis, J., Cuppen, E., and Lai, E.C. (2007). Mammalian mirtron genes. Mol Cell *28*, 328-336.

Bermejo, R., Lai, M.S., and Foiani, M. (2012). Preventing replication stress to maintain genome stability: resolving conflicts between replication and transcription. Mol Cell *45*, 710-718.

Bernstein, E., Kim, S.Y., Carmell, M.A., Murchison, E.P., Alcorn, H., Li, M.Z., Mills, A.A., Elledge, S.J., Anderson, K.V., and Hannon, G.J. (2003). Dicer is essential for mouse development. Nat Genet *35*, 215-217.

Berretta, J., and Morillon, A. (2009). Pervasive transcription constitutes a new level of eukaryotic genome regulation. EMBO Rep *10*, 973-982.

Bhaya, D., Davison, M., and Barrangou, R. (2011). CRISPR-Cas systems in bacteria and archaea: versatile small RNAs for adaptive defense and regulation. Annual review of genetics *45*, 273-297.

Birney, E., Stamatoyannopoulos, J.A., Dutta, A., Guigo, R., Gingeras, T.R., Margulies, E.H., Weng, Z., Snyder, M., Dermitzakis, E.T., Thurman, R.E.*, et al.* (2007). Identification and analysis of functional elements in 1% of the human genome by the ENCODE pilot project. Nature *447*, 799-816.

Biton, S., Barzilai, A., and Shiloh, Y. (2008). The neurological phenotype of ataxia-telangiectasia: solving a persistent puzzle. DNA Repair (Amst) *7*, 1028-1038.

Bolderson, E., Richard, D.J., Zhou, B.B., and Khanna, K.K. (2009). Recent advances in cancer therapy targeting proteins involved in DNA double-strand break repair. Clin Cancer Res *15*, 6314-6320.

Borchert, G.M., Lanier, W., and Davidson, B.L. (2006). RNA polymerase III transcribes human microRNAs. Nat Struct Mol Biol *13*, 1097-1101.

Borsani, O., Zhu, J., Verslues, P.E., Sunkar, R., and Zhu, J.K. (2005). Endogenous siRNAs derived from a pair of natural cis-antisense transcripts regulate salt tolerance in Arabidopsis. Cell *123*, 1279-1291.

Brangwynne, C.P., Eckmann, C.R., Courson, D.S., Rybarska, A., Hoege, C., Gharakhani, J., Julicher, F., and Hyman, A.A. (2009). Germline P granules are liquid droplets that localize by controlled dissolution/condensation. Science *324*, 1729-1732.

Branzei, D., and Foiani, M. (2008). Regulation of DNA repair throughout the cell cycle. Nat Rev Mol Cell Biol *9*, 297-308.

Branzei, D., and Foiani, M. (2010). Maintaining genome stability at the replication fork. Nat Rev Mol Cell Biol *11*, 208-219.

Britton, S., Coates, J., and Jackson, S.P. (2013). A new method for high-resolution imaging of Ku foci to decipher mechanisms of DNA double-strand break repair. J Cell Biol *202*, 579-595.

Buker, S.M., Iida, T., Buhler, M., Villen, J., Gygi, S.P., Nakayama, J., and Moazed, D. (2007). Two different Argonaute complexes are required for siRNA generation and heterochromatin assembly in fission yeast. Nat Struct Mol Biol *14*, 200-207.

Buscemi, G., Perego, P., Carenini, N., Nakanishi, M., Chessa, L., Chen, J., Khanna, K., and Delia, D. (2004). Activation of ATM and Chk2 kinases in relation to the amount of DNA strand breaks. Oncogene *23*, 7691-7700.

Bushnell, D.A., Cramer, P., and Kornberg, R.D. (2002). Structural basis of transcription: alpha-amanitin-RNA polymerase II cocrystal at 2.8 A resolution. Proceedings of the National Academy of Sciences of the United States of America *99*, 1218-1222.

Buske, F.A., Mattick, J.S., and Bailey, T.L. (2011). Potential in vivo roles of nucleic acid triple-helices. RNA Biol *8*, 427-439.

Bywater, M.J., Poortinga, G., Sanij, E., Hein, N., Peck, A., Cullinane, C., Wall, M., Cluse, L., Drygin, D., Anderes, K.*, et al.* (2012). Inhibition of RNA polymerase I as a therapeutic strategy to promote cancer-specific activation of p53. Cancer cell *22*, 51-65.

Caldecott, K.W. (2008). Single-strand break repair and genetic disease. Nat Rev Genet *9*, 619-631.

Cao, F., Li, X., Hiew, S., Brady, H., Liu, Y., and Dou, Y. (2009). Dicer independent small RNAs associate with telomeric heterochromatin. RNA *15*, 1274-1281.

Cao, L., Kim, S., Xiao, C., Wang, R.H., Coumoul, X., Wang, X., Li, W.M., Xu, X.L., De Soto, J.A., Takai, H.*, et al.* (2006). ATM-Chk2-p53 activation prevents tumorigenesis at an expense of organ homeostasis upon Brca1 deficiency. EMBO J *25*, 2167-2177.

Carninci, P., Kasukawa, T., Katayama, S., Gough, J., Frith, M.C., Maeda, N., Oyama, R., Ravasi, T., Lenhard, B., Wells, C.*, et al.* (2005). The transcriptional landscape of the mammalian genome. Science *309*, 1559-1563.

Caron, P., Aymard, F., Iacovoni, J.S., Briois, S., Canitrot, Y., Bugler, B., Massip, L., Losada, A., and Legube, G. (2012). Cohesin protects genes against gammaH2AX Induced by DNA double-strand breaks. PLoS Genet *8*, e1002460.

Carthew, R.W., and Sontheimer, E.J. (2009). Origins and Mechanisms of miRNAs and siRNAs. Cell *136*, 642-655.

Castel, S.E., and Martienssen, R.A. (2013). RNA interference in the nucleus: roles for small RNAs in transcription, epigenetics and beyond. Nat Rev Genet *14*, 100-112.

Castelnuovo, M., Massone, S., Tasso, R., Fiorino, G., Gatti, M., Robello, M., Gatta, E., Berger, A., Strub, K., Florio, T.*, et al.* (2010). An Alu-like RNA promotes cell differentiation and reduces malignancy of human neuroblastoma cells. Faseb J *24*, 4033-4046.

Celeste, A., Fernandez-Capetillo, O., Kruhlak, M.J., Pilch, D.R., Staudt, D.W., Lee, A., Bonner, R.F., Bonner, W.M., and Nussenzweig, A. (2003). Histone H2AX phosphorylation is dispensable for the initial recognition of DNA breaks. Nat Cell Biol *5*, 675-679.

Cernilogar, F.M., Onorati, M.C., Kothe, G.O., Burroughs, A.M., Parsi, K.M., Breiling, A., Lo Sardo, F., Saxena, A., Miyoshi, K., Siomi, H.*, et al.* (2011). Chromatin-associated RNA interference components contribute to transcriptional regulation in Drosophila. Nature *480*, 391-395.

Chapman, J.R., Taylor, M.R., and Boulton, S.J. (2012). Playing the end game: DNA double-strand break repair pathway choice. Mol Cell *47*, 497-510.

Charier, G., Couprie, J., Alpha-Bazin, B., Meyer, V., Quemeneur, E., Guerois, R., Callebaut, I., Gilquin, B., and Zinn-Justin, S. (2004). The Tudor tandem of 53BP1: a new structural motif involved in DNA and RG-rich peptide binding. Structure *12*, 1551-1562.

Chen, P.Y., Manninga, H., Slanchev, K., Chien, M., Russo, J.J., Ju, J., Sheridan, R., John, B., Marks, D.S., Gaidatzis, D.*, et al.* (2005). The developmental miRNA profiles of zebrafish as determined by small RNA cloning. Genes & development *19*, 1288-1293.

Cheng, J., Guo, J.M., Xiao, B.X., Miao, Y., Jiang, Z., Zhou, H., and Li, Q.N. (2011). piRNA, the new non-coding RNA, is aberrantly expressed in human cancer cells. Clin Chim Acta *412*, 1621-1625.

Cheung, A.C., and Cramer, P. (2011). Structural basis of RNA polymerase II backtracking, arrest and reactivation. Nature *471*, 249-253.

Chou, D.M., Adamson, B., Dephoure, N.E., Tan, X., Nottke, A.C., Hurov, K.E., Gygi, S.P., Colaiacovo, M.P., and Elledge, S.J. (2010). A chromatin localization screen reveals poly (ADP ribose)-regulated recruitment of the repressive polycomb and NuRD complexes to sites of DNA damage. Proc Natl Acad Sci U S A *107*, 18475-18480.

Chowdhury, D., Choi, Y.E., and Brault, M.E. (2013). Charity begins at home: non-coding RNA functions in DNA repair. Nat Rev Mol Cell Biol *14*, 181-189.

Chung, S.H., and Kennedy, R.A. (1991). Forward-backward non-linear filtering technique for extracting small biological signals from noise. J Neurosci Methods *40*, 71-86.

Ciccia, A., and Elledge, S.J. (2010). The DNA damage response: making it safe to play with knives. Mol Cell *40*, 179-204.

Clark, M.B., Amaral, P.P., Schlesinger, F.J., Dinger, M.E., Taft, R.J., Rinn, J.L., Ponting, C.P., Stadler, P.F., Morris, K.V., Morillon, A.*, et al.* (2011). The reality of pervasive transcription. PLoS Biol *9*, e1000625; discussion e1001102.

Clemson, C.M., Hutchinson, J.N., Sara, S.A., Ensminger, A.W., Fox, A.H., Chess, A., and Lawrence, J.B. (2009). An architectural role for a nuclear noncoding RNA: NEAT1 RNA is essential for the structure of paraspeckles. Molecular cell *33*, 717-726.

Cook, P.J., Ju, B.G., Telese, F., Wang, X., Glass, C.K., and Rosenfeld, M.G. (2009). Tyrosine dephosphorylation of H2AX modulates apoptosis and survival decisions. Nature *458*, 591-596.

Cummins, J.M., He, Y., Leary, R.J., Pagliarini, R., Diaz, L.A., Jr., Sjoblom, T., Barad, O., Bentwich, Z., Szafranska, A.E., Labourier, E.*, et al.* (2006). The colorectal microRNAome. Proceedings of the National Academy of Sciences of the United States of America *103*, 3687-3692.

d'Adda di Fagagna, F. (2008). Living on a break: cellular senescence as a DNA-damage response. Nat Rev Cancer *8*, 512-522.

d'Adda di Fagagna, F., Reaper, P.M., Clay-Farrace, L., Fiegler, H., Carr, P., Von Zglinicki, T., Saretzki, G., Carter, N.P., and Jackson, S.P. (2003). A DNA damage checkpoint response in telomere-initiated senescence. Nature *426*, 194-198.

da Costa Martins, P.A., Bourajjaj, M., Gladka, M., Kortland, M., van Oort, R.J., Pinto, Y.M., Molkentin, J.D., and De Windt, L.J. (2008). Conditional dicer gene deletion in the postnatal myocardium provokes spontaneous cardiac remodeling. Circulation *118*, 1567-1576.

Damsma, G.E., and Cramer, P. (2009). Molecular basis of transcriptional mutagenesis at 8-oxoguanine. J Biol Chem *284*, 31658-31663.

Davalos, V., Moutinho, C., Villanueva, A., Boque, R., Silva, P., Carneiro, F., and Esteller, M. (2012). Dynamic epigenetic regulation of the microRNA-200 family mediates epithelial and mesenchymal transitions in human tumorigenesis. Oncogene *31*, 2062-2074.

Davis, T.H., Cuellar, T.L., Koch, S.M., Barker, A.J., Harfe, B.D., McManus, M.T., and Ullian, E.M. (2008). Conditional loss of Dicer disrupts cellular and tissue morphogenesis in the cortex and hippocampus. J Neurosci *28*, 4322-4330.

De Bont, R., and van Larebeke, N. (2004). Endogenous DNA damage in humans: a review of quantitative data. Mutagenesis *19*, 169-185.

Deans, A.J., and West, S.C. (2011). DNA interstrand crosslink repair and cancer. Nat Rev Cancer *11*, 467-480.

Derr, L.K., and Strathern, J.N. (1993). A role for reverse transcripts in gene conversion. Nature *361*, 170-173.

Deuve, J.L., and Avner, P. (2011). The coupling of X-chromosome inactivation to pluripotency. Annu Rev Cell Dev Biol *27*, 611-629.

Di Micco, R., Fumagalli, M., Cicalese, A., Piccinin, S., Gasparini, P., Luise, C., Schurra, C., Garre, M., Nuciforo, P.G., Bensimon, A.*, et al.* (2006). Oncogene-induced senescence is a DNA damage response triggered by DNA hyper-replication. Nature *444*, 638-642.

Di Micco, R., Fumagalli, M., and d'Adda di Fagagna, F. (2007). Breaking news: high-speed race ends in arrest--how oncogenes induce senescence. Trends Cell Biol *17*, 529-536.

Difilippantonio, S., Gapud, E., Wong, N., Huang, C.Y., Mahowald, G., Chen, H.T., Kruhlak, M.J., Callen, E., Livak, F., Nussenzweig, M.C.*, et al.* (2008). 53BP1 facilitates long-range DNA end-joining during V(D)J recombination. Nature *456*, 529-533.

Dimitrova, N., Chen, Y.C., Spector, D.L., and de Lange, T. (2008). 53BP1 promotes non-homologous end joining of telomeres by increasing chromatin mobility. Nature *456*, 524-528.

Ding, H., Wong, P.T., Lee, E.L., Gafni, A., and Steel, D.G. (2009). Determination of the oligomer size of amyloidogenic protein beta-amyloid(1-40) by single-molecule spectroscopy. Biophysical journal *97*, 912-921.

Dinger, M.E., Amaral, P.P., Mercer, T.R., and Mattick, J.S. (2009). Pervasive transcription of the eukaryotic genome: functional indices and conceptual implications. Brief Funct Genomic Proteomic *8*, 407-423.

Doil, C., Mailand, N., Bekker-Jensen, S., Menard, P., Larsen, D.H., Pepperkok, R., Ellenberg, J., Panier, S., Durocher, D., Bartek, J.*, et al.* (2009). RNF168 binds and amplifies ubiquitin conjugates on damaged chromosomes to allow accumulation of repair proteins. Cell *136*, 435-446.

Dominguez-Sanchez, M.S., Barroso, S., Gomez-Gonzalez, B., Luna, R., and Aguilera, A. (2011). Genome instability and transcription elongation impairment in human cells depleted of THO/TREX. PLoS genetics *7*, e1002386.

Doyle, M., Badertscher, L., Jaskiewicz, L., Guttinger, S., Jurado, S., Hugenschmidt, T., Kutay, U., and Filipowicz, W. (2013). The double-stranded RNA binding domain of human Dicer functions as a nuclear localization signal. RNA *19*, 1238-1252.

Drygin, D., Lin, A., Bliesath, J., Ho, C.B., O'Brien, S.E., Proffitt, C., Omori, M., Haddach, M., Schwaebe, M.K., Siddiqui-Jain, A.*, et al.* (2011). Targeting RNA polymerase I with an oral small molecule CX-5461 inhibits ribosomal RNA synthesis and solid tumor growth. Cancer research *71*, 1418-1430.

Dupre, A., Boyer-Chatenet, L., Sattler, R.M., Modi, A.P., Lee, J.H., Nicolette, M.L., Kopelovich, L., Jasin, M., Baer, R., Paull, T.T.*, et al.* (2008). A forward chemical genetic screen reveals an inhibitor of the Mre11-Rad50-Nbs1 complex. Nat Chem Biol *4*, 119-125.

Emmerth, S., Schober, H., Gaidatzis, D., Roloff, T., Jacobeit, K., and Buhler, M. (2010). Nuclear retention of fission yeast dicer is a prerequisite for RNAi-mediated heterochromatin assembly. Dev Cell *18*, 102-113.

Esquela-Kerscher, A., and Slack, F.J. (2006). Oncomirs - microRNAs with a role in cancer. Nature reviews Cancer *6*, 259-269.

Esteller, M. (2011). Non-coding RNAs in human disease. Nat Rev Genet *12*, 861-874.

Eulalio, A., Behm-Ansmant, I., and Izaurralde, E. (2007). P bodies: at the crossroads of post-transcriptional pathways. Nat Rev Mol Cell Biol *8*, 9-22.

Evan, G.I., and d'Adda di Fagagna, F. (2009). Cellular senescence: hot or what? Curr Opin Genet Dev *19*, 25-31.

Farazi, T.A., Juranek, S.A., and Tuschl, T. (2008). The growing catalog of small RNAs and their association with distinct Argonaute/Piwi family members. Development *135*, 1201-1214.

Fattah, F., Lee, E.H., Weisensel, N., Wang, Y., Lichter, N., and Hendrickson, E.A. (2010). Ku regulates the non-homologous end joining pathway choice of DNA double-strand break repair in human somatic cells. PLoS Genet *6*, e1000855.

Fire, A., Xu, S., Montgomery, M.K., Kostas, S.A., Driver, S.E., and Mello, C.C. (1998). Potent and specific genetic interference by double-stranded RNA in Caenorhabditis elegans. Nature *391*, 806-811.

Flynn, R.L., Centore, R.C., O'Sullivan, R.J., Rai, R., Tse, A., Songyang, Z., Chang, S., Karlseder, J., and Zou, L. (2011). TERRA and hnRNPA1 orchestrate an RPA-to-POT1 switch on telomeric single-stranded DNA. Nature *471*, 532-536.

Fradet-Turcotte, A., Canny, M.D., Escribano-Diaz, C., Orthwein, A., Leung, C.C., Huang, H., Landry, M.C., Kitevski-LeBlanc, J., Noordermeer, S.M., Sicheri, F.*, et al.* (2013). 53BP1 is a reader of the DNA-damage-induced H2A Lys 15 ubiquitin mark. Nature *499*, 50-54.

Francia, S., Michelini, F., Saxena, A., Tang, D., de Hoon, M., Anelli, V., Mione, M., Carninci, P., and d'Adda di Fagagna, F. (2012). Site-specific DICER and DROSHA RNA products control the DNA-damage response. Nature *488*, 231-235.

Frank, F., Hauver, J., Sonenberg, N., and Nagar, B. (2012). Arabidopsis Argonaute MID domains use their nucleotide specificity loop to sort small RNAs. EMBO J *31*, 3588-3595.

Frank, F., Sonenberg, N., and Nagar, B. (2010). Structural basis for 5'-nucleotide base-specific recognition of guide RNA by human AGO2. Nature *465*, 818-822.

Fumagalli, M., Rossiello, F., Clerici, M., Barozzi, S., Cittaro, D., Kaplunov, J.M., Bucci, G., Dobreva, M., Matti, V., Beausejour, C.M.*, et al.* (2012). Telomeric DNA damage is irreparable and causes persistent DNA-damage-response activation. Nat Cell Biol *14*, 355-365.

Gagne, J.P., Hendzel, M.J., Droit, A., and Poirier, G.G. (2006). The expanding role of poly(ADP-ribose) metabolism: current challenges and new perspectives. Curr Opin Cell Biol *18*, 145-151.

Ganesan, S., Silver, D.P., Greenberg, R.A., Avni, D., Drapkin, R., Miron, A., Mok, S.C., Randrianarison, V., Brodie, S., Salstrom, J.*, et al.* (2002). BRCA1 supports XIST RNA concentration on the inactive X chromosome. Cell *111*, 393-405.

Gilder, A.S., Do, P.M., Carrero, Z.I., Cosman, A.M., Broome, H.J., Velma, V., Martinez, L.A., and Hebert, M.D. (2011). Coilin participates in the suppression of RNA polymerase I in response to cisplatin-induced DNA damage. Mol Biol Cell *22*, 1070-1079.

Gillet, L.C., and Scharer, O.D. (2006). Molecular mechanisms of mammalian global genome nucleotide excision repair. Chem Rev *106*, 253-276.

Goodarzi, A.A., Kurka, T., and Jeggo, P.A. (2011). KAP-1 phosphorylation regulates CHD3 nucleosome remodeling during the DNA double-strand break response. Nat Struct Mol Biol *18*, 831-839.

Gullerova, M., and Proudfoot, N.J. (2012). Convergent transcription induces transcriptional gene silencing in fission yeast and mammalian cells. Nat Struct Mol Biol *19*, 1193-1201.

Guo, S., and Kemphues, K.J. (1995). par-1, a gene required for establishing polarity in C. elegans embryos, encodes a putative Ser/Thr kinase that is asymmetrically distributed. Cell *81*, 611-620.

Gupta, R.A., Shah, N., Wang, K.C., Kim, J., Horlings, H.M., Wong, D.J., Tsai, M.C., Hung, T., Argani, P., Rinn, J.L.*, et al.* (2010). Long non-coding RNA HOTAIR reprograms chromatin state to promote cancer metastasis. Nature *464*, 1071-1076.

Hair, P., Cameron, F., and McKeage, K. (2013). Mipomersen sodium: first global approval. Drugs *73*, 487-493.

Halic, M., and Moazed, D. (2010). Dicer-independent primal RNAs trigger RNAi and heterochromatin formation. Cell *140*, 504-516.

Hannon, G.J. (2002). RNA interference. Nature *418*, 244-251.

Hansen, T.B., Jensen, T.I., Clausen, B.H., Bramsen, J.B., Finsen, B., Damgaard, C.K., and Kjems, J. (2013). Natural RNA circles function as efficient microRNA sponges. Nature *495*, 384-388.

Hayflick, L., and Moorhead, P.S. (1961). The serial cultivation of human diploid cell strains. Exp Cell Res *25*, 585-621.

He, L., He, X., Lim, L.P., de Stanchina, E., Xuan, Z., Liang, Y., Xue, W., Zender, L., Magnus, J., Ridzon, D.*, et al.* (2007). A microRNA component of the p53 tumour suppressor network. Nature *447*, 1130-1134.

Hecht, S.M. (2000). Bleomycin: new perspectives on the mechanism of action. J Nat Prod *63*, 158-168.

Helleday, T., Lo, J., van Gent, D.C., and Engelward, B.P. (2007). DNA double-strand break repair: from mechanistic understanding to cancer treatment. DNA Repair (Amst) *6*, 923-935.

Herbig, U., Jobling, W.A., Chen, B.P., Chen, D.J., and Sedivy, J.M. (2004). Telomere shortening triggers senescence of human cells through a pathway involving ATM, p53, and p21(CIP1), but not p16(INK4a). Mol Cell *14*, 501-513.

Hill, D.A., Ivanovich, J., Priest, J.R., Gurnett, C.A., Dehner, L.P., Desruisseau, D., Jarzembowski, J.A., Wikenheiser-Brokamp, K.A., Suarez, B.K., Whelan, A.J.*, et al.* (2009). DICER1 mutations in familial pleuropulmonary blastoma. Science *325*, 965.

Hirao, A., Cheung, A., Duncan, G., Girard, P.M., Elia, A.J., Wakeham, A., Okada, H., Sarkissian, T., Wong, J.A., Sakai, T.*, et al.* (2002). Chk2 is a tumor suppressor that regulates apoptosis in both an ataxia telangiectasia mutated (ATM)-dependent and an ATM-independent manner. Mol Cell Biol *22*, 6521-6532.

Hong, Z., Jiang, J., Lan, L., Nakajima, S., Kanno, S., Koseki, H., and Yasui, A. (2008). A polycomb group protein, PHF1, is involved in the response to DNA double-strand breaks in human cell. Nucleic Acids Res *36*, 2939-2947.

Hsin, J.P., and Manley, J.L. (2012). The RNA polymerase II CTD coordinates transcription and RNA processing. Genes Dev *26*, 2119-2137.

Huang, V., Zheng, J., Qi, Z., Wang, J., Place, R.F., Yu, J., Li, H., and Li, L.C. (2013a). Ago1 Interacts with RNA Polymerase II and Binds to the Promoters of Actively Transcribed Genes in Human Cancer Cells. PLoS genetics *9*, e1003821.

Huang, Y., Kesselman, D., Kizub, D., Guerrero-Preston, R., and Ratovitski, E.A. (2013b). Phospho-DeltaNp63alpha/microRNA feedback regulation in squamous carcinoma cells upon cisplatin exposure. Cell Cycle *12*, 684-697.

Huarte, M., Guttman, M., Feldser, D., Garber, M., Koziol, M.J., Kenzelmann-Broz, D., Khalil, A.M., Zuk, O., Amit, I., Rabani, M.*, et al.* (2010). A large intergenic noncoding RNA induced by p53 mediates global gene repression in the p53 response. Cell *142*, 409-419.

Huen, M.S., Grant, R., Manke, I., Minn, K., Yu, X., Yaffe, M.B., and Chen, J. (2007). RNF8 transduces the DNA-damage signal via histone ubiquitylation and checkpoint protein assembly. Cell *131*, 901-914.

Hung, T., Wang, Y., Lin, M.F., Koegel, A.K., Kotake, Y., Grant, G.D., Horlings, H.M., Shah, N., Umbricht, C., Wang, P.*, et al.* (2011). Extensive and coordinated transcription of noncoding RNAs within cell-cycle promoters. Nat Genet *43*, 621-629.

Iacovoni, J.S., Caron, P., Lassadi, I., Nicolas, E., Massip, L., Trouche, D., and Legube, G. (2010). High-resolution profiling of gammaH2AX around DNA double strand breaks in the mammalian genome. EMBO J *29*, 1446-1457.

Ichijima, Y., Ichijima, M., Lou, Z., Nussenzweig, A., Camerini-Otero, R.D., Chen, J., Andreassen, P.R., and Namekawa, S.H. (2011). MDC1 directs chromosome-wide silencing of the sex chromosomes in male germ cells. Genes Dev *25*, 959-971.

Iliakis, G., Wang, Y., Guan, J., and Wang, H. (2003). DNA damage checkpoint control in cells exposed to ionizing radiation. Oncogene *22*, 5834-5847.

Jackson, S.P. (2002). Sensing and repairing DNA double-strand breaks. Carcinogenesis *23*, 687-696.

Jackson, S.P., and Bartek, J. (2009). The DNA-damage response in human biology and disease. Nature *461*, 1071-1078.

Jackson, S.P., and Durocher, D. (2013). Regulation of DNA damage responses by ubiquitin and SUMO. Mol Cell *49*, 795-807.

Jacob, F., and Monod, J. (1961). Genetic regulatory mechanisms in the synthesis of proteins. J Mol Biol *3*, 318-356.

Jacome, A., and Fernandez-Capetillo, O. (2011). Lac operator repeats generate a traceable fragile site in mammalian cells. EMBO reports *12*, 1032-1038.

Janssen, H.L., Kauppinen, S., and Hodges, M.R. (2013). HCV infection and miravirsen. N Engl J Med *369*, 878.

Jaskiewicz, L., and Filipowicz, W. (2008). Role of Dicer in posttranscriptional RNA silencing. Curr Top Microbiol Immunol *320*, 77-97.

Jazayeri, A., Balestrini, A., Garner, E., Haber, J.E., and Costanzo, V. (2008). Mre11-Rad50-Nbs1-dependent processing of DNA breaks generates oligonucleotides that stimulate ATM activity. EMBO J *27*, 1953-1962.

Jazayeri, A., Falck, J., Lukas, C., Bartek, J., Smith, G.C., Lukas, J., and Jackson, S.P. (2006). ATM- and cell cycle-dependent regulation of ATR in response to DNA double-strand breaks. Nat Cell Biol *8*, 37-45.

Jepsen, J.S., Sorensen, M.D., and Wengel, J. (2004). Locked nucleic acid: a potent nucleic acid analog in therapeutics and biotechnology. Oligonucleotides *14*, 130-146.

Ji, L., and Chen, X. (2012). Regulation of small RNA stability: methylation and beyond. Cell Res *22*, 624-636.

Kanaar, R., and Wyman, C. (2008). DNA repair by the MRN complex: break it to make it. Cell *135*, 14-16.

Kanellopoulou, C., Muljo, S.A., Kung, A.L., Ganesan, S., Drapkin, R., Jenuwein, T., Livingston, D.M., and Rajewsky, K. (2005). Dicer-deficient mouse embryonic stem cells are defective in differentiation and centromeric silencing. Genes Dev *19*, 489-501.

Kapranov, P., and St Laurent, G. (2012). Dark Matter RNA: Existence, Function, and Controversy. Front Genet *3*, 60.

Karpenshif, Y., and Bernstein, K.A. (2012). From yeast to mammals: recent advances in genetic control of homologous recombination. DNA Repair (Amst) *11*, 781-788.

Karreth, F.A., Tay, Y., Perna, D., Ala, U., Tan, S.M., Rust, A.G., DeNicola, G., Webster, K.A., Weiss, D., Perez-Mancera, P.A.*, et al.* (2011). In vivo identification of tumor-suppressive PTEN ceRNAs in an oncogenic BRAF-induced mouse model of melanoma. Cell *147*, 382-395.

Kawai, S., and Amano, A. (2012). BRCA1 regulates microRNA biogenesis via the DROSHA microprocessor complex. J Cell Biol *197*, 201-208.

Kawamata, T., Yoda, M., and Tomari, Y. (2011). Multilayer checkpoints for microRNA authenticity during RISC assembly. EMBO Rep *12*, 944-949.

Kawano, M., Kawazu, C., Lizio, M., Kawaji, H., Carninci, P., Suzuki, H., and Hayashizaki, Y. (2010). Reduction of non-insert sequence reads by dimer eliminator LNA oligonucleotide for small RNA deep sequencing. Biotechniques *49*, 751-755.

Kedde, M., le Sage, C., Duursma, A., Zlotorynski, E., van Leeuwen, B., Nijkamp, W., Beijersbergen, R., and Agami, R. (2006). Telomerase-independent regulation of ATR by human telomerase RNA. J Biol Chem *281*, 40503-40514.

Kerzendorfer, C., and O'Driscoll, M. (2009). Human DNA damage response and repair deficiency syndromes: linking genomic instability and cell cycle checkpoint proficiency. DNA Repair (Amst) *8*, 1139-1152.

Khaitan, D., Dinger, M.E., Mazar, J., Crawford, J., Smith, M.A., Mattick, J.S., and Perera, R.J. (2011). The melanoma-upregulated long noncoding RNA SPRY4-IT1 modulates apoptosis and invasion. Cancer Res *71*, 3852-3862.

Khidir, M.A., Stachecki, J.J., Krawetz, S.A., and Armant, D.R. (1995). Rapid inhibition of mRNA synthesis during preimplantation embryo development: vital permeabilization by lysolecithin potentiates the action of alpha-amanitin. Experimental cell research *219*, 619-623.

Kim, J.A., Kruhlak, M., Dotiwala, F., Nussenzweig, A., and Haber, J.E. (2007). Heterochromatin is refractory to gamma-H2AX modification in yeast and mammals. J Cell Biol *178*, 209-218.

Kim, T.H., Barrera, L.O., Zheng, M., Qu, C., Singer, M.A., Richmond, T.A., Wu, Y., Green, R.D., and Ren, B. (2005). A high-resolution map of active promoters in the human genome. Nature *436*, 876-880.

Kleiman, F.E., Wu-Baer, F., Fonseca, D., Kaneko, S., Baer, R., and Manley, J.L. (2005). BRCA1/BARD1 inhibition of mRNA 3' processing involves targeted degradation of RNA polymerase II. Genes Dev *19*, 1227-1237.

Kohler, A., and Hurt, E. (2007). Exporting RNA from the nucleus to the cytoplasm. Nat Rev Mol Cell Biol *8*, 761-773.

Kolas, N.K., Chapman, J.R., Nakada, S., Ylanko, J., Chahwan, R., Sweeney, F.D., Panier, S., Mendez, M., Wildenhain, J., Thomson, T.M.*, et al.* (2007). Orchestration of the DNA-damage response by the RNF8 ubiquitin ligase. Science *318*, 1637-1640.

Koralov, S.B., Muljo, S.A., Galler, G.R., Krek, A., Chakraborty, T., Kanellopoulou, C., Jensen, K., Cobb, B.S., Merkenschlager, M., Rajewsky, N.*, et al.* (2008). Dicer ablation affects antibody diversity and cell survival in the B lymphocyte lineage. Cell *132*, 860-874.

Krietsch, J., Caron, M.C., Gagne, J.P., Ethier, C., Vignard, J., Vincent, M., Rouleau, M., Hendzel, M.J., Poirier, G.G., and Masson, J.Y. (2012). PARP activation regulates the RNA-binding protein NONO in the DNA damage response to DNA double-strand breaks. Nucleic Acids Res *40*, 10287-10301.

Krol, J., Loedige, I., and Filipowicz, W. (2010). The widespread regulation of microRNA biogenesis, function and decay. Nat Rev Genet *11*, 597-610.

Kruhlak, M., Crouch, E.E., Orlov, M., Montano, C., Gorski, S.A., Nussenzweig, A., Misteli, T., Phair, R.D., and Casellas, R. (2007). The ATM repair pathway inhibits RNA polymerase I transcription in response to chromosome breaks. Nature *447*, 730-734.

Kumar, M.S., Lu, J., Mercer, K.L., Golub, T.R., and Jacks, T. (2007). Impaired microRNA processing enhances cellular transformation and tumorigenesis. Nature genetics *39*, 673-677.

Kumar, M.S., Pester, R.E., Chen, C.Y., Lane, K., Chin, C., Lu, J., Kirsch, D.G., Golub, T.R., and Jacks, T. (2009). Dicer1 functions as a haploinsufficient tumor suppressor. Genes & development *23*, 2700-2704.

Kwak, H., and Lis, J.T. (2013). Control of Transcriptional Elongation. Annu Rev Genet.

Landick, R. (2006). The regulatory roles and mechanism of transcriptional pausing. Biochem Soc Trans *34*, 1062-1066.

Langerak, P., and Russell, P. (2011). Regulatory networks integrating cell cycle control with DNA damage checkpoints and double-strand break repair. Philos Trans R Soc Lond B Biol Sci *366*, 3562-3571.

Law, J.A., and Jacobsen, S.E. (2010). Establishing, maintaining and modifying DNA methylation patterns in plants and animals. Nature reviews Genetics *11*, 204-220.

Lee, H.C., Chang, S.S., Choudhary, S., Aalto, A.P., Maiti, M., Bamford, D.H., and Liu, Y. (2009). qiRNA is a new type of small interfering RNA induced by DNA damage. Nature *459*, 274-277.

Lee, J.H., Goodarzi, A.A., Jeggo, P.A., and Paull, T.T. (2010). 53BP1 promotes ATM activity through direct interactions with the MRN complex. EMBO J *29*, 574-585.

Lee, J.H., and Paull, T.T. (2005). ATM activation by DNA double-strand breaks through the Mre11-Rad50-Nbs1 complex. Science *308*, 551-554.

Lejeune, E., Bayne, E.H., and Allshire, R.C. (2010). On the connection between RNAi and heterochromatin at centromeres. Cold Spring Harb Symp Quant Biol *75*, 275-283.

Li, G.M. (2008). Mechanisms and functions of DNA mismatch repair. Cell Res *18*, 85-98.

Lieber, M.R. (2010). The mechanism of double-strand DNA break repair by the nonhomologous DNA end-joining pathway. Annu Rev Biochem *79*, 181-211.

Lindahl, T. (1993). Instability and decay of the primary structure of DNA. Nature *362*, 709-715.

Liu, Q., Guntuku, S., Cui, X.S., Matsuoka, S., Cortez, D., Tamai, K., Luo, G., Carattini-Rivera, S., DeMayo, F., Bradley, A.*, et al.* (2000). Chk1 is an essential kinase that is regulated by Atr and required for the G(2)/M DNA damage checkpoint. Genes Dev *14*, 1448-1459.

Lugli, G., Larson, J., Martone, M.E., Jones, Y., and Smalheiser, N.R. (2005). Dicer and eIF2c are enriched at postsynaptic densities in adult mouse brain and are modified by neuronal activity in a calpain-dependent manner. J Neurochem *94*, 896-905.

Luijsterburg, M.S., Dinant, C., Lans, H., Stap, J., Wiernasz, E., Lagerwerf, S., Warmerdam, D.O., Lindh, M., Brink, M.C., Dobrucki, J.W.*, et al.* (2009). Heterochromatin protein 1 is recruited to various types of DNA damage. J Cell Biol *185*, 577-586.

Lukas, C., Falck, J., Bartkova, J., Bartek, J., and Lukas, J. (2003). Distinct spatiotemporal dynamics of mammalian checkpoint regulators induced by DNA damage. Nat Cell Biol *5*, 255-260.

Lukas, C., Savic, V., Bekker-Jensen, S., Doil, C., Neumann, B., Pedersen, R.S., Grofte, M., Chan, K.L., Hickson, I.D., Bartek, J.*, et al.* (2011). 53BP1 nuclear bodies form around

DNA lesions generated by mitotic transmission of chromosomes under replication stress. Nat Cell Biol *13*, 243-253.

Ma, E., MacRae, I.J., Kirsch, J.F., and Doudna, J.A. (2008). Autoinhibition of human dicer by its internal helicase domain. J Mol Biol *380*, 237-243.

Machlin, E.S., Sarnow, P., and Sagan, S.M. (2012). Combating hepatitis C virus by targeting microRNA-122 using locked nucleic acids. Curr Gene Ther *12*, 301-306.

MacRae, I.J., Zhou, K., and Doudna, J.A. (2007). Structural determinants of RNA recognition and cleavage by Dicer. Nat Struct Mol Biol *14*, 934-940.

Mahaney, B.L., Meek, K., and Lees-Miller, S.P. (2009). Repair of ionizing radiation-induced DNA double-strand breaks by non-homologous end-joining. Biochem J *417*, 639-650.

Mailand, N., Bekker-Jensen, S., Faustrup, H., Melander, F., Bartek, J., Lukas, C., and Lukas, J. (2007). RNF8 ubiquitylates histones at DNA double-strand breaks and promotes assembly of repair proteins. Cell *131*, 887-900.

Maison, C., Bailly, D., Peters, A.H., Quivy, J.P., Roche, D., Taddei, A., Lachner, M., Jenuwein, T., and Almouzni, G. (2002). Higher-order structure in pericentric heterochromatin involves a distinct pattern of histone modification and an RNA component. Nat Genet *30*, 329-334.

Mallette, F.A., Mattiroli, F., Cui, G., Young, L.C., Hendzel, M.J., Mer, G., Sixma, T.K., and Richard, S. (2012). RNF8- and RNF168-dependent degradation of KDM4A/JMJD2A triggers 53BP1 recruitment to DNA damage sites. EMBO J *31*, 1865-1878.

Malumbres, M., and Barbacid, M. (2009). Cell cycle, CDKs and cancer: a changing paradigm. Nat Rev Cancer *9*, 153-166.

Margeat, E., Kapanidis, A.N., Tinnefeld, P., Wang, Y., Mukhopadhyay, J., Ebright, R.H., and Weiss, S. (2006). Direct observation of abortive initiation and promoter escape within single immobilized transcription complexes. Biophys J *90*, 1419-1431.

Martin, M., Terradas, M., Iliakis, G., Tusell, L., and Genesca, A. (2009). Breaks invisible to the DNA damage response machinery accumulate in ATM-deficient cells. Genes Chromosomes Cancer *48*, 745-759.

Martin, N.T., Nakamura, K., Davies, R., Nahas, S.A., Brown, C., Tunuguntla, R., Gatti, R.A., and Hu, H. (2013). ATM-dependent MiR-335 targets CtIP and modulates the DNA damage response. PLoS Genet *9*, e1003505.

Mastrocola, A.S., Kim, S.H., Trinh, A.T., Rodenkirch, L.A., and Tibbetts, R.S. (2013). The RNA-binding protein fused in sarcoma (FUS) functions downstream of poly(ADP-ribose) polymerase (PARP) in response to DNA damage. J Biol Chem *288*, 24731-24741.

Mattick, J.S. (2003). Challenging the dogma: the hidden layer of non-protein-coding RNAs in complex organisms. Bioessays *25*, 930-939.

McPherson, J.P., Lemmers, B., Hirao, A., Hakem, A., Abraham, J., Migon, E., Matysiak-Zablocki, E., Tamblyn, L., Sanchez-Sweatman, O., Khokha, R.*, et al.* (2004). Collaboration of Brca1 and Chk2 in tumorigenesis. Genes Dev *18*, 1144-1153.

McVey, M., and Lee, S.E. (2008). MMEJ repair of double-strand breaks (director's cut): deleted sequences and alternative endings. Trends Genet *24*, 529-538.

Meister, G. (2013). Argonaute proteins: functional insights and emerging roles. Nat Rev Genet *14*, 447-459.

Melo, S.A., Moutinho, C., Ropero, S., Calin, G.A., Rossi, S., Spizzo, R., Fernandez, A.F., Davalos, V., Villanueva, A., Montoya, G.*, et al.* (2010). A genetic defect in exportin-5 traps precursor microRNAs in the nucleus of cancer cells. Cancer Cell *18*, 303-315.

Melo, S.A., Ropero, S., Moutinho, C., Aaltonen, L.A., Yamamoto, H., Calin, G.A., Rossi, S., Fernandez, A.F., Carneiro, F., Oliveira, C.*, et al.* (2009). A TARBP2 mutation in human cancer impairs microRNA processing and DICER1 function. Nat Genet *41*, 365-370.

Memczak, S., Jens, M., Elefsinioti, A., Torti, F., Krueger, J., Rybak, A., Maier, L., Mackowiak, S.D., Gregersen, L.H., Munschauer, M.*, et al.* (2013). Circular RNAs are a large class of animal RNAs with regulatory potency. Nature *495*, 333-338.

Michalik, K.M., Bottcher, R., and Forstemann, K. (2012). A small RNA response at DNA ends in Drosophila. Nucleic Acids Res *40*, 9596-9603.

Miller, K.M., Tjeertes, J.V., Coates, J., Legube, G., Polo, S.E., Britton, S., and Jackson, S.P. (2010). Human HDAC1 and HDAC2 function in the DNA-damage response to promote DNA nonhomologous end-joining. Nat Struct Mol Biol *17*, 1144-1151.

Mochizuki, K., Fine, N.A., Fujisawa, T., and Gorovsky, M.A. (2002). Analysis of a piwi-related gene implicates small RNAs in genome rearrangement in tetrahymena. Cell *110*, 689-699.

Mudhasani, R., Zhu, Z., Hutvagner, G., Eischen, C.M., Lyle, S., Hall, L.L., Lawrence, J.B., Imbalzano, A.N., and Jones, S.N. (2008). Loss of miRNA biogenesis induces p19Arf-p53 signaling and senescence in primary cells. J Cell Biol *181*, 1055-1063.

Murchison, E.P., Stein, P., Xuan, Z., Pan, H., Zhang, M.Q., Schultz, R.M., and Hannon, G.J. (2007). Critical roles for Dicer in the female germline. Genes Dev *21*, 682-693.

Murga, M., Jaco, I., Fan, Y., Soria, R., Martinez-Pastor, B., Cuadrado, M., Yang, S.M., Blasco, M.A., Skoultchi, A.I., and Fernandez-Capetillo, O. (2007). Global chromatin compaction limits the strength of the DNA damage response. J Cell Biol *178*, 1101-1108.

Nakagawa, A., Shi, Y., Kage-Nakadai, E., Mitani, S., and Xue, D. (2010). Caspase-dependent conversion of Dicer ribonuclease into a death-promoting deoxyribonuclease. Science *328*, 327-334.

Nam, E.A., and Cortez, D. (2011). ATR signalling: more than meeting at the fork. Biochem J *436*, 527-536.

Newman, M.A., and Hammond, S.M. (2010). Emerging paradigms of regulated microRNA processing. Genes Dev *24*, 1086-1092.

Nguyen, V.T., Giannoni, F., Dubois, M.F., Seo, S.J., Vigneron, M., Kedinger, C., and Bensaude, O. (1996). In vivo degradation of RNA polymerase II largest subunit triggered by alpha-amanitin. Nucleic acids research *24*, 2924-2929.

Nicol, S.M., Bray, S.E., Black, H.D., Lorimore, S.A., Wright, E.G., Lane, D.P., Meek, D.W., Coates, P.J., and Fuller-Pace, F.V. (2013). The RNA helicase p68 (DDX5) is selectively required for the induction of p53-dependent p21 expression and cell-cycle arrest after DNA damage. Oncogene *32*, 3461-3469.

Nowacki, M., Vijayan, V., Zhou, Y., Schotanus, K., Doak, T.G., and Landweber, L.F. (2008). RNA-mediated epigenetic programming of a genome-rearrangement pathway. Nature *451*, 153-158.

Nussenzweig, A., and Nussenzweig, M.C. (2007). A backup DNA repair pathway moves to the forefront. Cell *131*, 223-225.

O'Donovan, P.J., and Livingston, D.M. (2010). BRCA1 and BRCA2: breast/ovarian cancer susceptibility gene products and participants in DNA double-strand break repair. Carcinogenesis *31*, 961-967.

O'Hagan, H.M., Wang, W., Sen, S., Destefano Shields, C., Lee, S.S., Zhang, Y.W., Clements, E.G., Cai, Y., Van Neste, L., Easwaran, H.*, et al.* (2011). Oxidative damage targets complexes containing DNA methyltransferases, SIRT1, and polycomb members to promoter CpG Islands. Cancer Cell *20*, 606-619.

O'Rourke, J.R., Georges, S.A., Seay, H.R., Tapscott, S.J., McManus, M.T., Goldhamer, D.J., Swanson, M.S., and Harfe, B.D. (2007). Essential role for Dicer during skeletal muscle development. Dev Biol *311*, 359-368.

Ogrunc, M., and d'Adda di Fagagna, F. (2011). Never-ageing cellular senescence. Eur J Cancer *47*, 1616-1622.

Ohrt, T., Muetze, J., Svoboda, P., and Schwille, P. (2012). Intracellular localization and routing of miRNA and RNAi pathway components. Curr Top Med Chem *12*, 79-88.

Olovnikov, I., Chan, K., Sachidanandam, R., Newman, D.K., and Aravin, A.A. (2013). Bacterial argonaute samples the transcriptome to identify foreign DNA. Mol Cell *51*, 594-605.

Orom, U.A., and Shiekhattar, R. (2013). Long Noncoding RNAs Usher In a New Era in the Biology of Enhancers. Cell *154*, 1190-1193.

Pak, J., and Fire, A. (2007). Distinct populations of primary and secondary effectors during RNAi in C. elegans. Science *315*, 241-244.

Panier, S., Ichijima, Y., Fradet-Turcotte, A., Leung, C.C., Kaustov, L., Arrowsmith, C.H., and Durocher, D. (2012). Tandem protein interaction modules organize the ubiquitin-dependent response to DNA double-strand breaks. Mol Cell *47*, 383-395.

Pankotai, T., Bonhomme, C., Chen, D., and Soutoglou, E. (2012). DNAPKcs-dependent arrest of RNA polymerase II transcription in the presence of DNA breaks. Nat Struct Mol Biol *19*, 276-282.

Papaioannou, M.D., Pitetti, J.L., Ro, S., Park, C., Aubry, F., Schaad, O., Vejnar, C.E., Kuhne, F., Descombes, P., Zdobnov, E.M., *et al.* (2009). Sertoli cell Dicer is essential for spermatogenesis in mice. Dev Biol *326*, 250-259.

Park, J.E., Heo, I., Tian, Y., Simanshu, D.K., Chang, H., Jee, D., Patel, D.J., and Kim, V.N. (2011). Dicer recognizes the 5' end of RNA for efficient and accurate processing. Nature *475*, 201-205.

Paroo, Z., Ye, X., Chen, S., and Liu, Q. (2009). Phosphorylation of the human microRNA-generating complex mediates MAPK/Erk signaling. Cell *139*, 112-122.

Pei, H., Zhang, L., Luo, K., Qin, Y., Chesi, M., Fei, F., Bergsagel, P.L., Wang, L., You, Z., and Lou, Z. (2011). MMSET regulates histone H4K20 methylation and 53BP1 accumulation at DNA damage sites. Nature *470*, 124-128.

Pellegrini, M., Celeste, A., Difilippantonio, S., Guo, R., Wang, W., Feigenbaum, L., and Nussenzweig, A. (2006). Autophosphorylation at serine 1987 is dispensable for murine Atm activation in vivo. Nature *443*, 222-225.

Pitchiaya, S., Androsavich, J.R., and Walter, N.G. (2012). Intracellular single molecule microscopy reveals two kinetically distinct pathways for microRNA assembly. EMBO reports *13*, 709-715.

Polo, S.E., Blackford, A.N., Chapman, J.R., Baskcomb, L., Gravel, S., Rusch, A., Thomas, A., Blundred, R., Smith, P., Kzhyshkowska, J.*, et al.* (2012). Regulation of DNA-end resection by hnRNPU-like proteins promotes DNA double-strand break signaling and repair. Mol Cell *45*, 505-516.

Polo, S.E., and Jackson, S.P. (2011). Dynamics of DNA damage response proteins at DNA breaks: a focus on protein modifications. Genes Dev *25*, 409-433.

Povirk, L.F. (1996). DNA damage and mutagenesis by radiomimetic DNA-cleaving agents: bleomycin, neocarzinostatin and other enediynes. Mutat Res *355*, 71-89.

Pryde, F., Khalili, S., Robertson, K., Selfridge, J., Ritchie, A.M., Melton, D.W., Jullien, D., and Adachi, Y. (2005). 53BP1 exchanges slowly at the sites of DNA damage and appears to require RNA for its association with chromatin. J Cell Sci *118*, 2043-2055.

Rastogi, R.P., Richa, Kumar, A., Tyagi, M.B., and Sinha, R.P. (2010). Molecular mechanisms of ultraviolet radiation-induced DNA damage and repair. J Nucleic Acids *2010*, 592980.

Rinn, J.L., and Chang, H.Y. (2012). Genome regulation by long noncoding RNAs. Annu Rev Biochem *81*, 145-166.

Rulten, S.L., Rotheray, A., Green, R.L., Grundy, G.J., Moore, D.A., Gomez-Herreros, F., Hafezparast, M., and Caldecott, K.W. (2013). PARP-1 dependent recruitment of the amyotrophic lateral sclerosis-associated protein FUS/TLS to sites of oxidative DNA damage. Nucleic Acids Res.

Salzman, D.W., Shubert-Coleman, J., and Furneaux, H. (2007). P68 RNA helicase unwinds the human let-7 microRNA precursor duplex and is required for let-7-directed silencing of gene expression. J Biol Chem *282*, 32773-32779.

Sayed, D., and Abdellatif, M. (2011). MicroRNAs in development and disease. Physiol Rev *91*, 827-887.

Schneider-Poetsch, T., Ju, J., Eyler, D., Dang, Y., Bhat, S., Merrick, W., Green, R., Shen, B., and Liu, J. (2010). Inhibition of Eukaryotic Translation Elongation by Cycloheximide and Lactimidomycin. Nat Chem Biol *6*, 209–217.

Schoeftner, S., and Blasco, M.A. (2008). Developmentally regulated transcription of mammalian telomeres by DNA-dependent RNA polymerase II. Nat Cell Biol *10*, 228-236.

Seiler, D.M., Rouquette, J., Schmid, V.J., Strickfaden, H., Ottmann, C., Drexler, G.A., Mazurek, B., Greubel, C., Hable, V., Dollinger, G.*, et al.* (2011). Double-strand break-induced transcriptional silencing is associated with loss of tri-methylation at H3K4. Chromosome Res *19*, 883-899.

Sellier, C., Freyermuth, F., Tabet, R., Tran, T., He, F., Ruffenach, F., Alunni, V., Moine, H., Thibault, C., Page, A.*, et al.* (2013). Sequestration of DROSHA and DGCR8 by expanded CGG RNA repeats alters microRNA processing in fragile X-associated tremor/ataxia syndrome. Cell reports *3*, 869-880.

Shanbhag, N.M., Rafalska-Metcalf, I.U., Balane-Bolivar, C., Janicki, S.M., and Greenberg, R.A. (2010). ATM-dependent chromatin changes silence transcription in cis to DNA double-strand breaks. Cell *141*, 970-981.

Shandilya, J., and Roberts, S.G. (2012). The transcription cycle in eukaryotes: from productive initiation to RNA polymerase II recycling. Biochim Biophys Acta *1819*, 391-400.

Sharma, V., and Misteli, T. (2013). Non-coding RNAs in DNA damage and repair. FEBS Lett *587*, 1832-1839.

Shiloh, Y., and Ziv, Y. (2013). The ATM protein kinase: regulating the cellular response to genotoxic stress, and more. Nat Rev Mol Cell Biol *14*, 197-210.

Simonson, P.D., Deberg, H.A., Ge, P., Alexander, J.K., Jeyifous, O., Green, W.N., and Selvin, P.R. (2010). Counting bungarotoxin binding sites of nicotinic acetylcholine receptors in mammalian cells with high signal/noise ratios. Biophysical journal *99*, L81-83.

Sinkkonen, L., Hugenschmidt, T., Filipowicz, W., and Svoboda, P. (2010). Dicer is associated with ribosomal DNA chromatin in mammalian cells. PLoS One *5*, e12175.

Siomi, M.C., Sato, K., Pezic, D., and Aravin, A.A. (2011). PIWI-interacting small RNAs: the vanguard of genome defence. Nat Rev Mol Cell Biol *12*, 246-258.

Soubeyrand, S., Pope, L., and Hache, R.J. (2010). Topoisomerase IIalpha-dependent induction of a persistent DNA damage response in response to transient etoposide exposure. Mol Oncol *4*, 38-51.

Soutoglou, E., Dorn, J.F., Sengupta, K., Jasin, M., Nussenzweig, A., Ried, T., Danuser, G., and Misteli, T. (2007). Positional stability of single double-strand breaks in mammalian cells. Nature cell biology *9*, 675-682.

Soutoglou, E., and Misteli, T. (2008). Activation of the cellular DNA damage response in the absence of DNA lesions. Science *320*, 1507-1510.

Spitale, R.C., Tsai, M.C., and Chang, H.Y. (2011). RNA templating the epigenome: long noncoding RNAs as molecular scaffolds. Epigenetics *6*, 539-543.

Starita, L.M., Horwitz, A.A., Keogh, M.C., Ishioka, C., Parvin, J.D., and Chiba, N. (2005). BRCA1/BARD1 ubiquitinate phosphorylated RNA polymerase II. J Biol Chem *280*, 24498-24505.

Steinmetz, E.J., Warren, C.L., Kuehner, J.N., Panbehi, B., Ansari, A.Z., and Brow, D.A. (2006). Genome-wide distribution of yeast RNA polymerase II and its control by Sen1 helicase. Mol Cell *24*, 735-746.

Stellwagen, A.E., Haimberger, Z.W., Veatch, J.R., and Gottschling, D.E. (2003). Ku interacts with telomerase RNA to promote telomere addition at native and broken chromosome ends. Genes Dev *17*, 2384-2395.

Stenvang, J., Petri, A., Lindow, M., Obad, S., and Kauppinen, S. (2012). Inhibition of microRNA function by antimiR oligonucleotides. Silence *3*, 1.

Stewart, G.S., Panier, S., Townsend, K., Al-Hakim, A.K., Kolas, N.K., Miller, E.S., Nakada, S., Ylanko, J., Olivarius, S., Mendez, M.*, et al.* (2009). The RIDDLE syndrome protein mediates a ubiquitin-dependent signaling cascade at sites of DNA damage. Cell *136*, 420-434.

Stewart, G.S., Stankovic, T., Byrd, P.J., Wechsler, T., Miller, E.S., Huissoon, A., Drayson, M.T., West, S.C., Elledge, S.J., and Taylor, A.M. (2007). RIDDLE immunodeficiency syndrome is linked to defects in 53BP1-mediated DNA damage signaling. Proc Natl Acad Sci U S A *104*, 16910-16915.

Stirling, P.C., Chan, Y.A., Minaker, S.W., Aristizabal, M.J., Barrett, I., Sipahimalani, P., Kobor, M.S., and Hieter, P. (2012). R-loop-mediated genome instability in mRNA cleavage and polyadenylation mutants. Genes & development *26*, 163-175.

Storici, F., Bebenek, K., Kunkel, T.A., Gordenin, D.A., and Resnick, M.A. (2007). RNA-templated DNA repair. Nature *447*, 338-341.

Stracker, T.H., Couto, S.S., Cordon-Cardo, C., Matos, T., and Petrini, J.H. (2008). Chk2 suppresses the oncogenic potential of DNA replication-associated DNA damage. Mol Cell *31*, 21-32.

Stracker, T.H., and Petrini, J.H. (2011). The MRE11 complex: starting from the ends. Nat Rev Mol Cell Biol *12*, 90-103.

Stucki, M., Clapperton, J.A., Mohammad, D., Yaffe, M.B., Smerdon, S.J., and Jackson, S.P. (2005). MDC1 directly binds phosphorylated histone H2AX to regulate cellular responses to DNA double-strand breaks. Cell *123*, 1213-1226.

Suarez, Y., Fernandez-Hernando, C., Yu, J., Gerber, S.A., Harrison, K.D., Pober, J.S., Iruela-Arispe, M.L., Merkenschlager, M., and Sessa, W.C. (2008). Dicer-dependent endothelial microRNAs are necessary for postnatal angiogenesis. Proc Natl Acad Sci U S A *105*, 14082-14087.

Sulli, G., Di Micco, R., and d'Adda di Fagagna, F. (2012). Crosstalk between chromatin state and DNA damage response in cellular senescence and cancer. Nat Rev Cancer *12*, 709-720.

Sustackova, G., Kozubek, S., Stixova, L., Legartova, S., Matula, P., Orlova, D., and Bartova, E. (2012). Acetylation-dependent nuclear arrangement and recruitment of BMI1 protein to UV-damaged chromatin. J Cell Physiol *227*, 1838-1850.

Suzuki, H.I., Yamagata, K., Sugimoto, K., Iwamoto, T., Kato, S., and Miyazono, K. (2009). Modulation of microRNA processing by p53. Nature *460*, 529-533.

Sydow, J.F., and Cramer, P. (2009). RNA polymerase fidelity and transcriptional proofreading. Curr Opin Struct Biol *19*, 732-739.

Tang, K.F., Ren, H., Cao, J., Zeng, G.L., Xie, J., Chen, M., Wang, L., and He, C.X. (2008). Decreased Dicer expression elicits DNA damage and up-regulation of MICA and MICB. J Cell Biol *182*, 233-239.

Tay, Y., Kats, L., Salmena, L., Weiss, D., Tan, S.M., Ala, U., Karreth, F., Poliseno, L., Provero, P., Di Cunto, F.*, et al.* (2011). Coding-independent regulation of the tumor suppressor PTEN by competing endogenous mRNAs. Cell *147*, 344-357.

Ting, N.S., Yu, Y., Pohorelic, B., Lees-Miller, S.P., and Beattie, T.L. (2005). Human Ku70/80 interacts directly with hTR, the RNA component of human telomerase. Nucleic Acids Res *33*, 2090-2098.

Trabucchi, M., Briata, P., Garcia-Mayoral, M., Haase, A.D., Filipowicz, W., Ramos, A., Gherzi, R., and Rosenfeld, M.G. (2009). The RNA-binding protein KSRP promotes the biogenesis of a subset of microRNAs. Nature *459*, 1010-1014.

Tritschler, F., Huntzinger, E., and Izaurralde, E. (2010). Role of GW182 proteins and PABPC1 in the miRNA pathway: a sense of deja vu. Nature reviews Molecular cell biology *11*, 379-384.

van Dijk, E.L., Chen, C.L., d'Aubenton-Carafa, Y., Gourvennec, S., Kwapisz, M., Roche, V., Bertrand, C., Silvain, M., Legoix-Ne, P., Loeillet, S.*, et al.* (2011). XUTs are a class of Xrn1-sensitive antisense regulatory non-coding RNA in yeast. Nature *475*, 114-117.

Vannini, A., and Cramer, P. (2012). Conservation between the RNA polymerase I, II, and III transcription initiation machineries. Mol Cell *45*, 439-446.

Vasudevan, S., Tong, Y., and Steitz, J.A. (2007). Switching from repression to activation: microRNAs can up-regulate translation. Science *318*, 1931-1934.

Vazquez, F. (2006). Arabidopsis endogenous small RNAs: highways and byways. Trends Plant Sci *11*, 460-468.

Verdel, A., Vavasseur, A., Le Gorrec, M., and Touat-Todeschini, L. (2009). Common themes in siRNA-mediated epigenetic silencing pathways. Int J Dev Biol *53*, 245-257.

Wagner, S.D., Yakovchuk, P., Gilman, B., Ponicsan, S.L., Drullinger, L.F., Kugel, J.F., and Goodrich, J.A. (2013). RNA polymerase II acts as an RNA-dependent RNA polymerase to extend and destabilize a non-coding RNA. The EMBO journal *32*, 781-790.

Wahba, L., Gore, S.K., and Koshland, D. (2013). The homologous recombination machinery modulates the formation of RNA-DNA hybrids and associated chromosome instability. Elife *2*, e00505.

Wan, G., Zhang, X., Langley, R.R., Liu, Y., Hu, X., Han, C., Peng, G., Ellis, L.M., Jones, S.N., and Lu, X. (2013). DNA-damage-induced nuclear export of precursor microRNAs is regulated by the ATM-AKT pathway. Cell Rep *3*, 2100-2112.

Wang, H., Perrault, A.R., Takeda, Y., Qin, W., and Iliakis, G. (2003). Biochemical evidence for Ku-independent backup pathways of NHEJ. Nucleic Acids Res *31*, 5377-5388.

Wang, X., Arai, S., Song, X., Reichart, D., Du, K., Pascual, G., Tempst, P., Rosenfeld, M.G., Glass, C.K., and Kurokawa, R. (2008). Induced ncRNAs allosterically modify RNA-binding proteins in cis to inhibit transcription. Nature *454*, 126-130.

Wang, Y., and Taniguchi, T. (2013). MicroRNAs and DNA damage response: implications for cancer therapy. Cell Cycle *12*, 32-42.

Wei, W., Ba, Z., Gao, M., Wu, Y., Ma, Y., Amiard, S., White, C.I., Rendtlew Danielsen, J.M., Yang, Y.G., and Qi, Y. (2012). A role for small RNAs in DNA double-strand break repair. Cell *149*, 101-112.

White, R.J. (2011). Transcription by RNA polymerase III: more complex than we thought. Nat Rev Genet *12*, 459-463.

Wilson, D.M., 3rd, and Bohr, V.A. (2007). The mechanics of base excision repair, and its relationship to aging and disease. DNA Repair (Amst) *6*, 544-559.

Wu, L., Pan, J., Thoroddsen, V., Wysong, D.R., Blackman, R.K., Bulawa, C.E., Gould, A.E., Ocain, T.D., Dick, L.R., Errada, P.*, et al.* (2003). Novel small-molecule inhibitors of RNA polymerase III. Eukaryot Cell *2*, 256-264.

Yuan, J., Adamski, R., and Chen, J. (2010). Focus on histone variant H2AX: to be or not to be. FEBS Lett *584*, 3717-3724.

Yuan, J., and Chen, J. (2010). MRE11-RAD50-NBS1 complex dictates DNA repair independent of H2AX. J Biol Chem *285*, 1097-1104.

Yuce, O., and West, S.C. (2013). Senataxin, defective in the neurodegenerative disorder ataxia with oculomotor apraxia 2, lies at the interface of transcription and the DNA damage response. Mol Cell Biol *33*, 406-417.

Zarebski, M., Wiernasz, E., and Dobrucki, J.W. (2009). Recruitment of heterochromatin protein 1 to DNA repair sites. Cytometry A *75*, 619-625.

Zeng, Y., and Cullen, B.R. (2005). Efficient processing of primary microRNA hairpins by Drosha requires flanking nonstructured RNA sequences. The Journal of biological chemistry *280*, 27595-27603.

Zhang, H., Kolb, F.A., Brondani, V., Billy, E., and Filipowicz, W. (2002). Human Dicer preferentially cleaves dsRNAs at their termini without a requirement for ATP. EMBO J *21*, 5875-5885.

Zhang, H., Kolb, F.A., Jaskiewicz, L., Westhof, E., and Filipowicz, W. (2004). Single processing center models for human Dicer and bacterial RNase III. Cell *118*, 57-68.

Zhang, X., Wan, G., Berger, F.G., He, X., and Lu, X. (2011). The ATM kinase induces microRNA biogenesis in the DNA damage response. Mol Cell *41*, 371-383.

Zimmermann, M., Lottersberger, F., Buonomo, S.B., Sfeir, A., and de Lange, T. (2013). 53BP1 regulates DSB repair using Rif1 to control 5' end resection. Science *339*, 700-704.

# Acknowledgments

Questo lavoro di ricerca non sarebbe stato possibile senza il supporto di molte persone, che vorrei calorosamente ringraziare.

Il mio supervisore, Fabrizio d'Adda di Fagagna, per avermi affidato questo rivoluzionario ed entusiasmante progetto, per la pazienza, per la disponibilità e per i consigli di cui ho fatto tesoro nel corso di questi anni di dottorato. Spero di essere riuscita ad assorbire, almeno in parte, la sua incredibile capacità comunicativa e le qualità per essere un buon capo.

Il Dr. Gioacchino Natoli (IEO, Milano, Italia) ed il Dr. Javier Martinez (IMBA, Vienna, Austria) per aver ricavato il tempo necessario ad essere i miei supervisori interno ed esterno, rispettivamente.

Il Prof. Marco Foiani (IFOM, Milano, Italia) ed il Prof. Witold Filipowicz (FMI, Basilea, Svizzera) per aver gentilmente accettato di essere i miei esaminatori interno ed esterno e per aver letto e revisionato la mia tesi di dottorato.

I servizi di Cell culture, Imaging, RT-PCR, FACS, Kitchen, Purchasing e Warehouse, senza i quali questo lavoro non sarebbe stato possibile.

La SEMM, ma soprattutto Francesca e Veronica per la loro incredibile capacità nel risolvere problemi burocratici e per la loro simpatia.

Sofia, per avermi insegnato tutto ciò che dovevo sapere per portare avanti questo progetto nel migliore dei modi, per aver lavorato con me – soprattutto all'inizio del mio percorso di dottorato – fianco a fianco e spesso fino a tardi, come solo una buona guida e una sorella maggiore potevano fare.

Aurora, Francesca e Valentina, mie colleghe e care amiche. Non dimenticherò mai i nostri momenti in laboratorio e fuori, le chiacchierate scientifiche e non, le pause caffè, le risate, il sostegno reciproco soprattutto nei periodi più duri delle rispettive vite lavorative (revisioni degli articoli, curve di crescita, giornate in stanza cellule). Con voi sono stata sempre libera di essere me stessa – e non mi riferisco solo all'accento romano – e spero davvero di non perdervi mai.

I membri del laboratorio FDA, presenti e passati, per l'incessante collaborazione, per la bella atmosfera e per essere stati il miglior gruppo in cui poter lavorare.

I lab F-riends, per aver reso piacevole e divertente l'ambiente lavorativo. In particolare Nadia, compagna di bancone per un anno. Non è stato più lo stesso lavorare senza le nostre colonne sonore quotidiane.

I SEMMers del mio anno di dottorato, specialmente Claudio, Marco, Pierluigi, Federica, Roberta, Andrea, Pietro e tutti coloro con cui ho condiviso le gioie e i dolori di questo lungo viaggio.

Stefano, che con la sua contagiosa passione per la scienza ed il suo lato autistico-divertente è spesso stato fondamentale nel mio percorso professionale e nella mia vita milanese.

Il Dr. Marco Crescenzi, per essere riuscito a far parte della mia vita professionale anche a distanza, per i suoi consigli, la stima e l'affetto reciproco.

I miei fantastici compagni di salsa, un'esperienza che mi ha aiutato a sorridere nei momenti più bui e che porterò con me per sempre. In particolare Gianluca, sempre disponibile ad uscire con me per una "birretta" e quattro chiacchiere.

Le mie coinquiline con cui ho convissuto per quattro anni, per il buonumore, per la loro pazienza a volte necessaria e per i momenti insieme.

Claudia, la mia "coinqui" ma soprattutto buona amica. Abbiamo iniziato insieme questo percorso, siamo cresciute insieme, ci siamo conosciute a fondo, in ogni lato del nostro carattere, e sostenute a vicenda. Ti ringrazio perché ho sempre saputo di poter bussare alla tua porta e condividere momenti di panico o gioia o semplicemente una pizza e un film. Sono contenta che quattro anni fa, in foresteria, ci siamo conosciute.

Alessia, per le serate insieme, i consigli su libri, film, serie TV, musica e vita. Io, te e Claudia siamo state un inseparabile trio e credo che il nostro legame non potrà mai perdersi.

I miei grandi amici di Roma, in particolare Matteo, Alba e Valentina. Anche se siamo e saremo distribuiti in varie parti del mondo rimarrete sempre i miei punti fermi. Un enorme grazie alle mie "romane", la nostra amicizia ha superato ogni confine di spazio e di tempo e continuerà a farlo sempre.

Loredana, per avermi incessantemente supportato (e sopportato) durante questo periodo di scrittura della tesi, per avermi spronato a dare il massimo, sempre, per aver creduto in me anche, e soprattutto, quando pensavo di non farcela, per avermi trasmesso il fuoco negli occhi e la sicurezza nella voce durante le presentazioni, per avermi regalato quel sorriso e quell'abbraccio di cui avevo bisogno proprio quando ne avevo bisogno, perché senza di te non ce l'avrei fatta. Questo e molto altro ancora, nonostante la lontananza, nonostante tutto e tutti, nonostante te, nonostante me. Hai visto il meglio, hai visto il peggio e sei rimasta sempre al mio fianco. La nostalgia per la fine di un percorso si mescola alla felicità per l'alba di un nuovo inizio.

La mia meravigliosa famiglia, per il loro amore incondizionato, per aver contribuito alla mia carriera, per aver supportato le mie scelte – anche se significava allontanarmi da casa – e per continuare a farlo.

Mia madre, spero di renderti sempre orgogliosa della persona che sono diventata, dei miei obiettivi così come dei risultati.

*Grazie di cuore,*
*Flavia*